ANALYTICA CHIMICA ACTA

International monthly devoted to all branches of analytical chemistry
Revue mensuelle internationale consacrée à tous les domaines de la chimie analytique
Internationale Monatsschrift für alle Gebiete der analytischen Chemie

ELSEVIER SCIENTIFIC PUBLISHING COMPANY

AMSTERDAM

Anal. Chim. Acta, Vol. 68, No. 1, 1–252, January 1974

Published monthly

Publication Schedule for 1974

Vol. **68**, No. **1**	January 1974	
Vol. **68**, No. **2**	February 1974	**(completing Vol. 68)**
Vol. **69**, No. **1**	March 1974	
Vol. **69**, No. **2**	April 1974	**(completing Vol. 69)**
Vol. **70**, No. **1**	May 1974	
Vol. **70**, No. **2**	June 1974	**(completing Vol. 70)**
Vol. **71**, No. **1**	July 1974	
Vol. **71**, No. **2**	August 1974	**(completing Vol. 71)**
Vol. **72**, No. **1**	September 1974	
Vol. **72**, No. **2**	October 1974	**(completing Vol. 72)**
Vol. **73**, No. **1**	November 1974	
Vol. **73**, No. **2**	December 1974	**(completing Vol. 73)**

Subscription price: Dfl. 492.00 plus Dfl. 36.00 postage. Subscribers in the U.S.A. and Canada receive their copies by airmail. Additional charges for airmail to other countries are available on request. For advertising rates apply to the publishers.

GENERAL INFORMATION

Languages

Papers will be published in English, French or German.

Submission of papers

Papers should be sent to:

PROF. PHILIP W. WEST,
Coates Chemical Laboratories,
College of Chemistry and Physics,
Louisiana State University,
Baton Rouge 3,
La. 70803 (U.S.A.)

or to:

DR. A. M. G. MACDONALD,
Department of Chemistry,
The University,
P.O. Box 363
Birmingham B15 2TT (Great Britain)

Reprints

Fifty reprints will be supplied free of charge. Additional reprints (minimum 100) can be ordered at quoted prices. They must be ordered on order forms which are sent together with the proofs.

PRINTED IN THE NETHERLANDS

40 000 scientifiques achètent chaque mois 'La Recherche' 10 000 d'entre eux ne sont pas français

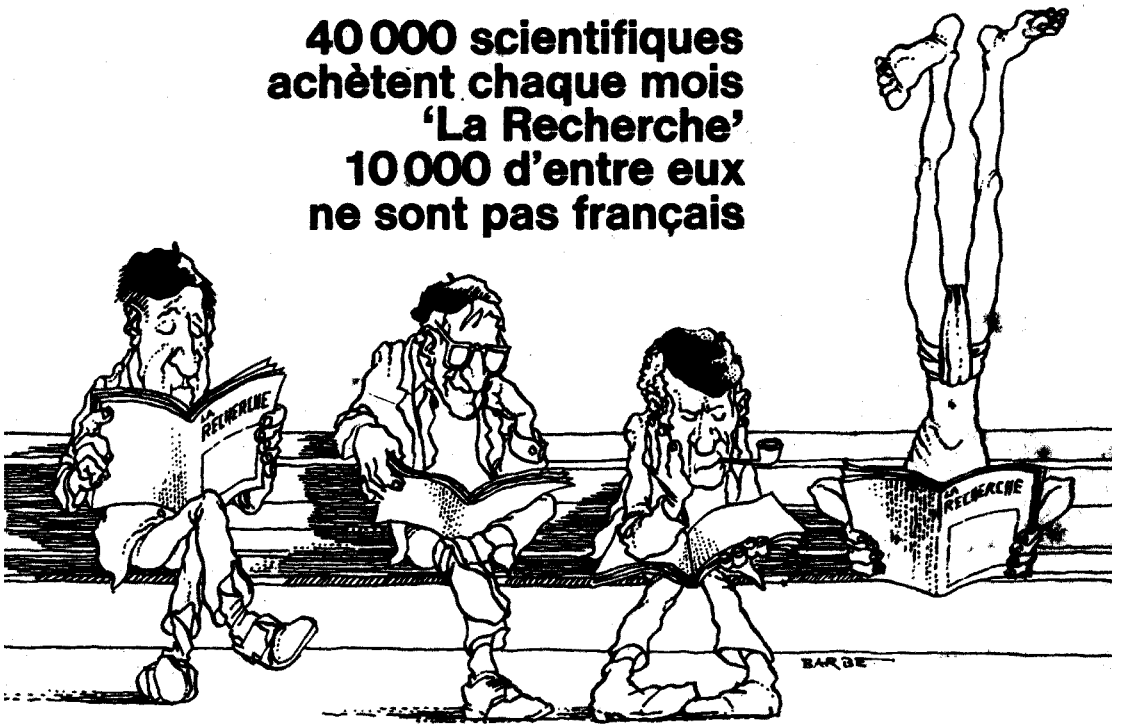

If LA RECHERCHE has an international readership, it's probably simply because its contents is international. You'll find well known French authors in LA RECHERCHE : E. Baulieu, F. Jacob, P. Jacquinot, F. Morel, X. Le Pichon, A. Leroi-Gourhan, L. Liboutry, J. Monod, C. Ropartz, Ch. Thibault among many others. But you'll also find articles by H. Alfvén, J.E. Cleaver, Hong Yee Chiu, Th. Dobzhansky, G. Natta, O. Morgenstern, C. Ponnamperuma, D.W. Sciama, J. Tuck, S. Uyeda...

Enough name-dropping. Distinguished names are not sufficient to make a good publication. (Some of our predecessors prove this.) Written by scientists for scientists, LA RECHERCHE covers everything from biochemistry to astrophysics. But it does not stop at doling out monthly slices of a cake baked of arbitrarily selected "good" articles.

You see, we think that LA RECHERCHE is the best interdisciplinary monthly. But, as its publishers, we have our prejudices.

What do you think? Even if your French is a little rusty, you can judge for yourself - free of charge - over a period of 3 months. All you need to do is fill in and return the coupon below.

Special offer

Name _____

Address _____

_____

Mail to LA RECHERCHE, 4, place de l'Odéon, 75006 Paris, France.

I wish to receive the next 3 issues of LA RECHERCHE on a trial basis. If interested, I'll settle your invoice on receipt of the third issue and benefit from the special subscription rate of fl. 46 instead of the usual fl.60 for a year's volume of 11 issues. Otherwise I'll keep the 3 issues received at no charge to me.

101a

Activation and decay tables of radioisotopes

by E. BUJDOSÓ, *Research Institute for Non-ferrous Metals, Budapest, Hungary,* I. FEHÉR, *Central Research Institute for Physics, Budapest, Hungary and* G. KARDOS, *UNIVAC, Division of Sperry Rand France, Paris, France.*

1973. 576 pages. Dfl. 100.00 (about US$38.50) ISBN 0-444-99937-X

With the widening use of radioisotopes in science and industry, the calculation of the activity of a sample irradiated by thermal neutrons and the rate of decay has become a routine task in many laboratories. The book greatly facilitates such calculations by means of tables compiled with the aid of a computer.
Activation and decay data are presented including half-lives, gamma-ray energies and intensities of 249 radioisotopes formed by (n,γ) reactions on 173 stable isotopes of 80 elements.
These clear tables will be of great help in activation analysis and in other investigations connected with the production and use of radioisotopes.

Contents:

Elsevier
Book Division P.O. Box 211,
Amsterdam, The Netherlands

1122E

DATA: MIRRORS OF SCIENCE

by **R. HOUWINK**

Wassenaar, The Netherlands

6 x 9", ix + 213 pages, illustrated
1970, US$9.50, ISBN 0-444-00068-2

". . . a treasure trove of interesting facts concerning the entire field of science-broadly interpreted. The intent is to put these data into a more common context through the use of aptly chosen analogies and comparisons . . . filled with fascinating tangential pieces of information: for example, the number of years that have elapsed since the earth solidified is equal to the number of people on earth, which is equal to the number of cells in a man's brain, which is equal to the number of heartbeats in a man's life . . . Houwink has managed to evolve examples that stick in the memory with the tenacity of sheep burrs . . . ideally suited to browsing, and if made required reading for anyone presenting any of the sciences to students at any level (the book) could have a revolutionary effect on all contemporary classroom exercises." — D. Allan Bromley, **American Scientist**

Of interest to: Scientists in all disciplines and at all levels; all laymen interested in the world in which they live.

Contents: Why this Book? Compiler's Note. Acknowledgments. Data and Images. Mathematics and Fundamental Physics. The Building Blocks: Atoms and Molecules. Space. Our Planet. The Source of Everything: Energy. Perception. The Biological World. Man and Science. Technical Flashes. The Hydroworld. Military. Sport and Games. Surprises for the Great. Bibliography. Units. Index.

Orders for this title may be placed with the publisher or with your regular bookseller

ELSEVIER PUBLISHING COMPANY

NEW YORK - LONDON - AMSTERDAM

618EV

NATURAL CHELATING POLYMERS

R A A MUZZARELLI

Professor of Quantitative Analytical Chemistry and Applied Radiochemistry, University of Bologna

For the first time three widespread natural polymers are described in terms of their chelating ability. These polymers fulfil in part the need for new chelating substances and also throw light on the important role that they play with trace transition metals in nature and in living organisms.
The book includes information on the occurrence of alginic acid and chitin, their isolation and their chemical treatment, the preparation of chitosan and other derivatives.
Chromatographic separations on thin layers and columns are described for nearly all metals in the Periodic Table. In addition there are original results from the Author's laboratory.
260 Pages £4.95 Hard cover January 1974

ORGANIC REAGENTS IN METAL ANALYSIS

K BURGER

In the light of modern chemical knowledge, more and more analytical problems can be solved via complexation reactions. Analytical chemists need to possess a coordination chemical view and apply this in their work. The first part of this book deals with this treatment of analytical reactions based on complexation. The second part provides tried and time-honoured analytical procedures for the accomplishment of many metal analytical tasks, employing examples covering a wide range of applications. Tabulated data at the end of the book facilitates experimental work.
270 Pages £5.80 Hard cover 1973

ALSO AVAILABLE:

N-BENZOYLPHENYLHYDROXYLAMINE AND ITS ANALOGUES
A K MAJUMDAR **£7.00 hard cover**

ISOTOPE DILUTION ANALYSIS
J TÖLGYESSY et al **£3.50 hard cover**

ANALYTICAL APPLICATIONS OF EDTA AND RELATED COMPOUNDS
R PRIBIL **£12.50 hard cover**

PERGAMON PRESS LTD
Headington Hill Hall Oxford OX3 0BW

596V

Developments in Inorganic Nitrogen Chemistry, Volume 2

edited by CHARLES B. COLBURN, *Department of Chemistry, School of Arts and Sciences, Auburn University, Alabama, U.S.A.*

1973. 238 pages. Dfl. 100.00 (about US$35.10) ISBN 0-444-40962-9

Contents:

Elsevier

BOOK DIVISION, P.O. BOX 211
AMSTERDAM - THE NETHERLANDS

1097E

ANALYTICA CHIMICA ACTA
Vol. 68 (1974)

ANALYTICA CHIMICA ACTA

International monthly devoted to all branches of analytical chemistry
Revue mensuelle internationale consacrée à tous les domaines de la chimie analytique
Internationale Monatsschrift für alle Gebiete der analytischen Chemie

ELSEVIER SCIENTIFIC PUBLISHING COMPANY
AMSTERDAM

PRINTED IN THE NETHERLANDS

Analytica Chimica Acta, 68 (1973) 1–10

A MULTI-ELEMENT SERUM STANDARD FOR NEUTRON ACTIVATION ANALYSIS

R. CORNELIS*, A. SPEECKE and J. HOSTE
Institute for Nuclear Sciences, Rijksuniversiteit Ghent, Ghent (Belgium)
(Received 4th June 1973)

Neutron activation analysis of biological samples, such as sera, permits the assessment of many elements, some of them at very low concentrations, *e.g.* chromium and cobalt. Although the use of flux monitors may sometimes be adequate to take care of changes in the neutron spectra of the reactor, the simultaneous irradiation of known amounts of the elements to be determined is most often necessary. However, the application of a multi-element standard material would be highly advisable for various reasons, such as gain of space in the irradiation container, prevention of cross-contamination, avoidance of neutron shadowing in the standards and of matrix effects in the samples, etc. Therefore, the purpose of this work was to study the feasibility of preparation and the quality at low sample size of a standard for internal laboratory use. This preparation would have to be regarded as an all-in-one standard and not as a reference material such as Bowen's kale powder or the N.B.S. orchard leaves or bovine liver.

The doping for the various elements of the matrix chosen, in this case serum, should be such that the amounts originally present are a negligible or a well-known contribution to the weighed-in quantities. An additional requirement and advantage is that after irradiation the resulting γ-ray spectrum will be very like those of the samples to be analysed. This eliminates corrections for differences in the dead-time and pulse pile-up of the multichannel analyser, and facilitates the interpretation of the measurements by computerized Ge-Li spectrometry.

The main problem with the preparation of such a standard is the correct way to homogenize the serum with the elements being used. The basic procedure developed consists of four parts:

1. thorough mixing of liquid serum with solutions containing all the desired elements;
2. solidifying in liquid nitrogen and cooling in the deep freeze at $-30°$;
3. lyophilization;
4. quality control.

PRELIMINARY EXPERIMENTS

The serum has to be doped with ten elements, which will act as standards for determinations based on long irradiation at a high neutron flux. These are Ag,

* Research Associate of the Inter-university Institute for Nuclear Sciences.

Co, Cr, Cs, Fe, Hg, Rb, Sb, Se and Zn. First of all, a medium has to be found, which is capable of retaining all the desired elements in solution and at the same time will not destroy the serum. Nitric acid must be avoided because it causes the immediate coagulation of the proteins. Although hydrochloric acid does not leave the serum completely unaltered, mixing appears to be possible. The high-purity compounds used of the ten elements are listed in Table I, together with the necessary dissolution treatment, the eventual standardization mode, and their respective concentrations in the stock solution.

TABLE I

CHEMICAL COMPOUNDS USED, THEIR MODE OF STANDARDIZATION, THE CONCENTRATION OF THE ELEMENTS IN THE STOCK SOLUTION AND IN THE DOPED SERUM STANDARD

Compound	*Starting dissolving agent*	*Standardization mode*	*Stock solution 6 M HCl (μg/2 ml)*	*Concentration in standard serum (p.p.m.)*
Ag	HNO_3	—	66.0	7.05
Co_3O_4	HCl	Titration with EDTA and xylenol orange as indicator	60.5	6.46
Cr	HCl	—	180.9	19.32
Cs_2CO_3	HCl	1) Precipitation as $2\ CsCl \cdot SnCl_4$ 2) Precipitation as $Cs_3Co(NO_2)_6 \cdot H_2O$	53.9	5.76
Fe	HC	—	9987	1067
HgO	HCl	Titration with EDTA and Erio T as indicator	210.8	22.5
RbCl	HCl	Drying at 100°	1077.5	115.1
Sb_2O_4	HCl	Na_2O_2 melt on Sb_2O_4, dissolution in 3 *M* HCl, reduction to Sb^{3+} with SO_3^{2-} and titration with $KBrO_3$ and methyl orange indicator	102.8	11.0
Se	HNO_3	—	123.0	13.9
ZnO	HCl	Titration with EDTA and eriochrome black T as indicator	2000	218.3
Al	HCl	—	13434	718
Mn_3O_4	HCl	Potentiometric titration with $KMnO_4$	7690	405
V	HCl	—	1978	105.6

The checks on the homogeneity of the ten elements, dissolved in 6 *M* hydrochloric acid and mixed with the liquid serum, were carried out with radiotracers, as was their behaviour during lyophilization. Liquid serum was doped with the ten elements and one tracer, respectively. The radioactivity of a fraction of this mixture was compared with an equivalent amount of the particular tracer, together with the ten carrier elements, in pure acid medium. In the ten cases, both activities appeared to be the same, within the error caused by counting statistics.

Afterwards the radioactive serum solutions were deep-frozen in liquid nitrogen and lyophilized. The activities of these samples proved to be still equal to those on the references. Apparently no losses due to precipitation nor evaporation occur. After this careful check of the mixing capacities of the elements with the serum by the aid of radiotracers, a successful preparation of a doped serum standard appeared very probable.

TESTS FOR INHOMOGENEITY

In order to carry out inhomogeneity tests on the ten elements mixed with the serum, long irradiations at high neutron flux would be necessary, but these were unacceptable because of the high costs involved. Therefore three elements, aluminium, manganese and vanadium were mixed with the serum as well (see Table I). These elements yield short-lived isotopes, suitable for quality control. They will build up a picture of the degree of homogeneity of the material.

Experimental procedure

Lyophilized serum (10 g) was dissolved in 100 ml of double-distilled water. 2 ml of the stock solution containing the 10 elements in 6 *M* hydrochloric acid and 1 ml of a stock solution containing Al, Mn and V in 6 *M* hydrochloric acid were added. This mixture was mechanically shaken for 30 min, frozen in liquid nitrogen and kept overnight in the deep-freezer at $-30°$. Lyophilization lasted five days. As the required sample size of the lyophilized serum standard was 20 mg, 500 samples could be made out of the 10 g. Part of these samples were packed in polyethylene vials, and the rest of the lot in quartz, a necessity for long irradiations at high neutron fluxes. The concentrations of the doped elements in the serum are also given in Table I.

The 20-mg doped serum samples, packed in polyethylene vials, were irradiated for 5 min at a flux of $2.56 \cdot 10^{12}$ n cm^{-2} s^{-1} in the Thetis reactor of the University of Ghent. After a 2-min cooling period, the samples were measured for 5 min on a Ge-Li detector (F.W.H.M. 2.0 keV, 1332.4-keV ^{60}Co, efficiency 15.6%). A pile-up rejector and a dead-time stabilizer were built into the electronic circuit[1,2]. The imposed dead-time was $\pm 25\%$. The γ-spectrum showed the activities of ^{24}Na, ^{38}Cl, ^{80}Br, ^{56}Mn, ^{52}V and ^{28}Al. The ^{24}Na activity is considered useful as a flux monitor and as an internal standard; it can be assumed that the sodium originates only from serum, that it is by nature homogeneously distributed, and that it remains so after the treatments. The ^{24}Na activity is also proportional to the dry weight of the lyophilized material. The attribution of an exact weight to lyophilized serum is difficult. As soon as lyophilization stops and the serum contacts the air, water is absorbed. This tends to stabilize around a 6.7% weight increase after a couple of hours.

The photopeaks taken into account were: 846.9-keV ^{56}Mn, 1368.4-keV ^{24}Na, 1434.4-keV ^{52}V and 1778.9-keV ^{28}Al. A γ-spectrum is given in Fig. 1. As can be seen all the net peak areas were of the order of 10^4 counts.

Sequential probability test

In sequential analysis (according to Wald[3]), the size of sample is not fixed

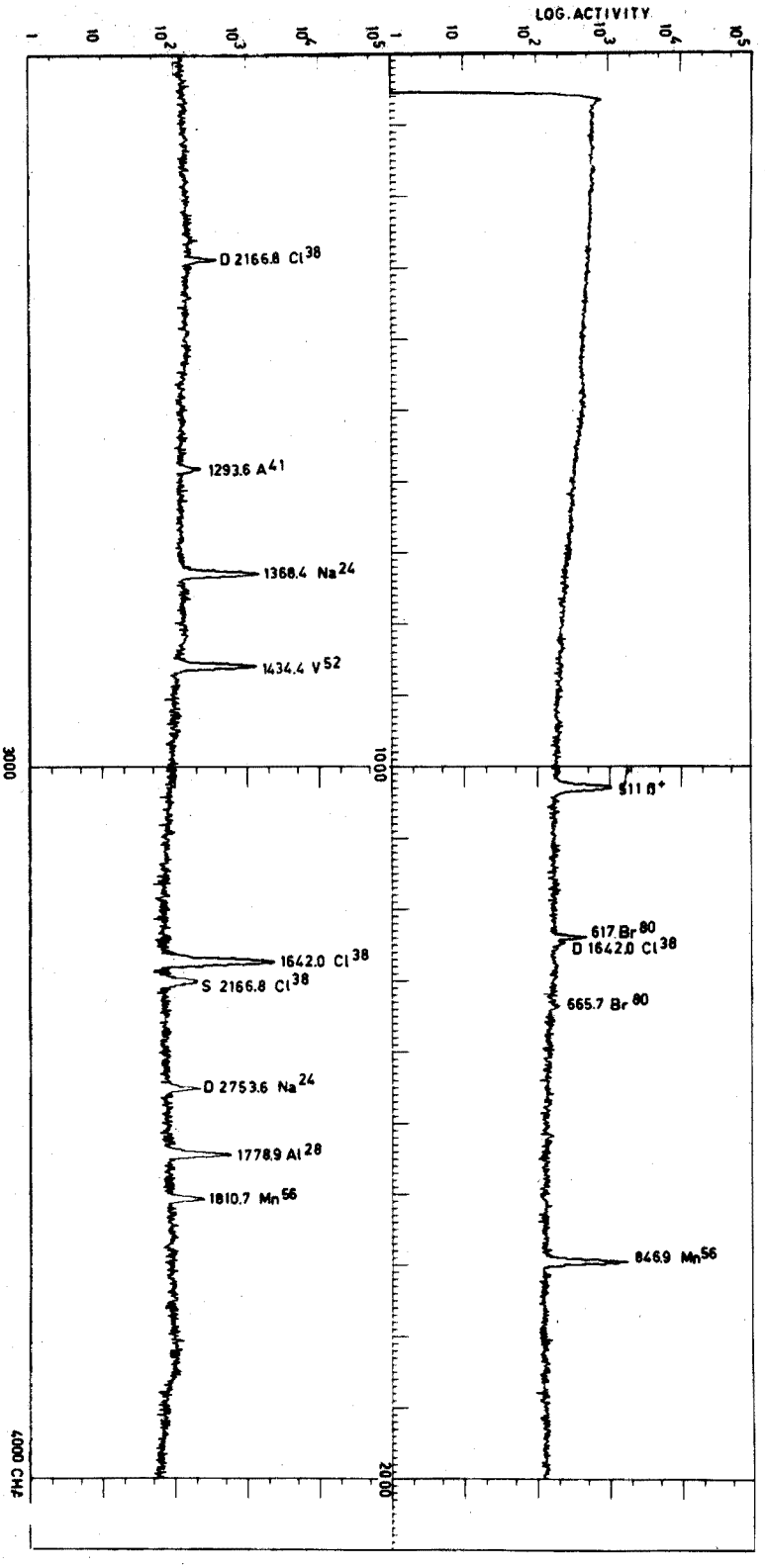

Fig. 1. γ-Spectrum of doped serum standard, after 5-min irradiation, 2-min cooling period and 5-min measurement on a Ge-Li detector.

in advance. A test is applied to the accumulated data after each sample has been examined, and sampling is terminated as soon as a decision either to accept the lot or to reject it, can be made with the required degree of confidence. The characteristics of a sequential plan are dependent on two values σ_0 and σ_1 (according to Wald's notation) specified by the tester and such that $\sigma_{lot} > \sigma_0$ and $\sigma_{lot} < \sigma_1$, and on the producer's and consumer's risks α and β (respectively, errors of type I and II).

The sequential probability test was applied to the ratios of the activities $^{56}Mn/^{24}Na$, $^{52}V/^{24}Na$ and $^{28}Al/^{24}Na$. The Z_i values ($Z_i = \Sigma_{1 \leqslant i \leqslant i} (x_i - x)^2$) were calculated, and the exactness of a set of hypothetical σ_0 and σ_1 values per ratio was demonstrated. The results are summarized in Table II. The σ_0–σ_1 sets concern the bulk of all samples with a confidence limit of 90%. These pair of σ_0–σ_1 values are higher than the s given by a simple calculation of the standard deviation on the 58 analyses (see Table II). The 90% confidence limits for the estimated standard deviation (58 analyses) vary between 0.84 times and 1.20 times its value.

TABLE II

RESULTS OF SEQUENTIAL ANALYSES

(58 samples analysed)

	Characteristics[a]	$^{56}Mn/^{24}Na$	$^{52}V/^{24}Na$	$^{28}Al/^{24}Na$
Sequential analysis				
	σ_0	2.60%	3.30%	4.50%
	σ_1	3.10%	3.80%	5.50%
Minus counting statistics	σ'_0	1.83%	2.55%	3.01%
	σ'_1	2.49%	3.17%	4.37%
Minus irradiation and measurement errors	σ''_0	0.89%	1.98%	2.55%
	σ''_1	1.91%	2.74%	4.07%
Estimated standard deviation on 58 analyses	s	2.32%	2.71%	4.01%
Minus counting statistics	s'	1.42%	1.82%	2.21%
Minus irradiation and measurement errors	s''	0.00%	0.87%	1.52%

[a] Risks $\alpha = \beta = 0.05$.

The calculated standard deviation comprises a variety of experimental errors which arise from:

1. the *inhomogeneity* of the added element and of the sodium reference;
2. the irradiation conditions (uncertainties regarding the position of the sample in the container, flux gradient, packing of the serum in the polyethylene vial, *instability of the reactor* and *error on the irradiation time*;
3. the measurement, which includes *cooling period, geometry*, dead-time correction, pile-up rejector, dead-time stabilizer, stability of the detector;
4. *counting statistics of the isotopes and γ-spectrometry.*

Some of these errors are preponderant (indicated by italics) whereas others are just secondary. The error from counting statistics can be subtracted and results in new sets of σ'_0–σ'_1 values (see Table II). Attributing these σ'_0 and σ'_1 values primarily to the inhomogeneity of the elements in the doped serum, still overrates this phenomenon. The influence of faulty measurement of the irradiation time can be quite important. The saturation factors for ^{24}Na and for ^{56}Mn are still linear ($T = 5$ min), whereas this is not the case for ^{52}V and for ^{28}Al. The increasing σ'_0 and σ'_1 values with decreasing half-life of the isotopes, may originate from these saturation factors. Errors caused by irradiation conditions and measurements were experimentally determined and appeared to be 1.60%. This variance was subtracted from the σ'_0 and σ'_1 values, resulting in a new pair of values σ''_0 and σ''_1.

It can thus be concluded that the doped serum standard, with a 20-mg sample size, shows a small variability over the entire lot, for the elements Mn, V and Al. With the preliminary trace experiments in mind, generalization of this conclusion to the other ten elements is justifiable. Nevertheless, a restricted number of analyses was carried out on these elements.

Variability of the ten doped elements in the serum standard

Nine serum samples (20 mg) were irradiated for 38 h at a flux of $1.8 \cdot 10^{12}$ n cm^{-2} s^{-1}. After a three-week cooling period, they were measured for 8 h on a Ge-Li detector, to ensure good counting statistics. Figure 2 shows a γ-spectrum of the doped serum. The γ-spectra were analysed with an appropriate computer program. The errors can now be mainly attributed to:

1. inhomogeneity of the added element and the inexact weight of the sample;
2. uncertainties in irradiation conditions reduced to the flux gradient, as all samples were contained in one irradiation can;
3. geometry and stability of the measurement;
4. counting statistics and peak area evaluation.

To eliminate the variability caused by inaccurate sample weight, ratios of

TABLE III

ESTIMATED STANDARD DEVIATIONS FOR THE LONG-LIVED ISOTOPES IN THE DOPED SERUM

Element	*s % ratios element/Zn*	*s % ratios minus counting statistics*
Ag	2.42	0.87
Co	1.32	0.00
Cr	1.34	0.00
Cs	1.65	0.89
Fe	3.50	2.09
Hg	3.39	3.15
Rb	1.07	0.00
Sb	2.79	2.27
Se	1.36	0.00
Zn	Reference	Reference

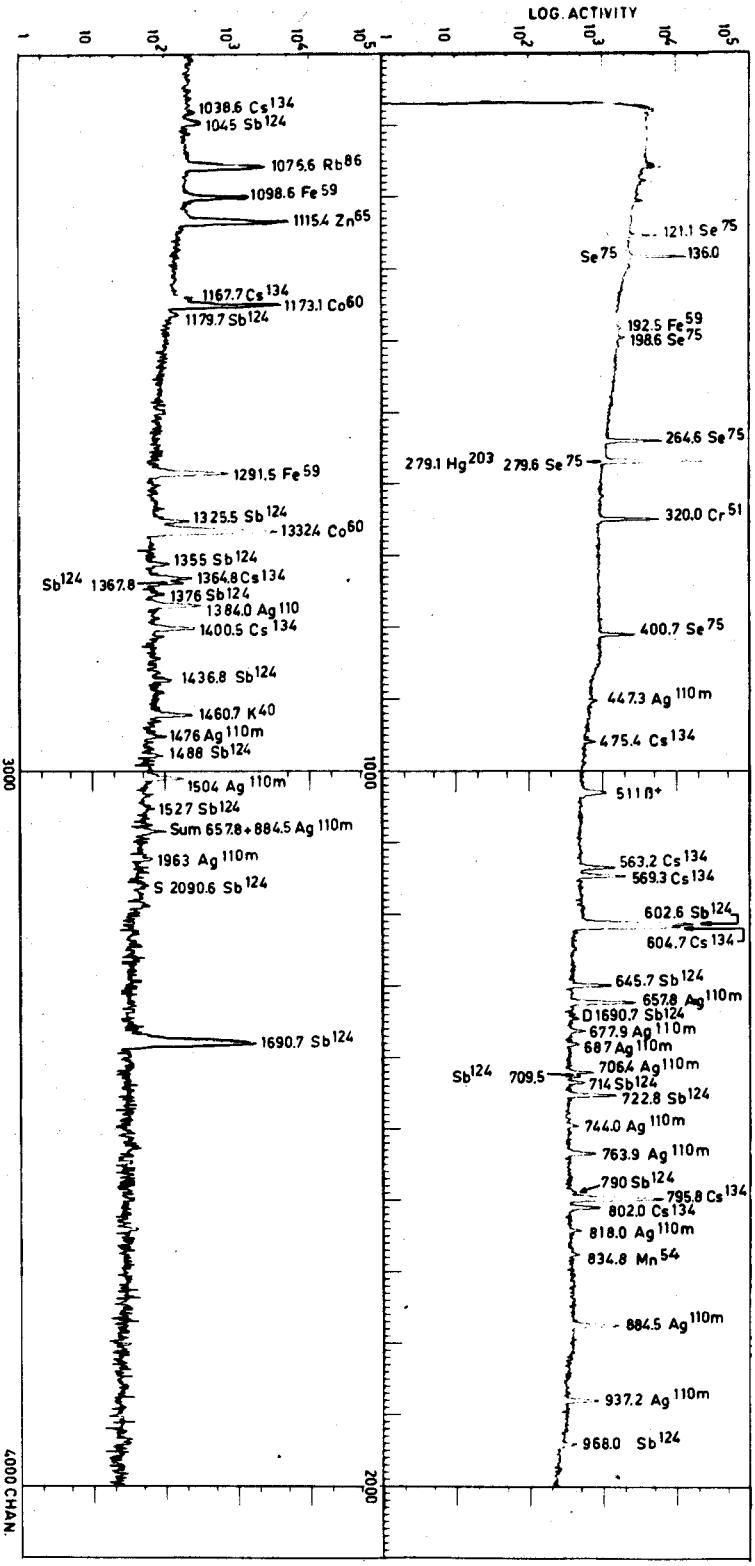

Fig. 2. γ-Spectrum of doped serum standard, irradiated for 32 h at a flux of $1.8 \cdot 10^{12}$ n cm^{-2} s^{-1}. Cooling period, 3 weeks.

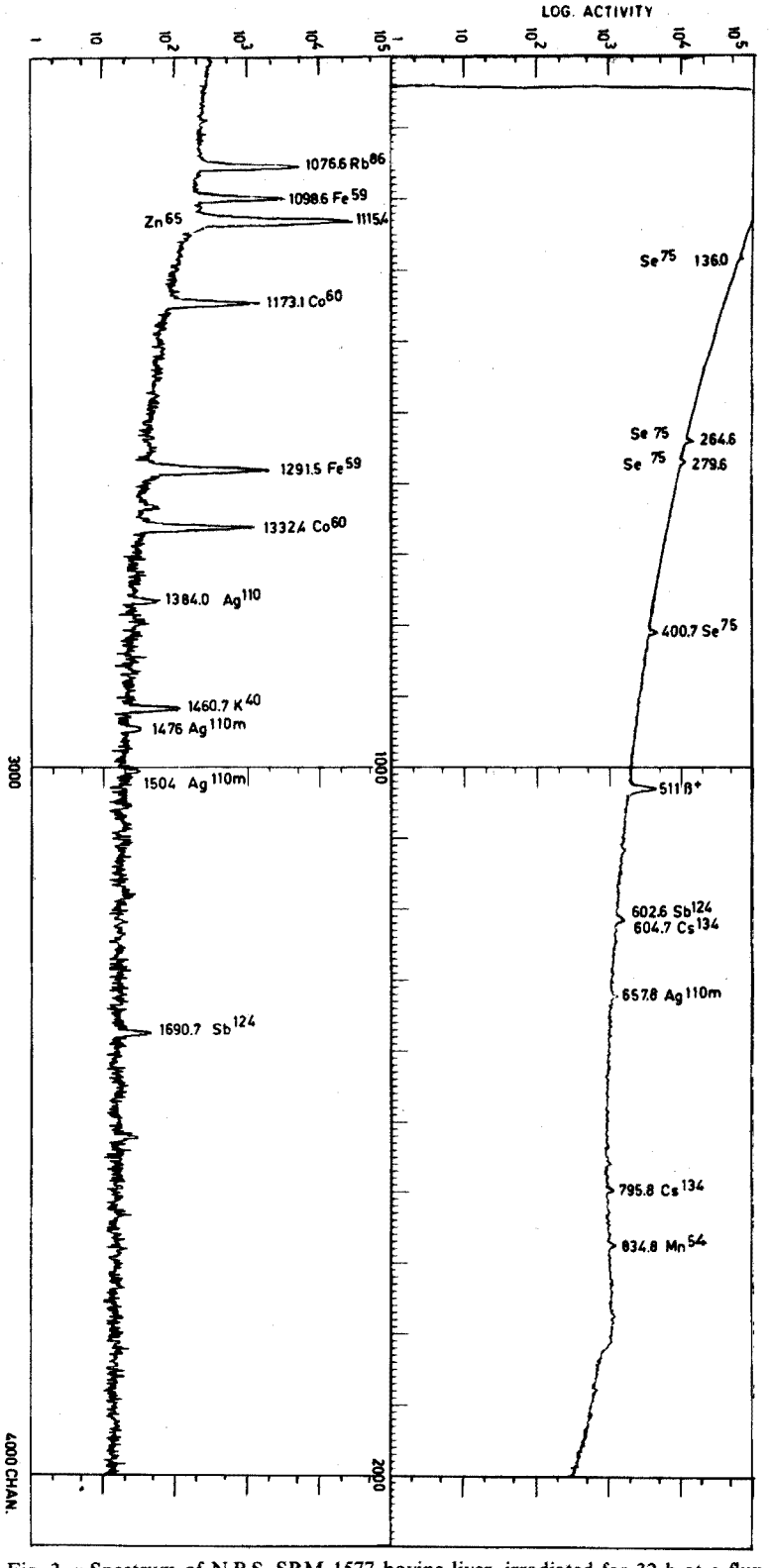

Fig. 3. γ-Spectrum of N.B.S. SRM 1577 bovine liver, irradiated for 32 h at a flux of $1.8 \cdot 10^{12}$ n cm^{-2} s^{-1}. Cooling period, 6 weeks.

the activities of each particular isotope *versus* the zinc activity were calculated (see Table III). After subtraction of the errors from counting statistics, the standard deviations appear to be entirely satisfactory.

COMPARISON WITH A STANDARD REFERENCE MATERIAL

To test the validity of the proposed standard, the bovine liver SRM 1577 of the National Bureau of Standards (Washington, U.S.A.) was analysed *versus* the serum standard by non-destructive neutron activation analysis. Before analysis the bovine matter was treated as suggested in the NBS specifications. The γ-spectrum is given in Fig. 3. The results are summarized in Table IV. It appears that there are no significant differences for the certified elements; there are, however, differences in the uncertified but estimated values of cobalt and silver. In addition, the concentrations of antimony and cesium could also be determined.

TABLE IV

TRACE CONTENTS OF N.B.S. SRM 1577 BOVINE LIVER—COMPARISON WITH THE RESULTS OBTAINED BY N.A.A. AND THE DOPED SERUM STANDARD

Element	*Content N.B.S. 95% confidence limit (p.p.m.)*	*Content n.a.a. with doped serum 95% confidence limit (p.p.m.)*[a]
	Certified values	
Zn	130 ±10	131.8 ± 6.5
Se	1.1± 0.1	1.13± 0.09
Rb	18.3± 1.0	18.7 ± 1.0
Fe	270 ±20	270 ±12
	Not certified	
Ag	(0.06)	0.091±0.026
Co	(0.18)	0.24 ±0.01
Sb	—	0.016±0.007
Cs	—	0.048±0.009

[a] Seven separate analyses were done.

The preparation procedure described for a multi-element serum standard proves to be very successful. The doped serum standard is satisfactorily homogeneous even for sample sizes as small as 20 mg. The standard yields very accurate results as demonstrated by the analytical results for the N.B.S. SRM 1577 bovine liver.

The authors acknowledge with gratitude the valuable technical assistance of Mr. L. Mees. They also thank the Inter-university Institute for Nuclear Sciences for financial support.

SUMMARY

A multi-element serum standard containing the elements Ag, Co, Cr, Cs, Fe,

Hg, Rb, Sb, Se and Zn, which is suitable for long irradiations at high neutron flux, is described. Tests showed that the homogeneity of the doped serum is satisfactory even for sample sizes of 20 mg. The accuracy obtainable with the proposed standard was demonstrated by analysis of the N.B.S. SRM 1577 bovine liver.

RÉSUMÉ

Une méthode de préparation d'un serum-étalon multi-élément est présentée. L'étalon contient les éléments Ag, Co, Cr, Cs, Fe, Hg, Rb, Sb, Se et Zn et se prête à des irradiations de longue durée à des flux de neutrons élevés. Le degré d'homogénéité est très satisfaisant, même à des prises d'échantillon de 20 mg. L'exactitude de l'étalon proposé est prouvée par l'analyse du foie bovin SRM 1577 du N.B.S.

ZUSAMMENFASSUNG

Es wird ein Serumstandard für mehrere Elemente beschrieben, der die Elemente Ag, Co, Cr, Cs, Fe, Hg, Rb, Sb, Se und Zn enthält und sich für lange Bestrahlungen bei hohem Neutronenfluss eignet. Kontrollen ergaben, dass die Homogenität des dotierten Serums sogar für Probenmengen von 20 mg zufriedenstellend ist. Die mit dem vorgeschlagenen Standard erreichbare Genauigkeit wurde durch Analyse der N.B.S. SRM 1577 Rinderleber belegt.

REFERENCES

1 J. Bartosek, G. Windels and J. Hoste, *Nucl. Instrum. Methods*, 103 (1972) 43.
2 J. Bartošek, J. Mašek, F. Adams and J. Hoste, *Nucl. Instrum. Methods*, 104 (1972) 221.
3 A. Wald, *Sequential Analysis*, Wiley, New York, 1947, Ch. 8.

Analytica Chimica Acta, 68 (1973) 11–24

DETERMINATION OF TRACE ELEMENTS IN COAL BY INSTRUMENTAL NEUTRON ACTIVATION ANALYSIS

C. BLOCK* and R. DAMS

Institute for Nuclear Sciences, Rijksuniversiteit Ghent, Ghent (Belgium)

(Received 2nd July 1973)

Although in recent years coal for home heating has been widely replaced by fuel oil, combustion of coal should still be considered as one of the major sources of air pollution in densely populated areas. Especially to the production of aerosols, combustion of coal contributes heavily.

According to Bertine and Goldberg[1], the total amount of coal and lignite burned on the globe amounted to $2.95 \cdot 10^9$ tons in 1970 while the amount of fossil fuel oil burned was $2.13 \cdot 10^9$ tons. The ash content of coal is, however, approximately two orders of magnitude larger than that of fuel oil. An estimated inventory from the same authors[1] indicates that for 29 elements out of a total of 34, the fly ash produced by coal combustion is more important than that produced by combustion of fuel oil. Therefore it seems important not only to study the gaseous emissions of coal combustion, but also the composition of fly ash. As a first approach to this problem a thorough analysis of the inorganic constituents of coal seems appropriate.

With a few exceptions[2], most analyses of coal described in the literature are limited to the determination of a few elements[3,4] usually based on analytical techniques which require the destruction of the sample[5,6]. This may introduce errors from reagent contamination or from loss of volatile elements. Non-destructive activation analysis, with 14-MeV neutrons, has been applied by several authors[7,8]. This technique is unfortunately limited to the determination of a few major constituents such as oxygen, silicon, aluminum and iron.

However, several minor and trace constituents, emitted as gases or as fly ash, become airborne and may represent a hazard to the environment. Since sensitive analyses of pollution aerosols recently proved the existence of a large variety of elements in airborne particulate matter[9,10], knowledge of the composition of fly ash is necessary in order to elucidate air pollution sources, atmospheric behaviour of the aerosols, and hazards of the fly ash.

Thus a selective, sensitive and preferably non-destructive multi-element method is needed for the determination of the inorganic constituents of coal. In this work, neutron activation analysis by means of Ge(Li) γ-spectrometry and computer-assisted data reduction were applied for the simultaneous determination of 43 elements in concentrations ranging from a few percent down to 1 p.p.b. for some elements. This instrumental approach is facilitated by the

* Research fellow of I.W.O.N.L.

low neutron cross-sections of the matrix elements carbon, oxygen and hydrogen.

In the present paper a detailed account is given of the applied procedure and its analytical possibilities.

EXPERIMENTAL

Apparatus

Samples were irradiated in the Thetis reactor of the University of Ghent. The γ-ray spectrometer system used, consists of a Princeton coaxial Ge(Li) detector (active volume 50 cm^3), a Princeton RG-10 preamplifier and an Ortec 450 amplifier. The detector is connected to an Intertechnique Didac-4000. The system resolution is 2.2 keV measured at the ^{60}Co 1332.4-keV photopeak with a peak-to-Compton ratio of 33/1. A gain setting of 1 keV/channel was applied.

The spectra were transferred on a TU-10 magnetic tape recorder, interfaced to the analyser by means of a PDP-11/20. Automatic data reduction was performed with a PDP-9 computer.

Preparation of the standards

The standards used were prepared to contain elemental concentrations approaching those encountered in an actual coal sample. In this way count rates of standards and samples were of the same magnitude and possible errors caused by coincidence-summing or broadening of peaks at high counting rates were minimized. For the elements present at levels approaching the detection limit, *e.g.* Zn, Ga, Mo, Cd, Ba, Se, W, Rb, Ag, somewhat larger amounts were added, in order to increase the precision on the counting statistics in the standard.

TABLE I

STANDARD SOLUTIONS FOR THE DETERMINATION OF ELEMENTS YIELDING SHORT-LIVED ISOTOPES

Solution number	*Element*	*Concn. ($\mu g\ ml^{-1}$) in the mixed solution*	*Concn. (μg) on the filter paper*
I	Al	100	20
	Cu	96.8	19.3
	Mg	2400	480
	Ca	5010	1000
	V	5.3	1.1
	In	0.32	0.65
	Na	250	51
	Dy	0.75	0.23
II	Cl	1008	202
	Br	64.9	13.0
	I	24.3	4.9
III	Mn	10.2	2.04
	Ti	1313	262
	S	—	40 mg

Aqueous solutions were prepared for all elements, either from the pure element, or from analytical-grade compounds. From these solutions, dilutions were prepared, the concentrations being determined by the half-lives of the isotopes used for detection and by possible chemical interactions.

The elements leading to short-lived isotopes were divided over three solutions containing, respectively: (I) Al, V, Cu, Mg, Na, Ca, In, Dy; (II) Cl, Br, I; (III) Ti, Mn. The metals (I, III) were dissolved in a dilute nitric acid solution. A separate alkaline solution was preferred for the halogens since an acidic medium leads to losses by evaporation. For Mn and Ti a separate solution was also preferred because the titanium solution contained sodium resulting from the sodium hydrogensulfate melt of titanium, and the large amount of magnesium present in solution I interfered with the determination of manganese. In the samples however, the magnesium activity is small compared to the manganese activity. The concentrations of the elements in these three solutions are given in Table I. Owing to the very low activation cross-section of sulfur, a relatively large amount of ammonium sulfate must be weighed and used as a sulfur standard.

The elements giving rise to long-lived isotopes were divided over two solutions. The first (IV) contained Zn, K, Hg, Ni, Fe, Co, Eu, Sm, As, Ce, Cu, Cr, La, Ga, Ag, Sc, Th, Se, Ba, Cd, Cs, Lu, Na, Yb, Hf, Rb and Ir in nitric acid; the second (V) contained Sb, Br, W, Au and Mo in slightly alkaline medium because these elements are either insoluble or volatile in acidic medium. The gold solution contained some chlorine and therefore could not be mixed with solution IV, as this would have caused the precipitation of silver and mercury. Table II shows the concentrations of the elements in solutions IV and V.

Small amounts (100–600 μl) of the described solutions (I–V) were spotted on a Whatman 41 filter paper, carefully dried and pressed into pellets of 25 mm diameter and 3 mm thickness. The concentrations for all elements, as present on the filter paper, are also given in Tables I and II.

Preparation of samples

The coal samples were pulverised and the powder was homogenized by shaking for a few hours. In order to irradiate and count the coal samples in the same geometry as the standards, weighed amounts of coal powder were wrapped in Whatman 41 filter paper and also pelletized. For short irradiations, 20–30 mg of coal were used; for the determination of long-lived isotopes, 70–200 mg were required.

Procedure

The method used for the non-destructive determination of 43 elements in coal samples consisted of two different irradiations and 3 or 5 γ-spectrometric measurements according to a procedure similar to that developed by Dams *et al.*[10] for the analysis of aerosols.

For the determination of the elements which give rise to short-lived isotopes, each coal sample was transferred with a pneumatic system to a position near the reactor core and irradiated during 5 min. The flux characteristics at the irradiation site were as follows[11]: thermal flux, $2.6 \cdot 10^{12}$ n cm^{-2} s^{-1}; epithermal flux, $1.1 \cdot 10^{11}$ n cm^{-2} s^{-1}; fast flux, $6.5 \cdot 10^{11}$ n cm^{-2} s^{-1}.

TABLE II

STANDARD SOLUTIONS FOR THE DETERMINATION OF ELEMENTS GIVING RISE TO LONG-LIVED ISOTOPES

Solution number	*Element*	*Concn. ($\mu g\ ml^{-1}$) in the mixed solution*	*Concn. (μg) on the filter paper*
IV	Zn	2000	400
	K	1000	206.8
	Hg	24.7	4.8
	Ni	400	80
	Fe	7200	1.44
	Co	8.7	1.74
	Eu	0.8	0.16
	Sm	2.0	0.41
	As	40.5	8.1
	Ce	39.9	8.0
	Cu	65.0	13.0
	Cr	64.0	12.8
	La	8.0	1.6
	Ga	20.7	2.14
	Ag	10.1	2.0
	Sc	0.8	0.16
	Th	2.16	0.43
	Se	25.2	5.0
	Ba	800	320
	Cd	156.8	27.2
	Cs	7.6	1.52
	Lu	0.9	0.2
	Na	296.5	59.4
	Yb	41	4.1
	Hf	56.6	5.6
	Ir	0.6	0.06
	Yb	645	64.5
V	Sb	80	8.0
	Br	110	11.0
	W	7.3	0.73
	Au	1.16	0.11
	Mo	376	37.6

3 min after irradiation the sample was counted for 6 min (count I). As the intense ^{28}Al activity made the measurement of longer-lived isotopes difficult, a second measurement of 20 min was started after a 15-min cooling time (count II). These two counts generally allowed the determination of the following elements: Al, S, Ca, Ti, V, Cu, Na, Mg, Mn, Cl, Br, In, I, Dy. Table III lists the isotopes and γ-ray energies used for the determination of these 14 elements.

Figure 1 shows a γ-ray spectrum obtained as described for count II. The multi-element standards described above were subjected to the same irradiation and counting scheme. Since subsequent measurements of standards and samples were not possible, because of the short half-lives of some isotopes, standards and samples were irradiated separately. Variations in rabbit placement

TABLE III

NUCLEAR DATA OF SHORT-LIVED ISOTOPES[a] WITH TYPICAL CONCENTRATIONS AND DETECTION LIMITS

Element	*Isotope*	*Half-life*	*γ-Energy used (keV)*	*Concn. ranges in home-heating coals (p.p.m.)*	L_D *(p.p.m.)*	
					1st method	*2nd method*
Na	^{24}Na	15 h	1368.6; 2754.1	470–200	60	150
Mg	^{27}Mg	9.5 min	1014.1	2500–1500	390	900
Al	^{28}Al	2.3 min	1778.9	10000–6500	13	20
S	^{37}S	5.1 min	3102.4	20000–8000	13000	—
Cl	^{38}Cl	37.3 min	1642.0; 2166.8	1500–300	160	210
Ca	^{49}Ca	8.5 min	3083.0	1900–900	480	1400
Ti	^{51}Ti	5.8 min	320.0	300–100	110	130
V	^{52}V	3.8 min	1434.4	30–10	1.1	1.1
Mn	^{56}Mn	2.58 h	846.8; 1810.9	60–25	1.0	1.0
Cu	^{66}Cu	5.1 min	1039.0	40–15	58	52
Br	^{80}Br	18 min	617.0	40–5	2.8	9
In	^{116m}In	54 min	417.0; 1293.3	0.03–0.01	0.015	0.09
I	^{128}I	25 min	442.7	4–1	0.9	4
Dy	^{165}Dy	2.3 h	94.7; 361.5	1.1–0.5	0.1	0.5

[a] See ref. 12.

and flux were then corrected by means of a flux monitor irradiated simultaneously with each standard and sample. This flux monitor, a small piece of titanium, was counted for 30 s, 12 min after irradiation. Owing to the short half-life of the ^{51}Ti isotope (5.1 min), the same monitor could be used for subsequent analyses. Conversion factors for all elements were calculated from the irradiated standard samples. These conversion factors were constants and once determined, they could be used as long as irradiations and countings were performed in the same circumstances.

A shorter method which took only half of the time of the preceding one was also used. This method consisted of only one sample measurement for 8 min after 5-min irradiation and 6-min cooling. The titanium flux monitor was replaced by an aluminum monitor which was counted for 60 s, 3 min after irradiation. A complete irradiation-counting cycle thus required only about 22 min. The sensitivity and precision for the elements Na, Cl, Mn, Br, In, I, Dy obtained with this procedure were lower than those obtained with the second count of the longer procedure owing to the superposition of almost all photopeaks on the high ^{28}Al Compton continuum.

For the determination of the elements giving rise to long-lived isotopes, samples and standards were irradiated during 7 h at an irradiation site with the following flux characteristics[11]: thermal flux, $1.6 \cdot 10^{12}$ n cm^{-2} s^{-1}; epithermal flux, $6.5 \cdot 10^{10}$ n cm^{-2} s^{-1}; fast flux, $2.6 \cdot 10^{11}$ n cm^{-2} s^{-1}. A first 15-min measurement, 1 day after irradiation (count III) was followed by a 1-h count after a 20-day cooling period (count IV), allowing the determination of K, Na, Cu, Ga, As, Br, Mo, Cd, La, Sm, W, Au (count III) and Sc, Fe, Co, Ni, Se, Rb, Ag, Cs, Ce, Cr, Lu, Hf, Ir, Hg, Th (count IV). A few elements, namely

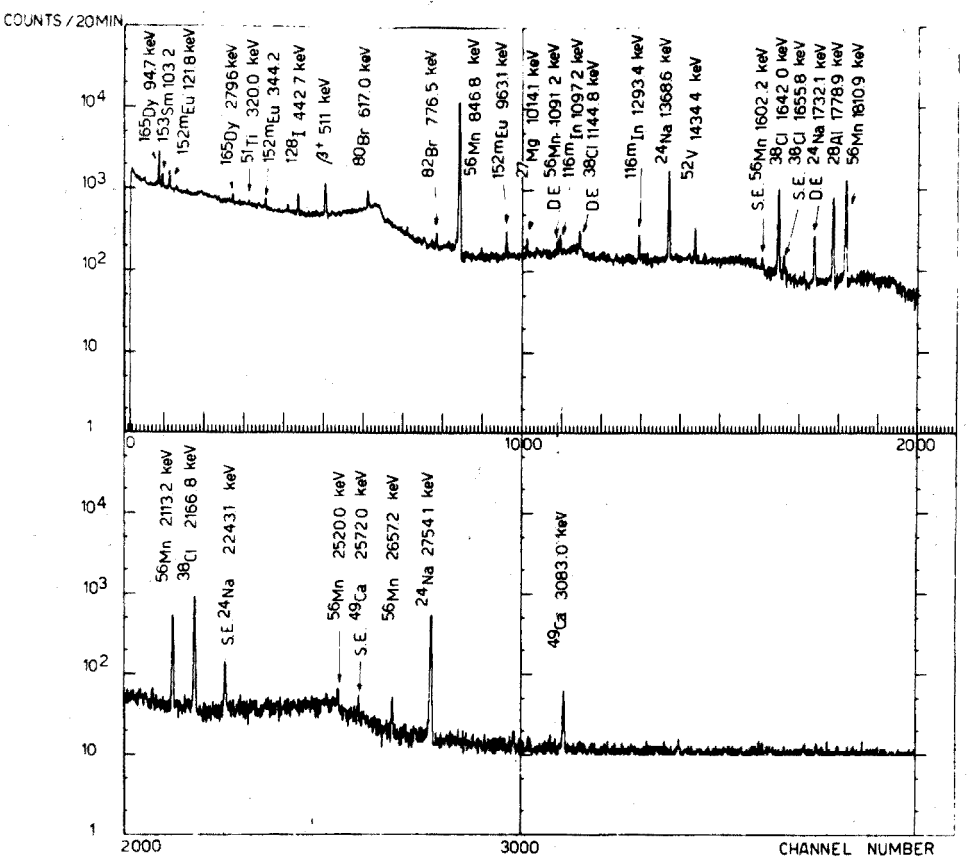

Fig. 1. Spectrum of neutron-activated coal sample. $T_{irr} = 5$ min; $T_{cool} = 15$ min; $T_{meas} = 20$ min.

Zn, Sb, Ba, Eu, Yb, were determined in counts III and IV, by means of different isotopes. Table IV lists the isotopes, with half-lives and γ-ray energies, measured in counts III and IV.

In count III, the ^{24}Na activity was generally predominant but still allowed the determination of some 15 other elements. However, especially for the determination of longer-lived isotopes, such as Br, Sb, La, Sm, Yb and Au, it was sometimes preferable to count the sample again 4–7 days after irradiation, when the ^{24}Na activity had decayed.

Figure 2 shows a γ-ray spectrum obtained from a 7-h irradiation and a 1-h measurement after 20 days' cooling time. Photopeaks of 16 isotopes can be recognised.

Standards and 10–15 samples were irradiated simultaneously in a polyethylene tube. It was consequently necessary to correct the results for the axial flux gradient in the rabbit.

The spectra were recorded on a TU-10 interfaced with the analyser by means of a PDP-11, and subsequently processed with a PDP-9 computer. The program used consisted of the following steps: photopeaks were identified, and

TABLE IV

NUCLEAR PROPERTIES OF LONG-LIVED ISOTOPES[a] WITH TYPICAL CONCENTRATIONS AND DETECTION LIMITS

Element determined	*Isotope*	*Half-life*	*γ-Energy used (keV)*	*Concn. ranges in home-heating coals (p.p.m.)*	L_D *(p.p.m.)*
Na	^{24}Na	15 h	1368.6	470–200	9
K	^{42}K	12.5 h	1524.7	1500–50	34
Cu	^{64}Cu	12.8 h	β^+	40–15	2.5
Zn	^{69m}Zn	13.9 h	438.7	100–20	50
Ga	^{72}Ga	14.0 h	834.1	2.8–1.4	1.0
As	^{76}As	26.5 h	559.1; 659.0; 1216.3	6–0.3	0.8
Br	^{82}Br	35.5 h	619.0; 776.5	40–5	3.2
Mo	^{99}Mo	66.7 h	140.3	<20	16
Cd	^{115}Cd	54 h	527.7	<40	100
Sb	^{122}Sb	67.2 h	564.0	1.7–0.5	0.5
Ba	^{135m}Ba	28.7 h	268.1	250–90	200
La	^{140}La	40.2 h	487.0; 1596.2	10–4	0.4
Sm	^{153}Sm	47 h	103.2	2.8–1.1	0.07
Eu	^{152m}Eu	9.3 h	963.1	0.9–0.3	0.06
Yb	^{175}Yb	4.28 h	396.1	0.8–0.2	0.2
W	^{187}W	23.8 h	479.5; 685.7	0.9–0.2	0.7
Au	^{198}Au	64.6 h	411.8	0.05–0.02	0.03
Sc	^{46}Sc	84 d	889.2; 1120.5	4–2	0.02
Cr	^{51}Cr	27.8 d	320.1	17–5	0.8
Fe	^{59}Fe	45 d	1099.3; 1291.6	4000–500	240
Co	^{60}Co	5.25 y	1173.2; 1332.4	12–7	0.8
Ni	^{58}Ni	71.3 d	810.8	50–20	60
Zn	^{65}Zn	244 d	1115.5	<900	210
Se	^{75}Se	120.4 d	264.6; 400.6	1.5–0.6	1.3
Rb	^{86}Rb	18.7 d	1076.6	4.7–1.0	3
Ag	^{110m}Ag	253 d	657.6; 937.3	1.2–0.5	1.0
Sb	^{124}Sb	60.3 d	602.7; 1691.0	1.7–0.5	0.2
Cs	^{134}Cs	2.05 y	795.8	0.3–0.03	0.1
Ba	^{131}Ba	12 d	216.0	250–40	90
Ce	^{141}Ce	33 d	145.4	20–5	0.9
Eu	^{152}Eu	12.4 y	964.2; 1408.1	0.8–0.2	0.05
Yb	^{169}Yb	32 d	177.0; 197.8	0.8–0.2	0.2
Lu	^{177}Lu	6.7 d	208.4	0.09–0.05	0.05
Hf	^{181}Hf	42.5 d	482.0	0.5–0.2	0.2
Ir	^{192}Ir	74 d	468.0	0.010–0.004	0.006
Hg	^{203}Hg	46.6 d	279.2	1.9–0.4	0.6
Th	^{233}Pa	27.4 d	311.9	1.2–0.5	0.2

[a] See ref. 12.

peak areas were calculated by subtraction of a generated baseline and converted to isotope weights by comparison to standard peak intensities. After corrections for interferences, decay, flux variation in the irradiation container, and subtraction of filter paper blanks, concentrations and their standard deviations were obtained in p.p.m. in the coal samples.

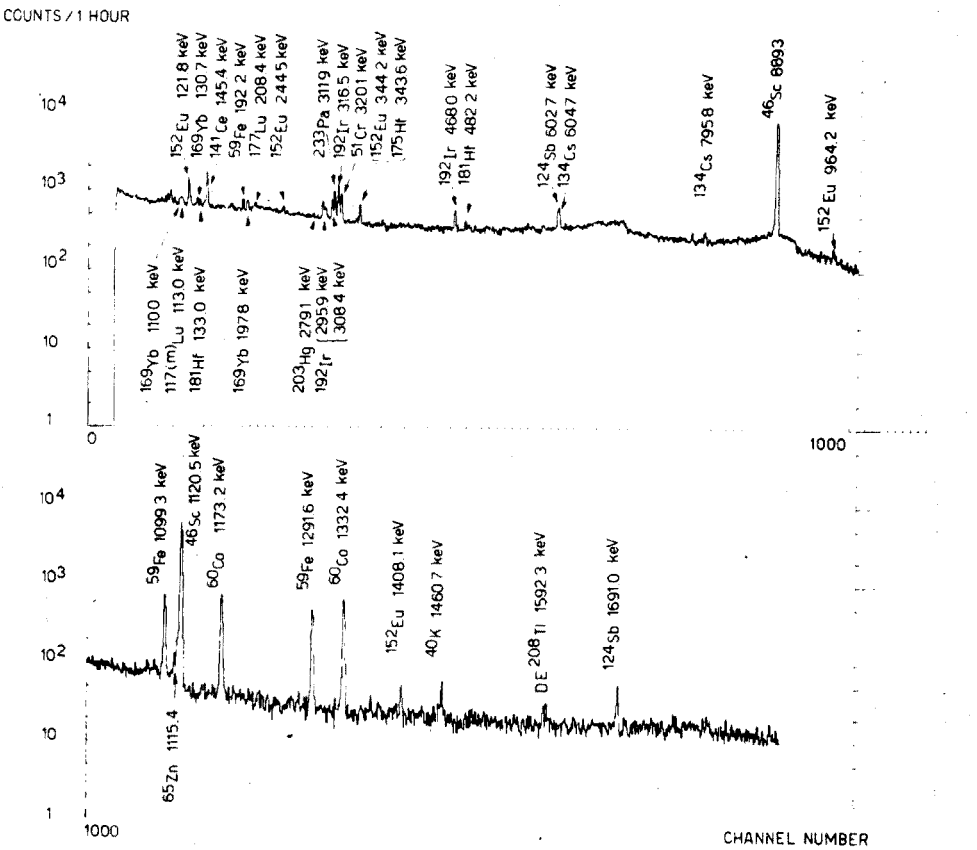

Fig. 2. Spectrum of neutron-activated coal sample. $T_{irr} = 7$ h; $T_{cool} = 20$ days; $T_{meas} = 1$ h.

Interferences

A few nuclear and spectrometric interferences must be taken into account.

The $^{27}Al(n,p)^{27}Mg$ reaction is known to interfere with the determination of magnesium. Aluminum (1 mg) was found to produce a ^{27}Mg activity equivalent to 0.20 mg of magnesium in the irradiation conditions used. The influences of other possible threshold reactions were calculated and checked. For the concentration ranges present in coal samples, they were found to cause errors smaller than 1%.

The measurement of ^{64}Cu (511-keV peak) is of course subject to interference from pair-production by high energy radiation, especially from ^{24}Na. A correction of *ca.* 15%, determined from a pure ^{24}Na spectrum, was applied. The influence of other highly energetic γ-rays in the spectrum of count III was very small.

A correction was also necessary for the determination of the count rate of the isotope ^{203}Hg, as its only photopeak (279.2 keV) is affected by the 279.6-keV photopeak of ^{75}Se. The interference was *ca.* 10% for the ^{203}Hg activity in coal samples.

Owing to the complexity of the spectrum, a number of high intensity peaks were unresolved. Other isotopes or interference-free peaks of the same isotope were then used; this was the case for the determination of the following isotopes: ^{27}Mg, ^{76}As, ^{122}Sb and ^{65}Zn.

Interfering isotopes and energies are summarized in Table V. This Table also contains the energies used for the determination of the above-mentioned elements. ^{51}Cr and ^{233}Pa were still determined from their main photopeak, because these isotopes have no other high-intensity γ-transitions.

TABLE V

INTERFERING ISOTOPES AND ENERGIES, AND ENERGIES USED FOR DETERMINATION

Isotope	*Energy of main peak (keV)*	*Interfering isotope*	*Energy of interfering isotope (keV)*	*Energy used (keV)*
^{27}Mg	844.0	^{56}Mn	846.9	1014.1
^{76}As	559.2	^{82}Br	554.3	657.0; 1216.3
^{122}Sb	564.0	^{76}As	559.2	1691.0; 795.8 (^{124}Sb)
^{65}Zn	1115.4	^{46}Sc	1120.3	438.7 (^{69m}Zn)
^{51}Cr	320.0	^{192}Ir	316.5	320.0
^{233}Pa	311.8	^{192}Ir	308.4; 316.5	311.8

RESULTS AND DISCUSSION

Tables III and IV list the concentration ranges encountered in 15 Belgian coal samples used for home heating together with the detection limits L_D calculated for a typical sample according to Currie's definition[13]. The detection limits are seen to be several times lower than the actual concentrations for most elements. For 10 elements, namely S, Zn, Ga, Mo, Cd, Ba, Se, W, Rb, Ag, the concentrations were slightly below the detection limits, while the Ti, In, Au, Ni, Cs, Ir concentrations were also often near the detection limit. It must, however, be borne in mind that these detection limits for instrumental neutron activation analysis depend on the composition of the sample and that they consequently will be different for each sample. Nevertheless, the figures listed in Tables III and IV may be considered as typical.

Table III also includes a comparison between detection limits for the two methods used for the determination of short-lived isotopes. The first method appears clearly to be more sensitive for all elements, except Ti, V, Mn, Cu, where the experimental detection limits are approximately the same for both methods. This is further illustrated in Table VI where results obtained for one coal sample after application of both methods, are summarized. All results agree within the standard deviations based on counting statistics, but the first method allows the determination of all elements with a better precision. This is due to the high ^{28}Al activity in the spectrum of the short method, resulting in a high Compton continuum, whereas in count II of the first method, ^{28}Al has already largely decayed, and other isotopes do not increase the Compton continuum

TABLE VI

COMPARISON BETWEEN TWO DIFFERENT PROCEDURES FOR THE DETERMINATION OF SHORT-LIVED ISOTOPES

Element determined	*1st method (p.p.m.) (Ti flux monitor)*	*2nd method (p.p.m.) (Al flux monitor)*
Na	200±30	220±40
Mg	1220±190	1120±380
Al	6420±160	6670±280
Cl	825±45	875±90
Ca	760±160	1100±640
V	18.0±0.6	18.0±0.9
Ti	170±45	145±50
Mn	77.7±3.0	76.9±2.9
Cu	40±20	27±23
Br	22±1.5	19±4
In	0.02±0.01	0.03±0.03
I	2.9±1.0	3.4±1.5
Dy	1.10±0.05	0.9±0.2

appreciably. Obviously the eventual choice will depend on whether speed or accuracy is judged to be the most important feature.

Reproducibility of irradiations and measurements, together with the homogeneity of the samples was carefully investigated. Table VII presents concentrations for a few representative elements (short-lived isotopes) determined in five replicate analyses of a single pellet. The overall experimental precision appears to be better than 10% for most elements and is mainly determined by counting statistics. The spread between different results is small for elements with good statistics (V, Mn, Al) while the large standard deviations for Mg, Ca, Ti are due to the limited number of counts under the respective photopeaks.

In instrumental activation analysis of samples, with multi-element standards, the complexity of the resulting γ-ray spectra may lead to erroneous results, when

TABLE VII

RESULTS OF FIVE REPLICATE ANALYSES OF A COAL SAMPLE (p.p.m.)

Element						S_r (%) *based on count. statist.*	*Mean*	S_r (%) *on the sample mean*
Al	6670±170	6420±170	6500±160	6110±180	6250±190	2.6	6390	3.4
Mg	1250±190	1420±200	1100±190	1480±200	1050±190	15	1260	15
Na	180±16	162±15	204±17	174±16	120±15	8.7	183	8.2
Cl	1100±75	890±65	1000±60	880±70	920±70	7.2	960	9.4
V	18.1±0.9	17.9±0.6	19.6±0.7	16.6±0.6	17.8±0.7	3.9	18.0	6.1
Ti	245±45	270±45	200±50	220±40	190±45	20	225	15
Mn	47.1±1.6	46.5±1.5	47.8±1.5	48.9±1.7	45.5±1.6	3.4	47.2	3.0
Ca	660±100	760±120	580±100	840±90	610±110	14	690	16
Br	19.4±1.5	20.2±1.5	18.7±1.6	17.0±1.4	17.5±1.3	9.5	18.6	7.5

TABLE VIII

REPLICATE ANALYSES OF THE SAME SAMPLE WITH 7 DIFFERENT STANDARDS

Element	*Standard*							*Mean* ± *s.d.*	*S*, *(%)*
	1	*2*	*3*	*4*	*5*	*6*	*7*		
K	17730 ± 230[a]	16200 ± 1120	16480 ± 290	15990 ± 760	17600 ± 300	16860 ± 670	15880 ± 350	16700 ± 700	4.2
Sb	5.0 ± 0.8	4.5 ± 0.6	5.5 ± 0.4	5.9 ± 0.4	4.9 ± 0.6	5.6 ± 0.1	4.8 ± 0.8	5.2 ± 0.5	9.6
La	32.4 ± 1.6	29.2 ± 3.7	32.3 ± 1.3	28.3 ± 3.2	31.7 ± 1.7	32.4 ± 1.3	29.7 ± 1.0	30.1 ± 1.0	5.9
Ga	17.6 ± 2.9	14.3 ± 5.1	19.3 ± 4.0	24.2 ± 11.6	3.7 ± 2.3[b]	21.2 ± 1.5	18.2 ± 3.0	19.1 ± 3.5	18
Sc	15.4 ± 0.2	16.9 ± 0.2	15.9 ± 0.2	16.1 ± 0.2	16.4 ± 0.2	16.3 ± 0.2	15.3 ± 0.2	16.0 ± 0.5	3.1
Fe	19600 ± 220	21300 ± 270	20130 ± 260	19030 ± 240	20970 ± 270	21250 ± 270	19870 ± 230	20310 ± 870	4.3
Cu	37.4 ± 2.5	45.9 ± 2.5	35.2 ± 2.6	39.6 ± 2.4	46.3 ± 5.7	43.0 ± 3.2	34.1 ± 6.3	40.2 ± 4.9	12
Cl	89.0 ± 1.3	92.7 ± 1.5	87.4 ± 1.3	93.8 ± 1.5	93.6 ± 1.6	89.9 ± 1.4	89.0 ± 1.1	90.1 ± 2.5	2.8
Co	18.6 ± 0.3	20.2 ± 0.4	19.0 ± 0.3	19.5 ± 0.3	20.3 ± 0.4	20.1 ± 0.4	18.7 ± 0.3	19.3 ± 0.8	4.1
Ba	600 ± 160	390 ± 140	830 ± 180	330 ± 180	730 ± 170	500 ± 150	500 ± 150	550 ± 180	33

[a] Concentrations are given in p.p.m.
[b] Not used in calculation of the mean.

the composition of the standard samples is strongly different from the unknowns. This was checked by analysing one sample with seven different standards, all with the same elements present but in concentration ratios varying from the lower to the higher limits found in actual samples. Results for a few elements are given in Table VIII. For almost all elements, the results agree except for those with very low intensities in some standard spectra. The best example is the gallium concentration in standard 5.

For copper, the experimental error was also found to be larger than that expected from counting statistics. This is, of course, due to the interference on the 511-keV photopeak by highly energetic γ-rays of other isotopes. As already mentioned, only the interference due to ^{24}Na was taken into account for the determination of copper. However, when the standards contained high concentrations of other elements yielding highly energetic isotopes, such as lanthanum and potassium, the contribution of their isotopes to the 511-keV photopeak should also be taken into account. Generally, it may be concluded, as is shown in Table VIII, that the error resulting from the complexity of the γ-ray spectra is small compared to the statistical error, even when a standard is used with a composition which differs to a considerable extent from the samples.

TABLE IX

HOMOGENEITY OF 5 DIFFERENT SAMPLES

(All results are given in p.p.m.)

Element	*Sample*					*S_r (%) based on count. statist.*	*Mean*	*S_r (%) on sample m*
	1	*2*	*3*	*4*	*5*			
K	640±20	640±18	650±19	630±18	650±19	2.9	640	1.6
Na	208.2±3.8	218.8±3.9	210.0±3.6	209.6±3.4	212.1±3.2	1.7	211.3	2.1
Cu	23.1±1.5	21.3±1.5	22.3±1.4	24.9±1.0	24.5±1.3	5.8	23.2	6.4
La	6.3±0.2	5.9±0.3	6.1±0.2	6.3±0.3	6.0±0.2	3.9	6.1	3.3
Sm	1.66±0.03	1.59±0.03	1.62±0.03	1.64±0.03	1.60±0.03	1.9	1.62	1.9
Sc	2.39±0.04	2.57±0.04	2.53±0.04	2.60±0.04	2.43±0.04	1.5	2.50	3.6
Fe	2630±70	2490±70	2860±70	2850±70	2630±80	2.6	2690	5.3
Co	7.3±0.3	7.7±0.2	7.1±0.2	7.1±0.2	7.5±0.3	3.2	7.3	4.1
Sb	0.64±0.09	0.65±0.09	0.68±0.09	0.69±0.09	0.64±0.09	13	0.66	3.0
Ce	9.2±0.4	8.7±0.4	9.5±0.4	9.2±0.4	9.1±0.4	4.3	9.1	3.2
Ba	32±23	29±24	12±26	15±23	33±21	90	26	50
Hf	0.44±0.08	0.46±0.08	0.38±0.08	0.37±0.07	0.40±0.07	18	0.41	10

The homogeneity of the samples was checked by analysing five different samples of the same coal. Typical results for a few elements are given in Table IX. The spread of the results is in agreement with the statistical error. Only for Na, Sc, Co and Fe, which have very good counting statistics, do smaller contributions, such as differences in counting geometry, become determining factors for the overall uncertainty. Thus no obvious inhomogeneity of the samples was detected.

CONCLUSION

Instrumental neutron activation analysis is well suited for the determination of most inorganic constituents of coal samples. Its sensitivity is adequate to allow the determination of 43 elements in concentrations for some elements down to 1 p.p.b. Even a 22-min irradiation and counting scheme suffices for the determination of 14 elements. The absence of any chemical treatment eliminates many possible sources of errors. A study of the precision showed that errors resulting from variation in irradiation and counting conditions are small compared to errors caused by counting statistics. Differences between sample and standard composition do not introduce significant errors and inhomogeneity of the samples was not found. The standard deviation resulting from counting statistics can thus be considered as a good approximation of the overall standard deviation.

Thanks are due to Prof. J. Hoste for the interest taken in this investigation. This research was sponsored in part by the "Nationaal Centrum voor de Studie van Luchtverontreiniging door Verbranding". One of us (C.B.) also expresses her gratitude to the I.W.O.N.L. for financial support.

SUMMARY

A completely instrumental neutron activation analysis, with Ge(Li) γ-spectrometry and computer-assisted data reduction, has been developed for the measurement of more than 40 elements in coal samples. Two neutron irradiations and 3–5 γ-spectrometric measurements are performed for each sample. Sensitivity and reproducibility of the analysis and homogeneity of the samples have been investigated. The overall standard deviation for nearly all elements is determined by the counting statistics.

RÉSUMÉ

Une analyse par activation neutronique, entièrement instrumentale, avec spectrométrie γ-Ge(Li) et ordinateur est proposée pour le dosage de plus de 40 éléments dans des échantillons de charbon. Deux irradiations neutroniques, et 3 à 5 mesures spectrométriques-γ sont effectuées pour chaque échantillon. On examine la sensibilité et la reproductibilité de l'analyse, de même que l'homogénéité des échantillons. La déviation standard totale pour presque tous les éléments est déterminée par des statistiques de comptage.

ZUSAMMENFASSUNG

Eine vollständig instrumentelle Neutronenaktivierungsanalyse mit Ge(Li)-γ-Spektrometrie und computerunterstützter Auswertung wurde für die Bestimmung von mehr als 40 Elementen in Kohleproben entwickelt. Es werden zwei Neutronenbestrahlungen und 3–5 γ-spektrometrische Messungen für jede Probe durchgeführt. Empfindlichkeit und Reproduzierbarkeit der Analyse sowie die Homogenität der Proben wurden untersucht. Die Gesamt-Standardabweichung für nahezu alle Elemente wird durch die Zählstatistik ermittelt.

REFERENCES

1 K. K. Bertine and E. D. Goldberg, *Science*, 173 (1971) 233.
2 R. Brown, M. L. Jacobs and H. E. Taylor, *Intern. Lab.*, Jan.–Feb. (1973) 32.
3 H. J. Gluskoter and R. R. Ruch, *Fuel*, 50 (1971) 65.
4 A. E. Vasilevskaya and V. P. Shcherbakov, *Zh. Anal. Khim.*, 19 (1964) 1200.
5 R. F. Abernethy and F. H. Gibson, *U.S., Bur. Mines, Rep. Invest., RI 7184*, 1968.
6 S. Tardon and M. Balcarkovâ, *Chem. Listy*, 60 (1966) 334.
7 J. C. Martin and S. C. Mathur, *Report TID-18883, Contract AT 2980*, February 27, 1963, p. 40.
8 R. Kurosowa, *J. Mining Metallurgy*, 84 (1968) 101.
9 W. H. Zoller and G. E. Gordon, *Anal. Chem.*, 42 (1970) 256.
10 R. Dams, J. A. Robbins, K. A. Rahn and J. W. Winchester, *Anal. Chem.*, 42 (1970) 861
11 W. Maenhaut, personal communication.
12 H. H. Pagden, G. J. Pearson and J. M. Bewers, *J. Radioanal. Chem.*, 8 (1971) 127.
13 L. A. Currie, *Anal. Chem.*, 40 (1968) 586.

Analytica Chimica Acta, 68 (1974) 25–30

DETERMINATION OF NICKEL IN ROCKS AFTER EPITHERMAL NEUTRON ACTIVATION

E. STEINNES

Institutt for Atomenergi, Isotope Laboratories, Kjeller (Norway)

(Received 11th June 1973)

Nickel is not among those elements which show extremely high sensitivity in neutron activation analysis. In spite of this fact, several authors have described methods for the determination of nickel in geological material based on this analytical technique. Procedures based on 2.58-h ^{65}Ni with radiochemical separations have been reported for application to meteorites[1,2], tektites[3], rocks and marine sediments[2], and lunar materials[4]. These procedures are rather lengthy and may often involve handling of samples of high radioactivity which arises mainly from ^{56}Mn and ^{24}Na. Fisher and Currie[5] made nickel determinations without radiochemical separation, using NaI(Tl) γ-spectrometry for measurement of the 1481-keV peak, in meteorites at the 1% level. Extension of this determination to the p.p.m. level[6] with a Ge(Li) detector and Compton suppression turned out to be difficult (see Table II).

The reaction ^{58}Ni(n,p)^{58}Co, although even less sensitive than the ^{64}Ni(n,γ)-^{65}Ni reaction, has also been used to some extent. Morgan and Ehmann[7] were able to make useful determinations on chondritic meteorites, using multiparameter coincidence spectrometry, but did not analyze samples with nickel contents in the p.p.m. range. Turekian and Kharkar[8] and Wänke *et al.*[9] used radiochemical separations for the isolation of ^{58}Co–^{60}Co from irradiated lunar rocks. This approach becomes difficult at high Co/Ni ratios because of the high activation cross-section of ^{59}Co for thermal neutrons.

Perhaps the most promising method of purely instrumental activation analysis for nickel in rocks reported so far is that by Schmitt *et al.*[10], who used 28-MeV bremsstrahlung from an electron linear accelerator to produce 36.0-h ^{57}Ni.

Advantage of epithermal activation

The epithermal irradiation technique involving activation within a suitable cadmium cover for the exclusion of thermal neutrons, may be useful in reactor activation analysis if reactions induced by resonance or fast neutrons are to be employed. In the case of fast-neutron induced reactions, the interference from an (n,γ) reaction is reduced by a factor equal to the cadmium ratio of the interfering nuclide in the irradiation position involved[11]. Several major long-lived nuclides induced in silicate rocks upon reactor neutron activation show comparatively low activation by resonance neutrons[12], hence it is evident that the feasibility of nickel determination in rocks by purely instrumental reactor activation

analysis based on the $^{58}Ni(n,p)^{58}Co$ reaction, should be considerably improved by introducing the epi-cadmium irradiation technique. In a reactor position with a neutron energy distribution corresponding to a cadmium ratio of 3.0 for ^{197}Au, the advantage to be gained with respect to ^{46}Sc and ^{59}Fe would be 74 and 31, respectively, if a cadmium cover is employed. Similarly, if a radiochemical separation of cobalt is used, the $^{58}Co/^{60}Co$ ratio which is a limiting factor in that case, would be about 16 times higher than without cadmium.

During work in the author's laboratory with lunar samples[13] from Apollo 14 and subsequent missions, it became evident that nickel could be determined instrumentally after epithermal activation, to a precision of about ± 5–10% in samples with concentrations exceeding 100 p.p.m. The purpose of the work described in the present paper was to extent this method down to lower concentration levels in order to see how good determinations could be performed either by purely instrumental analysis or with radiochemical separation of ^{58}Co–^{60}Co. An additional goal was to attempt a contribution to the improvement of nickel data on the U.S. Geological Survey standard silicate rocks.

EXPERIMENTAL

Irradiation

Rock samples of about 100 mg, wrapped in 30 mm × 30 mm sheets of aluminium foil, were irradiated in cylindrical cadmium boxes of 1.0 mm thickness, 20 mm internal diameter and 10 mm internal height. The irradiations were performed for 7 days in the JEEP II reactor (Kjeller, Norway) in a vertical irradiation channel inside the core where the thermal neutron flux was about $2 \cdot 10^{13}$ n cm^{-2} s^{-1}, the cadmium ratio of ^{197}Au was 1.7 and the fast neutron flux was about 10% of the thermal flux.

In an initial run the ultramafic standard rocks DTS-1 and PCC-1 were analyzed against nickel standards prepared by evaporating aliquots of a solution of appropriate concentration on sheets of aluminium foil. In the subsequent work, DTS-1 was used as standard. This should help to minimize systematic errors which may occur when samples and standards of slightly different shape are subjected to measurements close to a Ge(Li) detector.

Activity measurements

After 3 weeks' delay, the γ-activities were measured by means of a coaxial Ge(Li) detector system connected to a 2000-channel analyzer, with a conversion factor of 1 keV/channel.

The energy resolution at 1332 keV was 2.5 keV FWHM, and the full-energy peak efficiency at the same energy was 5% at 25 cm distance, compared to a 3″ × 3″ NaI(Tl) detector. Counting periods of 30–120 min were used, except for samples of G-2 and GSP-1, in which case 300-min counting was applied. Compensation for dead-time losses was accomplished by means of a precision pulse generator as proposed by Anders[14]. Peak areas were calculated by the method of Sterlinski[15], and the 811-keV γ-ray of ^{58}Co was made the basis for the analyses.

Radiochemical separation

In order to see whether an isolation of ^{58}Co–^{60}Co from the other activities present would result in improved data, a radiochemical separation based on anion exchange[16] was carried out after the end of the γ-spectrometry measurements. For this purpose, the rock samples and DTS-1 monitors were transferred to 100-ml teflon beakers containing 5 ml of concentrated hydrofluoric acid, 5 ml of concentrated nitric acid and 10 mg of cobalt carrier. After evaporation of the solution to dryness on a hot plate, an additional 5 ml of concentrated hydrofluoric acid was added, and the mixture was evaporated to dryness again. The residue was dissolved in 10 ml of 9 *M* hydrochloric acid and 1 ml of 2% boric acid solution, and the solution was allowed to stand for at least 2 h. The solution was then passed through a column of Dowex 1-X8 (100–200 mesh, Cl^--form; 85 ± 5 mm bed height; 10 mm internal diameter) pre-equilibrated with 9 *M* hydrochloric acid. A flow-rate of *ca.* 0.5 ml min^{-1} was used. The column was subsequently washed with four 5-ml portions of 9 *M* hydrochloric acid. Cobalt was then eluted with four 5-ml portions of 4 *M* hydrochloric acid. The eluates were collected in 100-ml polyethylene screwcap bottles and subjected to γ-spectrometry in the same manner as described above.

The chemical yield of cobalt by the use of this procedure is about 98%, and no activities apart from that of the cobalt isotopes are contained in the isolated fractions, with the exception of some ^{233}Pa which does not interfere in the subsequent measurements, unless present in very high amounts.

RESULTS AND DISCUSSION

Results obtained for seven U.S. Geological Survey standard rocks by means of epithermal activation analysis are given in Table I. The data for DTS-1 and PCC-1 were obtained in an initial run in which synthetic nickel standards were

TABLE I

CONTENT OF NICKEL IN U.S.G.S. STANDARD ROCKS (p.p.m.)

	AGV-1	*BCR-1*	*G-2*	*GSP-1*	*W-1*	*DTS-1*	*PCC-1*
Instrumental	15.8	7.1	2.5	6.5	71.7	2370	2380
	14.4	8.9	2.2	4.0	74.3	2440	2410
	19.8	9.7	2.3	5.5	69.8	2430	2520
	12.7	8.7	2.8	5.9	73.3	2350	2420
Mean value:						2400 ± 40	2430 ± 60
After radiochemical separation	13.3	10.2	2.4	6.2	76.7		
	13.3	10.2	2.0	7.5	76.8		
	12.0	9.6	2.4	6.5	75.4		
	13.2	10.0	2.3	7.6	73.7		
Mean value:	13.0 ± 0.6	10.0 ± 0.3	2.3 ± 0.2	7.0 ± 0.7	75.7 ± 1.4		
Co/Ni[a]	1.1	3.6	1.9	0.90	0.46	0.056	0.047

[a] Calculated on the basis of cobalt data from previous work in the author's laboratory[16,17].

used. These samples were not run according to the radiochemical procedure. The data for the other five rocks were obtained by two different irradiations, with DTS-1 as standard with an assigned nickel value of 2400 p.p.m.

Although the purely instrumental version seems to be capable of giving useful data down to a few p.p.m. of nickel, it appears that introduction of a simple radiochemical separation is likely to improve the data considerably. It seems that nickel determinations with a precision of $\pm 10\%$ or better are possible at concentrations of a few p.p.m. The factor limiting the precision and sensivity of the method is probably the cobalt-to-nickel ratio rather than the absolute level of nickel present in the rock. It appears from the present examples that a Co/Ni ratio of 3.6 or a nickel concentration of 2.3 p.p.m. do not represent marginal cases of determination.

It is assumed that the mean values obtained after radiochemical separation are the "best values" from this work for the five rocks that are low in nickel. This is so not only because of the improved precision, but also because spectral interferences are not likely to be present in this case. In the purely instrumental method, γ-rays such as 803 keV from ^{134}Cs, 808 keV from ^{47}Ca, 811 keV from ^{152}Eu and 816 keV from ^{154}Eu may interfere with the measurement of the 811-keV γ-ray of ^{58}Co.

In Table II, the present values are compared with some literature values of interest. The value of 75.7 p.p.m. for W-1 is in good agreement with the recommended value by Fleischer[18] as well as previous values obtained by activation analysis[2,4]. The values obtained for the six new standard rocks up to 1969, mostly by emission spectrography, were compiled by Flanagan[19], and the mean values calculated by him are given in the Table along with the range of reported values. Considering the large spread in the observed results and the fact that many of the values were close to the limit of detection of the procedures used, it seems likely that Flanagan's average values may not be the best basis for

TABLE II

COMPARISON OF PRESENT RESULTS WITH PREVIOUS NICKEL DATA (p.p.m.)

	AGV-1	*BCR-1*	*G-2*	*GSP-1*	*W-1*	*DTS-1*	*PCC-1*
Present work	13.0±0.6	10.0±0.3	2.3±0.2	7.0±0.7	75.7±1.4	2400±40	2430±60
Schmitt *et al.* (ref. 10), photon activation	24±3	10±3	3±1	9±1	73±4	2140±80	2460±80
Morrison *et al.* (ref. 6), instrumental neutron activation	34	39	7.5				
Other neutron activation values		12.4±3.2[4]			73[2]		
Flanagan (ref. 19), average value	17.8	15.0	6.4	10.7		2330	2430
range	11–27	8–30	2–14	3–25		1770–3300	1750–340
Fleischer (ref. 18), recommended value					78		
Sutton *et al.* (ref. 20), emission spectrography	13.0	10.0	3	7.7		2470	2480
Sarma and Das (ref. 21), emission spectrography	17	15	2	7		2200	2300

assessment of accuracy for nickel determination in these rocks. It might be more useful to consider two specific sets of data, notably those by Sutton *et al.*[20] obtained in the U.S.G.S. laboratories, and those by Sarma and Das[21]. Both sets of data are in good agreement with the present work, and in the case of Sutton *et al.*, the agreement may be characterized as excellent. The agreement with the values obtained by Schmitt *et al.*[10], who used a technique of activation analysis that is entirely different from that used in the present work is also remarkable.

Although it appears difficult to assess the accuracy of the results from this work on the basis of literature data, it seems likely from an evaluation of possible sources of systematic error that data obtained by the present epithermal activation method employing radiochemical separation of the cobalt radionuclides, should be reasonably accurate. Neutron shielding effects and interfering nuclear reactions are insignificant in this case, and spectral interferences are not likely to be present in the radiochemically isolated fractions. The method should be useful for the determination of nickel in most geological materials.

SUMMARY

Nickel has been determined in seven U.S.G.S. standard rocks by reactor activation analysis based on the $^{58}Ni(n,p)^{58}Co$ reaction. Irradiation in cadmium containers is used in order to reduce interference from nuclides formed by (n,γ) reactions. Samples with nickel contents down to a few p.p.m. can be analyzed instrumentally by Ge(Li) γ-spectrometry, but considerable improvement is observed by introducing a simple radiochemical separation. The data obtained are compared with previous literature values. The method is applicable to most geological samples.

RÉSUMÉ

Le nickel a été dosé dans sept roches étalon U.S.G.S. par activation, basée sur la réaction $^{58}Ni(n,p)^{58}Co$. L'irradiation s'effectue dans des récipients de cadmium, afin de diminuer l'interférence de nucléides formés par les réactions (n,γ). Des échantillons avec des teneurs en nickel allant jusqu'à quelques p.p.m. peuvent être analysés par spectrométrie γ (Ge(Li)) ; cependant une nette améliozation est observée par introduction d'une simple séparation radiochimique. Les valeurs obtenues sont comparées avec celles de la littérature. Cette méthode peut s'appliquer à la plupart des échantillons géologiques.

ZUSAMMENFASSUNG

Nickel wurde in sieben U.S.G.S.-Standard-Gesteinen mittels Reaktor-Aktivierungsanalyse aufgrund der Reaktion $^{58}Ni(n,p)^{58}Co$ bestimmt. Zur Verminderung von Störungen durch Nuklide, die durch (n,γ)-Reaktionen entstehen, wurde die Bestrahlung in Cadmium behältern vorgenommen. Proben mit Nickelgehalten bis zu wenigen p.p.m. herab können instrumentell durch Ge(Li)-γ-Spektrometrie analysiert werden, jedoch wird durch eine einfache radiochemische Trennung eine

erhebliche Verbesserung erzielt. Die Ergebnisse werden mit früheren Literaturwerten verglichen. Die Methode ist auf die meisten geologischen Proben anwendbar.

REFERENCES

1 E. Goldberg, A. Uchiyama and H. Brown, *Geochim. Cosmochim. Acta*, 2 (1951) 1.
2 A. A. Smales, D. Mapper and A. J. Wood, *Analyst*, 82 (1957) 75.
3 W. D. Ehmann, *Geochim. Cosmochim. Acta*, 19 (1960) 149.
4 R. O. Allen, L. A. Haskin, M. R. Anderson and O. Müller, *J. Radioanal. Chem.*, 6 (1970) 115.
5 D. E. Fisher and R. L. Currie, *Radiochemical Methods of Analysis*, Vol. 1, I.A.E.A., Vienna, 1965, p. 217.
6 G. H. Morrison, J. T. Gerard, A. Travesi, R. L. Currie, S. F. Peterson and N. M. Potter, *Anal. Chem.*, 41 (1969) 1633.
7 J. W. Morgan and W. D. Ehmann, *Anal. Lett.*, 2 (1969) 537.
8 K. K. Turekian and D. P. Kharkar, in A. A. Levinson, *Proc. Apollo 11 Lunar Science Conf.*, Vol. 2, Pergamon, New York, 1970, p. 1659.
9 H. Wänke, R. Rieder, H. Baddenhausen, B. Spettel, F. Tesche, M. Quijano-Rico and A. Balacescu, in A. A. Levinson, *Proc. Apollo 11 Lunar Science Conf.*, Vol. 2, Pergamon, New York, 1970, 1719.
10 R. A. Schmitt, T. A. Linn and H. Wakita, *Radiochim. Acta*, 13 (1970) 200.
11 E. Steinnes, in A. O. Brunfelt and E. Steinnes, *Activation Analysis in Geochemistry and Cosmochemistry*, Universitetsforlaget, Oslo, 1971, p. 113.
12 A. O. Brunfelt and E. Steinnes, *Anal. Chim. Acta*, 48 (1969) 13.
13 A. O. Brunfelt, K. S. Heier, B. Nilssen, B. Sundvoll and E. Steinnes, in D. Heymann, *Proc. Third Lunar Science Conf.*, Vol. 2, The MIT Press, Cambridge, Mass. and London, 1972, p. 1133.
14 O. U. Anders, *Nucl. Instrum. Methods*, 68 (1969) 205.
15 S. Sterlinski, *Anal. Chem.*, 40 (1968) 1995.
16 O. Johansen and E. Steinnes, *Talanta*, 17 (1970) 407.
17 A. O. Brunfelt and E. Steinnes, *Geochim. Cosmochim. Acta*, 30 (1966) 921.
18 M. Fleischer, *Geochim. Cosmochim. Acta*, 33 (1969) 65.
19 F. J. Flanagan, *Geochim. Cosmochim. Acta*, 33 (1969) 81.
20 A. L. Sutton, H. G. Neiman and J. Haffty, private communication (1965) cited in ref. 19.
21 B. D. Sarma and H. B. Das, private communication (1966) cited in ref. 19.

Analytica Chimica Acta, 68 (1974) 31–36

A SIMPLE METHOD FOR SIMULTANEOUS RADIOCHEMICAL SEPARATIONS IN ACTIVATION ANALYSIS

M. CSAJKA

Central Research Institute for Physics, 1525 Budapest 114 (Hungary)

(Received 27th June 1973)

Activation analytical methods combined with chemical destruction are usually laborious, particularly if several elements have to be determined in a sample. Successive separations take a long time, even if selective fast separation techniques are used for each of the elements or groups of elements involved. Attempts were made therefore in this Laboratory to develop methods for the simultaneous separation of different activities from an irradiated sample.

The heterogeneous processes taking place between solids and the solutions of activated samples, such as adsorption, isotopic exchange, ion exchange, etc., have been already successfully exploited for radiochemical separations in activation analysis[1–8]. Our investigations of such procedures resulted among others in the isolation of radiocopper by retention of copper(I) thiocyanate[9] and in the recovery of rare earth activities on lanthanum oxalate precipitate by group separation techniques[10]. Radiochemical separations of this type are often carried out from similar solutions, *i.e.* a weakly acidic solution of the activated sample. It seemed feasible to bring simultaneously different precipitates in contact with the activated solution in order to achieve the radiochemical separations of the different elements from the solution and from one another in a single step. To prevent the precipitates from mixing, the solid particles were pasted on plexiglas discs which could be easily removed from the solution on termination of the separation. This method was used for the simultaneous separation of copper and the group of rare earth activities from each other and from an activated rock sample.

EXPERIMENTAL

Apparatus

The radiochemical separator consists of a low performance motor connected to a removable tubular glass shaft. The plexiglas discs coated with the precipitate can be drawn onto this shaft through the holes drilled in their middle (Fig. 1). The broadened bottom of the shaft prevents the discs from slipping down and the small plexiglas rings between the discs serve to separate them from each other and to keep both sides of the discs in contact with the solution while they are being rotated therein. On termination of the rotation, the container of the solution is removed, the shaft is pulled out from the motor and the discs are taken off through the upper straight end of the glass rod.

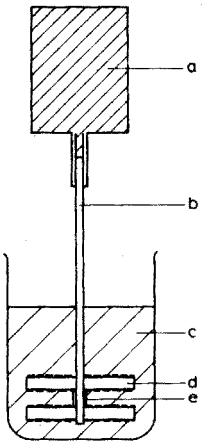

Fig. 1. Apparatus for simultaneous radiochemical separations. (a) Electric motor; (b) glass shaft; (c) container of activated sample solution; (d) plexiglas discs coated on both sides with the precipitate; (e) plexiglas ring.

Coating of discs

Copper(I) thiocyanate and lanthanum oxalate were prepared as described in earlier reports[9,10].

For the pasting of the precipitates, discs of 3 cm in diameter and 0.4 cm in height with a hole in the middle were prepared from plexiglas. The plexiglas was made sticky by dipping the discs into chloroform which dissolves the polymer at a slow rate. In this state the discs were pressed on a plane surface onto which the precipitate had been evenly distributed. The discs coated on both sides in this manner were dried, and the non-adhering particles were washed off with distilled water. The vertical sides were also carefully cleaned. The mechanical resistance of the coating was then tested by rotating the discs in a hot dilute solution of hydrochloric acid. The discs from which no more precipitate could be removed were used in the experiments. The coatings thus obtained varied from 150 to 200 mg in weight.

Determination of the retention conditions on disc

Tracer techniques were employed to establish the experimental conditions under which copper and rare earth activities could be retained on a disc coated with thiocyanate and lanthanum oxalate, respectively. For these experiments weakly acidic solutions of 10^{-5} g of copper or europium with 10^4 c.p.m. ^{64}Cu or ^{152}Eu activity were used. The disc coated with the retaining precipitate was rotated for different periods. The solution activity was measured with a Ge/Li detector and a multichannel analyser before and after the separation in order to evaluate the percentual retention.

Radiochemical separation for activation analysis

A rock sample of 0.01 g was irradiated for 10 h in nuclear reactor. The irradiated sample was placed in a platinum crucible where it was evaporated to dryness first with 0.2 ml of concentrated hydrofluoric acid, and secondly with a

fresh 0.2-ml portion of hydrofluoric acid and 0.2 ml of 72% perchloric acid; finally, the inside of the crucible was washed down with 1 ml of 2 *M* perchloric acid, and the mixture was evaporated to dryness. The residue was then dissolved in 1 ml of 0.1 *M* hydrochloric acid and 0.5 ml of reducing solution (1% sodium sulphate solution neutralized with sulphurous acid) and diluted with distilled water to 15 ml. Two discs, one coated with copper(I) thiocyanate, and the other with lanthanum oxalate, were rotated in the hot solution for 10 min. After their removal from the solution the discs were washed with distilled water and packed in aluminium foils for the activity measurement.

Copper and rare earth standards were irradiated along with the sample, and then dissolved in 0.01 *M* hydrochloric acid. The activities were recovered on the same types of discs as used for the sample and were thus measured in the same geometry as the sample activities.

A 45-cm^3 Ge/Li detector and a 1024-channel analyzer were used in the measurements. The spectra were evaluated on a computer.

RESULTS

It was found that under the experimental conditions used (10-min rotation in 15 ml of hot 0.02 *M* hydrochloric acid solution) the rare-earth metal activities could be recovered to 90% on the disc coated with lanthanum oxalate, and the copper activity to 60% on the disc coated with cuprous thiocyanate. The dependence of the recovery on such experimental parameters as solution volume, temperature, rotation velocity and time was studied in a set of experiments by means of radioactive tracer techniques. The results of the tracer experiments are listed in Tables I and II. The reproducibility of these data was $\pm 2\%$. In the earlier batch experiments[9,10], it had been already established that the recovery was reduced by

TABLE I

INFLUENCE OF EXPERIMENTAL PARAMETERS ON THE RETENTION OF RARE EARTH ACTIVITIES BY LANTHANUM OXALATE COATED ON A PLEXIGLAS DISC

Solution	*Time of rotation (min)*	*Rotation velocity (r.p.m.)*	*Recovery (%)*
Experiments with hot solution			
15 ml 0.01 *M* HCl	5	~300	77
15 ml 0.01 *M* HCl	10	~300	90
15 ml 0.01 *M* HCl	15	~300	92
15 ml 0.025 *M* HCl + 0.5 ml reducing solution	10	~300	90
15 ml 0.01 *M* HCl	10	~150	77
15 ml 0.01 *M* HCl	10	~500	90
20 ml 0.01 *M* HCl	10	~300	88
25 ml 0.01 *M* HCl	10	~300	70
Experiments at room temperature			
15 ml 0.01 *M* HCl	10	~300	80

TABLE II

INFLUENCE OF THE EXPERIMENTAL PARAMETERS ON THE RETENTION OF RADIO-COPPER BY COPPER(I) THIOCYANATE COATED ON PLEXIGLAS DISCS

Solution[a]	*Time of rotation (min)*	*Rotation velocity (r.p.m.)*	*Recovery (%)*
Experiments with hot solution			
15 ml 0.01 *M* HCl	5	~300	54
15 ml 0.01 *M* HCl	10	~300	61
15 ml 0.01 *M* HCl	15	~300	63
15 ml 0.01 *M* HCl	20	~300	65
20 ml 0.01 *M* HCl	10	~300	56
15 ml 0.05 *M* HCl	10	~300	52
15 ml 0.01 *M* HCl	10	~500	68
Experiments at room temperature			
15 ml 0.01 *M* HCl	10	~300	49

[a] 0.5 ml of reducing solution was added in all cases.

high acidity of the solution. It has to be noted that the activities are retained in a shorter time with the batch technique than with the same quantity of precipitate on disc. This is probably due to the larger solid surface areas in contact with the solution in the former case.

The accuracy and reproducibility of the activation analysis combined with the simultaneous radiochemical separations can be seen from the results obtained on USGS W1 rock standard are listed in Table III.

TABLE III

EUROPIUM, SAMARIUM AND COPPER CONTENTS OF USGS W1 ROCK

(All results given in p.p.m.)

	This work				*Lit. value*	*Average*	*Ref*
	run 1	*run 2*	*run 3*	*Average*			
Eu	1.16	1.20	1.19	1.18	1.18–1.2–1.08–1.102–1.13–1.0–1.18–1.09–1.29–1.04–1.4–0.9–0.95–1.20–1.09	1.12±0.2	10
Sm	3.3	3.6	3.3	3.4	3.4–3.4–2.8–3.356–3.55–3.0–3.62–3.79–3.46–3.78–3.2–3.8–3.3–3.76	3.44±0.6	10
Cu	102	117	104	108	80–103–109–110–110–110–110–110–110–115–118–118–120–124–130–130	113±2	11

The selectivity of the method is satisfactory as is apparent from the γ-spectrum taken on a small volume (0.15 ml) of the 15-ml solution of the sample after separation and the spectra taken on the discs in Fig. 2.

Finally, it can be stated that the copper and rare earth activities can be selectively and reproducibly separated from each other and from irradiated rock samples by this simple and relatively fast method which gives, in addition, samples of well defined geometry for the activity measurement.

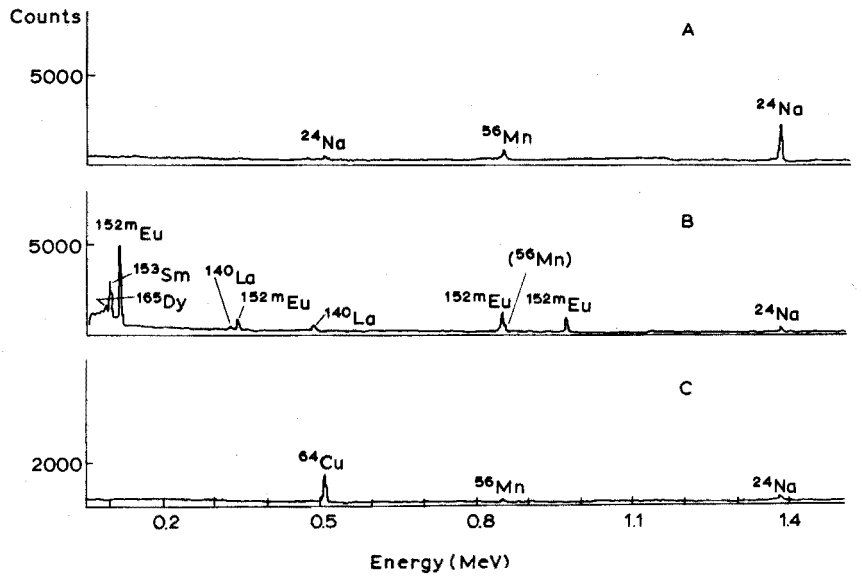

Fig. 2. γ-Spectra of (A) 0.15-ml portion of the 15-ml solution of the sample; (B) disc with lanthanum oxalate; (C) disc with copper(I) thiocyanate.

SUMMARY

A radiochemical separation technique is described which permits several elements or groups of elements to be isolated in a single step from the activated sample and from one another. The inexpensive apparatus considerably simplifies radiochemical procedures for activation analysis. It has been used for the simultaneous separation of copper and rare earth activities from irradiated rock samples.

RÉSUMÉ

Une technique radiochimique est décrite permettant d'isoler plusieurs éléments ou groupes d'éléments, en un seul stade, à partir d'un échantillon activé. L'appareil peu coûteux simplifie considérablement les procédés radiochimiques de l'analyse par activation. Il a été utilisé pour la séparation simultanée des activités du cuivre et des terres rares dans des échantillons de roches irradiés.

ZUSAMMENFASSUNG

Es wird ein radiochemisches Trennverfahren beschrieben, mit dem in einer einzigen Stufe verschiedene Elemente oder Elementgruppen von der aktivierten Probe und voneinander getrennt werden können. Die wenig aufwendige Apparatur vereinfacht radiochemische Verfahren für die Aktivierungsanalyse erheblich. Sie wurde für die simultane Abtrennung von Kupfer- und Seltenerdaktivitäten von bestrahlten Gesteinsproben angewendet.

REFERENCES

1 D. N. Sunderman and W. W. Meinke, *Anal. Chem.*, 29 (1957) 1579.
2 J. H. Qureshi and M. Shabbir, *Talanta*, 13 (1966) 847.
3 F. Tera and G. H. Morrison, *Anal. Chem.*, 38 (1966) 959.
4 S. Giovannetti, Q. Maggiore and R. Malvano, *Proc. Symp. Nuclear Activation Techniques in the Life Sciences*, I.A.E.A., Vienna, 1967, p. 511.
5 M. Csajka, *Talanta*, 17 (1967) 1157.
6 F. Girardi, R. Pietra and E. Sabbioni, *EUR-4287e*, 1969.
7 O. Gimesi, É. Bányai, M. Csajka and A. Szabadházy, *Talanta*, 17 (1970) 1183.
8 É. Bányai, O. Gimesi and A. Farkas, *Int. Conf. Modern Trends in Activation Analysis*, Saclay, 1972, M48.
9 M. Csajka, *J. Radioanal. Chem.*, 13 (1973) 329.
10 M. Csajka, *Radiochem. Radioanal. Lett.*, 13 (1973) 151.
11 H. J. M. Bowen, *Advances in Activation Analysis*, Vol. 1, Academic Press, London and New York, 1969, p. 101.

Analytica Chimica Acta, 68 (1973) 37–48

A STUDY OF THE OPTIMAL CONDITIONS FOR FLAMELESS ATOMIC ABSORPTION SPECTROMETRY OF IRIDIUM, PLATINUM AND RHODIUM

E. ADRIAENSSENS

Laboratory of Analytical Chemistry, University of Ghent, Ghent (Belgium)

P. KNOOP

Analytical Department, Glass Development Centre, H.I.G. Glas, N.V. Philips' Gloeilampen Fabrieken, Eindhoven (The Netherlands)

(Received 19th March 1973)

Very little is known about the determination of high-melting noble metals by flameless atomic absorption spectrometry[1–3]. In a preliminary investigation, the possibilities and satisfactory conditions for the determination of some of these elements were established. The determination of iridium, platinum and rhodium in a glass matrix in the range 1–100 p.p.m. was found to be possible. Inter-element interferences could not be detected. Sensitivity and detection limits of about 10^{-10}–10^{-9} g were achieved.

EXPERIMENTAL

Apparatus

A Perkin–Elmer model 403 atomic absorption spectrophotometer fitted with a Massmann furnace, the HGA-70 flameless atomization device[4], a recorder Model 165, a deuterium background corrector and intensitron hollow-cathode lamps were used in this work. Eppendorf microlitre pipettes with disposable plastic tips were used for sample injections.

Reagents and standard solutions

All chemicals were p.a. products and all solutions were prepared with deionized water.

A platinum stock solution (1000 μg ml^{-1}) was prepared by dissolving 1.000 g of pure platinum metal in aqua regia. The final volume was made up to 1 l and the hydrochloric acid concentration was 1 *M*.

A rhodium stock solution (1000 μg ml^{-1}) was prepared by dissolving 0.2559 g of rhodium chloride trihydrate in 25 ml of 4 *M* hydrochloric acid and diluting with water to a final volume of 100 ml.

An iridium stock solution (1000 μg ml^{-1}) was prepared by dissolving 0.2533 g of ammonium hexachloroiridate ($\cdot 1.5\ H_2O$) in 25 ml of 4 *M* hydrochloric acid and diluting with water to a final volume of 100 ml.

Freshly prepared dilutions were made from these stock solutions, stored in polyethylene bottles; the solutions used contained 2.0, 1.0 and 0.25 μg metal ml^{-1}, in a 0.1 *M* hydrochloric acid medium.

For each measurement, 20 μl of the solution was injected into the Massmann furnace and dried for 40 s at 100°. Before each series of measurements, the furnace was adjusted in the optical path so that minimal absorbance (*ca.* 0.050) was obtained. To achieve this value, it was necessary to move the hollow-cathode lamp as far back in its holder as possible, because the furnace is not symmetrically located in the burner compartment of the 403.

OPTIMAL WORKING CONDITIONS

For the three elements, iridium, platinum and rhodium, the combination of parameters leading to the highest sensitivity was sought, but in some cases better stability and/or reproducibility were preferred at the cost of a small signal decrease. The optimal conditions found are given in Table I. The reported results are the arithmetical mean of at least 5 measurements. The sensitivity of the recorder was adjusted so that 100 scale units corresponded to 0.25 absorbance units.

TABLE I

OPTIMAL WORKING PARAMETERS

(In all cases, the optimal lamp current was 30 mA and the atomization voltage was 10 V. Argon was used as the inert gas, and the water coolant flow was 3.0 l min^{-1})

Element	*Wavelength (nm)*	*Slit setting (rel. value)*	*Atom. time (s)*	*Max. mineralz. temp. (°)*	*Max. mineralz. time (s)*
Ir	263.97	4	20	1280	20
Pt	265.95	4	20	1100	600
Rh	343.49	3	30	1440	20

Slit setting

For each element the absorption was measured at slit settings varying from 1 to 6; these settings correspond to band passes of 0.02, 0.07, 0.2, 0.7, 2 and 7 nm, respectively. The optimal values were 3 or 4 (Table I); at higher slit settings, strong emission from the red-hot graphite furnace caused very unstable signals or no signal at all.

Lamp current

The lamp currents were varied from 10 mA to the maximal permissible value as stated by the manufacturer. The signals were essentially stable in the range 20–35 mA for each of the elements. The lifetime of the lamp was taken into account in choosing the optimal current.

Atomization voltage and atomization time

The atomization voltage was varied from 10.0 to 8.0 V for iridium and platinum, and from 10.0 to 6.5 V for rhodium, in both cases with steps of 0.5 V. From Fig. 1, it can be seen that the absorbance of the three elements is very temperature-dependent. This would be expected in view of the high melting and

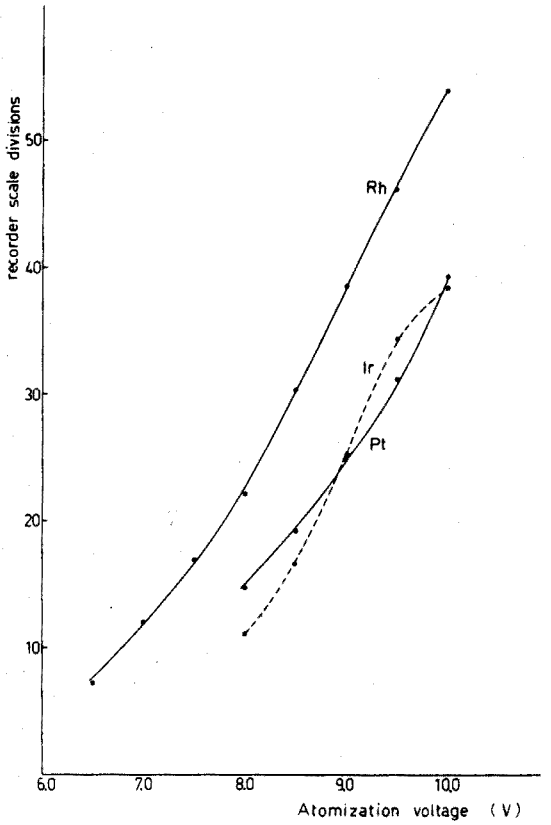

Fig. 1. Influence of atomization voltage on the absorption signals of iridium, platinum and rhodium.

boiling points of iridium (m.p. 2454°, b.p. 4800°), platinum (m.p. 1774°, b.p. 4300°) and rhodium (m.p. 1966°, b.p. 2500°). The atomization time was chosen so that no memory effects could occur, *i.e.* long enough for the transport of all the absorbing material out of the graphite tube.

Temperature and time for mineralization

Reference signals for iridium, platinum and rhodium were recorded by mineralizing the samples for 30 s at temperatures of 750° for iridium, 490° for platinum, and 750° for rhodium; with these values, one can be sure that no element losses occur during mineralization. The temperature and time of the mineralization step were then varied, and the percentage difference of the recorded absorption signal from the reference signal was calculated in each case. The results are summarized in Table II. From these values the maximum allowable mineralization temperature and time were deduced; differences up to -2.5% were not taken into account.

It must be noted that atomization of these elements can be done safely by pressing the "maximum temperature" button just after the third time clock has stopped. With this procedure this third clock can be used as a mineralization step

TABLE II

PERCENTAGE DIFFERENCE BETWEEN THE SIGNALS OBTAINED UNDER VARIOUS MINERALIZATION CONDITIONS AND THE REFERENCE SIGNALS

Mineralz. temp. (°)	*Time* (s)	*Percentage difference*		
		Ir	*Pt*	*Rh*
1100 (prog. 7)	180	—[a]	—	+0.2
	600	—	−1.5	+1.7
1280 (4.0 V)	20	−1.7	−4.4	−0.2
	40	—	−6.1	—
	60	—	—	−2.2
1440 (4.5 V)	20	−4.6	−6.9	−2.5
	40	—	−8.0	−6.5
1580 (5.0 V)	20	−4.8	−10.2	−10.9
1705 (5.5 V)	20	−7.4	—	−25.8
1815 (6.0 V)	20	−9.3	−22.3	−44.8

[a] Not measured.

for temperatures above 1100° (prog. 7), because the voltage can be set at an arbitrary value between *ca.* 3.5 and 10.0 V and maintained during the whole series of measurements. The atomization at 10.0 V is then started with the help of the "maximum temperature" button as already mentioned; this solves the problem of reproducible adjustment of the "mineralization voltage" for each measurement.

The results in Table II show that losses occur at temperatures much lower than the melting points of the metals. L'vov[3] has indicated that losses often occur below normal vaporization temperatures.

Inert gas

The absorption signals for the different elements were compared with argon or nitrogen as the purging gas at a flow rate of 1.5 l min^{-1}. The use of nitrogen led to a decrease in signal height of *ca.* 20% for each of the three elements (see columns 2 and 4 of Table III).

The HGA-70 furnace was equipped with a simple "gas-stop" system by

TABLE III

INFLUENCE OF THE GAS-STOP MECHANISM WITH ARGON AND NITROGEN AS INERT GASES

Element	*Argon*		*Nitrogen*	
	Gas	*Gas-stop*	*Gas*	*Gas-stop*
Ir	31.2[a]	21.9	22.2	18.4
Pt	43.3	51.8	30.8	39.8
Rh	50.9	40.8	35.1	27.6

[a] Recorder scale divisions.

placing a 3-way valve in the gas line between the power supply and the furnace. By turning the valve quickly just before atomization started, the gas flow could be turned off just before it entered the furnace. This simple procedure allowed the effect of the gas-stop mechanism on the atomization of an element to be checked. However, it was difficult to obtain reproducible results because the moment of stopping the gas is very critical. Gas-stop effects on the atomization signals of iridium, platinum and rhodium were checked with argon and nitrogen as inert gases. The gas-stop caused a signal decrease for iridium and rhodium, but an increase in signal height for platinum (Table III). Hansen[5] has shown that by using the gas-stop method the detection limit of most elements can be improved by a factor of 2 to 5; however, the lowest factors occur for high-melting metals, and molybdenum and vanadium, for example, show no improvement in the detection limit. The fact that the signals for iridium and rhodium decrease may be explained as follows. These high-melting elements have at atomization temperature (about 2700°) a vapour pressure that approximates to the saturation pressure at that temperature; hence at the moment of atomization, with the gas-stop, vaporization is slower because of local saturation. The expected increase in signal height as a result of a longer retention time of the absorbing atoms in the light path is suppressed by this second phenomenon so that the normal signal is lowered.

Water cooling

The flow rate of the cooling water was varied from 3.0 l min^{-1} to 0.6 l min^{-1} in steps of 0.6 l min^{-1}. It was intended to lower this flow rate to obtain a higher atomization temperature, and so a higher recorder signal. Unfortunately, the opposite effect was obtained, the signals decreasing as the water flow decreased. A possible explanation for this could be the greater expansion of the inert gas on atomization so that atoms are removed more quickly from the absorption path.

The results of the following experiment can probably be explained in the same way. As stated earlier, elements can be atomized at 10 V by means of the "maximum temperature" button. This is especially useful when the technique of selective vaporization is applied to remove a matrix, above 1100°, before atomization starts. This process was used with pure iridium and rhodium solutions. After drying (40 s at 100°), mineralization (30 s at 750°) and selective vaporization (20 s at 1280° = 4.0 V), atomization was obtained by pressing the "maximum temperature" button. The absorption signals of iridium and rhodium were about 10% higher when atomization started 30 s after the selective vaporization had finished, instead of immediately afterwards. This difference must be connected with the fact that in the first case atomization starts from about room temperature and in the second from about 1280°. It appears that when the initial furnace temperature is high, the absorption signals decrease because of greater expansion of the inert gas.

Calibration curves

With the optimal working conditions (Table I), except that lower mineralization temperatures were used, adjusted calibration curves for the three elements were recorded. The curves obtained are shown in Figs. 2 and 3. The sensitivities calculated from these curves are given in Table IV, together with the detection limit determined for each element.

TABLE IV

SENSITIVITIES AND DETECTION LIMITS

Element	*Sensitivity (g)*[a]	*Detection limit (g)*[b]
Ir	$2 \cdot 10^{-9}$	$7.5 \cdot 10^{-9}$
Pt	$1 \cdot 10^{-9}$	$1.1 \cdot 10^{-9}$
Rh	$1.8 \cdot 10^{-10}$	$2.5 \cdot 10^{-10}$

[a] The weight corresponding to 1% absorption.
[b] For a signal:noise ratio of 2:1.

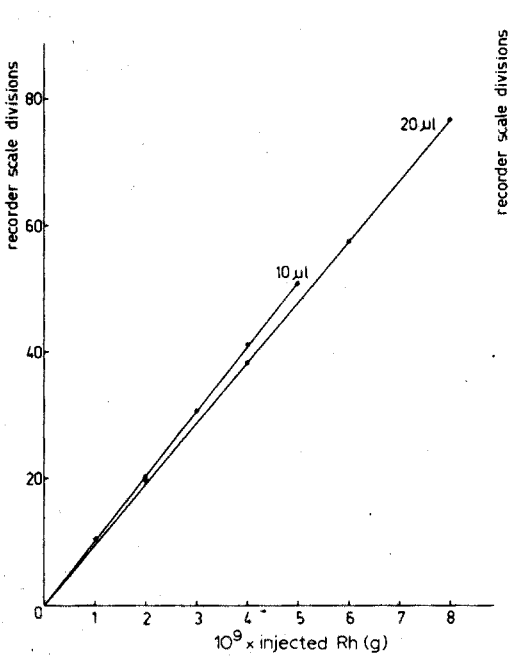

Fig. 2. Calibration curves for rhodium with 10- and 20-μl aliquots injected.

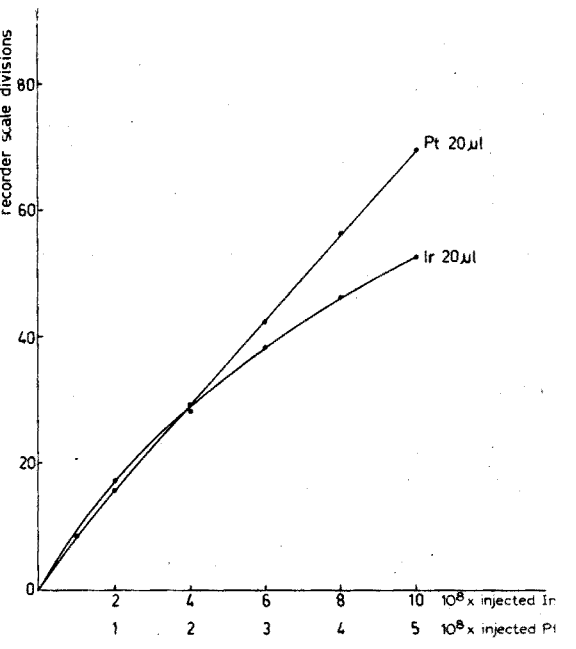

Fig. 3. Calibration curves for iridium and platinum with 20-μl aliquots injected.

INTERFERENCE EFFECTS

Acid interferences

The influences of hydrochloric and nitric acid on the absorption signals of iridium, platinum and rhodium were investigated up to maximal concentrations of 2 *M*. The concentrations of the elements were 2.0, 1.0 and 0.2 μg metal ml^{-1}, respectively, and 20-μl aliquots were injected. The results are shown in Figs. 4 and 5. The influence of nitric acid is more pronounced than that of hydrochloric acid, with regard to both sensitivity and reproducibility, especially for platinum and rhodium (see below). The decrease in sensitivity with increasing acid concentration can be avoided by neutralization with ammonia. If there is no danger of hydrolysis, this can be done in advance, otherwise it should be done in the furnace. Care

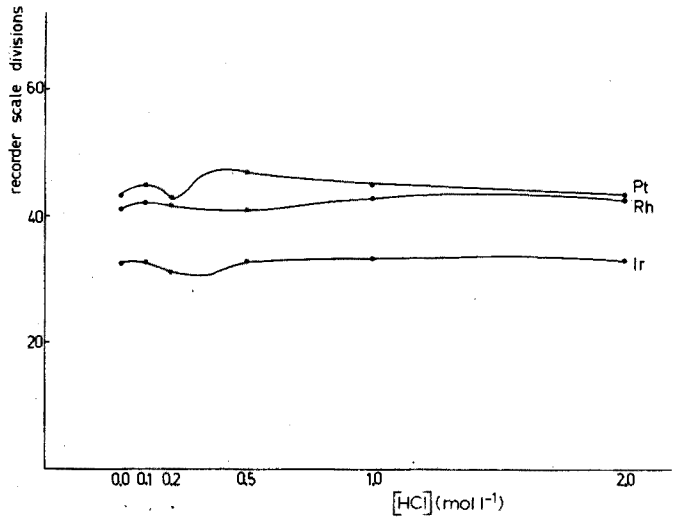

Fig. 4. Effect of hydrochloric acid concentration on the absorbance signals of iridium, platinum and rhodium.

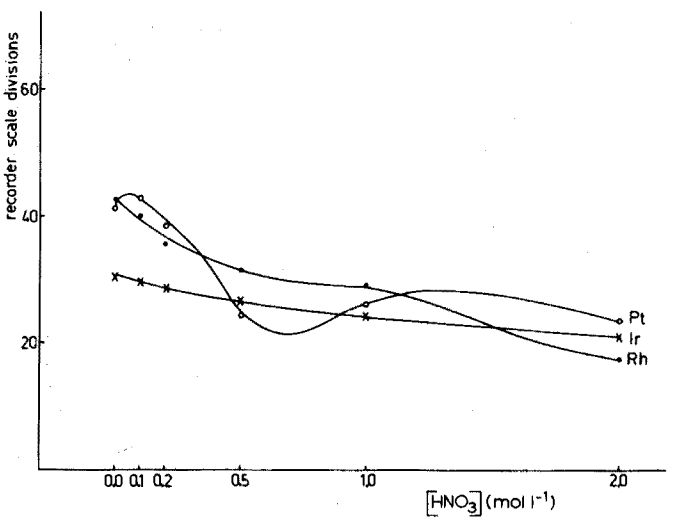

Fig. 5. Effect of nitric acid concentration on the absorbance signals of iridium, platinum and rhodium.

should be taken that all the ammonium chloride and ammonium nitrate present is completely removed during the drying and mineralization steps to avoid non-specific absorption during the atomization step.

Interelement interferences

Interelement interferencs for the three metals were investigated for the binary systems. To solutions of iridium, platinum and rhodium containing 2.0, 1.0 and 0.2 μg metal ml^{-1}, respectively, increasing amounts of one of the two other metals

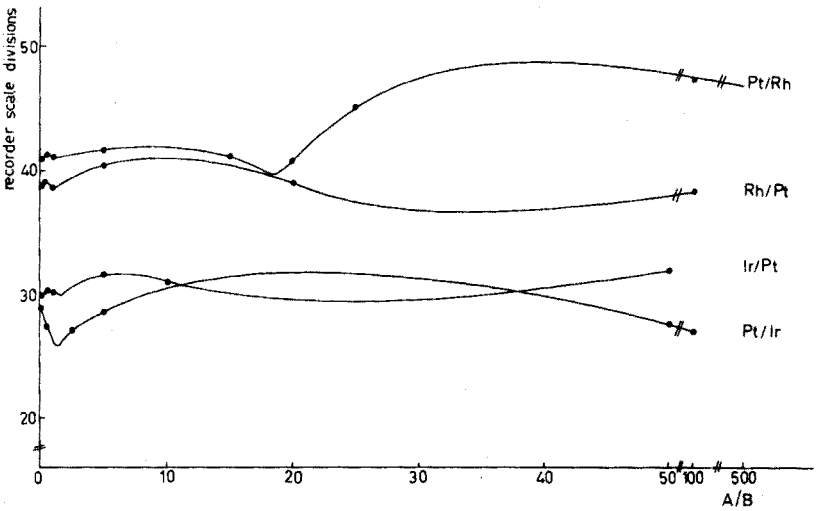

Fig. 6. Interelement interferences for some binary systems of iridium, platinum and rhodium. (A) Interfering element concentration in $\mu g\ ml^{-1}$; (B) concentration of the element to be determined in $\mu g\ ml^{-1}$.

were added; in each case 20 μl of the solution was injected and the absorption signals were recorded. The results are given in Fig. 6. When "blank" measurements were made on a solution containing iridium, no signals for platinum or rhodium were obtained at the appropriate wavelengths; similarly, neither platinum nor rhodium gave signals at the wavelengths used for the other metals.

DISCUSSION

Furnace temperature profile and influence of sample volume

It is well known that there is a temperature gradient along the furnace tube. Relatively small differences in temperature could be important in analysis for very

TABLE V

INFLUENCE OF SAMPLE VOLUME

Injected volume (μl)	*Longitud. section of the drop* (*mm*)	*Drying time* (*s*)	*Ir*		*Pt*		*Rh*	
			Solution concn.[a] ($\mu g\ ml^{-1}$)	*Recorder scale div.*	*Solution concn.*[b] ($\mu g\ ml^{-1}$)	*Recorder scale div.*	*Solution concn.*[c] ($\mu g\ ml^{-1}$)	*Recorder scale div.*
5	2.9	10	8.0	29.3	4.0	48.1	1.00	53.6
10	4.4	20	4.0	27.7	2.0	45.9	0.50	52.9
20	5.5	40	2.0	27.3	1.0	44.1	0.25	50.9
50	7.8	100	0.8	25.0	0.4	41.6	0.10	48.1
100	11.0	120	0.4	24.0	0.2	40.6	0.05	48.4

[a] Injected weight, 0.04 μg.
[b] Injected weight, 0.02 μg.
[c] Injected weight, 0.005 μg.

"temperature-dependent" elements, and such differences can be caused by injecting varying volumes of solution.

It was found for iridium, platinum and rhodium that absorption signals decreased as volumes were increased for the same injected weight of metal (Table V). If the signal decrease is related to a decrease in temperature and the increase in volume leading to an increased sample area at the centre of the tube, the results in Table V can serve as an indication of the temperature profile around the middle of the graphite tube. A graphite tube was therefore partly cut open and after different volumes had been deposited on the graphite surface, the longitudinal sections of the drops were measured. For each sample volume of the three elements, the percentage decrease in absorption signal relative to the maximum value was plotted as a function of the distance between the end and the centre of the drop (half the longitudinal section) on both sides of the centre. The temperature profile round the centre of the graphite tube obtained in this way is shown in Fig. 7. Mainly because of these local differences in temperature, the height of the absorption signal depends on the volume used when equal weights of analyte are injected. Accordingly, it is essential always to inject the same volume of solution, *e.g.* 20 μl, in the preparation of calibration curves, so as to reduce the risk of curvature.

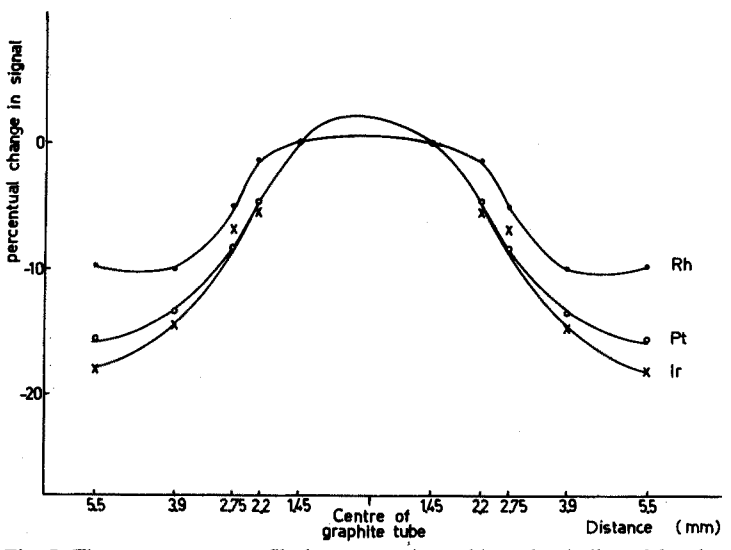

Fig. 7. The temperature profile in a normal graphite tube, indicated by the effect of volume on the absorption signals of fixed amounts of iridium, platinum and rhodium.

The results in Table V show that 100 μl of an aqueous solution can easily be put into a normal graphite tube (P.E. model no. 045057), because the longitudinal section of the drop is only about 11 mm while the tube length is about 50 mm. However, when these larger volumes were used, it was difficult to remove water vapour completely before atomization. This problem of water condensing on the windows of the model 403 was overcome by installing an exhaust system made of Teflon on both ends of the furnace.

When organic liquids are used, the wetted area of the graphite tube is much larger than for water. The injection of 5 μl of MIBK resulted in a wetted graphite area about 20 mm long, while 20 μl covered the tube surface completely.

Reproducibility

All the values given in this paper are the arithmetical means of at least 5 measurements; at the 95% confidence level, larger numbers of tests provide little improvement[6]. For iridium, platinum and rhodium, the percentage standard deviations for series of five measurements on pure solutions under optimal working conditions were calculated; values of 2.8, 3.2 and 1.9%, respectively, were found. Typical traces showing the stability of the base-line, the signal reproducibility and the background noise are given in Fig. 8. Among the various factors which can affect the reproducibility, the most important is the age and general condition of the graphite tube. With a new tube, reproducible results can be obtained only after about 10 measurements, but there was no decrease in reproducibility with older tubes that had been used for 100–200 times. The presence of carbon particles and dust decreased the reproducibility, but this could be avoided by cleaning the tube surface with a soft brush or cloth.

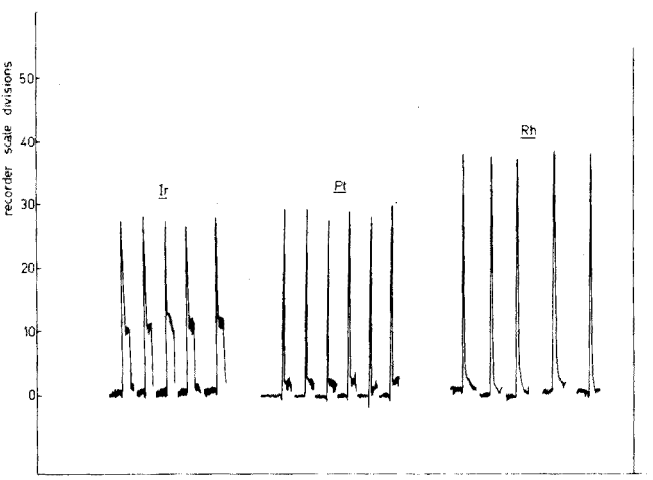

Fig. 8. Reproducibility and background emission of the atomic absorption signals of iridium, platinum and rhodium under optimal working conditions.

The background emission of the graphite tube during atomization increased linearly with the voltage applied. When the 10 V maximum was used, this strong emission caused an increase in noise; the noise depended on such factors as wavelength, lamp intensity, slit setting, photomultiplier gain. It would be advantageous in some cases (*e.g.* iridium) to have a continuously adjustable slit built into the instrument. It should also be noted that optimal adjustment of the furnace in the light path does not always give rise to the lowest background emission signals.

Another important factor is the sample injection into the tube. With normal tubes, the hole through which the samples are injected is so small that the drop

may adhere partly to the edges. To overcome this problem, the hole was enlarged so that the pipette tip nearly reached the opposite side of the tube, and the whole sample drop could be deposited at one place. There was no significant difference in reproducibility whether the volume used was 10 or 100 μl; even with 5 μl, the percentage standard deviation did not exceed 5%.

Finally, it was found that certain media can affect the reproducibility considerably. For example, increasing nitric acid concentrations may greatly reduce the reproducibility for iridium, platinum and rhodium (Table VI).

TABLE VI

PERCENTAGE STANDARD DEVIATION AS A FUNCTION OF NITRIC ACID CONCENTRATION

Element	*Nitric acid concentration (M)*					
	0.0	*0.1*	*0.2*	*0.5*	*1.0*	*2.0*
Ir	2.3[a]	2.3	5.0	2.2	3.7	2.8
Pt	2.4	4.1	6.0	12.5	17.0	23.0
Rh	3.0	3.9	8.2	20.0	25.0	6.1

[a] Percentage standard deviation.

SUMMARY

The optimal working conditions under which iridium, platinum and rhodium can be determined with the aid of flameless atomic-absorption spectrometry with a Massmann furnace were examined. The limits of detection were in the range 10^{-9}–10^{-10} g. The influence of acids and mutual interferences was checked. The effect of the sample volume on the atomic absorption signals was related to temperature differences in the graphite tube. Factors affecting reproducibility are discussed.

RÉSUMÉ

Une étude est effectuée pour déterminer les conditions de travail optimales pour le dosage de l'iridium, du platine et du rhodium à l'aide de la spectrométrie par absorption atomique sans flamme, avec un four Massman. Les limites de détection sont de l'ordre de 10^{-9} à 10^{-10} g. On examine divers paramètres et l'influence des acides et des interférences mutuelles en particulier.

ZUSAMMENFASSUNG

Die optimalen Arbeitsbedingungen für die Bestimmung von Iridium, Platin und Rhodium durch flammenlose Atomabsorptionsspektrometrie unter Verwendung eines Massman-Ofens wurden untersucht. Die Nachweisgrenzen lagen im Bereich 10^{-9}–10^{-10} g. Der Einfluss von Säuren und gegenseitigen Störungen wurde geprüft. Der Einfluss des Probenvolumens auf die Atomabsorptionssignale wurde auf Temperaturunterschiede im Graphitrohr zurückgeführt. Die Reproduzierbarkeit beeinflussende Faktoren werden diskutiert.

REFERENCES

1 G. F. Kirkbright, *Analyst*, 96 (1971) 609.
2 S. Slavin, *Atomic Absorption Spectroscopy*, Interscience, New York, 1968.
3 B. V. L'vov, *Atomic Absorption Spectroscopy*, Israel Program for Scientific Translations, 1969.
4 F. J. Fernandez and D. C. Manning, *At. Absorption Newslett.*, 10 (1971) 65.
5 P. Hansen, *General and Methodical References for the Application of the Heated Graphite Atomizer HGA 70*, unpublished work 705/8. 71 from Bodenseewerk Perkin Elmer & Co. GMBH, Überlingen, Western-Germany.
6 P. H. Müller and P. Knoop, *Silic. Ind.*, 12 (1969).

Analytica Chimica Acta, 68 (1973) 49–60

EIN BEITRAG ZUM PROBLEM DER BANDENVERSCHIEBUNGEN IN DEN I.R.-SPEKTREN VON DIALKYLDITHIOCARBAMIDATEN

TEIL II. DIÄTHYL- UND TETRAMETHYLENDITHIOCARBAMIDATE. DER BEREICH VON 500–32 cm^{-1}

R. KELLNER

Institut für Analytische Chemie und Mikrochemie, Technische Hochschule, Wien (Österreich)

(Eingegangen den 29. Juli 1973)

In früheren Arbeiten wurde über die Bandenverschiebungen in den I.R.-Spektren von Diäthyl- und Tetramethylendithiocarbamidaten (DEDTC bzw. TMDTC) im Bereich von 4000 bis *ca.* 270 cm^{-1} und deren Anwendung zur qualitativen und quantitativen Analyse von Metallchelatgemischen berichtet[1,2]. Besonders die starken Verschiebungen der υ-M–S zwischen 400 und 300 cm^{-1} sowie gegebenenfalls auch der υ-C–N bei *ca.* 1500 cm^{-1} können zur direkten Analyse von bestimmten Metallionen ohne vorhergehenden Trennschritt herangezogen werden. In manchen Fällen kommt es jedoch auch im M–S bzw. C–N-Bereich der I.R.-Spektren zu Koinzidenzen, sodass der I.R.-spektroskopischen Analyse ein dünnschichtchromatographischer Trennschritt vorgeschaltet werden muss[3].

Bei der angegebenen Grenze von *ca.* 270 cm^{-1} handelte es sich nicht um eine physikalisch gegebene, sondern um eine rein messtechnisch begründete wilkürliche Grenze des Aufnahmebereiches. Daher war es von grossem Interesse, weiter in den Bereich des F.I.R. vorzustossen, um zu untersuchen, ob durch die in diesem Bereich in Analogie zu einfacheren Modellen[4] zu erwartenden weiteren M–S-, sowie Gitter- und Deformationsschwingungen Koinzidenzen höherfrequenter Banden umgangen werden können.

Mit dem Infrarotspektrophotometer Perkin-Elmer 180 wurden daher die I.R.-Spektren der DEDTC und der TMDTC von Mn^{3+}, Fe^{3+}, Co^{3+}, Ni^{2+}, Cu^{2+}, Zn^{2+}, MoO_2^{2+}, Cd^{2+}, Hg^{2+} und Pb^{2+} im Bereich von 500 bis 32 cm^{-1} registriert und im obengenannten Sinne ausgewertet. Es soll an dieser Stelle nicht unerwähnt bleiben, dass auch 32 cm^{-1} eine willkürliche, durch die Gerätetechnik begründete Grenze darstellt.

EXPERIMENTELLER TEIL

Die Herstellung und elementaranalytische Charakterisierung der untersuchten Verbindungen erfolgte wie früher beschrieben[2]. Die Substanzen wurden als Verreibungen in Paraffinöl zwischen Polyäthylenscheiben präpariert.

Die I.R.-Spektren wurden mit einem Gitterspektrophotometer Perkin-Elmer 180 mit F.I.R.-Zusatz (Gesamtaufnahmebereich 4000–32 cm^{-1}) registriert.

Die Aufnahmeparameter für den Bereich 500–32 cm^{-1} waren wie folgt: Strahlungsquelle: Hg-Dampflampe; Detektor: Triglycinsulfat; Spaltsteuerung: PROG 5, AGC on; Auflösung bei 500 cm^{-1}: 1.5 cm^{-1}, im Gesamtbereich stets unter 2 cm^{-1}; Registriergeschwindigkeit: 17 cm^{-1} min^{-1}; Zeitkonstante: 8.

Für die Bestimmung der relativen Intensitäten ist die Kenntnis der Abhängigkeit der Auflösung von der Wellenlänge der I.R.-Strahlung wesentlich. Um grössere Fehler zu vermeiden, darf die Auflösung nicht schlechter als 1/7 der Bandenhalbwertsbreite werden, was stets gegeben war.

SPEKTRENAUSWERTUNG UND DISKUSSION

Der Bereich unter 400 cm^{-1} zeigt sowohl bei den Diäthyl- als auch bei den Tetramethylendithiocarbamidaten eine Reihe von stark lage- und intensitätsinkonstanten Absorptionsbanden, die nach der Literatur[4,5] symmetrischen Metall–Ligand- sowie Gerüst- und Deformationsschwingungen zuzuordnen sind. Diese Banden können, wie nun gezeigt werden soll, sehr gut zur Charakterisierung ähnlich aufgebauter Moleküle herangezogen werden. Während sich die Spektren der Metallchelate im Bereich von 1400 cm^{-1} bis 400 cm^{-1} kaum voneinander unterscheiden lassen[2], kann der Bereich unter 400 cm^{-1} als echter "Fingerprint"-Bereich bezeichnet werden. Als Bezug für die Bestimmung der relativen Intensität der Absorptionsbanden im F.I.R.-Bereich wurde die jeweilige υ_{as}-M–S ausgewählt (s. Tabelle I).

TABELLE I

LAGE DER υ_{as}-M–S VON DEDTC UND TMDTC IN NUJOL UND KBr

	DEDTC (cm^{-1})		*TMDTC (cm^{-1})*	
	Nujol	*KBr*	*Nujol*	*KBr*
Mn(III)	376	380, 370	317	320
Fe(III)	355, 334	355, 330	325	325
Co(III)	360	363	354	355
Ni(II)	388	392	383	385
Cu(II)	356	360	339	340
Zn(II)	333	335	343	343
Mo(VI)	382	383	369	370
Cd(II)	329	330	323	325
Hg(II)	331	333	365	370
Pb(II)	324	325	305	305

Tetramethylendithiocarbamidate

Abbildung 1 zeigt die F.I.R.-Spektren der untersuchten TMDTC in reduzierter Form zum besseren Überblick über die Bandenverschiebungen. Besonders bezeichnet (●) sind die υ_{as}-M–S, denen willkürlich die Intensität 1 zugeordnet wurde. Der Abbildung liegen Spektren zu Grunde, deren maximale Absorption 40% nicht übersteigt (mit Ausnahme von Ni–TMDTC). Dadurch werden einige schwache Absorptionsbanden nicht sichtbar, das Bild wird übersichtlicher.

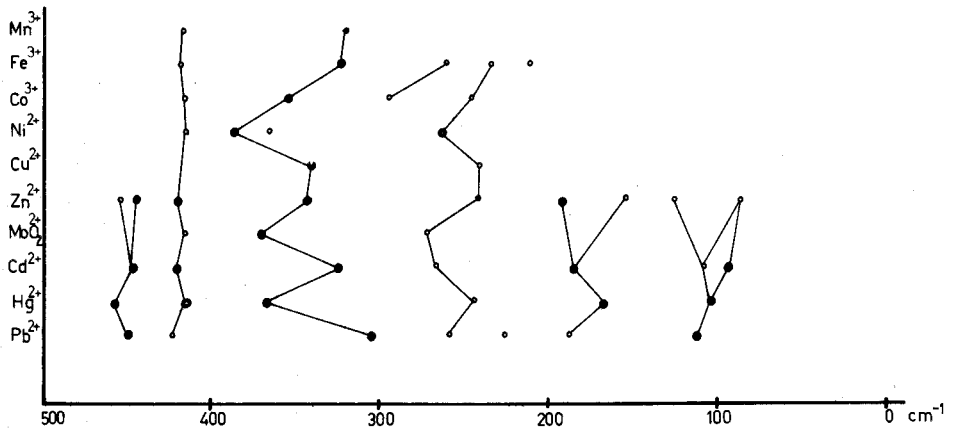

Abb. 1. Übersicht über die F.I.R.-Spektren einiger Tetramethylendithiocarbamidate (in Nujol, Polyäthylenfenster).

Es zeigt sich, dass die Verbindungen auf Grund der Lage der Banden und deren relativer Intensitäten in Gruppen eingeteilt werden können, welche der zu erwartenden Koordination der Liganden am Zentralatom entsprechen[6–8].

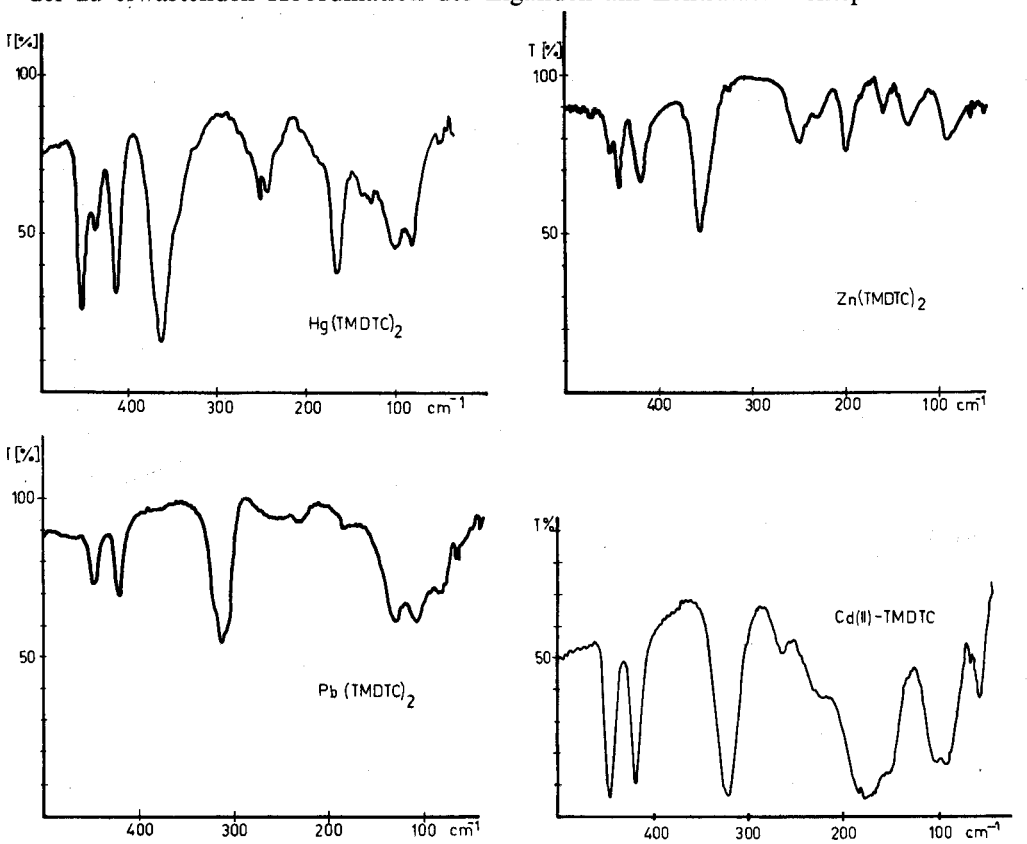

Abb. 2. F.I.R.-Spektren von TMDTC mit tetraedrischer Koordination.

TABELLE II

F.I.R.-SPEKTREN VON TMDTC MIT TETRAEDRISCHER KOORDINATION

$Zn(TMDTC)_2$		$Cd(TMDTC)_2$		$Hg(TMDTC)_2$		$Pb(TMDTC)_2$	
$\upsilon(cm^{-1})$	E_{M-S}/E	$\upsilon(cm^{-1})$	E_{M-S}/E	$\upsilon(cm^{-1})$	E_{M-S}/E	$\upsilon(cm^{-1})$	E_{M-S}/E
454	sh	446	0.8	455	1.3	446	2.5
444	1.7	419	1.2	440	3.8	420	2.0
419	1.9	323	1.0	415	1.6	312	sh
343	1.0	266	9.5	365	1.0	305	1.0
241	0.9	225	sh	244	2.5	230	8.0
225	sh	180	1.1	166	1.5	129	sh
192	0.7	156	sh	100	2.6	107	1.1
156	2.4	107	1.8	81	2.6	79	sh
129	2.0	95	1.7				
89	1.9	61	3.3				

Auftreten starker Absorptionen unter 100 cm^{-1}: TMDTC mit tetraedrischer Koordination: Zn^{2+}, Cd^{2+}, Hg^{2+} und Pb^{2+}. Abbildung 2 zeigt die I.R.-Spektren der Vertreter dieser Gruppe mit linearer Darstellung der Durchlässigkeit. Die genaue Lage sämtlicher, auch der erst bei 100%iger Absorption der υ-M–S auftretender Banden bis 32 cm^{-1} sowie deren relative Intensitäten, bezogen auf die υ_{as}-M–S gibt Tabelle II an.

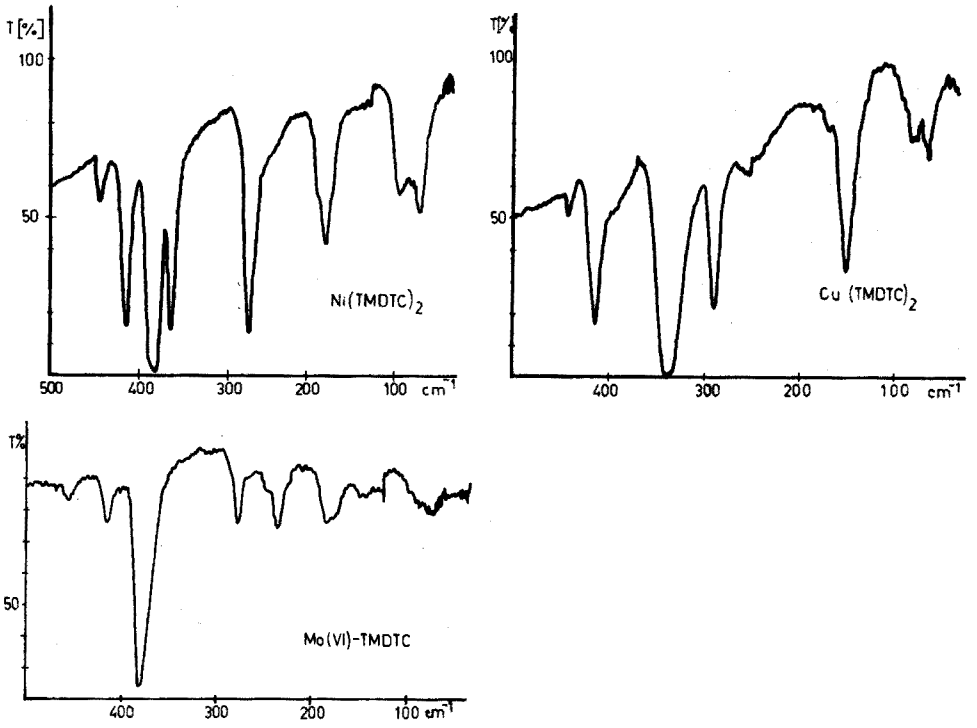

Abb. 3. F.I.R.-Spektren von TMDTC mit quadratisch-planarer Koordination.

Die F.I.R.-Spektren dieser Verbindungen unterscheiden sich von allen übrigen untersuchten Spektren durch das Auftreten einer starken Absorption bei und unter 100 cm^{-1} sowie durch weitere breite Absorptionsbanden, die zusammen ein charakteristisches Fingerprintmuster ergeben.

Fehlen starker Absorptionen im Bereich unter 250 cm^{-1}: TMDTC mit planarer Koordination: Ni^{2+}, Cu^{2+} und MoO_2^{2+}. Abbildung 3 zeigt die F.I.R.-Spektren von $Ni(TMDTC)_2$, $Cu(TMDTC)_2$ und $MoO_2(TMDTC)_2$. Die genaue Lage sämtlicher, auch der erst bei 100%iger Absorption der υ-M–S auftretender Banden bis 32 cm^{-1} sowie deren relative Intensitäten, bezogen auf die υ-M–S, gibt Tabelle III an. Werden die F.I.R.-Spektren dieser Verbindungen mit einer Extinktion der υ-M–S von maximal 0.4 registriert, so treten nur noch eine (Mo, Cu), höchstens zwei (Ni) Banden geringer Intensität im Bereich unter der υ-M–S auf. Dieses Fehlen von starken Absorptionsbanden ist charakteristisch.

TABELLE III

F.I.R.-SPEKTREN VON TMDTC MIT PLANARER KOORDINATION

$Ni(TMDTC)_2$		$Cu(TMDTC)_2$		$MoO_2(TMDTC)_2$	
$\upsilon(cm^{-1})$	E_{M-S}/E	$\upsilon(cm^{-1})$	E_{M-S}/E	$\upsilon(cm^{-1})$	E_{M-S}/E
444	28	444	42	455	20
415	4.8	415	3.5	416	7
383	1	339	1	369	1
364	4	290	4.2	272	4.5
262	3	252	40	234	6
182	sh	148	10	183	7.5
174	12	78	>40	175	sh
92	35				

Auftreten charakteristischer starker Absorptionen zwischen 300 und 115 cm^{-1}: TMDTC mit oktaedrischer Koordination: Mn^{3+}, Fe^{3+} und Co^{3+}. Abbildung 4 zeigt die F.I.R.-Spektren der Vertreter dieser Gruppe. Die genaue Lage sämtlicher, auch der erst bei 100%iger Absorption der υ-M–S, auftretender Banden bis 32 cm^{-1} sowie deren relative Intensitäten, bezogen auf die υ-M–S, gibt Tabelle IV an. Die F.I.R.-Spektren der TMDTC mit oktaedrischer Struktur zeigen zum Unterschied zu den Analoga mit tetraedrischer Koordination keine starke Absorption bei 100 cm^{-1}.

Diäthyldithiocarbamidate

Die F.I.R.-Spektren der DEDTC unterscheiden sich von den Spektren der analogen TMDTC prinzipiell durch das Auftreten mehrerer (meist dreier) Absorptionsbanden zwischen 400 und 300 cm^{-1}, von denen eine infolge ihrer grossen Frequenzverschiebung der υ-M–S zugeordnet wird[2]. Die übrigen Banden sind dagegen weitaus lagestabiler und dürften von Deformationsschwingungen der Äthylgruppen stammen, die in den TMDTC infolge der Ringbildung im Liganden nicht auftreten können (s. Abb. 5).

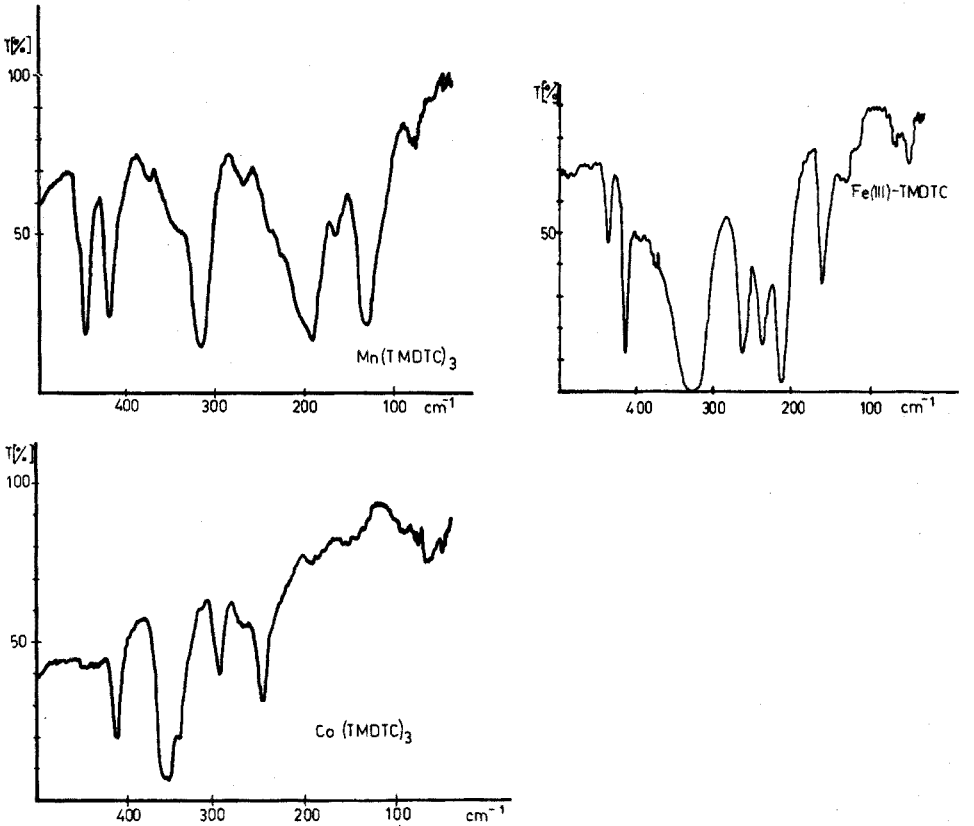

Abb. 4. F.I.R.-Spektren von TMDTC mit oktaedrischer Koordination.

TABELLE IV

F.I.R.-SPEKTREN VON TMDTC MIT OKTAEDRISCHER KOORDINATION

$Mn(TMDTC)_3$		$Fe(TMDTC)_3$		$Co(TMDTC)_3$	
$\upsilon(cm^{-1})$	E_{M-S}/E	$\upsilon(cm^{-1})$	E_{M-S}/E	$\upsilon(cm^{-1})$	E_{M-S}/E
454	sh	449	28	450	>30
446	1	418	5.7	414	2.6
419	1.6	325	1	359	sh
375	15	259	7.8	351	1
345	sh	235	8.5	340	sh
317	1	210	1.8	295	5.2
270	15	159	25	266	sh
228	sh	130	>30	246	2.5
205	sh	50	>30	190	>30
192	1.4			150	>30
165	11				
128	2.5				

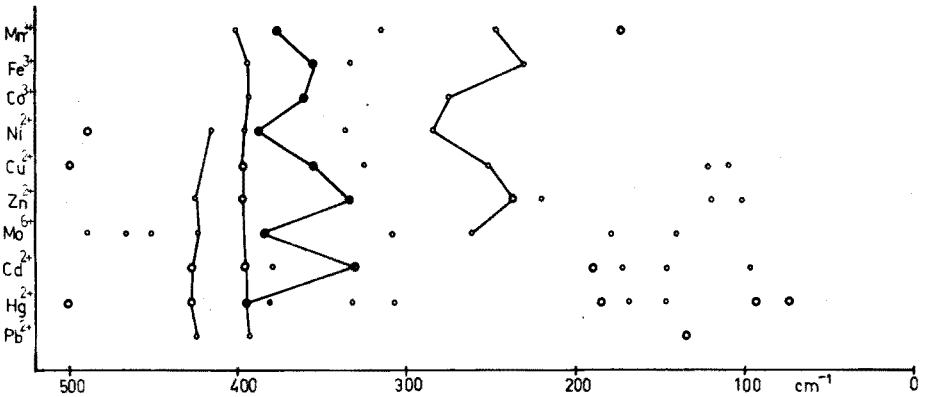

Abb. 5. Übersicht über die F.I.R.-Spektren einiger Diäthyldithiocarbamidate (in Nujol, Polyäthylenfenster).

Durch Vergleich von Lage und relativer Intensität der Banden im F.I.R.-Bereich ergibt sich jedoch eine ähnliche Möglichkeit zur Einteilung in Strukturklassen wie bei den TMDTC (s. oben).

Lediglich die Verbindungen $Cu(DEDTC)_2$ und $MoO_2(DEDTC)_2$ lassen sich nicht exakt in Gruppen einordnen. Offensichtlich treten hier—besonders bei $Cu(DEDTC)_2$—Abweichungen von der quadratisch-planaren Koordination auf (s. Diskussion).

Auftreten starker Absorptionen um 100 cm^{-1}: DEDTC mit tetraedrischer Koordination: Zn^{2+}, Cd^{2+}, Hg^{2+} und Pb^{2+} (Abb. 6). Die genaue Lage sämtlicher, auch der erst bei 100%iger Absorption der υ-M–S auftretender Banden bis 32 cm^{-1} sowie deren relative Intensitäten, bezogen auf die υ-M–S gibt Tabelle V an. Auf Grund des Auftretens einer Bande bei 126 cm^{-1} mit einer Schulter bei 110 cm^{-1} könnte $Cu(DEDTC)_2$ ebenfalls dieser Strukturklasse zugeordnet werden. Allerdings ist das Verhältnis E_{M-S}/E mit 7.3 zu gross (vgl. $Pb(TMDTC)_2$: $E_{M-S}/E_{132}=0.8$).

TABELLE V

F.I.R.-SPEKTREN VON DEDTC MIT TETRAEDRISCHER KOORDINATION

$Zn(DEDTC)_2$		*$Cd(DEDTC)_2$*		*$Hg(DEDTC)_2$*		*$Pb(DEDTC)_2$*	
$\upsilon(cm^{-1})$	E_{M-S}/E	$\upsilon(cm^{-1})$	E_{M-S}/E	$\upsilon(cm^{-1})$	E_{M-S}/E	$\upsilon(cm^{-1})$	E_{M-S}/E
425	0.8	506	1.1	508	1.2	502	3.3
398	0.3	432	sh	427	0.7	423	3.3
377	0.4	426	0.7	394	0.6	390	1.4
333	1	395	0.4	380	1	357	1
238	0.3	379	0.5	331	3.3	350	sh
222	sh	329	1	306	4.3	324	1
152	1.1	311	4	183	1.2	154	sh
100	2	190	0.5	146	sh	133	0.8
76	1.5	146	1.3	94	1.2		
		96	0.9	75	0.7		

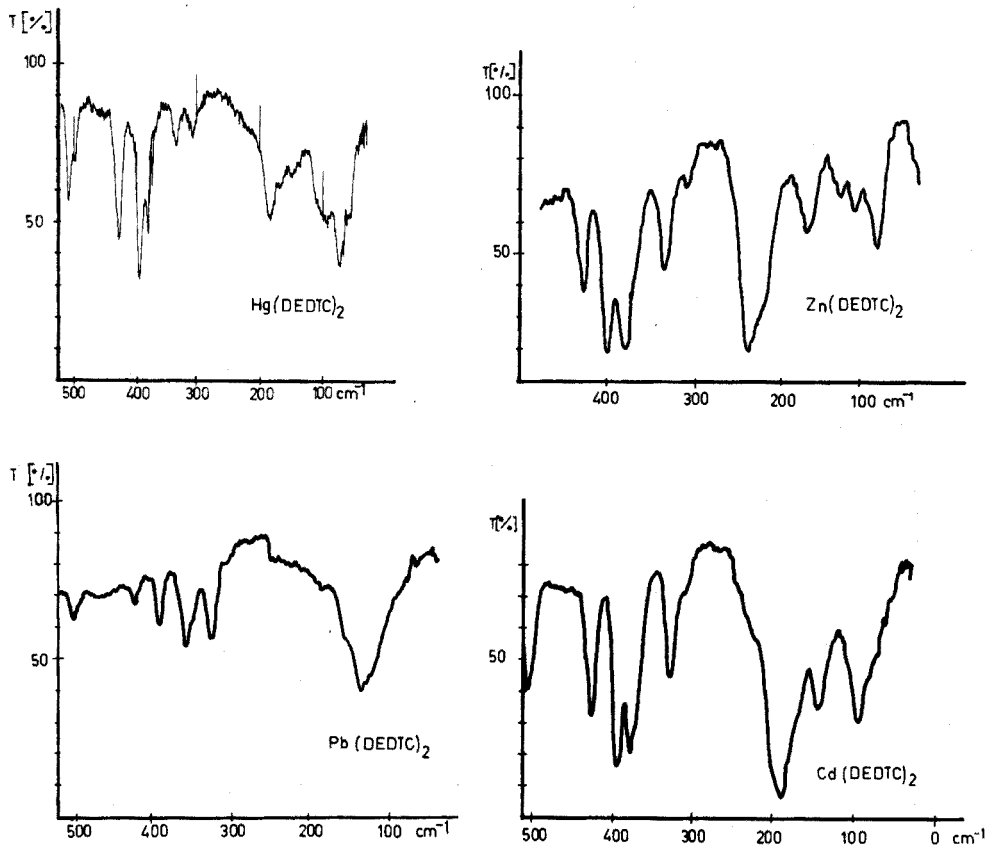

Abb. 6. F.I.R.-Spektren von DEDTC mit tetraedrischer Koordination.

Fehlen starker Absorptionen im Bereich unter 250 cm^{-1}: DEDTC mit planarer oder verzerrt planarer Koordination: Ni^{2+}, MoO_2^{2+} und Cu^{2+} (Abb. 7). Die genaue Lage sämtlicher, auch der erst bei 100%iger Absorption der υ-M–S

TABELLE VI

F.I.R.-SPEKTREN VON DEDTC MIT PLANARER ODER VERZERRT PLANARER KOORDINATION

$Ni(DEDTC)_2$		*$Cu(DEDTC)_2$*		*$MoO_2(DEDTC)_2$*	
$\upsilon(cm^{-1})$	E_{M-S}/E	$\upsilon(cm^{-1})$	E_{M-S}/E	$\upsilon(cm^{-1})$	E_{M-S}/E
490	6	498	4.4	488	4.9
417	6.3	397	2.3	423	10
397	sh	392	sh	402	sh
388	1	356	1	382	1
336	3	326	2.2	308	1
285	5.4	253	8.3	260	3
183	3	126	7.3	178	4.2

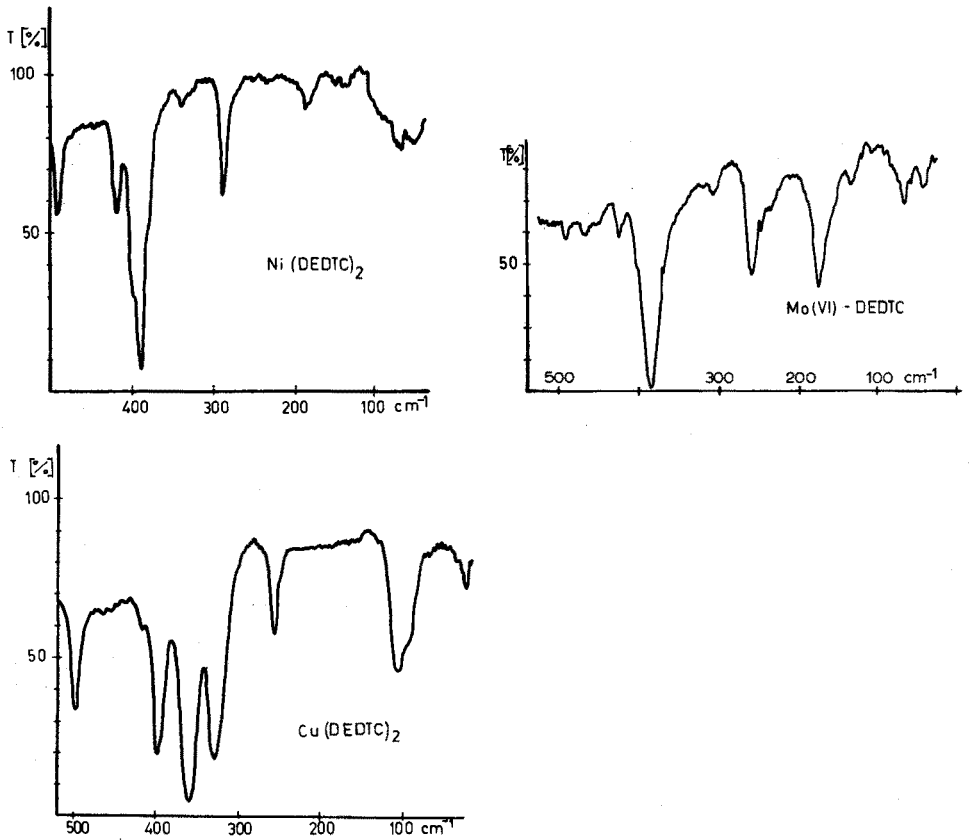

Abb. 7. F.I.R.-Spektren von DEDTC mit planarer oder verzerrt planarer Koordination.

auftretender Banden bis 32 cm^{-1} sowie deren relative Intensitäten, bezogen auf die υ-M–S gibt Tabelle VI an. Auf Grund von Literaturdaten[4] ist zu erwarten, dass das Kupfer in $Cu(DEDTC)_2$ planar koordiniert ist. Die vorliegenden I.R.-Spektren lassen jedoch eine eindeutige Zuordnung zu einer der beiden Gruppen (planar oder tetraedrisch) nicht zu. Da auch die Lage der υ-C–N (in KBr 1500 cm^{-1}, in Nujol 1505 cm^{-1}) nicht eindeutig ist[2,7], wird angenommen, dass es sich hier um einen Grenzfall handelt. Ähnliches gilt[8] auch für $MoO_2(DEDTC)_2$.

Auftreten einer charakteristischen Absorption zwischen 300 und 150 cm^{-1}: DEDTC mit oktaedrischer Koordination: Mn^{3+}, Fe^{3+} und Co^{3+}. Als charakteristische Vertreter zeigt Abb. 8 die F.I.R.-Spektren von $Fe(DEDTC)_3$, $Mn(DEDTC)_3$, und $Co(DEDTC)_3$. Die genaue Lage sämtlicher, auch der erst bei 100%iger Absorption der υ-M–S auftretender Banden bis 32 cm^{-1} sowie deren relative Intensitäten, bezogen auf die υ-M–S, gibt Tabelle VII an. In dieser Verbindungsklasse tritt nur eine Bande unter 300 cm^{-1} auf, die im Falle des $Co(DEDTC)_3$ äusserst schwach ist.

DISKUSSION

Wie die angegebenen Daten beweisen, lässt sich auf Grund der Lage und

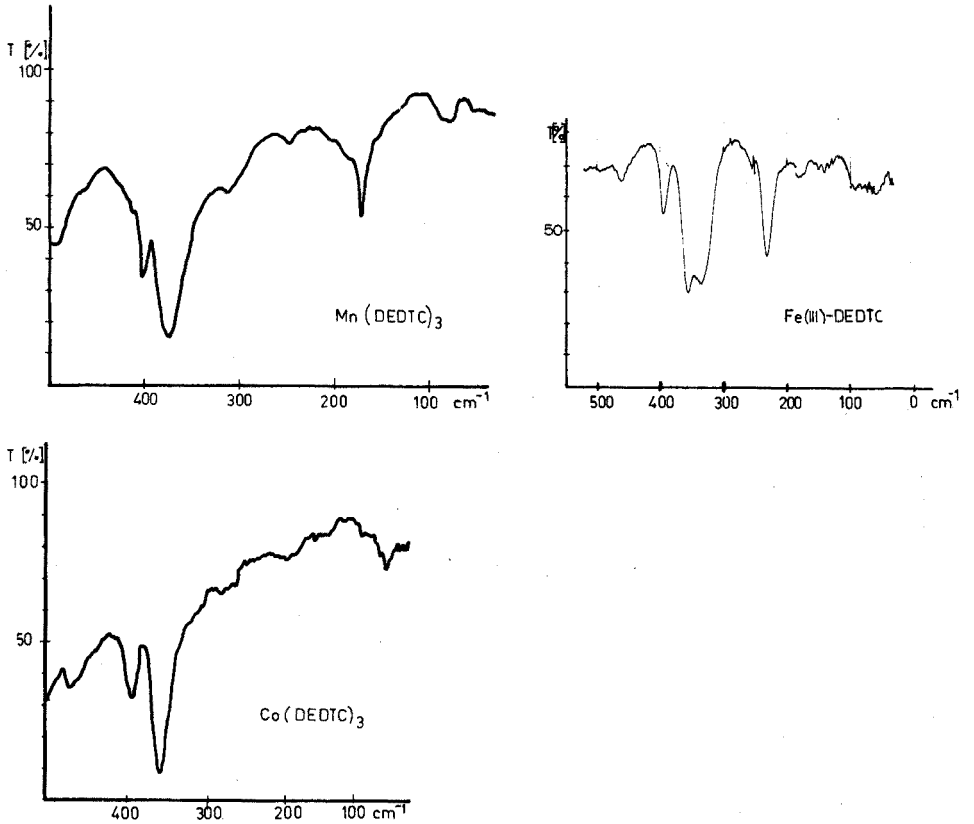

Abb. 8. F.I.R.-Spektren von DEDTC mit oktaedrischer Koordination.

TABELLE VII

F.I.R.-SPEKTREN VON DEDTC MIT OKTAEDRISCHER KOORDINATION

$Mn(DEDTC)_3$		$Fe(DEDTC)_3$		$Co(DEDTC)_3$	
$\upsilon(cm^{-1})$	E_{M-S}/E	$\upsilon(cm^{-1})$	E_{M-S}/E	$\upsilon(cm^{-1})$	E_{M-S}/E
401	3.2	460	7.6	500	9
376	1	355	1	470	11
315	sh	334	sh	393	4.1
248	33	230	2.2	360	1
174	3.5	190	7.6	184	30
85	35	150	30	61	30

der relativen Maximalextinktionen der Absorptionsbanden in den F.I.R.-Spektren von TMDTC und – mit Ausnahmen—auch von DEDTC eine Klassifizierung der Verbindungen in die Strukturklassen tetraedrisch, oktaedrisch und quadratisch-planar durchführen. Wie Abb. 9 zeigt, gilt als Kennzahl für die Zugehörigkeit einer Verbindung zu einer bestimmten Gruppe das Verhältnis der Extinktionen

der υ_{as}-M–S (s. Tabelle I) und der jeweils stärksten der übrigen Banden im F.I.R.

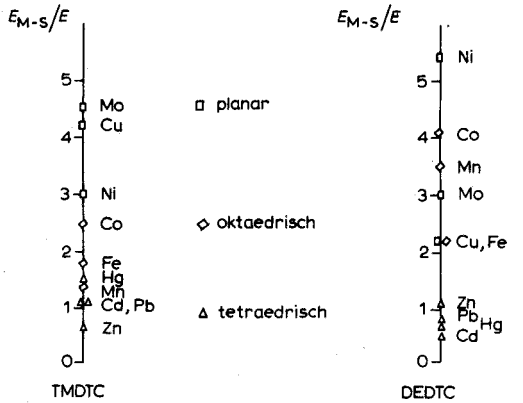

Abb. 9. Charakteristische Grenzwerte der E_{M-S}/E-Verhältnisse zur Einteilung der TMDTC und DEDTC in Strukturklassen.

Die sich bei den TMDTC ergebende Überlappung im Falle $Hg(TMDTC)_2$ und $Mn(TMDTC)_3$ ist durch die unterschiedliche Bandenlage kompensiert (s. Tabellen II und IV).

Bei den DEDTC ist nur der Bereich der tetraedrischen Koordination ausser Diskussion gestellt. $Ni(DEDTC)_2$ zeigt wie $Ni(TMDTC)_2$ ein hohes E_{M-S}/E-Verhältnis. Dagegen kommen $MoO_2(DEDTC)_2$ und $Cu(DEDTC)_2$ in der Gruppe der oktaedrisch koordinierten Chelate zu liegen. Diese Abweichung deutet darauf hin, dass verzerrte Strukturen vorliegen. Auch die Lage der strukturempfindlichen ν-C–N deutet auf ein Grenzverhalten hin[7].

Neben der Bedeutung der F.I.R.-Spektren zur Klassifizierung der TMDTC und der DEDTC in Strukturgruppen ermöglichen die unterschiedlichen Bandenlagen unter 300 cm^{-1} die Umgehung der im M–S-Bereich und darüber auftretenden Koinzidenzen.

Es können z.B. $Cu(TMDTC)_2$–$Zn(TMDTC)_2$ sowie $Fe(DEDTC)_3$–$Cu(DEDTC)_2$ und $Zn(DEDTC)_2$–$Cd(DEDTC)_2$ auf Grund ihrer F.I.R.-Spektren erstmals leicht identifiziert werden. Diese Möglichkeit zur Analyse ähnlicher Verbindungen im F.I.R. lässt sich prinzipiell für alle ähnlich aufgebauten Verbindungen anwenden.

Herrn Prof. Dr. H. Malissa möchte ich an dieser Stelle für die wertvolle Förderung dieser Arbeit herzlich danken. Dem Fonds zur Förderung der wissenschaftlichen Forschung danke ich für das zur Verfügung gestellte Infrarotspektrophotometer Perkin-Elmer 180.

ZUSAMMENFASSUNG

Die unter konstanten Registrierbedingungen aufgenommenen F.I.R.-Spektren der Diäthyl- und Tetramethylendithiocarbamidate von Co^{3+}, Mn^{3+}, Fe^{3+}, Ni^{2+}, Cu^{2+}, Zn^{2+}, MoO_2^{2+}, Cd^{2+}, Hg^{2+} und Pb^{2+} im Bereich von 500–32 cm^{-1}

werden erstmals beschrieben. Die Auswertung der F.I.R.-Spektren nach der Lage und der relativen Intensität der unter 400 cm^{-1} auftretenden Absorptionsbanden erlaubt eine Klassifizierung der untersuchten Metallchelate nach der Koordination des Zentralatoms in planare, tetraedrische und oktaedrische Komplexe. Daneben kann der Bereich unter 400 cm^{-1} als echter "Fingerprint"-Bereich dienen und zur Umgehung von Koinzidenzen im höherfrequenten Teil der I.R.-Spektren einiger Metalldithiocarbamidate herangezogen werden, was für die Analyse ähnlich aufgebauter Substanzen allgemein von grosser Bedeutung ist.

SUMMARY

The far infrared spectra of the diethyl- and tetramethylenedithiocarbamates (DEDTC and TMDTC) of Mn^{3+}, Fe^{3+}, Co^{3+}, Ni^{2+}, Cu^{2+}, Zn^{2+}, MoO_2^{2+}, Cd^{2+}, Hg^{2+} and Pb^{2+} in the region of 500–32 cm^{-1} are described. The evaluation of both position and absorbance of the bands in the far i.r. enables a classification of the metal chelates as planar, tetrahedral and octahedral coordinated compounds. Moreover, the region below 400 cm^{-1} can be used as a real "fingerprint"-region and can serve to bypass several coincidences in the higher frequency part of the i.r. spectra of metal chelates. This is of general importance for the i.r.-spectrometric analysis of solid substances with similar structure.

RÉSUMÉ

Une étude est effectuée sur les spectres infra-rouges (région de 500 à 32 cm^{-1}) des diéthyl- et tétraméthylènedithiocarbamates (DEDTC et TMDTC) de Mn^{3+}, Fe^{3+}, Co^{3+}, Ni^{2+}, Cu^{2+}, Zn^{2+}, MoO_2^{2+}, Cd^{2+}, Hg^{2+} et Pb^{2+}. L'évaluation de la position et de l'absorbance des bandes permet de classifier les chélates métalliques en composés diversément coordinés. En outre, la zone en dessous de 400 cm^{-1} peut être utilisée comme une réelle "empreinte digitale" et permettre d'éviter plusieurs coïncidences dans la partie de fréquence plus élevée du spectre i.r. des chélates métalliques. Ceci est d'une importance générale pour l'analyse spectrométrique i.r. de substances solides ayant une structure similaire.

LITERATUR

1 H. Malissa und R. Kellner, *Anal. Chim. Acta*, 63 (1973) 263.
2 R. Kellner, *Anal. Chim. Acta*, 63 (1973) 277.
3 H. Malissa, R. Kellner und P. Prokopowski, *Anal. Chim. Acta*, 63 (1973) 225.
4 K. Nakamoto, *Infrared Spectra of Inorganic and Coordination Compounds*, Wiley, New York, 2. Aufl., 1970.
5 A. Finch, P. N. Gates, K. Radcliffe, F. N. Dickson und F. F. Bentley, *Chemical Application of Far Infrared Spectroscopy*, Academic Press, London, 1970.
6 M. Bonamico, G. Dessy, C. Mariani, A. Vaciago und L. Zambonelli, *Acta Crystallogr.*, 19 (1965) 619.
7 J. Chatt, L. A. Duncanson und L. M. Venanzi, *Suom. Kemistilehli B*, 29 (1956) 75.
8 R. N. Jowitt und P. C. N. Mitchell, *J. Chem. Soc., A*, (1970) 1702.

Analytica Chimica Acta, 68 (1974) 61–71

ANALYTICAL STUDY OF TWO DIAZOTIZATION–COUPLING REACTIONS

APPLICATION TO THE DETERMINATION OF NANO-AMOUNTS OF NITRITE IN WATER

F. CELARDIN, M. MARCANTONATOS and D. MONNIER

Department of Inorganic and Analytical Chemistry, University of Geneva, Geneva (Switzerland)

(Received 20th July 1973)

The methods for the detection and determination of nitrite and nitrite precursors have been reviewed by Kolthoff and Elving[1], Streuli and Averell[2] and Sawicki *et al.*[3]. Sawicki *et al.* discussed a series of autocatalytic methods for the determination of nitrite by free radical chromogens[4] and reported a preliminary comparison between 36 new spectrophotometric methods many of which have a higher sensitivity than the Griess reagent[5]. Among those methods only the one using a *p*-nitroaniline–azulene reagent has been developed by Garcia[6]. Another method for nitrite determination by solvent extraction and spectrophotometry of the azo dye, and more recently a very sensitive fluorimetric method which has the disadvantage of being more lengthy than the Griess-type methods, have been published by Foris and Sweet[7] and by Dombrowski and Pratt[8], respectively.

In view of the increasing interest in the quality of natural waters, very sensitive and rapid methods for nitrite ion determination seem desirable. With this scope in mind, a method, among those reported by Sawicki *et al.*[5], based on the formation of an azo dye anion ($\varepsilon_{618} = 89000$) between 4-aminoacetophenone and N-phenyl-1-naphthylamine, has been developed and is proposed for the determination of nano-traces of nitrite. Methods based on the azo dye cation of the same reagents in strong acidic medium ($\varepsilon_{568} = 49000$), and on the use of 4-aminoacetophenone and N-phenyl-2-naphthylamine have also been developed. The azo dye formed in this last case has an absorption wavelength at 524 nm which is independent of pH within the limits 0 to 13.3 and has a molar absorptivity of 18300. The structures of the absorbing species are discussed below. Except for their differences in sensitivity, these techniques have in common the advantages of procedural simplicity, colour stability, selectivity and reproducibility.

The reactions involved are the diazotization of 4-aminoacetophenone by nitrous acid followed by coupling with either N-phenyl-1-naphthylamine or N-phenyl-2-naphthylamine.

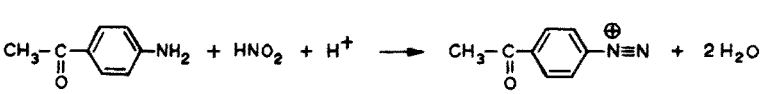

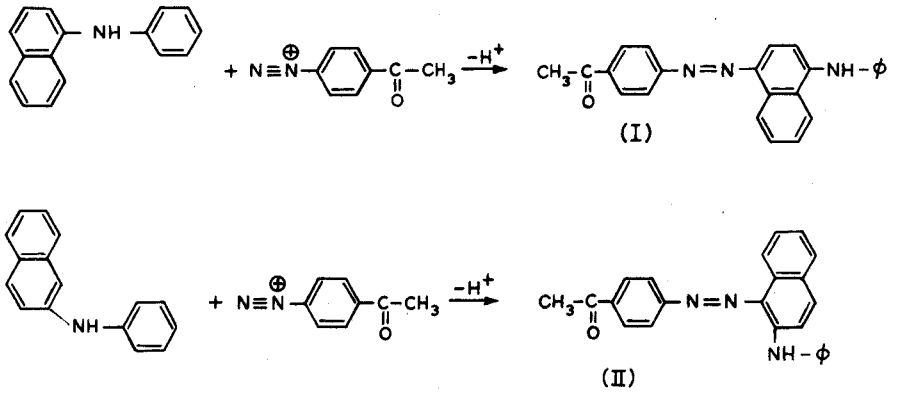

EXPERIMENTAL

Apparatus

Spectra and absorbance values were recorded with Unicam SP 8000, Beckman DB-G and Zeiss PMQ-II spectrophotometers with either 1-cm or 5-cm quartz cells. pH values were determined with a Metrohm E 520 pH meter equipped with a combined glass electrode. A Tottoli apparatus was used for melting point determinations.

Reagents

4-Aminoacetophenone (Fluka) and N-phenyl-2-naphthylamine (Fluka) were recrystallized in a chloroform–methanol mixture to give melting points of 104° and 107°, respectively. N-Phenyl-1-naphthylamine (Schuchardt) was used without recrystallization. No difference was noticed between the absorbances measured in N,N-dimethylformamide (Merck) "Uvasol" and "for synthesis", hence the latter quality was adopted without further purification. Tetraethylammonium hydroxide, 25% in water, was Fluka pract. All other solvents were Merck G.R.

Synthesis and isolation of the dyes

4-Aminoacetophenone (1.35 g; 0.01 mole) was dissolved in 300 ml of 2 *M* hydrochloric acid cooled to 0–5° by addition of ice. To this, an aqueous solution of sodium nitrite (0.69 g; 0.01 mole) was added slowly with stirring. A solution of 2.15 g (0.0098 mole) of N-phenyl-1-naphthylamine (or N-phenyl-2-naphthylamine) in 10 ml of DMF was then added dropwise with strong stirring. The dye was filtered, washed and recrystallized from a water–ethanol mixture.

Compound I precipitated as a chlorohydrate (m.p. 260° decomp.). Its free amino forms were obtained by recrystallization from an alkaline water–ethanol mixture (m.p. 186°).

Elemental analysis of the amine and its chlorohydrate yielded results that agreed well with the theoretical values. For the chlorohydrate of I: found: 71.67% C, 5.00% H, 10.45% N; calculated: 71.73% C, 4.98% H, 10.46% N. For the free amine of I: found: 78.92% C, 5.33% H, 11.35% N; calculated: 78.94% C, 5.20% H, 11.50% N.

RESULTS AND DISCUSSION

Absorption spectra

N-Phenyl-1-naphthylamine–4-azoacetophenone (I) exhibits an absorption spectrum which is pH-dependent (Fig. 1). The absorption peak at 618 nm in strong basic medium shifts to 520 nm at lower pH values. In strong acidic medium the

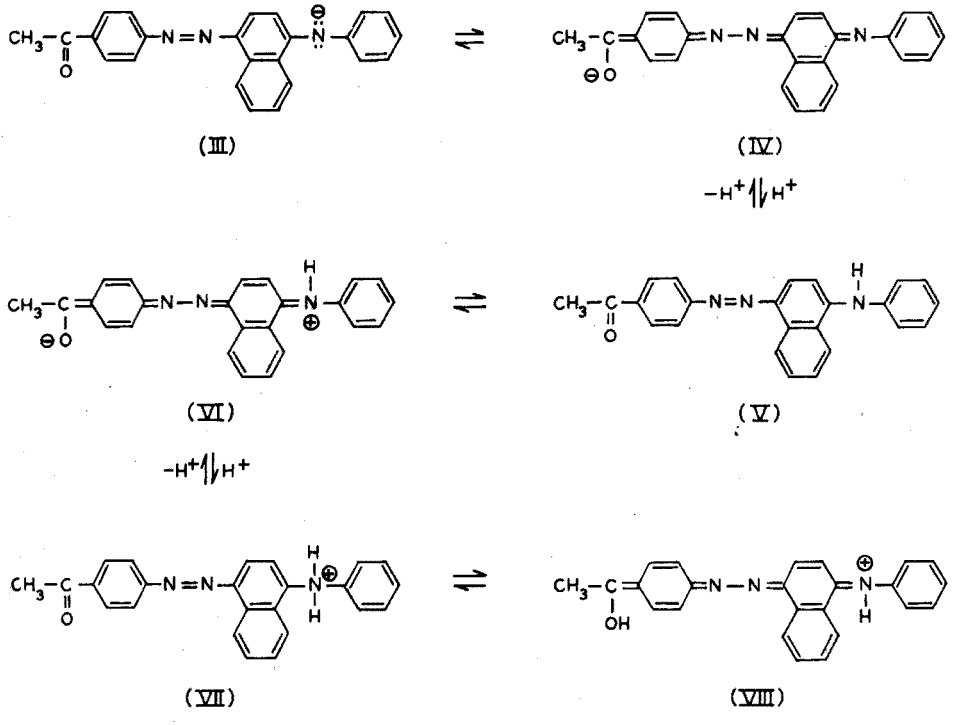

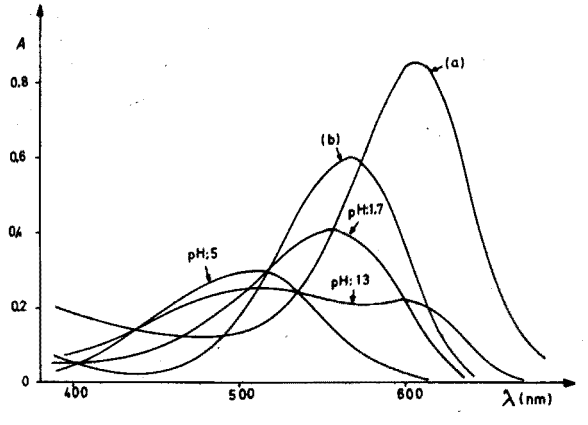

Fig. 1. Absorption spectra of N-phenyl-1-naphthylamine–4-azoacetophenone at different pH. $C_T = 1.1 \cdot 10^{-5}$ *M*. (a) (1+1) ethanol–tetraethylammonium hydroxide (25% in H_2O); (b) (1+1) ethanol–HCl conc. (37%).

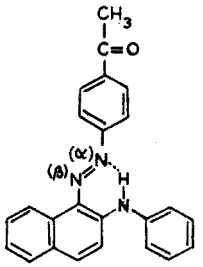

(IX)

absorption is displaced to 568 nm. Those variations in absorption maxima occur via two isosbestic points at 545 and 525 nm.

This behaviour may be explained by the following equilibria between the anionic, zwitterionic and cationic forms of (I).

The bathochromic shift with the anionic form results most probably from the strong charge delocalization; in the cationic form, the charge is localized on the nitrogen of the amino group, and the absorption occurs at a shorter wavelength. With regard to the zwitterionic form, it appears from the bathochromic displacements caused by a proton addition to the negatively charged end and by the increase of solvent polarity (Table I), that the neutral form (V) of the molecule is responsible for the observed absorption spectrum[9].

TABLE I

MAXIMAL ABSORBANCE WAVELENGTHS IN DIFFERENT SOLVENTS

Solvent	*Wavelength (nm)*
Benzene	470
Acetone	482
2-Methoxyethanol	496
N,N-Dimethylformamide	500
Pyridine	502

N-Phenyl-2-naphthylamine–1-azoacetophenone (II) has an absorption at 524 nm which is independent of the pH in the range 0 to 14. This feature of the reagent may be explained by the presence of a strong intramolecular hydrogen bond (IX). Thus, in acidic medium the electron pair of the nitrogen cannot participate in the resonance of the cationic structure and in basic medium, the hydrogen of the amino group which exhibits a very low acidity (see next paragraph) is further retained by the hydrogen bond and the anionic species is not formed.

Determination of the dissociation constants of N-phenyl-1-naphthylamine–4-azoacetophenone (I)

The spectral observations above indicate that in the case of (I) the following equilibria are operative:

$$R^- + H^+ \rightleftharpoons RH \qquad K_1 = [R^-][H^+]/[RH] = 1/\beta_1$$
$$RH + H^+ \rightleftharpoons RH_2^+ \qquad K_2 = [RH][H^+]/[RH_2^+] = \beta_1/\beta_2$$

The method described by Yatsimirskii and Vasil'ev[10] was applied to determine β_1 and β_2. Since the dye is insoluble in water alone, a solvent mixture (1+1 ethanol+water) was used for this determination. The pH was varied with hydrochloric acid or tetraethylammonium hydroxide.

Three series of measurements of 120 points each at 500, 550 and 570 nm were performed within the pH range 0–13.3.

Starting from the relation:

$$\bar{\varepsilon} - \varepsilon_0 = \frac{(\varepsilon_1 - \varepsilon_0)\beta_1[H^+] + (\varepsilon_2 - \varepsilon_0)\beta_2[H^+]^2}{1 + \beta_1[H^+] + \beta_2[H^+]^2} \tag{1}$$

where $\bar{\varepsilon} = D/C_T$, D is the absorbance measured at the given wavelength, ε_0, ε_1, ε_2 are the molar absorptivities of R^-, RH, and RH_2^+, and C_T is total concentration of the dye; one can deduce the following simultaneous equations:

$$a_1 = (\varepsilon_1 - \varepsilon_0)\beta_1$$
$$a_2 = (\varepsilon_2 - \varepsilon_0)\beta_2 - (\varepsilon_1 - \varepsilon_0)\beta_1^2$$
$$b_1 = (\varepsilon_2 - \varepsilon_0)$$
$$b_2 = [(\varepsilon_1 - \varepsilon_0) - (\varepsilon_2 - \varepsilon_0)]\frac{\beta_1}{\beta_2}$$

The value of ε_0 which is required at the start was obtained directly from the absorption spectra. a_1, a_2, b_1 and b_2 were obtained by successive extrapolations from experimental results. With those values, the equations yielded ε_1, ε_2, β_1 and β_2, which were reintroduced into eqn. (1) and were adjusted to give the best fit with the experimental curves (Fig. 2). The results are given in Table II.

TABLE II

DISSOCIATION CONSTANTS FOR N-PHENYL-1-NAPHTHYLAMINE-4-AZO-ACETOPHENONE

λ(nm)	ε_0	ε_1	ε_2
500	9000	25000	12000
550	26000	18000	46000
570	42000	10000	53000
$\beta_1 = 5 \cdot 10^{13}$		$K_1 = 2 \cdot 10^{-14}$	
$\beta_2 = 5 \cdot 10^{15}$		$K_2 = 10^{-2}$	

Determination of reaction parameters

In procedure C (see below) for 0.90 μg of nitrite per ml, the pH of diazotization was varied by adding reagent solutions with different quantities of hydrochloric acid. Figure 3a shows that for pH values between 0.9 and 2 the absorbance is at its maximal value, the reaction time being 5 min (Fig. 3b).

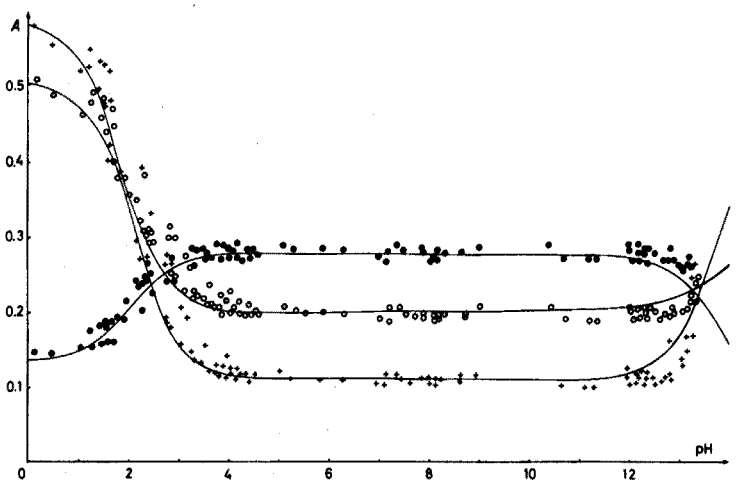

Fig. 2. Experimental points and calculated curves (according to eqn. 1) for the absorption of N-phenyl-1-naphthylamine–4-azoacetophenone *versus* pH at 500 (●), 550 (○) and 570 (+) nm. $C_T = 1.1 \cdot 10^{-5}$ *M*.

The same conditions for diazotization were adopted for procedure A. But, since in this case the maximal absorbance occurs at a very basic pH, and in order to obtain the minimal dilution factor and to bring the reaction time within 5 min (Fig. 3c), the concentration of the diazotization reagent was doubled.

Since the maximal absorbance of the cationic form of the dye in procedure B occurs at a pH of 0–0.5, a very acidic solution of the diazotization reagent was chosen in order to avoid any further adjustments to reach the optimal pH conditions.

It was then observed that for a diazotization time above 2 min, the absorbance is at its maximum value (Fig. 3d).

The coupling reaction in procedure C is rapid and yields constant absorbance values for reagent concentrations above $5 \cdot 10^{-3}$ *M* (Fig. 3e). The colour is stable for at least 1 h.

The same rapid colour development and stability was observed for procedure A, at least 15 min are required for total colour development (Fig. 3f). The absorbance remains constant for at least 30 min.

For all the procedures, the solvent was chosen so as to completely solubilize the dye and the excess of coupling reagent which are insoluble in water alone. Mixtures of water–ethanol (1 + 1) or water–DMF (1 + 1) proved to be satisfactory.

The concentrations and volumes of the reagents in the reaction mixture were determined in order to attain the minimal dilution factor and a fast reaction rate. Dilution factors obtained for procedures A, B and C are 3.57, 2.5 and 2.5, respectively. By using a methanolic solution of tetraethylammonium hydroxide, the dilution factor for procedure A may be further decreased. This base has the advantage of being odorless and easy to manipulate, compared to benzyltrimethylammonium methoxide.

It is very important to use the recommended order of adding the solutions during the analysis. Results up to 30% low were obtained by reversing the order of

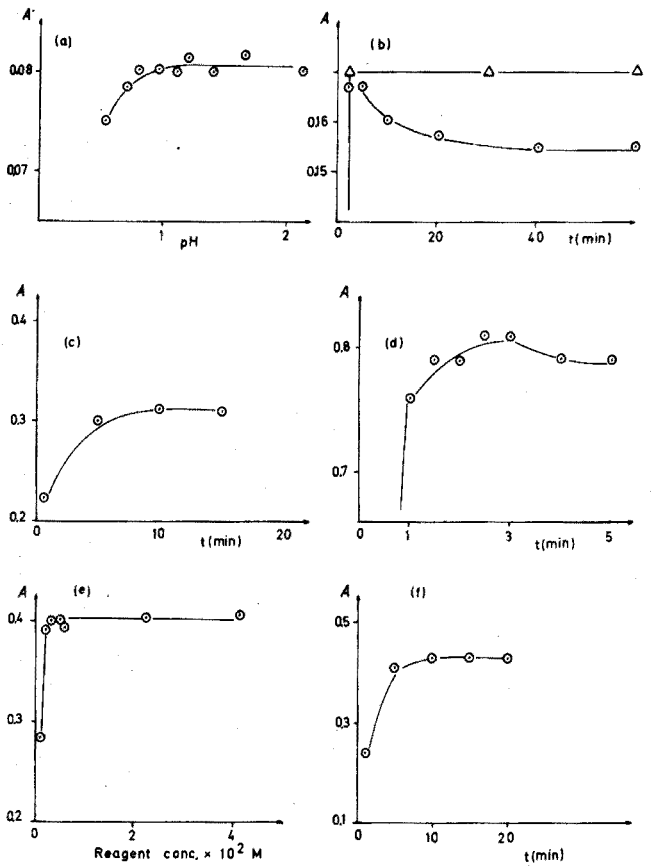

Fig. 3. (a) Effect of pH on diazotization. (b) Reaction times for diazotization (⊙) and coupling (△) in Procedure C. (c) Diazotization time in Procedure A. (d) Diazotization time in Procedure B. (e) Effect of coupling reagent concentration in Procedure C. (f) Coupling time in Procedure A.

addition of the nitrite solution and the diazotization reagent because of the loss of nitrogen dioxide. Low results were also obtained by the use of mixed reagent solution. The temperature was 20–25°; no variations in the absorbance were detected within these temperature limits.

Calibration curves were obtained for the procedures described below (Figs. 4 and 5). Even though the reagent blank does not absorb at the working wavelengths, it was used for all measurements. Procedure A has the highest sensitivity with a molar absorptivity 89000; when 5-cm cells are used, this allows detection of 1 ng NO_2^- ml^{-1}. Since the dilution factor is 3.57, the effective detection limit is 3.57 ng NO_2^- ml^{-1}. For procedures B and C, the molar absorptivities are 49000 and 18300 respectively.

Since the methods were designed mainly for water analysis, the interference by foreign ions was checked by preparing an arbitrary sample which had the following composition in the measuring cell:
$2.5 \cdot 10^{-6}$ *M* $NaNO_2$, $2.5 \cdot 10^{-3}$ *M* $Ca(NO_3)_2$, $1.4 \cdot 10^{-4}$ *M* $CuSO_4$, $1.87 \cdot 10^{-3}$ *M*

$MgSO_4$, $2.5 \cdot 10^{-5}$ *M* $FeCl_3$, $10.2 \cdot 10^{-3}$ *M* KCl, $4.4 \cdot 10^{-3}$ *M* KNO_3, $9.3 \cdot 10^{-4}$ *M* $Al_2(SO_4)_3$, $12.6 \cdot 10^{-3}$ *M* NH_4Cl.

The absorbance observed (0.21) was the same as a sample containing only the nitrite ion. The interference limits of concentration were not determined in the present work.

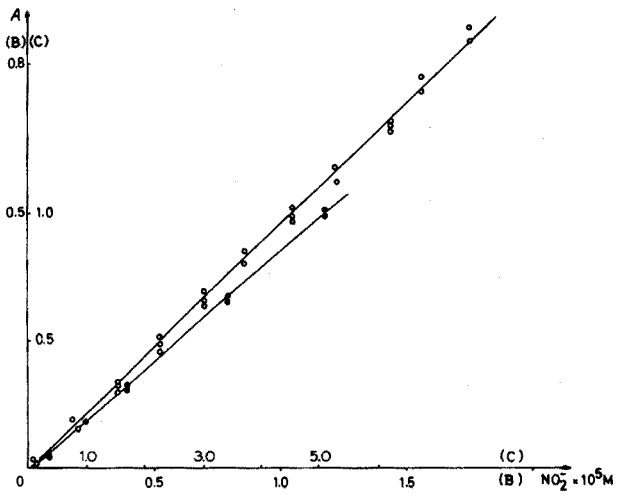

Fig. 4. Calibration curves for Procedure C (●) and Procedure B (○).

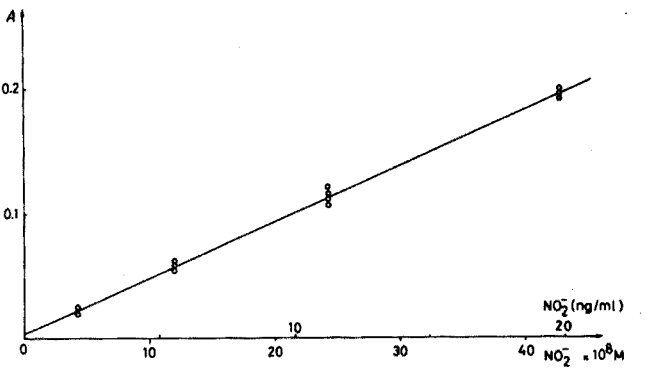

Fig. 5. Calibration curve for Procedure A ($l = 5$ cm).

ANALYTICAL PROCEDURES

Calibration curves were obtained with nitrite solutions prepared by dilutions from a stock solution of 1.5 g of sodium nitrite (Merck G.R.) in 1 l of water. This stock solution was standardized by titration with permanganate as in the U.S.P. method[11].

Procedure A

Solution a. Dissolve 1 g of 4-aminoacetophenone in 1 l of 1% hydrochloric acid solution.

Solution b. Dissolve 1 g of N-phenyl-1-naphthylamine in a mixture of 500 ml of absolute ethanol and 2 ml of anhydrous acetic acid. This solution is photosensitive and should be kept in a brown glass bottle.

Procedure. Pipet 1.25 ml of solution a into a 25-ml volumetric flask. Add. 7 ml of sample solution. Allow 5 min for diazotization. Add 1.25 ml of solution b and allow 15 min for coupling. Add 12.5 ml of tetraethylammonium hydroxide solution and complete to the mark with absolute ethanol. Centrifuge if necessary and measure the absorbance at 618 nm *versus* a blank prepared in the same fashion. The colour is stable for at least 30 min.

Procedure B

Solution c. Dissolve 0.5 g of 4-aminoacetophenone in 1 l of 18% hydrochloric acid solution.

Solution d. Dissolve 0.5 g of N-phenyl-1-naphthylamine in 500 ml of DMF and add 2 ml of concentrated hydrochloric acid. The DMF may be replaced by absolute ethanol. This solution should be kept in a brown glass bottle.

Procedure. Pipet 1 ml of solution c into a 10-ml volumetric flask. Add 4 ml of sample solution and allow 5 min for reaction. Then add 2 ml of solution d and make up to the mark with DMF (or ethanol). Measure the absorbance at 568 nm *versus* a blank solution prepared in the same way. The colour is stable for at least 1 h.

Procedure C

Solution e. Dissolve 0.5 g of 4-aminoacetophenone in 1 l of 1% hydrochloric acid solution.

Solution f. Dissolve 0.5 g of N-phenyl-2-naphthylamine in 500 ml of DMF and add 2 ml of concentrated hydrochloric acid. This solution should be kept in a brown glass flask.

Procedure. The procedure is the same as for Procedure B. The absorbance is measured at 524 nm. The colour is stable for at least 1 h.

Determination of nitrite content in an original water sample

Water collected from the river Arve was filtered twice on millipore membrane and a known amount of nitrite was added to give a concentration of 105 ng ml^{-1} in addition to the original amount present. The determination was done by Procedure A by the internal standard method. Thus, reaction mixtures containing from 1 to 6 ml of sample diluted to 7 ml with nitrite-free water were measured as well as reaction mixtures containing the same amount of sample plus 1 ml of a $5.4 \cdot 10^{-6}$ *M* nitrite solution. The results were calculated as follows:

$$\frac{D_x \cdot E}{(D_{x+E} - D_x)n} = \text{ng}NO_2^- \text{ ml}^{-1}$$

where D_x, D_{x+E} = absorbances of samples of unknown and unknown plus internal standard solution; E = ng of nitrite in the internal standard; n = ml of unknown solution added.

$$\text{Error } \% = 100\, tS_M/\bar{X}$$

where S_M is the standard deviation/$\sqrt{N}$, and N is the number of determinations.

The amount of nitrite found was 121 ng ml^{-1} with a relative error of $\pm 11\%$ (5 determinations).

SUMMARY

Three spectrophotometric methods for the determination of nitrite have been developed based on diazotization of 4-aminoacetophenone followed by coupling with N-phenyl-1-naphthylamine or N-phenyl-2-naphthylamine. In the former case, the coloured species shows an absorption maximum which depends on pH; the dissociation constants were established for a (1+1) water–ethanol system: $K_1 = 2 \cdot 10^{-14}$ and $K_2 = 10^{-2}$. The anion of the coloured species has a molar absorptivity of 89000 at 618 nm and traces of nitrite of the order of 1 ng ml^{-1} (dilution factor 3.57) can be determined. The cationic form AH_2^+ present in strongly acidic media has a molar absorptivity of 49000 at 568 nm. The absorbing species formed with N-phenyl-2-naphthylamine has a molar absorptivity of 18,300 at 524 nm, and the absorbance is independent of pH, probably because of intramolecular hydrogen bonding. The method has been applied to the determination of nitrite in natural waters.

RÉSUMÉ

Trois méthodes spectrophotométriques pour le dosage de nitrite, basées sur la diazotation du 4-aminoacétophénone suivie par la copulation avec le N-phényl-1-naphtylamine (I) ou le N-phényl-2-naphtylamine (II) ont été développées. Dans le cas de la copulation avec (I), le colorant formé présente un maximum d'absorption qui dépend du pH de la solution suivant les équilibres:

$$A^- + H^+ \overset{K_1}{\rightleftharpoons} AH, \text{ et } AH + H^+ \overset{K_2}{\rightleftharpoons} AH_2^+$$

Les constantes de dissociation sont déterminées dans un système de solvant eau–éthanol (1+1): $K_1 = 2 \cdot 10^{-14}$, $K_2 = 10^{-2}$. L'anion du colorant présente un $\varepsilon = 89000$ à 618 nm et permet de déceler des traces de nitrite de l'ordre de 1 ng ml^{-1} (facteur de dilution 3.57). Le cation AH_2^+ présent en milieu acide fort, a un $\varepsilon = 49000$ à 568 nm. Le colorant formé avec (II) ($\varepsilon = 18300$ à 524 nm) a la particularité d'avoir une absorption qui est indépendante du pH. Ceci semble être dû à la présence d'une liaison hydrogène intramoléculaire. La méthode est appliquée au dosage de nitrite dans des échantillons d'eau naturelle.

ZUSAMMENFASSUNG

Es wurden drei spektrophotometrische Methoden für die Bestimmung von Nitrit entwickelt. Sie beruhen auf der Diazotierung von 4-Aminoacetophenon und der anschliessenden Kupplung mit N-Phenyl-1-naphthylamin oder N-Phenyl-2-naphthylamin. Im ersten Fall hängt das Absorptionsmaximum der gefärbten Spezies vom pH-Wert ab; die Dissoziationskonstanten für das System Wasser-Äthanol (1+1) wurden ermittelt: $K_1 = 2 \cdot 10^{-14}$ und $K_2 = 10^{-2}$. Das Anion der gefärbten Spezies hat einen molaren Extinktionskoeffizienten von 89000 bei 618 nm,

und Nitritspuren der Grössenordnung 1 ng ml^{-1} (Verdünnungsfaktor 3.57) können bestimmt werden. Die in stark sauren Medien vorliegende kationische Form AH_2^+ hat einen molaren Extinktionskoeffizienten von 49000 bei 568 nm. Die mit N-Phenyl-2-naphthylamin gebildete absorbierende Spezies hat einen molaren Extinktionskoeffizienten von 18300 bei 524 nm, und die Extinktion ist, wahrscheinlich aufgrund einer intramolekularen Wasserstoffbindung, vom pH-Wert unabhängig. Die Methode wurde auf die Bestimmung von Nitrit in der Natur vorkommendem Wasser bestimmt.

REFERENCES

1 I. M. Kolthoff and P. J. Elving, *Treatise on Analytical Chemistry*, Part II, Vol. 5, Interscience, New York, 1961, p. 275.
2 C. A. Streuli and P. R. Averell, *Analytical Chemistry of Nitrogen and its Compounds*, Part I, Wiley–Interscience, New York, 1970, p. 117.
3 E. Sawicki, J. Pfaff and T. W. Stanley, *Rev. Univ. Ind. Santander*, 5 (1963) 337.
4 E. Sawicki, T. W. Stanley, J. Pfaff and H. Johnson, *Anal. Chem.*, 35 (1963) 3183.
5 E. Sawicki, T. W. Stanley, J. Pfaff and A. D'Amico, *Talanta*, 10 (1963) 641.
6 E. E. Garcia, *Anal. Chem.*, 39 (1967) 1605.
7 A. Foris and T. R. Sweet, *Anal. Chem.*, 37 (1965) 701.
8 L. J. Dombrowski and E. J. Pratt, *Anal. Chem.*, 44 (1972) 2268.
9 E. Sawicki, *Photometric Organic Analysis*, Part I, Wiley–Interscience, New York, 1970.
10 K. B. Yatsimirskii and V. P. Vasil'ev, *Instability Constants of Complex Compounds*, Pergamon, Oxford, 1960.
11 *U. S. Pharmacopoeia*, 17th Ed., 1965, p. 631.

Analytica Chimica Acta, 68 (1974) 73–82

ARSENAZO III AS A SPECTROPHOTOMETRIC REAGENT FOR ZINC AND CADMIUM

V. MICHAYLOVA and L. YUROUKOVA

Department of Chemistry, University of Sofia, Sofia 26 (Bulgaria)

(Received 2nd April 1973)

The absence of the crystal-field stabilization energy of d^{10} configuration of zinc(II) and cadmium(II) restricts the use of complexation reactions for the photometric determination of these metals. The reagents usually recommended are ligands with nitrogen or sulphur donor atoms. Accordingly, arsenazo III (3,6-bis(2'-arsenophenylazo)-4,5-dihydroxynaphthalene-2,7-disulphonic acid) was selected and studied as a spectrophotometric reagent for zinc and cadmium. Arsenazo III has been widely applied as an excellent complexing agent in the photometric determination of rare metals such as U, Th, Zr, etc., but its reactions with zinc(II) and cadmium(II) have not previously been studied. Moreover, Savvin[1] has reported that arsenazo III does not react with zinc(II) and cadmium(II) because of their small ionic radii. In our previous work[2], however, it was shown that these reactions do occur. It seems probable that the nature of the bonding groups of the reagent is important in these reactions.

The reactions of zinc(II) and cadmium(II) with arsenazo III, their sensitivity and selectivity, the properties and stabilities of the complexes formed are described in the present paper. The molar absorptivities of the zinc(II)– and cadmium(II)–arsenazo III complexes were found to be 28,000 and 26,000, respectively. The sensitivity of the zinc(II)–arsenazo III reaction was increased by using suitable ligands; potassium iodide and allyl alcohol increased the molar absorptivities to 42,800 and 38,500, respectively. This effect may be explained by the formation of ternary complexes between zinc(II), arsenazo III and iodide or ally alcohol. The use of ammonium fluoride as a masking agent permitted the determination of micro amounts of zinc in the presence of the macro quantities of cadmium. In this connection, other halide complexes of cadmium were also studied. For masking of zinc(II), pyridine in the form of its nitric acid salt was used; this allowed the determination of 35.6 μg of cadmium in the presence of 120 μg of zinc.

EXPERIMENTAL

Reagents

Zinc sulphate solution. A 10^{-2} *M* solution was prepared from Merck, p.a. reagent, and standardized complexiметrically with xylenol orange or eriochrome black T as indicators.

Cadmium sulphate solution. A 10^{-2} *M* solution was prepared from the Merck, p.a. reagent (octahydrate) and standardized complexiметrically with xylenol orange as indicator.

Arsenazo III solution. An aqueous 10^{-4} *M* solution of the reagent (Fluka) was standardized by spectrophotometric titration with thorium(IV) nitrate solution at 600 nm and pH 3. An aqueous 0.04% (w/v) solution of arsenazo III was used for analytical purposes.

Buffer solutions. Biphthalate and borate buffer solutions were prepared by conventional methods[3].

Pyridine. Analytical-grade pyridine (Merck) was used and its nitric acid salt was prepared with reagent-grade nitric acid. Stock 2 *M* solutions of this salt were prepared.

All other reagents were of analytical-reagent grade.

Apparatus

Absorbance spectra were obtained with a Specord u.v.-vis Spectrophotometer (Zeiss). Spectrophotometric measurements were performed with Universal Spectrophotometer VSU-1 (Zeiss). For pH checks of the solutions, a pH-meter LPU-01 (USSR) with a glass electrode was used.

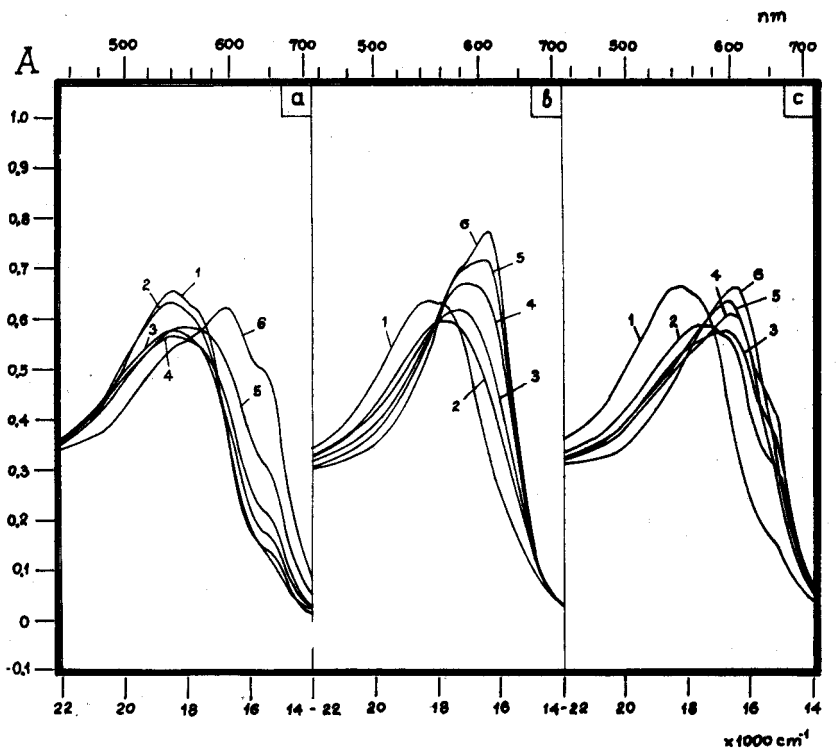

Fig. 1. Absorption spectra of arsenazo III and its complexes with zinc(II) and cadmium(II) at various pH values (buffer solutions). (a) Arsenazo III. $C_R = 2.47 \cdot 10^{-5}$ *M*. 1-cm cells against a water reference. pH: (1) 6.25; (2) 7.48; (3) 8.35; (4) 9.22; (5) 10.05; (6) 11.50. (b) Zinc–arsenazo III complex. $C_R = 2.47 \cdot 10^{-5}$ *M*, $C_{Zn} = 2.78 \cdot 10^{-5}$ *M*. 1-cm cells against a water reference. pH: (1) 6.10; (2) 7.05; (3) 7.80; (4) 8.70; (5) 9.30; (6) 11.25. (c) Cadmium–arsenazo III complex. $C_R = 2.47 \cdot 10^{-5}$ *M*, $C_{Cd} = 2.74 \cdot 10^{-5}$ *M*. 1-cm cells against a water reference. pH: (1) 6.20; (2) 7.48; (3) 8.36; (4) 9.25; (5) 10.00; (6) 11.40.

REACTION OF ARSENAZO III WITH ZINC(II) AND CADMIUM(II)

The complex formation was studied at various pH values because of the acid–base behaviour of arsenazo III and the tendency of zinc(II) and cadmium(II) to form hydroxo complexes in alkaline media. It was found that arsenazo III formed blue complexes with zinc(II) and cadmium(II) with absorption maxima at 590 nm and 600 nm, respectively. The absorbance spectra presented in Figs. 1 and 2 show that the complex formation began just above pH 6 and maximal absorbance was observed in alkaline medium, pH 10–11. In strongly alkaline medium above pH 9, the zinc complex spectra changed, probably because of hydrolysis of the complex.

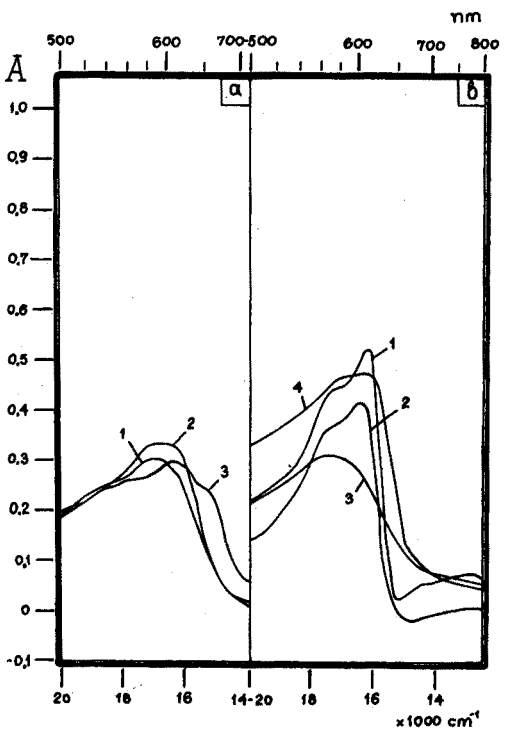

Fig. 2. Absorption spectra of zinc(II)- and cadmium(II)-arsenazo III complexes with excess of reagent; and the influence of halide ions and allyl alcohol on the zinc(II)–arsenazo III complex absorbance. (a) $C_R = 4.12 \cdot 10^{-5}$ *M*, $C_{Zn} = 1.28 \cdot 10^{-5}$ *M*, $C_{Cd} = 1.26 \cdot 10^{-5}$ *M*. 1-cm cells against $2.84 \cdot 10^{-5}$ *M* reagent. (1) Zn complex, pH 9.10; (2) Zn complex, pH 10.05; (5) Cd complex, pH 9.10. (b) $C_R = 4.12 \cdot 10^{-5}$ *M*, $C_{Zn} = 1.28 \cdot 10^{-5}$ *M*, $C_{X^-} = 4\%$, $C_{al.alc.} = 40\%$, pH 9.05. 1-cm cells against $2.84 \cdot 10^{-5}$ *M* reagent. In the presence of: (1) KI, (2) KBr, (3) NH_4F, (4) allyl alcohol.

Absorbance of arsenazo III was also studied at pH values corresponding to acid–base equilibria according to the distribution curves of the reagent reported previously[4]. It can be seen from Fig. 1 that in more alkaline medium, a bathochromic effect is obtained; therefore, the absorbance of the reagent must be taken into account for the reactions studied.

Composition of the complexes

As reported by Savvin[5], arsenazo III usually forms 1:1 complexes with di- and trivalent cations. This was confirmed for the arsenazo III complexes of zinc(II) and cadmium(II) by the molar ratio method, by the straight-line method of Asmus[6] and by the Bent-French method[7]. The results obtained at pH 9 and 600 nm from these methods proved the 1:1 composition of the complexes.

Sensitivity of the reactions and conformity to Beer's law

The molar absorptivity of the reactions was determined in the presence of at least a 3–4-fold amount of arsenazo III. The least-squares procedure was applied to the straight line $\Delta A = \varepsilon lc$, ΔA being the absorbance of the complex; correct account was taken of the reagent absorbance. The results are shown in Table I

TABLE I

MOLAR ABSORPTIVITY

(All results are given as $\varepsilon \cdot 10^{-4}$ in l mole^{-1} cm^{-1})

Zn complex			*Cd complex*			*pH*
590 nm	*600 nm*	*610 nm*	*590 nm*	*600 nm*	*610 nm*	
2.08	1.94	1.74	2.55	2.59	2.35	7.05
2.50	2.44	2.32	2.60	2.60	2.56	9.02
2.80	2.78	2.75	2.54	2.59	2.54	9.96

The corresponding sensitivities as defined by Sandell are 0.0023 μg Zn cm^{-2} and 0.0043 μg Cd cm^{-2}, calculated from the optimal values of the molar absorptivity.

The absorbances of the complexes studied obey Beer's law over the ranges 0.14–1.26 μg Zn ml^{-1} and 0.24–2.38 μg Cd ml^{-1}.

Recommended procedure

Place the test solutions (0.50–5.00 ml) containing 3.5–34.9 μg of zinc(II) or 5.9–59.5 μg of cadmium(II) in 25-ml volumetric flasks. Add 2.50 ml of 0.04% arsenazo III solution followed by 5.0 ml of buffer solution, make up to 25 ml, and mix thoroughly. The blue or blue-violet colour develops immediately and remains stable during 24 h. Read the absorbance in 3-cm cuvettes at 590–610 nm against a reagent blank solution.

Effect of diverse ions

Table II summarizes the results of the interference study for the determination of zinc(II) and cadmium(II) at pH 10. Presented data show the amounts of the ions which did not interfere.

The selectivity of the reactions decreased at pH 9. At this pH, only 20 μg Al(III), 3 μg Fe(III) or 10 μg Ti(IV) could be tolerated in the determination of 21 μg of zinc and only 34 μg Al(III), 6 μg Fe(III) or 5 μg Ti(IV) could be tolerated in the determination of 35.6 μg of cadmium. Best results for Al(III), Fe(III), Ti(IV) and Mn(II) were obtained in the presence of 4 ml of 20% triethanolamine (Table

TABLE II

INTERFERENCE OF DIVERSE IONS

(The solutions tested contained 21 μg Zn or 35.6 μg Cd)

Diverse ion	*Zinc(II)*		*Cadmium(II)*	
	Amount added (μg)	*λ (nm)*	*Amount added (μg)*	*λ (nm)*
Ag(I)	240	590	240	600
Al(III)	47	600	108	600
Bi(III)	16	600	25	600
Co(II)	44	600	11	600
Cu(II)	10	590	9	600
Fe(III)	28	590	5	600
Mn(II)	11	590	8	600
Ni(II)	17	590	8	600
Pb(II)	31	590	62	600
Sn(II)	97	590	97	600
Ti(IV)	14	600	21	600

TABLE III

TOLERANCE FOR DIVERSE IONS IN THE PRESENCE OF TRIETHANOLAMINE

(pH 10.10; 600 nm; 21 μg Zn or 35.6 μg Cd were used)

Diverse ion	*Zinc(II) amount added (μg)*	*Cadmium(II) amount added (μg)*
Al(III)	505	675
Fe(III)	1886	2695
Mn(II)	137	82
Ti(IV)	29	59

III). Apparent pH values of 10.10 for the final solutions were obtained with a borate buffer solution of pH 7.96 and of a triethanolamine solution of pH 10.68.

Zinc(II) and cadmium(II) are electronic homologues, and their determination in the presence of each other is important. In this connection, the conditional stability constants of the zinc(II)– and cadmium(III)–arsenazo III complexes were determined.

Determination of the conditional stability constants

The graphical method of Frank and Oswalt[8] was used at pH 9.12 and $\mu = 0.06$. The following expression is valid in an excess of the reagent:

$$C_M C_R / \Delta A = 1/\beta \Delta\varepsilon + (C_M + C_R)/\Delta\varepsilon \quad (1)$$

where β is the stability constant; C_M and C_R are the concentrations of the metal and the reagent; $\Delta A = A - A_R$; $\Delta\varepsilon = \varepsilon_{complex} - \varepsilon_R$. The data were calculated according to

eqn. (1), and the results are presented in Fig. 3. Regression analysis was applied and the values found were as follows:

For the zinc(II)–arsenazo III complex: $\log \beta = 5.7 \pm 0.1$; $\varepsilon = (2.49 \pm 0.07) \cdot 10^4$ (graphically: $\log \beta = 5.7$; $\varepsilon = 2.51 \cdot 10^4$)

For the cadmium(II)–arsenazo III complex: $\log \beta = 4.7 \pm 0.2$; $\varepsilon = (2.80 \pm 0.10) \cdot 10^4$ (graphically: $\log \beta = 4.7$; $\varepsilon = 2.77 \cdot 10^4$)

The lower stability of the cadmium complex can be related to the larger ionic radius of cadmium and therefore to the weaker ionic bonding in the complex. It is probable that ionic bonds are principally responsible for the complex formation of arsenazo III with these metals.

DETERMINATION OF ZINC(II) AND CADMIUM(II) IN THE PRESENCE OF EACH OTHER

The difference between the stabilities of the halide complexes of zinc and cadmium[9] was used to achieve masking of cadmium. Since the stabilities of the cadmium(II) complexes with arsenazo III and with halides are similar, high concentrations of halide ions were used; aqueous 10% solutions of potassium iodide, potassium bromide and ammonium fluoride were prepared. Ammonium fluoride proved the best masking agent; this was unexpected on the basis of the stabilities of the halide complexes alone, but many other factors must be considered, such as ionic potential, polarization, back donor-bonding, etc. The hydroxo complexes of cadmium are stronger than those of zinc[10], hence masking of cadmium was done in more alkaline media.

The stability of the cadmium(II) complexes with pyridine is of the same order as that of zinc(II)[10]; however, zinc(II) could be masked by using the nitric acid salt of pyridine which shows buffer properties and maintains the pH at *ca.* 5. Under these conditions, the sensitivity of the cadmium(II)–arsenazo III reaction was sufficient ($\varepsilon = 16{,}600$), and Beer's law was followed in the range 0.96–2.16 μg Cd ml^{-1}. The results are presented in Table IV.

TABLE IV

DETERMINATION OF ZINC(II) AND CADMIUM(II) IN THE PRESENCE OF EACH OTHER

Ion determined	*Amount taken (μg)*	*Ion masked*	*Amount added (mg)*	*Masking agent, conc.*	*pH*	*λ (nm)*
Zn(II)	21	Cd(II)	110.0	NH_4F, 2.8%	8.16[a]	600
Zn(II)	21	Cd(II)	5.6	KBr, 4%	8.35[a]	600
Zn(II)	21	Cd(II)	16.8	KI, 4%	8.96	590
Zn(II)	21	Cd(II)	0.14	Borate buffer	11.35	620
Cd(II)	35.6	Zn(II)	0.15	$PyHNO_3$, $2 \cdot 10^{-3}$ *M*	5.03	600

[a] Apparent pH of the final solution (buffer solution pH 8.96).

INCREASING THE SENSITIVITY OF THE ZINC(II)–ARSENAZO III REACTION

When the halide ions were used as masking agents for cadmium(II) an increase in the sensitivity of the zinc(II)–arsenazo III reaction was obtained, which

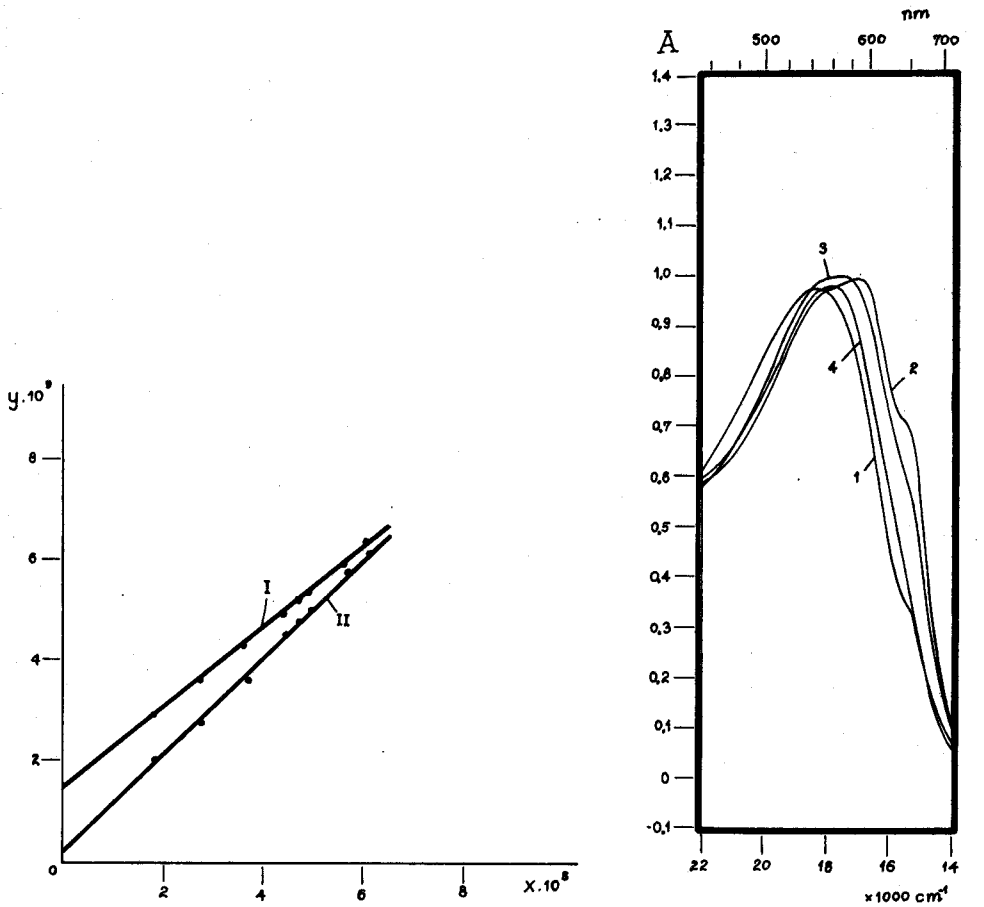

Fig. 3. Plots according to eqn. (1) for determination of conditional stability constants. pH 9.12, $\mu = 0.06$, 600 nm, $l = 1$ cm *vs.* water. $y = (C_R \cdot C_M)/\Delta A$, $x = C_R + C_M$. (I) Cd complex, (II) Zn complex.

Fig. 4. Effect of halide ions on arsenazo III absorbance. $C_R = 4.12 \cdot 10^{-5}$ *M*, $C_{X^-} = 4\%$, pH 8.96. (1) Arsenazo III, (2) arsenazo III plus KI, (3) arsenazo III plus KBr, (4) arsenazo III plus NH_4F.

suggested the formation of ternary complexes between zinc(II), arsenazo III and halide. The unoccupied coordination positions of zinc(II) and the low stability of the zinc(II)–halide complexes favour such formation.

The experimental data showed that ternary complexes were formed only at high concentration of halide ions. Aqueous 10% (w/v) solutions of potassium iodide, potassium bromide and ammonium fluoride were used in studying the sensitivity of the zinc(II)–arsenazo III reaction.

The formation of ternary complexes was estimated directly by the electronic absorption spectra of the systems. The spectra shown in Fig. 2b were measured at a reagent excess corresponding to analytical conditions. The influence of the halide ions on the arsenazo III equilibria is shown in Fig. 4. The formation of ternary complexes causes an increase in sensitivity compared with the simple system (Table V).

TABLE V

THE MOLAR ABSORPTIVITY OF THE ZINC(II)–ARSENAZO III COMPLEX IN THE PRESENCE OF HALIDES

(pH 8.16 for NH_4F; pH 9 for KI and KBr)

Halide	$\varepsilon \cdot 10^{-4}$ *(l mole^{-1} cm^{-1})*	λ *(nm)*
KI	3.98	610
	3.49	590
KBr	3.63	610
	3.50	600
NH_4F	2.56	600

Such an effect may be explained as follows. With bromide and chloride ions, the unoccupied d_π-orbitals can participate in the formation of $\pi(M \rightarrow L)$ bonds with metals possessing a d^{10} configuration[11]. Such back-donation bonds lead to a lowering of the electron density on the metal ion and hence to increase in its effective charge. The large effect of iodide may be explained by the more diffuse character of its 5d-orbitals compared with the 4d-orbital of bromide ion, which ensures a greater overlap with the d_π-orbitals of zinc(II). With such bonding, the replacement of the remaining water molecules in the coordination sphere of zinc(II) by halide ions would ensure a higher effective charge on the metal ion in the ternary complex. As a result the sensitivity, which is due to the polarization effect of zinc(II) on the arsenazo III molecule increases. The lower energy difference of the 5p–5d orbitals of iodine compared with the 4p–4d orbitals of bromine also contributes to

TABLE VI

INFLUENCE OF HALIDE CONCENTRATION ON THE MOLAR ABSORPTIVITY OF THE ZINC(II)–ARSENAZO III COMPLEX

(pH 9; pH 7.8 for NH_4F)

Halides	*Amount taken (%)*	$\varepsilon \cdot 10^{-4}$ *(l mole^{-1} cm^{-1})*	λ *(nm)*
KI	0.4	2.80	610
	1.2	3.11	610
	2.0	3.72	610
	2.8	3.83	610
	4.0	3.98	610
KBr	2.0	3.64	610
	2.8	3.66	610
	4.0	3.63	610
NH_4F	0.8	3.06	600
	2.0	2.75	600
	2.8	2.63	600
	4.0	2.56	600

the larger effect of iodide. Fluoride ions, as good electron-acceptors, also influence the effective charge of zinc(II), but the effect is smaller.

The influence of the concentration of halide ions on the sensitivity of the zinc(II)–arsenazo III reaction was studied; some results are shown in Table VI. In general, the present data are in accord with the stability of the zinc(II)–halide complexes which increases in the order $F^- > Br^- > I^-$.

The influence of the acidity on the reaction sensitivity was studied for iodide (Table VII). It can be seen that the optimal pH value is about 8. This fact can be related to the more intense arsenazo III absorption at high pH values which effect is increased by iodide.

TABLE VII

MOLAR ABSORPTIVITY OF THE ZINC(II)-ARSENAZO III COMPLEX AT 610 nm IN THE PRESENCE OF 4% KI AT DIFFERENT pH VALUES

pH	7.04	8.10	9.06	10.10
ε	3.74	4.28	3.98	3.84

Other compounds, such as dioxane, ethanol and allyl alcohol, were also studied for increasing the reaction sensitivity, but only allyl alcohol was effective (Fig. 2b). The molar absorptivity was found to be 38,500 at pH 9.05 and 610 nm in the presence of 40% allyl alcohol; the absorption spectra again indicated the formation of a ternary complex. Allyl alcohol is a monodentate ligand with a less basic donor oxygen atom than water, and its conjugated bonds probably participate in he arsenazo III system, increasing the chromophoric effect.

SUMMARY

Arsenazo III forms blue 1:1 complexes with zinc(II) and cadmium(II) in alkaline media, the absorpion maxima occurring at 590 nm and 600 nm, respectively; the molar absorptivities are 28,000 and 26,000, respectively. Halide ions and allyl alcohol increase the sensitivity of the zinc(II)–arsenazo III reaction. With iodide and allyl alcohol, molar absorptivities increase to 42,800 and 38,500 respectively, owing to the formation of ternary complexes. Zinc(II) and cadmium(II) can be determined in the presence of each other if suitable masking agents are used: 21 μg of zinc can be determined in the presence of 110 mg of cadmium with 10% ammonium fluoride, and 35.6 μg of cadmium in the presence of 120 μg of zinc with pyridine nitrate The conditional stability constants of the zinc(II)– and cadmium(II)–arsenazo III complexes are given.

RÉSUMÉ

L'arsènazo III forme des complexes bleus 1:1 avec le zinc et le cadmium, en milieu alcalin avec maximum d'absorption à 590 et 600 nm et coefficient d'extinction molaire de 28000 et 26000, respectivement. Les halogénures et l'alcool allylique permettent d'augmenter la sensibilité de la réaction zinc–arsènazo. Il est possible de

doser zinc et cadmium, l'un en présence de l'autre, en utilisant des agents de masquage (fluorure d'ammonium ou nitrate de pyridine).

ZUSAMMENFASSUNG

Arsenazo III bildet mit Zink(II) und Cadmium(II) in alkalischem Medium blaue 1:1-Komplexe, deren Absorptionsmaxima bei 590 nm bzw. 600 nm liegen. Die molaren Extinktionskoeffizienten sind 28000 bzw. 26000. Halogenidionen und Allylalkohol erhöhen die Empfindlichkeit der Zink(II)–Arsenazo III-Reaktion. Mit Jodid und Allylalkohol steigen die molaren Extinktionskoeffizienten auf 42800 bzw. 38500, was durch die Bildung ternärer Komplexe verursacht wird. Zink und Cadmium können in Gegenwart geeigneter Maskierungsmittel neben einander bestimmt werden: 21 μg Zink können neben 110 mg Cadmium in Gegenwart von 10% Ammoniumfluorid und 35.6 μg Cadmium neben 120 μg Zink in Gegenwart von Pyridinnitrat bestimmt werden. Die konditionalen Beständigkeitskonstanten der Zink(II– und der Cadmium(II)–Arsenazo III-Komplexe werden angegeben.

REFERENCES

1 S. B. Savvin, *Zh. Anal. Khim.*, 17 (1962) 785.
2 V. Michaylova and P. Ilkova, *Anal. Chim. Acta*, 53 (1971) 194.
3 I. M. Kolthoff, *Acid–Base Indicators*, Academic Press, New York, 1937.
4 V. Michaylova and N. Kouleva, *Talanta*, 20 (1973) 453.
5 S. B. Savvin, *Organic Reagents from the Group of Arsenazo III*, in Russian, Atomizdat, Moscow, 1971, p. 120.
6 E. Asmus, *Z. Anal. Chem.*, 178 (1960) 104.
7 H. Bent and C. French, *J. Amer. Chem. Soc.*, 63 (1941) 569.
8 H. Frank and R. Oswalt, *J. Amer. Chem. Soc.*, 69 (1947) 1321.
9 F. Albert Cotton and G. Wilkinson, *Advanced Inorganic Chemistry*, Part II, in Russian, Mir, Moscow, 1969, p. 471.
10 L. G. Sillen and A. E. Martell, *Stability Constants of Metal-ion Complexes*, The Chemical Society, London, 1964.
11 D. D. Perrin, *Organic Complexing Reagents*, in Russian, Mir, Moscow, 1967, p. 367.

Analytica Chimica Acta, 68 (1974) 83–92

HIGH-PRECISION DETERMINATION OF CALCIUM IN THE PRESENCE OF HIGHER CONCENTRATIONS OF MAGNESIUM BY MEANS OF A COMPUTERIZED PHOTOMETRIC TITRATION

APPLICATION TO SEA WATER

DANIEL JAGNER

Department of Analytical Chemistry, University of Göteborg, Fack, S-402 20 Göteborg 5 (Sweden)

(Received 22nd May 1973)

The determination of calcium in the presence of magnesium is a classical problem in complexometry. In sea water, where the calcium and magnesium concentrations are approximately 0.01 *M* and 0.05 *M*, respectively, at 35‰ salinity, the determination of calcium involves a particular aspect of this problem, namely the precision determination of calcium in the presence of higher concentrations of magnesium. In order to be able to establish significantly the small variations in the calcium/chlorinity ratio occurring in the oceans, a method yielding a relative standard deviation less than 0.001 is required. Moreover, it is an advantage if the method is automatic, thus facilitating the analysis of a large number of samples. At the present time, only titration methods can meet these requirements, because flame absorption and emission methods do not yet yield precisions of this order, while gravimetric methods are unsuitable for automation.

Of the titration methods hitherto used for the determination of calcium in sea water, that of Riley and Tongudai[1] yields by far the highest precision. The method requires, however, ion-exchange separation of the alkaline earth metals before titration and is, consequently, time-consuming and difficult to automate.

Potentiometric titration methods based on the Orion ion-exchanger calcium-sensitive electrode have been found to yield poor results in sea water[2,3], mainly because of interference with the electrode from sodium and magnesium. A new calcium-sensitive electrode, developed by Růžička *et al.*[4], is, however, being tested at this laboratory and the preliminary results would seem to be promising. The advantage of using a calcium-sensitive electrode is, of course, that it is not necessary to separate calcium from the other alkaline earths before titration.

Another procedure for the determination of calcium in sea water which does not require previous separation of calcium is that proposed by Culkin and Cox[5]. This is a photometric titration method, with zinc–zincon as an indirect calcium indicator, based on principles originally suggested by Ringbom *et al.*[6]. The theory is analogous to that first outlined by Reilley and Schmid[7]. Ringbom *et al.*[6] did not, however, cover the case where the magnesium to calcium ratio was as unfavourable as five to one. Such a high ratio ought to give rise to systematic errors and decreasing precision, as is also shown in the present paper by means of computer-simulated titration curves.

A new approach to the determination of calcium in sea water by photometric titration based on the zinc–zincon indicator system is described in this paper. The evaluation procedure used has similarities with those outlined by Higuchi *et al.*[8], Dyrssen *et al.*[9] and Johansson[10].

THEORY

In order to be able to estimate the magnitudes of the accuracy and precision associated with different methods of evaluating the titration of calcium in sea water with zinc–zincon as an indirect indicator, theoretical titration curves were calculated by means of the computer program HALTAFALL[11,12]. The total concentrations used in the calculations were: calcium 0.00128 *M*, magnesium 0.0066 *M*, strontium 0.00004 *M*, zinc–EGTA 0.000128 *M*, zincon $6 \cdot 10^{-6}$ *M*, EGTA 0.016 *M*, the latter being the obvious choice as complexing agent for the titration of calcium in the presence of magnesium. The calculations were performed at pH values between 8 and 10, an initial volume of 200 ml being assumed. The total concentrations chosen correspond to 25 g of sea water (of 35‰ salinity) diluted to 200 ml. The equilibrium constants, relevant at 0.1 *M* ionic strength, have been taken from Ringbom[6,13] and are specified in Table I. In order to avoid confusion, the notation for the indicator species used in this paper is the same as that used by Ringbom *et al.*, namely ZnOHI (blue) for the zinc–zincon complex and HI (yellow) and I (yellow-red) for the proton–indicator complexes. According to preliminary experiments carried out at this laboratory, these complexes would, however, appear to be better represented by ZnI, H_2I and HI, respectively.

TABLE I

STABILITY CONSTANTS USED IN THE HALTAFALL CALCULATION OF THE TITRATION OF CALCIUM IN DILUTED SEA WATER WITH EGTA

(H_4Y denotes EGTA and H_3I denotes zincon)

Equilibrium	*Log. of constant*
$H+Y \rightleftharpoons HY$	9.46
$2\,H+Y \rightleftharpoons H_2Y$	18.31
$Ca+Y \rightleftharpoons CaY$	10.70
$Mg+Y \rightleftharpoons MgY$	5.40
$Sr+Y \rightleftharpoons SrY$	8.10
$Zn+Y \rightleftharpoons ZnY$	12.80
$H+I \rightleftharpoons HI$	8.25
$Zn+H_2O+I \rightleftharpoons ZnOHI+H$	−1.00
$Zn+H_2O \rightleftharpoons ZnOH+H$	−9.60
$Zn+3\,H_2O \rightleftharpoons Zn(OH)_3+3\,H$	−27.60

The results of the calculations are illustrated in Fig. 1, in which the concentration of the zinc–indicator complex has been plotted against v ml of EGTA added for different pH values.

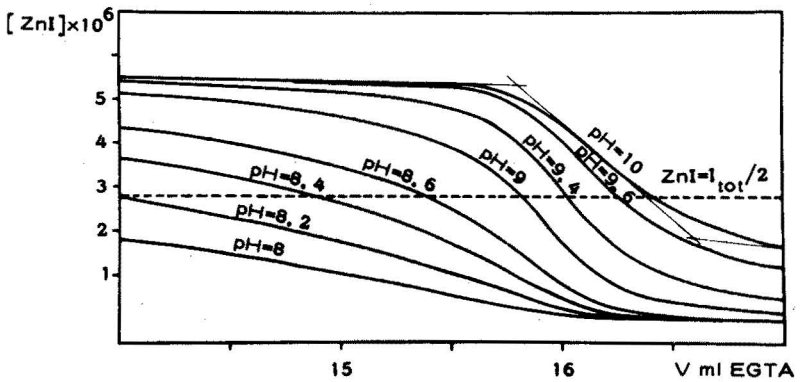

Fig. 1. Computer-simulated titration curves for the determination of calcium in sea water.

Visual evaluation

If the visual end-point, v_{end}, is defined as the v value corresponding to

$$[ZnOHI] = [HI] + [I] \quad (1)$$

then the percentage systematic error is given by

$$\% \text{ error} = 100(v_{end} - v_{eq})/v_{eq} \quad (2)$$

The v_{end} value for a specific pH value is obtained from Fig. 1 as the value corresponding to the intersection of the dashed horizontal line $[I]_{tot}/2$ and the relevant [ZnOHI] plot. The results are summarized in Table II. From Fig. 1 it can also be concluded that, apart from giving rise to systematic errors, visual evaluation is also associated with a poor precision.

Maximum slope

The v value corresponding to the maximum slope of the absorbance curve is often taken to be v_{end}. The systematic errors thus obtained for the system under consideration are given in Table II. In spite of the fact that these errors are con-

TABLE II

PERCENTAGE SYSTEMATIC ERROR OBTAINED BY DIFFERENT EVALUATION METHODS FOR THE TITRATION OF CALCIUM IN DILUTED SEA WATER AT DIFFERENT pH VALUES (*cf.* Fig. 1)

pH	*Evaluation method*				
	Visual	*Linear extrapolation*	*Maximum slope*	F_1	F_1'
8.0	< −20	0.2	—	0.5	0.1
8.2	−13.0	0.4	—	0.4	0.1
8.4	−7.4	0.7	−1.4	0.3	0.1
8.6	−3.9	1.0	−0.9	0.3	0.1
9.0	−1.2	1.2	−0.3	—	—
9.4	0.2	−2.0	0.3	—	—
9.8	1.5	−1.5	0.6	—	—
10.0	2.6	−1.3	0.9	—	—

siderably smaller than those obtained in the visual evaluation, it can be concluded from Fig. 1 that the precision of this method is not sufficiently high.

Linear extrapolation

Break-point curves[14,15], *i.e.* curves yielding large systematic errors in visual evaluation, can be evaluated by linear extrapolation. Straight lines are approximated through the almost linear parts of the absorbance curve before and after the equivalence point. These lines are allowed to intersect the best line drawn through the steepest part of the absorbance curve and one of the two points of intersection thus obtained is taken as v_{end}. Which of the two intersection points should be used in order to obtain the best accuracy can normally be seen directly from the shape of the plot. This procedure is illustrated by means of the fine lines in Fig. 1 for the plot at pH 10, and the systematic errors are specified in Table II.

Visual, maximum slope and linear extrapolation methods have all been tested in practice and the orders of magnitude of all errors given in Table II have been verified experimentally.

Linear regression

The methods discussed above exploit only a small part of the titration curve in the evaluation of the equivalence point. From the aspect of precision it would, of course, be advantageous if as many titration points as possible could be used in this evaluation *e.g.* by a linear regression method analogous to the Gran[16] method used in potentiometric titrations. In the derivation of Gran plots it is, however, assumed that there is a dominating main reaction. This requirement is, of course, never fulfilled in an indicator titration since in the part of the titration curve where measurable colour changes occur there must always be interfering side-reactions between the metal to be titrated and the indicator. These side-reactions can be neglected only if the total indicator concentration is very low in comparison with the total metal ion concentration. The importance of indicator side-reactions can easily be ascertained from theoretical titration curves calculated with *e.g.* HALTAFALL.

Supposing that, in the titration under consideration, the only reaction before the equivalence point, v_{eq}, is the formation of calcium–EGTA, then

$$(v_o + v)[\mathrm{Ca}] \propto v_{eq} - v \qquad (v_o \text{ here } 200) \tag{3}$$

$$(v_o + v)[\mathrm{CaY}] \propto v \tag{4}$$

and, consequently,

$$[\mathrm{Y}] \propto v/(v_{eq} - v) \tag{5}$$

Assuming, moreover, that only a minor part of the Zn–EGTA added dissociates, then

$$(v_o + v)[\mathrm{ZnY}] = \text{constant} \tag{6}$$

and, after combination with eqn. (5),

$$v(v_o + v)[\mathrm{Zn}] \propto v_{eq} - v \tag{7}$$

In the photometric titration, absorbance values proportional to either [ZnOHI] or

$[I'] = [HI] + [I]$ are the only measurable parameters. These are related to the free zinc concentration by

$$[Zn] \propto [ZnOHI]/[I'] \tag{8}$$

provided that pH is constant.

Thus, as seen from eqns. (7) and (8), F_1, where

$$F_1 = v(v_o + v)[ZnOHI]/[I']$$

is a linear function of v ml of titrant added, provided that all the assumptions made above are valid. Moreover, this line when extrapolated to $F_1 = 0$ will intersect the v-axis at $v = v_{eq}$.

Plots of F_1 applied to the HALTAFALL simulated titration data at different pH values are shown in Fig. 2, and the dependence of the systematic error on the pH is evident from Table II. As is seen from the figure, the F_1 plots are very nearly linear in the pH range under consideration.

The main reason for the systematic errors and the slight non-linearity of F_1 is the formation of the calcium–EGTA complex from the EGTA liberated from the zinc–EGTA complex during the formation of the zinc–indicator complex. Also, of course, very close to the equivalence point, magnesium– and strontium–EGTA complexes are present. Interference from the latter complexes is best overcome by choosing a pH value such that the measurable colour changes occur before their formation commences.

Interference from zinc–EGTA is partly compensated for by introducing v_1

$$v_1 = v + v_o[ZnOHI]/t_{EGTA} \tag{9}$$

and plotting F_1'

$$F_1' = v_1(v_o + v)[ZnOHI]/[I'] \tag{10}$$

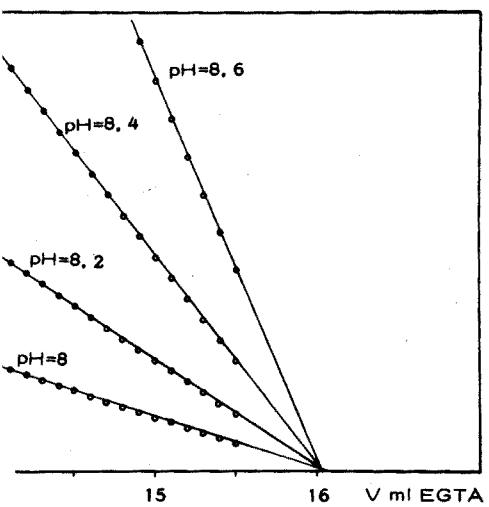

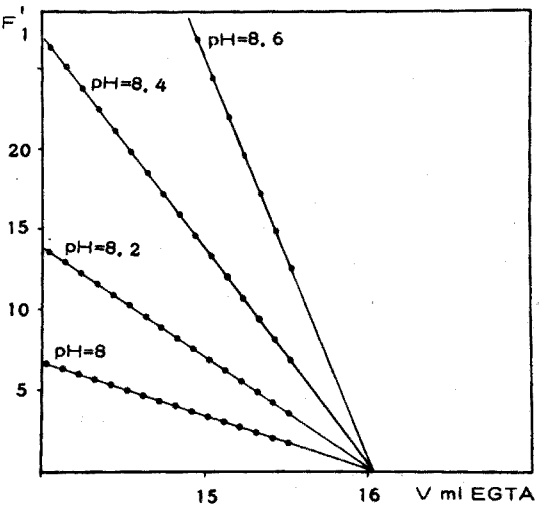

Fig. 2. Straight-line regression evaluation of the equivalence point by means of the plot F_1 (arbitrary scale).

Fig. 3. Straight-line regression evaluation of the equivalence point by means of the plot F_1' (arbitrary scale).

against v_1. As is seen from Fig. 3, the theoretical plots thus obtained are linear and on extrapolation to $F_1' = 0$, they intersect the v-axis very close to the theoretical end-point. The systematic error is small and independent of pH, as is seen from Table II.

As pointed out above, the concentrations of the indicator species cannot be measured directly. The relationship between these values and the experimentally measurable absorbance, A, at constant pH, is

$$A = \varepsilon_1[\mathrm{ZnOHI}] + \varepsilon_2[\mathrm{I}'] \tag{11}$$

Furthermore, if the wavelength is such that $\varepsilon_1 > \varepsilon_2$, then

$$A_{max} = f\varepsilon_1[\mathrm{I}]_{tot} \tag{12}$$

$$A_{min} = f\varepsilon_2[\mathrm{I}]_{tot} \tag{13}$$

where

$$f = v_0/(v_0 + v) \tag{14}$$

and

$$f[\mathrm{I}]_{tot} = [\mathrm{ZnOHI}] + [\mathrm{I}'] \tag{15}$$

By combining eqns. (12) and (15)

$$A_{max} - A = (\varepsilon_1 - \varepsilon_2)[\mathrm{I}'] \tag{16}$$

and by combining eqns. (13) and (15)

$$A - A_{min} = (\varepsilon_1 - \varepsilon_2)[\mathrm{ZnOHI}] \tag{17}$$

Thus,

$$[\mathrm{ZnOHI}]/[\mathrm{I}'] = (A - A_{min})/(A_{max} - A) \tag{18}$$

which is used to calculate F_1 and F_1'.

Moreover, by combining eqns. (16), (17) and (18)

$$[\mathrm{ZnOHI}] = (A - A_{min}) f[\mathrm{I}]_{tot}/(A_{max} - A_{min}) \tag{19}$$

which can be used to calculate F_1', provided that a value for $[\mathrm{I}]_{tot}$ is known.

EXPERIMENTAL

Apparatus

The photometer used was an EEL filter photometer with a selenium photocell. Since it is not necessary to protect the titration vessel from external light, the instrument has many advantages, *e.g.*, samples can be changed rapidly. The main drawback of the instrument, the non-linearity between the illumination and the output current, due to the external load resistance, was overcome by means of an operational amplifier (Fairchild μA 725 C) used as an current amplifier, as shown in Fig. 4. Calibration of the photocell response against zincon concentration yielded linear plots in the range 0–1.0 absorbance units. The computer-processed titrator used was that described previously[17] and the automatic burets were of type Metrohm Dosimat E 412.

Reagents

All reagents were of analytical grade and were analysed for calcium im-

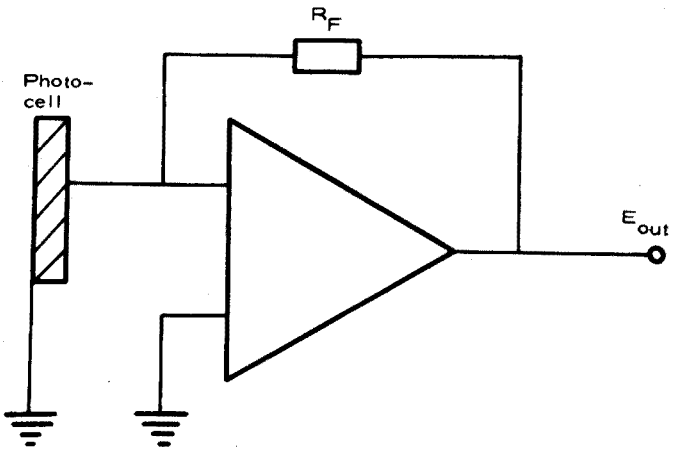

Fig. 4. Current amplification of photocell signal.

purities by means of atomic absorption spectrometry. A *ca.* 0.15 *M* solution of tetrasodium–EGTA was prepared by dissolving the acid in sodium hydroxide. Calcium standards corresponding to "sea water" of 35‰ salinity were prepared by dissolving calcium carbonate in hydrochloric acid. After neutralization, sodium, potassium, magnesium, strontium, chloride, sulphate and hydrogencarbonate were added in the same proportions as in sea water. Standard Sea Water was obtained from Charlottenlund Slot, Denmark. Buffer solutions (pH 8.6) were prepared from boric acid and the indicator solution was prepared by dissolving the monosodium salt in ethanol.

Computerized titration procedure

A portion (25 g) of a 35‰ salinity sea water sample was accurately weighed into the titration vessel and diluted with calcium-free doubly distilled water and buffer solution. For water samples of lower salinity, a proportionately greater amount was weighed in, the ionic strength and composition thus always being approximately the same. The procedure commenced with the titrator asking for the weight of the sample and the temperature in the EGTA storage vessel. The latter information was used by the processing computer program to correct for variations in the EGTA concentration caused by fluctuations in temperature. Such a correction is necessary in high-precision analysis unless the temperature can be kept constant to within 0.2°. Density variation corrections were calculated by the processing computer program according to experimental data relevant for 0.5 *M* sodium chloride. Information concerning the concentration of EGTA, at a given temperature, and the total indicator concentration were specified in the processing program and not as input data for each separate titration, since these parameters were changed only when new stock solutions were prepared.

The reference intensity, I_0, for the solution without indicator was measured for 10 s, after which the titrator added one-half the amount of indicator from an automatic syringe buret and measured the absorbance. The amount of indicator was chosen so that the absorbance value obtained, $A_{max}/2$, was between 0.4 and

0.5 units, *i.e.* within the optimal range for accurate photometric measurement. From the measured value of A_{max}, the relevant A_{min} value was calculated, using the value of the ratio A_{max}/A_{min} specified in the processing program. This ratio was determined separately and is, of course, relevant for the specific photometric equipment only at a given pH value. It would be possible to determine A_{min} in each separate titration by programming the computer to add a large excess of titrant at the end of each titration. In this region the absorbance value is, however, so small that the photometric precision is poor. In the separate determination of the ratio A_{max}/A_{min}, the value of A_{min} was determined for a total indicator concentration approximately ten times higher than that used in the titrations.

The remainder of the indicator was then added, followed by EGTA titrant, until the value of $(A-A_{min})/(A_{max}-A)$ approached 2, after which increments of 0.1 ml of titrant were added, the values being stored in the core memory. Addition of titrant was continued until $(A-A_{min})/(A_{max}-A)\approx 0.3$. The criterion for a stable absorbance reading after an addition of titrant was that two consecutive sets of mean values differed by less than 0.1%, each mean value being calculated from twenty readings, which took a little longer than 1 s. Stable readings were normally achieved in less than 10 s after the addition of a new increment of titrant.

In the evaluation of the equivalence point by means of F_1', only titration points for which $(A-A_{min})/(A_{max}-A)$ lay between 2 and 0.3 were included. This was because even small errors in A cause large errors in this ratio if the absorbance value is close to either A_{max} or A_{min}. Moreover, interference from magnesium–EGTA can be neglected if data for which $(A-A_{min})/(A_{max}-A)<0.3$ are excluded.

Tests were made to establish whether or not improved precision was obtained if a weighting scheme was applied to the experimental points included in F_1', those values with high F_1' values being, of course, assigned the lowest weights. Since the computerized titrator permits the titration of a larger number of samples, the weighting function was derived empirically rather than theoretically, that finally adopted being

$$\text{Weight of point No. Q} = \text{Integer } (1.5\ \text{Q})^{\frac{1}{2}} \qquad (20)$$

point No. 1 being the first experimental point with $(A-A_{min})/(A_{max}-A)$ less than 2. It should be emphasized that the weighting function improves the analytical precision only by *ca.* 20%. The time required for a single titration is about 10 min, including the time needed for evaluation and printing out of the edited results.

RESULTS AND DISCUSSION

Precision

Ten sets of measurements, each set consisting of twenty titrations of 20–25 g sea-water samples, yielded a mean value with a relative standard deviation of 0.00028. This is considerably better than the relative standard deviations obtained previously from linear regression photometric titrations, *e.g.* reference 18. The main reasons for this were found experimentally to be:

(i) the method does not require pretreatment of the samples;

(ii) the current amplifier coupled to the photocell results in a linear absorbance *vs.* concentration relationship;

(iii) the plot F_1' takes interfering indicator side-reactions into account and permits exploitation of a part of the titration curve where the formation of magnesium–EGTA complex is negligible;

(iv) both A_{max} and A_{min} are measured within the optimal region for absorbance measurement;

(v) the titration procedure is automatic, permitting the collection of a large number of titration data in a reasonable space of time; it is, of course, possible to perform the titration manually but this will increase the time needed for one titration considerably;

(vi) temperature variations in the titrant storage vessel are compensated for;

(vii) evaporation from the titrant storage vessel is kept at a minimum by using a syringe-shaped vessel, thus reducing the volume of air above the titrant solution.

Accuracy

The accuracy of the titration procedure depends on the accuracy of the calcium concentration in the standard solution and on how closely the ionic composition of the standard resembles that of sea water. Calcium carbonate is an accurate calcium standard, and since the relative compositions of the main sea water constituents differ only very slightly from one sample to another it is possible to prepare a representative "sea water" standard. The great sensitivity obtainable in the atomic absorption analysis for calcium ensures, moreover, that calcium impurities are not introduced with chemicals used in preparing the standards. The suggested method ought to be sufficiently accurate for sea-water samples with salinities greater than 5‰. Nevertheless, it is the author's opinion that, in order to be able to compare results obtained by different methods, it is imperative to agree on an international standard to be used, as emphasised by Culkin and Cox[5], for example.

Calcium concentration in sea water

The calcium concentration of Copenhagen Standard Sea Water of 19.3745‰ chlorinity was determined to be 10.28 mmoles kg^{-1}. This value is in good agreement with the mean values of 10.26 and 10.29 obtained for North Atlantic samples by Riley and Tongudai[19] and Culkin and Cox[5], respectively.

Field experiments

The suggested method has been used by Dyrssen *et al.* to determine the calcium concentration in samples of Pacific sea water taken by Eng. Dmitry Mendeleev. The preliminary results[20] show that the method is well suited to analysis on board ship.

Financial support from Knut och Alice Wallenbergs Stiftelse and the Swedish Natural Research Council (NFR) is gratefully acknowledged.

SUMMARY

A computerized photometric titration procedure for the determination of

calcium in the presence of magnesium with zinc–zincon as indicator is described. The evaluation method is based on straight-line regression, the method yielding a relative precision of 0.00028 when applied to sea water samples in the salinity range 5–35‰.

RÉSUMÉ

On décrit une méthode de titrage photométrique avec ordinateur pour le dosage du calcium en présence de magnésium, en'utilisant le zinc–zincon comme indicateur. Cette méthode est basée sur une régression en ligne droite permettant une précision relative de 0.00025 pour des échantillons d'eau de mer de salinité comprise entre 5 et 35‰.

ZUSAMMENFASSUNG

Es wird ein photometrisches Titrationsverfahren unter Verwendung eines Computers für die Bestimmung von Calcium in Gegenwart von Magnesium mit Zink–Zincon als Indikator beschrieben. Die Auswertmethode beruht auf einer geradlinigen Regression und ergibt eine relative Reproduzierbarkeit von 0.00025, wenn sie auf Meerwasser-Proben mit einem Salzgehalt von 5–35‰ angewendet wird.

REFERENCES

1 J. P. Riley and M. Tongudai, *Anal. Chim. Acta*, 36 (1966) 439.
2 M. Whitfield and J. V. Leyendekkers, *Anal. Chim. Acta*, 45 (1969) 383.
3 D. Dyrssen, D. Jagner and H. Johansson, *Reports on the Chemistry of Sea Water*, V, University of Göteborg, 1968.
4 J. Růžička, E. H. Hansen and J. C. Tjell, *Anal. Chim. Acta*, 67 (1973) 155.
5 F. Culkin and R. A. Cox, *Deep-Sea Res.*, 13 (1966) 789.
6 A. Ringbom, G. Pensar and E. Wänninen, *Anal. Chim. Acta*, 19 (1958) 525.
7 C. N. Reilley and R. W. Schmid, *Anal. Chem.*, 30 (1958) 947.
8 T. Higuchi, C. Rehm and C. Barnstein, *Anal. Chem.*, 28 (1956) 1506.
9 D. Dyrssen, D. Jagner and F. Wengelin, *Computer Calculations of Ionic Equilibria and Titration Procedures*, Almqvist et Wiksell, Stockholm, 1968.
10 A. Johansson, *Anal. Chim. Acta*, 61 (1972) 285.
11 N. Ingri, W. Kakotowicz, L.-G. Sillén and B. Warnqvist, *Talanta*, 14 (1967) 1261.
12 T. Anfält and D. Jagner, *Anal. Chim. Acta*, 57 (1971) 165.
13 A. Ringbom, *Complexation in Analytical Chemistry*, Interscience, New Nork and London, 1963.
14 E. Still and A. Ringbom, *Anal. Chim. Acta*, 33 (1965) 50.
15 E. Still, *Suom. Kemistil.*, 41 (1968) 33.
16 O. Gran, *Analyst*, 77 (1952) 661.
17 T. Anfält and D. Jagner, *Anal. Chim. Acta*, 57 (1971) 177.
18 D. Jagner and Årén, *Anal. Chim. Acta*, 57 (1971) 185.
19 J. P. Riley and M. Tongudai, *Chem. Geol.*, 2 (1967) 263.
20 T. Almgren, D. Dyrssen and M. Strandberg, to be published in *Deep-Sea Res.*

Analytica Chimica Acta, 68 (1974) 93–102

EINE KINETISCHE DIFFERENZMETHODE UNTER VERWENDUNG VON REAKTIONEN DES LANDOLT-TYPS

H. WEISZ und K. ROTHMAIER

Lehrstuhl für Analytische Chemie, Chemisches Laboratorium, Universität Freiburg i.Br., Freiburg i.Br. (Bundesrepublik Deutschland)

(Eingegangen den 28 Mai 1973)

Eine kinetische Differenzmethode unter Verwendung katalysierter Reaktionen wurde bereits in einer früheren Veröffentlichung beschrieben[1].

Bei dieser Methode werden in zwei gleichartigen Gefässen zwei völlig gleiche Ansätze mit verschiedenen Katalysatormengen simultan gestartet. Das eine Gefäss enthält jeweils die gleiche bekannte Katalysatormenge, das andere die unbekannte zu bestimmende Katalysatormenge. Wird der Ablauf der Reaktion in den beiden Gefässen anhand der Abnahme der Konzentration eines Partners oder der Zunahme eines Produktes verfolgt, z.B. durch Messung der Extinktion oder des Potentials, so ist die Differenz der beiden Messgrössen zum Zeitpunkt des Starts null. Die Differenz nimmt nach dem Start zu, bis schliesslich ein Maximum erreicht ist. Nach vollständigem Ablauf der Reaktion in beiden Gefässen erhalten wir wieder den Wert Null. Wird der Reaktionsverlauf mittels eines Schreibers aufgezeichnet, dann kann die Steigung der Kurve, das Maximum der Differenz oder die Fläche unter der Kurve als Mass für die unbekannte Katalysatorkonzentration verwendet werden.

Wir haben nun diese Differenzmethode auf Reaktionen vom Landolt-Typ angewendet, die auf der Ausscheidung von Jod beruhen. Solche Systeme lassen sich vereinfachend durch nachstehendes Reaktionsschema beschreiben:

$$Ox_1 + 2\,J^- \xrightarrow{k_1} J_2 + Red_1 \qquad \text{langsam} \qquad (1)$$

$$J_2 + Red_2 \xrightarrow{k_2} 2\,J^- + Ox_2 \qquad \text{schnell} \qquad (2)$$

Auf die langsam ablaufende Reaktion (1) folgt die schnellverlaufende Reaktion (2). Das als Indikatorsubstanz dienende freie Jod kann erst dann auftreten, wenn das im definierten Unterschuss vorhandene Reduktionsmittel Red_2, das "Landolt-Reagens", verbraucht ist. Die Zeit vom Start der Reaktion bis zum ersten Auftreten von Jod nennt man Induktionsperiode. Ist die langsame Reaktion (1) katalysierbar, so lassen sich unbekannte Katalysatorkonzentrationen bestimmen, wobei die Länge der Induktionsperiode ein Mass für die Katalysatorkonzentration darstellt. Svehla und Mitarbeiter[2–5] sowie Bognár und Jellinek[6,7] haben eine Reihe von Metallionen auf diese Weise bestimmt.

Bei Verwendung von Reaktionen des Landolt-Typs in der katalytischen Differenzmethode werden wiederum zwei gleiche Ansätze, die sich nur in der

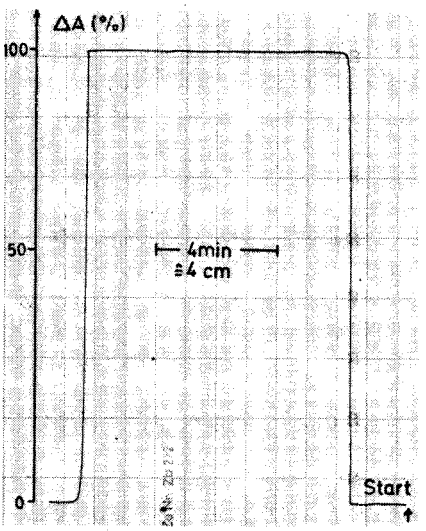

Abb. 1. Registrierung des Reaktionsablaufes (Bestimmung von Molybdän). $[Mo]_p = 4$ µg Mo pro 10 ml und $[Mo]_v = 30$ µg Mo pro 10 ml.

Katalysatorkonzentration unterscheiden, simultan gestartet. Verfolgt man das Auftreten von freiem Jod während des Reaktionsablaufes mit Hilfe einer geeigneten Methode, z.B. durch Messung der Extinktion, so erhält man zunächst für die Differenz der beiden Messgrössen den Wert Null. Erst nach Ablauf der Reaktion mit der höheren Katalysatorkonzentration tritt eine rasche und deutliche Zunahme der Differenz des Messeffektes auf. Die Differenz wird erst dann wieder null, wenn auch die zweite Reaktion vollständig abgelaufen ist. Abb. 1 zeigt einen solchen Kurvenverlauf. Wird die Katalysatorkonzentration in einem der Ansätze als konstant vorgegeben ($[K]_v$ = Katalysatorkonzentration im Vergleichsansatz), so ist die Zeit zwischen der Zu- und Abnahme der Differenz des Messeffektes (jeweilige Ausscheidung von Jod in den beiden Ansätzen) ein Mass für die unbekannte Katalysatorkonzentration im Probeansatz $[K]_p$.

Wir haben das System Wasserstoffperoxid–Jodid–Ascorbinsäure verwendet, um Molybdän(VI) zu bestimmen. Die beschleunigende Wirkung von Jodid auf die Jodat–Arsenit-Reaktion wurde zu dessen Bestimmung ausgenutzt. Der Reaktionsablauf wurde in beiden Fällen photometrisch verfolgt. Bei der Bestimmung von Vanadin(V) unter Verwendung des Bromat–Jodid–Ascorbinsäure-Systems, sowie bei der Kupferbestimmung mit dem Peroxodisulfat–Jodid–Thiosulfat-System wurde der Reaktionsablauf potentiometrisch verfolgt.

BESTIMMUNG VON MOLYBDÄN(VI) MIT EINER KINETISCH-PHOTOMETRISCHEN DIFFERENZMETHODE

Das System Jodid–Wasserstoffperoxid–Ascorbinsäure wurde von Svehla und Erdey zur Bestimmung von Molybdän benutzt[2,8].

$$2\,J^- + H_2O_2 + 2\,H^+ \rightarrow J_2 + 2\,H_2O$$

$$J_2 + \text{Ascorbinsäure} \rightarrow 2\,J^- + 2H^+ + \text{Dehydroascorbinsäure}$$

Experimentelles

Bei der Differenzmethode wird die durch Molybdän katalysierte Wasserstoffperoxid–Jodid–Ascorbinsäure-Reaktion unter Verwendung einer geeigneten Startpipette (vgl. Weisz und Ludwig[1]) in zwei Reaktionsgefässen gleichzeitig gestartet. Dabei werden zu zwei Lösungen, welche gleiche Mengen Jodid und Ascorbinsäure, aber unterschiedliche Molybdänmengen enthalten, jeweils gleiche Mengen Wasserstoffperoxid gegeben. Zur photometrischen Verfolgung des Reaktionsablaufes haben wir das "Universal Kolorimeter Modell J" der Fa. Lange, Berlin, verwendet, das mit zwei temperierbaren Küvettenhaltern ausgestattet wurde. Diese wurden nach den Massen der Küvettenschächte des Kolorimeters und der verwendeten Küvetten (H-Küvette, Fa. Zeiss, Schichtlänge 20 mm) hergestellt. Die Thermostatierung erfolgte mit einem Umwälzthermostaten ("Ultra-Thermostat", Messgerätewerk Lauda/Tauber). Zur Durchmischung der Reaktionslösungen dienten zwei Magnetrührer. Die Registrierung erfolgte durch den Kompensations-Linienschreiber "Servogor" der Fa. Metrawatt, Nürnberg.

Lösungen. Lösung I. 4.35 g Kaliumjodid, 9.125 g Natriumacetat-3-hydrat, 6 ml Eisessig und 10 g Ascorbinsäure werden in bidest. Wasser gelöst und auf 250 ml aufgefüllt.

Lösung II. 2 ml 30%iges Wasserstoffperoxid und 10 ml 0.5 *M* Schwefelsäure werden mit bidest. Wasser auf 100 ml aufgefüllt.

Durchführung. In die beiden Küvetten werden je 2 ml der Lösung I und jeweils 0.5 ml Stärkelösung (1%ig) einpipettiert. In Küvette I werden 3 ml Molybdännvergleichslösung (10 μg Mo ml^{-1}; ($Na_2MoO_4 \cdot 2\ H_2O$)), in Küvette II 5 ml Probelösung gegeben. Beide Küvetten werden mit bidest. Wasser auf 9 ml aufgefüllt. Die Küvette mit dem Vergleichsansatz wird in den rechten, die Küvette mit dem Probeansatz in den linken Strahlengang des Photometers eingesetzt. Die Temperatur der beiden Lösungen wird auf $23.0 \pm 0.1°$ gebracht. Die Reaktion wird in beiden Gefässen durch Zugabe von je 1 ml der Lösung II (Startpipette) ge-

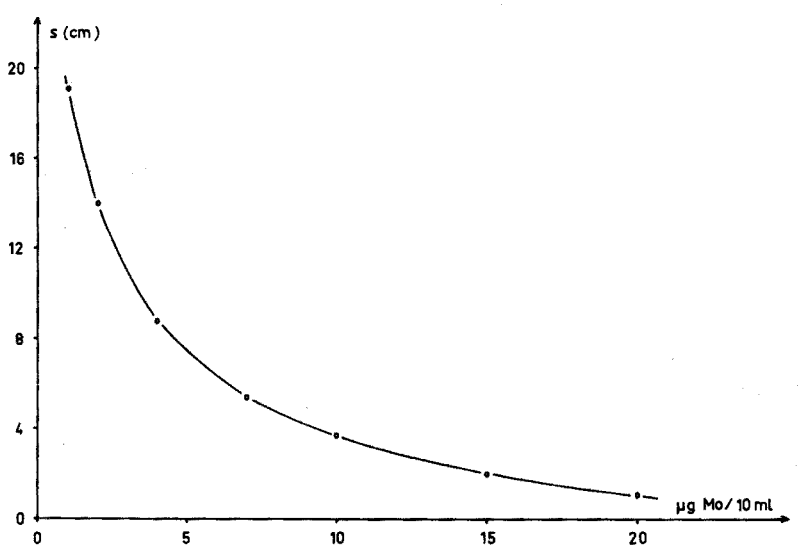

Abb. 2. Abhängigkeit der gemessenen Abstände *s* (ausgedrückt in cm) von der Molybdänkonzentration.

startet. Die zeitliche Änderung der Absorptionsdifferenz (Grünfilter, max. *ca.* 525 nm) wird durch den Schreiber (Vorschubgeschwindigkeit 600 mm h^{-1}) registriert. Der Verlauf einer Kurve ist in Abb. 1 dargestellt. Der scharf ausgebildete Kurvenverlauf wird durch den Kunstgriff erreicht, dass man die Extinktion von freiem Jod stark erhöht, indem man dem System von Anfang an Stärkelösung zusetzt.

Auswertung und Ergebnisse

Zur Auswertung der Messungen wurden die Abstände *s* (cm) zwischen den auf- und absteigenden Kurvenästen bei einer gleichbleibenden, einmal vorgewählten Absorptionsdifferenz (in diesem Falle bei 50%) gemessen.

Zur Herstellung der Eichkurve wurden die Abstände für 1, 2, 4, 7, 10, 15 und 20 μg Mo pro 10 ml gemessen und gegen die Katalysatorkonzentration aufgetragen ($[Mo]_v$ ist stets 30 μg Mo pro 10 ml). Die Eichkurve ist in Abb. 2 wiedergegeben.

Wir haben zahlreiche Bestimmungen im Bereich von 1–20 μg Mo pro 10 ml durchgeführt. Einige Ergebnisse sind in Tabelle I aufgeführt. Die gemessenen Abstände *s* lagen zwischen 19.8 und 1.1 cm (bzw. min).

TABELLE I

BESTIMMUNG VON MOLYBDÄN

Mo gegeben (μg/10 ml)	*Mo gefunden (μg/10 ml)*	*Relativer Fehler (%)*
1.47	1.42	−3.4
2.44	2.43	−0.4
3.07	3.01	−2.0
4.24	4.20	−0.9
5.57	5.58	+0.2
8.13	8.24	+1.4
9.36	9.40	+0.4
12.35	12.53	+1.5
17.10	16.70	−2.4
19.34	19.43	+0.5

BESTIMMUNG VON JODID MIT EINER KINETISCH-PHOTOMETRISCHEN DIFFERENZMETHODE

Als weiteres Beispiel sei die Bestimmung von Jodid mit der Jodat–Arsenit-Reaktion beschrieben. Hierbei handelt es sich im Gegensatz zur vorher beschriebenen Reaktion um ein autokatalytisches System, in welchem Jodid als Katalysator wirkt[9]. Ein willkürlicher Zusatz von Jodid führt zu einer Beschleunigung der Reaktion. Bognár und Sárosi haben diese beschleunigende Wirkung auf die Jodat–Arsenit-Reaktion zur Bestimmung von Jodid herangezogen[10].

$$3\ AsO_3^{3-} + JO_3^- \rightarrow 3\ AsO_4^{3-} + J^-$$

$$5\ J^- + JO_3^- + 6\ H^+ \rightarrow 3\ J_2 + 3\ H_2O$$

$$J_2 + AsO_3^{3-} + H_2O \rightleftharpoons 2\ J^- + AsO_4^{3-} + 2\ H^+$$

Experimentelles

Bei der Differenzmethode wird die Reaktion wiederum mit Hilfe der Startpipette in zwei Reaktionsgefässen gleichzeitig gestartet. Als Reaktionsgefässe dienen Rundküvetten (innerer Durchmesser 22 mm, Höhe *ca.* 50 mm) mit den entsprechenden temperierbaren Haltern. Um Störungen zu vermeiden, werden die Gefässe nach jeder Bestimmung mit Ascorbinsäure und anschliessend mit Königswasser behandelt.

Lösungen. Lösung I. 10 g Arsentrioxid werden in 200 ml 1 *M* Natronlauge gelöst. Die Lösung wird nach Zugabe von 200 ml 0.5 *M* Schwefelsäure mit bidest. Wasser auf 1 Liter aufgefüllt.

Lösung II. 2%ige Kaliumjodatlösung.

Pufferlösung. 26.5 ml 0.1 *N* Natriumcitratlösung (tri-Natriumcitrat-2-hydrat) mit 0.1 *N* Salzsäure ad 100 ml.

Durchführung. In die beiden Bechergläser werden je 1 ml der Lösung I, 2 ml Pufferlösung und 0.5 ml Stärkelösung (1%ig) einpipettiert. In das eine Gefäss wird 1 ml Jodidvergleichslösung (100 μg J^- ml^{-1} (KJ)) gegeben. In das andere Gefäss werden 5 ml Probelösung gegeben. Beide Gefässe werden mit bidest. Wasser auf 9 ml aufgefüllt und in das Photometer eingesetzt. Die Vergleichslösung befindet sich dabei wieder im rechten Strahlengang. Die Temperatur der beiden Lösungen wird auf $23.0 \pm 0.1°$ gebracht. Mit Hilfe der Startpipette wird die Reaktion in den beiden Gefässen durch Zugabe von je 1 ml Lösung II simultan gestartet.

Die registrierte Kurve hat die gleiche Form wie die in Abb. 1 beschriebene.

Auswertung und Ergebnisse

Zur Aufnahme einer Eichkurve wurden hier die Abstände s (cm) für 1, 3, 5, 10, 20 und 30 μg J^- pro 10 ml bei der Absorptionsdifferenz 50% gemessen ($[J^-]_v$ ist stets 100 μg J^- pro 10 ml). Die Eichkurve ist der in Abb. 2 dargestellten ähnlich.

Es wurden mehrere Bestimmungen im Bereich von 1–30 μg Jodid pro 10 ml durchgeführt. Einige Ergebnisse sind in Tabelle II aufgeführt. Die Abstände s lagen zwischen 24.5 und 3.8 cm (bzw. min).

TABELLE II

BESTIMMUNG VON JODID

J^- gegeben (μg/10 ml)	*J^- gefunden (μg/10 ml)*	*Relativer Fehler (%)*
1.40	1.35	−3.6
2.66	2.60	−2.3
3.92	4.00	+2.0
5.82	6.00	+3.1
7.14	6.80	−4.8
9.50	9.30	−2.1
16.50	17.10	+3.6
19.30	20.30	+5.2
25.00	26.60	+6.4
29.00	30.20	+4.1

BESTIMMUNG VON KUPFER MIT EINER KINETISCH-POTENTIOMETRISCHEN DIFFERENZMETHODE

Die durch Kupfer und Eisen(II) katalysierte Reaktion zwischen Peroxodisulfat und Jodid wurde von Páll, Svehla und Erdey durch Zugabe von Thiosulfat in eine Reaktion vom Landolt-Typ umgewandelt[3].

$$2\,J^- + S_2O_8^{2-} \rightarrow J_2 + 2\,SO_4^{2-}$$
$$J_2 + 2\,S_2O_3^{2-} \rightarrow 2\,J^- + S_4O_6^{2-}$$

Experimentelles

Bei der Differenzmethode wurde zur potentiometrischen Verfolgung des Reaktionsablaufes die bereits früher beschriebene Versuchsanordnung (Weisz und Ludwig[1]) verwendet. Die Potentialmessung erfolgte mit zwei Platinelektroden (4.5 mm lange und 1 mm starke in den Glasschaft eingeschmolzene Metallstifte, die am unteren Ende in eine Kugel vom Durchmesser 1.7 mm auslaufen) und dem Labor-pH-Meter "pH 70" der Fa. Knick, Berlin. Die beiden Halbzellen wurden durch eine Elektrolytbrücke (0.6% Agar; 0.2 *M* KCl) miteinander verbunden. Zur Durchmischung der beiden Lösungen verwendeten wir zwei Rührer, die von einem Motor über eine Transmission (1:1) angetrieben wurden.

Lösungen. Lösung I. 7.0 g Kaliumperoxodisulfat, 6.8 g Natriumacetat-3-hydrat und 10 ml 0.5 *M* Schwefelsäure mit bidest. Wasser ad 250 ml.

Lösung II. 1.65 g Kaliumjodid und 0.4 g Natriumthiosulfat mit bidest. Wasser ad 250 ml.

Kupferstammlösung. 100 μg Cu ml^{-1} ($CuSO_4 \cdot 5\,H_2O$).

Durchführung. In zwei thermostatierbare 10 ml-Bechergläser werden je 1 ml Lösung I einpipettiert. In das Gefäss I werden 5 ml Kupfervergleichslösung (2 μg Cu ml^{-1}), in das Gefäss II 5 ml Probelösung gegeben. Das Gesamtvolumen in beiden Gefässen beträgt 6 ml. Die Platinelektroden und die Elektrolytbrücke werden eingeführt. Nachdem die Temperatur der beiden Lösungen 25° erreicht hat, wird die Reaktion in den beiden Gefässen durch Zugabe von je 1 ml Lösung II (Startpipette) gestartet. Die zeitliche Änderung der Potentialdifferenz der beiden Jod/Jodid-Halbzellen wird durch den Schreiber (Vorschubgeschw. 600 mm h^{-1}) registriert. Der Verlauf einer Kurve ist in Abb. 3 dargestellt.

Die Platinelektroden werden zwischen den Messungen in Chromschwefelsäure und die Elektrolytbrücke in einer 0.2 *M* Kaliumchloridlösung aufbewahrt. Die Bechergläser werden nach jeder Messung mit Königswasser gereinigt.

Auswertung und Ergebnisse

Zur Auswertung der Messungen wurden hier die Abstände s (cm) zwischen den auf- und absteigenden Kurvenästen bei einer gleichbleibenden, einmal gewählten Potentialdifferenz (in diesem Fall bei $\Delta E = 106$ mV, entsprechend etwa der Hälfte der maximalen Potentialdifferenz) gemessen.

Zur Herstellung der Eichkurve wurden die Abstände für 0.1, 0.3, 0.5, 1.0, 1.5 und 2.0 μg Cu pro 7 ml gemessen und gegen die Katalysatorkonzentration aufgetragen ($[Cu]_v$ ist stets 10 μg Cu pro 7 ml). Die Eichkurve ist der in Abb. 2 dargestellten ähnlich.

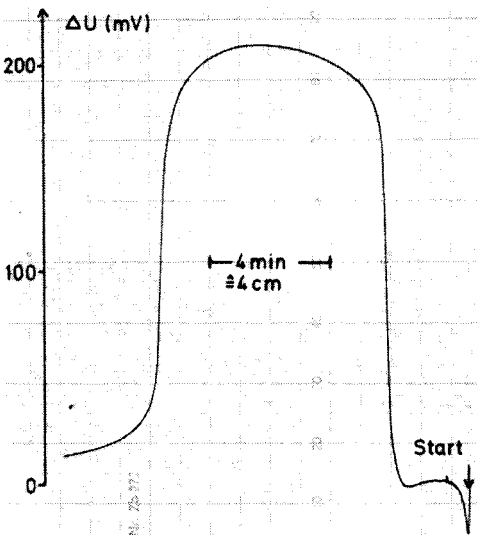

Abb. 3. Registrierung des Reaktionsablaufes (Bestimmung von Kupfer). $[Cu]_p = 1$ µg Cu pro 7 ml und $[Cu]_v = 10$ µg Cu pro 7 ml.

TABELLE III

BESTIMMUNG VON KUPFER

Cu gegeben (µg/7 ml)	*Cu gefunden (µg/7 ml)*	*Relativer Fehler (%)*
0.133	0.142	+ 6.8
0.225	0.223	− 0.9
0.358	0.370	+ 3.4
0.446	0.515	+15.5
0.581	0.644	+10.8
0.711	0.750	+ 5.5
0.955	0.960	+ 0.5
1.204	1.185	− 1.6
1.522	1.490	− 2.1
1.912	1.860	− 2.7

Es wurden mehrere Bestimmungen im Bereich von 0.1–2.0 µg Cu pro 7 ml durchgeführt. In Tabelle III sind einige Ergebnisse aufgeführt. Die gemessenen Abstände *s* lagen zwischen 20.3 und 4.2 cm (bzw. min).

BESTIMMUNG VON VANADIN(V) MIT EINER KINETISCH-POTENTIOMETRISCHEN DIFFERENZMETHODE

Die Bestimmung von Vanadin(V) mit Hilfe des Bromat–Jodid–Ascorbinsäure-Systems wurde von Bognár und Jellinek beschrieben[7,11].

$$BrO_3^- + 6\,J^- + 6\,H^+ \rightarrow 3\,J_2 + Br^- + 3\,H_2O$$

$$J_2 + \text{Ascorbinsäure} \rightarrow 2\,J^- + 2\,H^+ + \text{Dehydroascorbinsäure}$$

Experimentelles

Zur Bestimmung von Vanadin mit der Differenzmethode wurde die bei der Kupferbestimmung verwendete Versuchsanordnung benutzt.

Lösungen. Lösung I. 0.697 g Kaliumbromat und 63 g Citronensäure werden in bidest. Wasser gelöst und auf 250 ml aufgefüllt.

Lösung II. 2.075 g Kaliumjodid, 0.294 g Ascorbinsäure und 2.762 g tri-Natriumcitrat-2-hydrat werden in bidest. Wasser gelöst und auf 250 ml aufgefüllt.

Vanadinstammlösung. 100 μg V ml^{-1} (NH_4VO_3).

Durchführung. In die beiden Bechergläser gibt man je 1 ml Lösung I. In das eine Gefäss werden 3 ml Vanadinvergleichslösung (2 μg V ml^{-1}), in das andere 5 ml Probelösung gegeben. Beide Gefässe werden mit bidest. Wasser auf 7 ml aufgefüllt. Anschliessend werden die beiden Platinelektroden und die Elektrolytbrücke eingeführt. Die Temperatur der beiden Lösungen wird auf 25° gebracht. Der gleichzeitige Start (Startpipette) erfolgt mit je 1 ml Lösung II. Der Reaktionsverlauf wird auch hier durch den Schreiber registriert (Vorschubgeschwindigkeit 600 mm h^{-1}). Die Form der Kurve ist der in Abb. 3 dargestellten ähnlich.

Die Gefässe werden nach jeder Messung mit Königswasser gereinigt. Die Platinelektroden werden in Jod/Jodidlösung und die Elektrolytbrücke in einer 0.2 *M* Kaliumchloridlösung aufbewahrt.

Auswertung und Ergebnisse

Die Auswertung der Messungen erfolgte auf die gleiche Weise, wie vorstehend beschrieben. Die Abstände *s* (cm) wurden hier bei der Potentialdifferenz $\Delta E = 93$ mV gemessen (entsprechend etwa der Hälfte der maximalen Potentialdifferenz).

Zur Aufstellung der Eichkurve wurden die Abstände *s* für 0.1, 0.2, 0.5, 1.0, 2.0 und 3.0 μg V pro 8 ml gemessen und gegen die Katalysatorkonzentration aufgetragen ($[V]_v$ ist stets 6 μg V pro 8 ml). Die Eichkurve ist der in Abb. 2 dargestellten ähnlich.

Wir haben mehrere Bestimmungen im Bereich von 0.1–3.0 μg Vanadin pro 8 ml durchgeführt. In Tabelle IV haben wir einige Ergebnisse zusammengestellt. Die Abstände *s* liegen hier zwischen 23.8 und 2.5 cm (bzw. min).

TABELLE IV

BESTIMMUNG VON VANADIN

V gegeben (μg/8 ml)	*V gefunden (μg/8 ml)*	*Relativer Fehler (%)*
0.174	0.187	+ 7.5
0.310	0.279	− 10.0
0.526	0.540	+ 2.7
0.740	0.758	+ 2.4
0.905	0.936	+ 3.4
1.210	1.180	− 2.5
1.679	1.676	− 0.2
2.290	2.236	− 2.4
2.458	2.437	− 0.9
2.860	2.780	− 2.8

ZUSAMMENFASSUNG

Es wird eine kinetische Differenzmethode unter Verwendung von Reaktionen des Landolt-Typs beschrieben. Das Prinzip besteht darin, dass eine Reaktion in zwei Ansätzen gleichzeitig abläuft. Unter sonst identischen Bedingungen enthält ein Ansatz eine bekannte, jeweils gleiche Katalysatormenge und der andere die unbekannte Katalysatormenge. Aus der Differenz der beiden auftretenden Landolteffekte wird die zu bestimmende Katalysatorkonzentration ermittelt. Das System Wasserstoffperoxid–Jodid–Ascorbinsäure wurde verwendet, um Molybdän im Bereich von 1–20 μg pro 10 ml zu bestimmen. Jodid wurde aufgrund seiner beschleunigenden Wirkung auf die Jodat–Arsenit-Reaktion im Bereich von 1–30 μg pro 10 ml bestimmt. In beiden Fällen wurde der Reaktionsverlauf photometrisch verfolgt. Bei der Bestimmung von Vanadin im Bereich von 0.1–3.0 μg pro 8 ml unter Verwendung des Bromat–Jodid–Ascorbinsäure-Systems, sowie bei der Bestimmung von Kupfer im Bereich von 0.1–2.0 μg pro 7 ml mit dem Peroxodisulfat–Jodid–Thiosulfat-System wurde der Reaktionsverlauf potentiometrisch verfolgt.

SUMMARY

A kinetic difference method based on Landolt-type reactions is described. The reaction is allowed to proceed simultaneously in two mixtures, one of which contains a known constant amount of the catalyst and the other the unknown amount. The catalyst can be determined by means of the difference between the two Landolt effects. The system hydrogen peroxide–iodide–ascorbic acid was used to determine molybdenum in the range 1–20 μg. Iodide was determined by its effect on the iodate–arsenite reaction in the range 1–30 μg. In both cases, the reactions were followed photometrically. Vanadium (0.1–3.0 μg) was determined by means of the bromate–iodide–ascorbic acid system, and copper (0.1–2 μg) by the peroxydisulphate–iodide–thiosulphate system, both reactions being followed potentiometrically.

RÉSUMÉ

On décrit une méthode cinétique par différence, basée sur des réactions de type Landolt. On effectue la réaction simultanément dans deux mélanges, l'un d'eux renferme une quantité connue du catalyseur, l'autre la quantité à déterminer. Le système peroxyde d'hydrogène–iodure–acide ascorbique est utilisé pour le dosage du molybdène, en quantités de l'ordre de 1 à 20 μg. Les iodures (1 à 30 μg) sont dosés par leur action sur la réaction iodate–arsénite. Dans les deux cas, les réactions sont suivies photométriquement. Le vanadium (0.1 à 3.0 μg) est dosé par la réaction bromate–iodure–acide ascorbique, potentiométriquement. Le cuivre (0.1 à 2.0 μg) est dosé également potentiométriquement par le système peroxydisulfate–iodure–thiosulfate.

LITERATUR

1 H. Weisz und H. Ludwig, *Anal. Chim. Acta*, 55 (1971) 303.

2 G. Svehla und L. Erdey, *Microchem. J.*, 7 (1963) 221.
3 A. Páll, G. Svehla und L. Erdey, *Talanta*, 17 (1970) 211.
4 H. Thompson und G. Svehla, *Microchem. J.*, 13 (1968) 576.
5 H. Thompson und G. Svehla, *Z. Anal. Chem.*, 247 (1969) 244.
6 J. Bognár und O. Jellinek, *Mitt. in fremden Sprachen Tech. Univ. Schwerind., Miskolc, Ungarn*, 24 (1964) 111; *Chem. Abstr.*, 65 (1966) 12848 h.
7 J. Bognár und O. Jellinek, *Mitt. in fremden Sprachen Tech. Univ. Schwerind., Miskolc, Ungarn*, 25 (1965) 127; *Chem. Abstr.*, 65 (1966) 12849 a.
8 G. Svehla und L. Erdey, *Microchem. J.*, 7 (1963) 206.
9 J. Bognár, *Mikrochim. Acta*, (1968) 485.
10 J. Bognár und Sz. Sárosi, *Anal. Chim. Acta*, 29 (1963) 406.
11 J. Bognár und O. Jellinek, *Mikrochim. Acta*, (1969) 318.

Analytica Chimica Acta, 68 (1974) 103–110

COMPLEX FORMATION OF GALLIUM(III) WITH 8-HYDROXY-7-IODOQUINOLINE-5-SULPHONIC ACID (FERRON)

A. MASSOUMI*, P. OVERVOLL and F. J. LANGMYHR
Department of Chemistry, University of Oslo, Oslo 3 (Norway)
(Received 11th June 1973)

The complex formation of 8-hydroxy-7-iodoquinoline-5-sulphonic acid (ferron) with metal ions has been studied by various authors[1–12]. In the earlier investigations the calculations of the stability constants had to be based on approximations; the numbers of reactions that could be taken into consideration were limited, so that important equilibria had to be neglected. The advances in computer technology made during recent years have made it possible to make allowance for far more equilibria in studies of complex chemistry.

The present paper describes a potentiometric study of the system gallium(III)–ferron, a system which does not seem to have been studied before.

A new computer program was applied in the calculations; the program made it possible to allow for a considerable number of equilibria.

EXPERIMENTAL

Apparatus

For the potentiometric titrations and for the measurement and adjustment of pH, a Metrohm potentiograph (model E-436) and a Beckman research pH-meter equipped with a Beckman glass electrode (type 39301 0-14 pH) and a Beckman 39071 calomel frit junction reference electrode were used. Standard solution of base was added from a Metrohm multi-burette (model E-485).

The titrations were made in a double-walled titrating vessel placed on a magnetic stirrer. Water from a thermostat ($25.0 \pm 0.1°$) was circulated through the jacket. Before and during the titrations a stream of high-purity nitrogen was passed through the solution.

The computer program was written in Fortran IV, and was used with a CDC 3300 computer.

The activity coefficient of the hydrogen ion was determined experimentally and found to be 0.81. Recalculation of the hydrogen ion activities (determined by the pH measurements) to concentrations was made by the computer. At the present constant ionic strength, the activity coefficients were assumed to be constant in the range 2.4–10.0 pH.

* On leave from Department of Chemistry, Pahlavi University, Shiraz, Iran.

Reagents

The ferron (Analar, Hopkin and Williams) was checked by alkalimetric titration and was found to be satisfactory. Gallium nitrate octahydrate (Fluka) was used.

All other chemicals were of reagent-grade quality.

Standard solutions

A $5 \cdot 10^{-3}$ *M* ferron solution, 0.1 *M* in potassium nitrate, was prepared by dissolving 1.756 g of ferron and 10.11 g of potassium nitrate in boiled distilled water and diluting the solution to 1 l.

A solution of gallium (about $5 \cdot 10^{-2}$ *M*) was prepared by dissolving 4.998 g of the nitrate in about 20 ml of boiled distilled water and diluting to 25 ml with water. The solution was standardized by indirect EDTA titration[13], a manganese(II) standard solution being used for the back-titration. More dilute ($5 \cdot 10^{-3}$ *M*) solutions of gallium, also 0.1 *M* in potassium nitrate, were prepared.

Standard solutions of sodium hydroxide (about 0.05 *M*) were prepared by diluting proper volumes of a 50% solution with freshly boiled distilled water; the solutions were standardized with potassium hydrogeniodate.

A 1 *M* solution of potassium nitrate was prepared.

For the adjustment of pH, 0.05 *M* and 0.01 *M* solutions of potassium hydrogenphthalate (pH 4.008 at 25°) and borax (pH 9.180 at 25°), respectively, were prepared.

Titrations

Aliquots (25 ml) of $5 \cdot 10^{-3}$ *M* ferron solution were titrated with standard alkali and the titration curves were recorded. Then 25 ml of $5 \cdot 10^{-3}$ *M* gallium solution were mixed with 25, 50 or 75 ml of $5 \cdot 10^{-3}$ *M* ferron solution and titrated as above.

DEFINITIONS AND CALCULATIONS

The following equilibria were taken into account (M representing the metal, L the ligand, DK_n the dissociation constants of the ligand, K_n the stability constants of the complexes, HK_n the hydrolysis constants of the metal ion). For simplicity ionic charges are omitted.

I. The dissociation constants of the ligand

DK_1: $HL \rightleftarrows H+L$; DK_2: $H_2L \rightleftarrows H+HL$

II. The stability constants of the complexes

K_1: $M+H_2L \rightleftarrows MH_2L$; K_2: $M+HL \rightleftarrows MHL$

K_3: $M+L \rightleftarrows ML$; K_4: $M+OH+L \rightleftarrows MOHL$

K_5: $M+2OH+L \rightleftarrows M(OH)_2L$; K_6: $M+2HL \rightleftarrows M(HL)_2$

K_7: $M+2L \rightleftarrows ML_2$; K_8: $M+OH+2L \rightleftarrows MOHL_2$

K_9: $M+3L \rightleftarrows ML_3$

III. The hydrolysis constants of the metal

HK_1: $M + H_2O \rightleftarrows MOH + H$; HK_2: $M + 2H_2O \rightleftarrows M(OH)_2 + 2H$

HK_3: $M + 3H_2O \rightleftarrows M(OH)_3 + 3H$; HK_4: $M + 4H_2O \rightleftarrows M(OH)_4 + 4H$

HK_5: $M + 5H_2O \rightleftarrows M(OH)_5 + 5H$

The computer program was developed from the following three basic equations:

The total metal concentration (C_M):

$$C_M = [MH_2L] + [MHL] + [ML] + [MOHL] + [M(OH)_2L] + [M(HL)_2] + [ML_2] + [MOHL_2] + [ML_3] + [M] + [MOH] + [M(OH)_2] + [M(OH)_3] + [M(OH)_4] + [M(OH)_5] \quad (1)$$

The total ligand concentration (C_L):

$$C_L = [H_2L] + [HL] + [L] + [MH_2L] + [MHL] + [ML] + [MOHL] + [M(OH)_2L] + 2[M(HL)_2] + 2[ML_2] + 2[MOHL_2] + 3[ML_3] \quad (2)$$

The degree of neutralization of the acid as defined by Schwarzenbach[14] (a being the number of moles of sodium hydroxide added per mole of ligand; NH representing the number of ligand protons):

$$(NH - a)C_L = 2[H_2L] + [HL] + 2[MH_2L] + [MHL] - [MOHL] - 2[M(OH)_2L] + 2[M(HL)_2] - [MOHL_2] - [MOH] - 2[M(OH)_2] - 3[M(OH)_3] - 4[M(OH)_4] - 5[M(OH)_5] + [H] - [OH] \quad (3)$$

Equation (1) was now simplified to:

$$C_M = \left(K_1P_2 + K_2P_1 + K_3 + K_4\frac{K_W}{[H]} + K_5\frac{K_W^2}{[H]^2}\right)[M][L] + \left(K_6P_1^2 + K_7 + K_8\frac{K_W}{[H]}\right)[M][L]^2 + K_9[M][L]^3 + \left(1 + \frac{HK_1}{[H]} + \frac{HK_2}{[H]^2} + \frac{HK_3}{[H]^3} + \frac{HK_4}{[H]^4} + \frac{HK_5}{[H]^5}\right)[M] \quad (4)$$

In this equation

$$P_1 = \frac{[H]}{DK_1}; \quad P_2 = \frac{[H]^2}{DK_1 \cdot DK_2}$$

Previous data[15–17] for the hydrolysis constants were used in the calculations, and, to fit the above definitions, the values were converted from stepwise to overall constants.

Similarly, eqn. (2) was rearranged to:

$$C_L = (P_2+P_1+1)[L] + \left(K_1P_2+K_2P_1+K_3+K_4\frac{K_W}{[H]} + K_5\frac{K_W^2}{[H]^2}\right)[M][L]$$
$$+2\left(K_6P_1^2+K_7+K_8\frac{K_W}{[H]}\right)[M][L]^2+3K_9[M][L]^3 \qquad (5)$$

Equation (3) was transformed to:

$$(NH-a)C_L = (2P_2+P_1)[L] + \left(2K_1P_2+K_1P_2-K_4\frac{K_W}{[H]} - 2K_5\frac{K_W^2}{[H]^2}\right)[M][L] +$$
$$+\left(2K_6P_1^2-K_8\frac{K_W}{[H]}\right)[M][L]^2$$
$$-\left(\frac{HK_1}{[H]} + 2\frac{HK_2}{[H]^2} + 3\frac{HK_3}{[H]^3} + 4\frac{HK_4}{[H]^4} + 5\frac{HK_5}{[H^5]}\right)[M]$$
$$+[H] - \frac{K_W}{[H]} \qquad (6)$$

From eqns. (4) and (5), M was eliminated, and also between eqns. (5) and (6), the value of L found in the former equation was inserted in the latter; the value of a was then calculated, $a_{calc.}$ now being expressed as a function of the constants: $a_{calc.} = f(K_1 \ldots K_9)$.

The simplified version of the above calculations was translated into a Fortran language*.

The values for pH and the volume of base added at each experimental point were inserted in the program. An initial value was then given to all stability constants and the square sum $\Sigma_i(a_{i_{exp.}} - a_{i_{calc.}})^2$ (i being the specific experimental point number) was calculated. One constant at a time was then varied until the square sum reached a minimum; constants which did not improve the square sum were eliminated.

When a satisfactory set of constants had been established, the computer printed out the titration curves and the calculated absolute stability constants, as well as the mole fractions of the various complexes; the values of m (moles of sodium hydroxide per mole of metal ion) were calculated from the data for a.

The root mean square error sum defined by $[n^{-1}\Sigma(a_{exp.} - a_{calc.})^2]^{\frac{1}{2}}$, where n is the number of experimental points, was calculated to be 0.069 for all the constants.

RESULTS

From the titration curve of the ligand (Fig. 1), the dissociation constants were calculated with a computer program based on the principles outlined above. The present and earlier data are listed in Table I.

* The present computer program is an application of a new general program developed for mono- and binuclear complex equilibria[18].

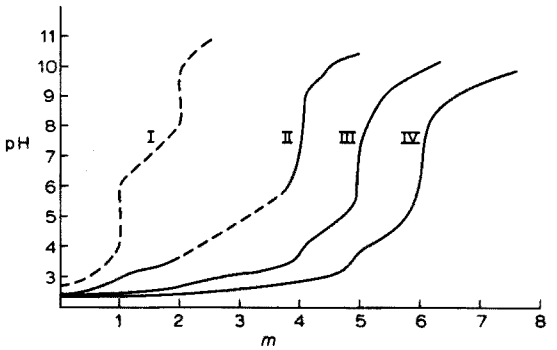

Fig. 1. Alkalimetric titration curves of ferron alone (I) and of 1:1 (II), 1:2 (III) and 1:3 (IV) mixtures of gallium with ferron. m = mole sodium hydroxide added per mole of metal.

TABLE I

DISSOCIATION CONSTANTS OF FERRON

pDK_1	pDK_2	*Experimental conditions*	*Method*	*References*
2.45	7.15	Not given	Colorimetric	4
2.44	7.17	25°, 0.005 *M* KCl	Potentiometric	5
2.96	6.46	25°, 2 *M* NaCl	Potentiometric	9
2.41	7.10	25°, 0.1 *M* acetate buffer	Spectrophotometric	11
2.50	7.11	25°, 0.1 *M* KCl	Potentiometric	6
2.35	7.05	25°, 0.1 *M* KNO_3	Potentiometric	This work

The titration curves of the mixtures of gallium with ferron are also reproduced in Fig. 1. The 1:1 curve exhibits inflections corresponding to the addition of one and four equivalents of base per mole of metal.

With reference to the equilibria listed above, the following reactions are likely to predominate in 1:1 mixtures.

$$Ga + HL \rightleftarrows GaHL$$

$$Ga + L \rightleftarrows GaL$$

$$GaL + OH \rightleftarrows GaOHL$$

$$Ga + 2OH + L \rightleftarrows Ga(OH)_2L$$

After the addition of two equivalents of alkali per mole of metal, the neutral slightly soluble compound GaOHL started to precipitate, but by further addition of base it dissolved.

In Fig. 2 the mole fractions of the various species appearing in the 1:1 mixtures are shown as a function of pH. The dotted parts of the curves represent the range in which the precipitate appeared. It is seen that—in addition to the complexes listed above—small amounts of GaL_2, $GaOHL_2$ and GaL_3 are also present.

The 1:2 curve exhibited inflections at $m=4$ and $m=5$. No precipitate appeared. The main reactions are believed to be:

$$Ga + 2L \rightleftarrows GaL_2$$
$$Ga + 2L + OH \rightleftarrows GaOHL_2$$
$$Ga + 3L \rightleftarrows GaL_3$$

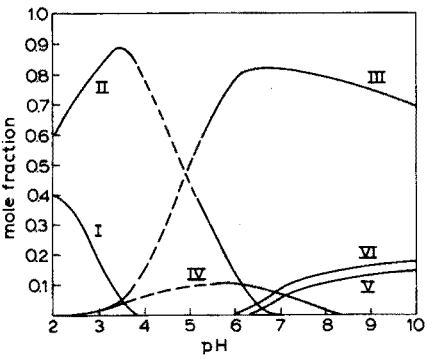

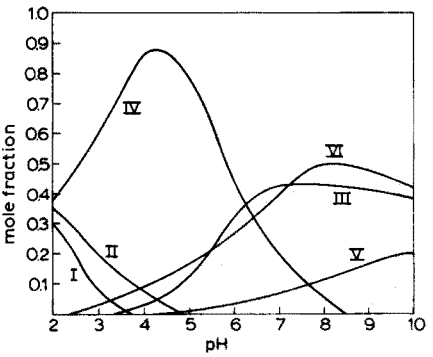

Fig. 2. The mole fractions in 1:1 mixtures of GaHL (I), GaL (II), $Ga(OH)_2L$ (III), GaL_2 (IV), $GaOHL_2$ (V) and GaL_3 (VI) plotted as a function of pH.

Fig. 3. The mole fractions in 1:2 mixtures of GaHL (I), GaL (II), $Ga(OH)_2L$ (III), GaL_2 (IV), $GaOHL_2$ (V), and GaL_3 (VI) plotted as a function of pH.

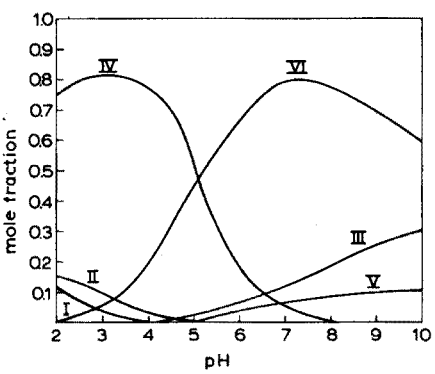

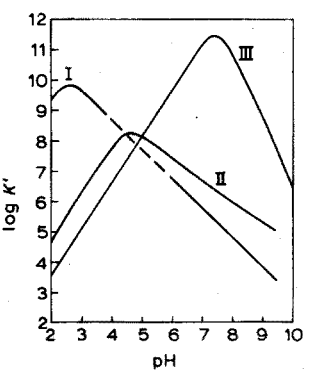

Fig. 4. The mole fractions in 1:3 mixtures of GaHL (I), GaL (II), $Ga(OH)_2L$ (III), GaL_2 (IV), $GaOHL_2$ (V) and GaL_3 (VI) plotted as a function of pH.

Fig. 5. The logarithm of the conditional constants of GaL (I), GaL_2 (II) and GaL_3 (III) plotted as a function of pH.

The mole fractions of the various species present in the 1:2 mixtures are apparent from Fig. 3; in the pH range studied small amounts of the complexes GaHL, GaL and $Ga(OH)_2L$ are also formed.

The 1:3 curve showed inflections at $m=5$ and $m=6$, the major reactions probably being:

$$Ga + 2L \rightleftarrows GaL_2$$

$$Ga + L + 2OH \rightleftarrows Ga(OH)_2L$$

$$Ga + 3L \rightleftarrows GaL_3$$

Figure 4 shows that GaL_2 and GaL_3 are the predominant species, but small amounts of GaHL, GaL and $GaOHL_2$ also appear.

The absolute stability constants of the major complexes were calculated as described above. The data are given in Table II.

TABLE II

ABSOLUTE STABILITY CONSTANTS OF THE GALLIUM–FERRON COMPLEXES

Complex	*Const. (as defined above)*	*Logarithm of stab. const.*
GaHL	K_2	11.3
GaL	K_3	14.7
$Ga(OH)_2L$	K_5	32.3
GaL_2	K_7	23.9
$GaOHL_2$	K_8	31.0
GaL_3	K_9	29.6

As expected, the present system is characterized by the strong tendency of gallium to form hydroxy complexes, which are detectable at pH values as low as about 2. The calculations gave no evidence for the presence of the proton complexes GaH_2L or GaH_2L_2.

The computer was also utilized to calculate the conditional constants K'_{GaL}, K'_{GaL_2} and K'_{GaL_3} as defined by Ringbom[19]. In Fig. 5 the logarithms of the conditional constants are plotted as a function of pH.

SUMMARY

The complex formation of gallium(III) with 8-hydroxy-7-iodoquinoline-5-sulphonic acid (ferron) (L) was studied by potentiometry; and the dissociation constants of the ligand were redetermined. A new computer program made it possible to make allowance for a considerable number of equilibria. In the pH range 2–10, the main species were as follows (the logarithm of the absolute stability constants at 25.0±0.1° for ionic strength 0.1 *M* are given in parentheses): GaHL (11.3), GaL (14.7), $Ga(OH)_2L$ (32.3), GaL_2 (23.9), $GaOHL_2$ (31.0) and GaL_3 (29.6). For 1:1, 1:2 and 1:3 mixtures of metal with ferron, the mole fractions of the various complexes as a function of pH were calculated; the effect of pH on the conditional constants of the species GaL, GaL_2 and GaL_3 was also established.

RÉSUMÉ

Une étude potentiométrique est effectuée sur la formation du complexe

gallium(III)–acide hydroxy-8-iodo-7-quinoléinesulfonique-5 (ferron). On détermine à nouveau les constantes de dissociation du ligand, grâce à un nouveau programme d'ordinateur tenant compte d'un nombre considérable d'équilibres. Du pH 2 à 10. les principales espèces sont les suivantes: GaHL (11.3), GaL (14.7), $Ga(OH)_2L$ (32.3), GaL_2 (23.9), $GaOHL_2$ (31.0) et GaL_3 (29.6); entre parenthèses: le logarithme des constantes de stabilité absolue à $25.0 \pm 0.1°$ et force ionique 0.1 *M*. L'influence du pH est examinée, en particulier sur les constantes conditionnelle de GaL, GaL_2 et GaL_3.

ZUSAMMENFASSUNG

Die Komplexbildung zwischen Gallium(III) und 8-Hydroxy-7-jodchinolin-5-sulfonsäure (Ferron) (L) wurde potentiometrisch untersucht; die Dissoziationskonstanten des Liganden wurden erneut bestimmt. Ein neues Rechenprogramm ermöglichte die Berücksichtigung einer beträchtlichen Zahl von Gleichgewichten. Im pH-Bereich 2–10 lagen im wesentlichen folgende Spezies vor (die Logarithmen der absoluten Stabilitätskonstanten bei $25.0 \pm 0.1°$ und Ionenstärke 0.1 *M* sind in Klammern angegeben): GaHL (11.3), GaL (14.7), $Ga(OH)_2L$ (32.3), GaL_2 (23.9), $GaOHL_2$ (31.0) und GaL_3 (29.6). Für 1:1-, 1:2- und 1:3-Gemische des Metalls mit Ferron wurden die Molenbrüche der verschiedenen Komplexe als Funktion des pH-Wertes berechnet; der Einfluss des pH-Wertes auf die konditionalen Konstanten der Spezies GaL, GaL_2 und GaL_3 wurde ebenfalls festgestellt.

REFERENCES

1 J. H. Yoe, *J. Amer. Chem. Soc.*, 54 (1932) 4139.
2 H. W. Swank and M. G. Mellon, *Anal. Chem.*, 9 (1937) 406.
3 J. H. Yoe and R. T. J. Hall, *J. Amer. Chem. Soc.*, 59 (1937) 872.
4 H. B. Feldman and A. L. Powell, *J. Amer. Chem. Soc.*, 62 (1940) 3107.
5 R. Näsänen and A. Ekman, *Acta Chem. Scand.*, 6 (1952) 1384.
6 F. J. Langmyhr and Å. R. Storm, *Acta Chem. Scand.*, 15 (1961) 1461.
7 Å. R. Storm and F. J. Langmyhr, *Acta Chem. Scand.*, 15 (1961) 1765.
8 Å. R. Storm, *Acta Chem. Scand.*, 17 (1963) 667.
9 T. Chang, J. Lin, T. Chan and S. Yang, *J. Chin. Chem. Soc.*, 2 (1964) 125.
10 A. Malik, *Indian J. Chem.*, 3 (1965) 446.
11 Tong Ming Hseu and Li-Shu Chen, *J. Chin. Chem. Soc.*, 4 (1966) 150.
12 N. Kurmaih, D. Satyanarayana and R. V. Panda, *Anal. Chim. Acta*, 35 (1966) 484.
13 G. Schwarzenbach, H. Flaschka and H. M. N. H. Irving, *Complexometric Titration*, Methuen, London, 1969, p. 273.
14 G. Schwarzenbach, *Helv. Chim. Acta*, 33 (1950) 947.
15 D. D. Perrin, *J. Pure Appl. Chem.*, 20 (1969) 165.
16 I. P. Alimarin, S. Abdelkhamid and I. V. Puzchenkova, *Russ. J. Inorg. Chem. (English Transl.)*, 10 (1965) 209.
17 B. N. Ivanov-Emin, L. A. Niselson and L. E. Larionova, *Russ. J. Inorg. Chem. (English Transl.)*, 7 (1962) 266.
18 W. Lund and P. Overvoll, to be published.
19 A. Ringbom, *Complexation in Analytical Chemistry*, Interscience, New York, 1963, p. 37.

Analytica Chimica Acta, 68 (1974) 111–118

THE PURITY OF COMMERCIAL DIPHENYLCARBAZONE

G. J. WILLEMS and C. J. DE RANTER

Department of Pharmacy, Laboratory of Analytical Chemistry, University of Leuven, 3000 Leuven (Belgium)

(Received 29th May 1973)

In a previous paper[1] it has been shown that most commercial diphenylcarbazide (DPCI) samples are approximately equimolar mixtures of DPCI (61%) and phenylsemicarbazide (PSCI) (39%), when they are prepared by heating urea with phenylhydrazine. Since diphenylcarbazone (DPCO) is prepared by partial oxidation of DPCI with hydrogen peroxide, it would be expected that commercially available DPCO would be a mixture of DPCI, DPCO and also of PSCI. Krumholz and Krumholz nevertheless stated[2] that DPCO is an equimolar mixture of DPCI and DPCO. They also described a method for separating the DPCO ($K_a = 10^{-8}$) from the DPCI, which shows no acidic character, by extracting the latter with ether from an alcoholic solution of sodium hydroxide. After acidification and recrystallization, they obtained DPCO with a melting point of 127°, which is considerably lower than the 156–158° given for the commercial mixture. The purified product did not react with chromium(VI), in contrast to the reaction mechanism proposed by Bose[3]:

$$\mathrm{Cr(VI)} + 3\ \mathrm{DPCO} \rightarrow [\mathrm{Cr(II)(DPCO)}] + 2\ \mathrm{DPCDO} + 6\ \mathrm{H^+}\,.$$

Da Silva *et al.*[4] achieved separation by thin-layer chromatography on silica gel, by which they also concluded that commercial DPCO is a mixture of DPCI and DPCO. These authors also described a method for separating DPCO from DPCI, based on continuous liquid–liquid extraction.

Earlier, Krumholz and Watzek[5] reported that DPCO solutions undergo an oxidative decomposition to diphenylcarbadiazone (DPCDO) catalyzed by traces of copper(II) ions. The possibility of further oxidation of DPCO to DPCDO had previously been noted by Heller[6] and by Bamberger *et al.*[7], who defined it as diphenyltetrazolium betaine.

Although various papers have been published about this problem, it has not been properly solved. A rigorous examination of the DPCO reagent was considered necessary, because a purification method was required on a preparative scale in order to obtain the pure DPCO reagent that can be used in complex formation studies with chromium.

EXPERIMENTAL

Apparatus

The chromatographic experiments and the melting point determinations

were performed as described previously[1]. The u.v. spectra were recorded on an Unicam spectrophotometer, and the mass spectra on a MS 12 AET mass-spectrometer (Manchester, U.K.).

Materials

The following DPCO samples were investigated: (A) BDH, Poole, G.B.; (B) Fluka, Buchs, Switzerland; (C) Matheson, Coleman and Bell, Norwood, U.S.A.; (D) Carlo Erba, Milano, Italy; (E) Schuchardt, München, W. Germany; (F) U.C.B., Brussels, Belgium; (G) Merck, Darmstadt, W. Germany; (H) Eastman Kodak, N.Y., U.S.A.; (I) Aldrich, Milwaukee, U.S.A.; (J) DPCO prepared in this laboratory by reaction of hydrogen peroxide in alkaline solution on DPCI from Schuchardt; (K) DPCO prepared in this laboratory by reaction of hydrogen peroxide in alkaline solution on DPCI from B.D.H., Analar.

Pure DPCDO (melting point 160.8°) was prepared from DPCO by the method described by Da Silva *et al.*[8]. The following commercial t.l.c. sheets were used for the chromatographic experiments: t.l.c. aluminium sheets Silica Gel (without fluorescence indicator) and t.l.c. aluminium sheets Silica Gel F_{254}, both from Merck, Darmstadt, W. Germany; MN-polygram polyamid-11, t.l.c.-grade and MN-polygram polyamid-11, UV_{254} t.l.c.-grade, both from Macherey-Nagel & Co, Düren, W. Germany.

The separations on an analytical scale were achieved on a column SR 25/45 (Pharmacia Fine Chemicals, Uppsala, Sweden); the separations on a preparative scale were made with a column 3500-75 × 90, fitted with a plunger 3500-A-75, an eluent reservoir and a sample valve (Glenco, Houston, Texas, U.S.A.).

Chromatographic procedures

Solvent system A (ethanol 4%, chloroform 96%) was used for thin-layer separations on silica gel sheets, and solvent system B (water–ethanol–acetic acid, 1 : 3 : 0.04) for the thin-layer experiments on polyamide sheets. When non-fluorescing sheets were used, the spots were detected by irradiation with light at 366 nm during 1 h. With fluorescing sheets, instant detection was possible by irradiation with u.v. light of 254 nm.

The column chromatographic experiments on an analytical scale were performed with a two-fold aqueous dilution of solvent B. The effluents from the column were collected at intervals of 160 s, at a rate of 1 drop per s, and monitored with the spectrophotometer at a wavelength of 234 nm.

The preparative column was charged with about 1 g of commercial DPCO sample, and the separations were performed with a three-fold diluted aqueous solution of solvent B, except for the last fraction, which was finally eluted with solvent B as such.

RESULTS AND DISCUSSION

The t.l.c. results on silica gel sheets confirm the presence of DPCI and DPCO in all the DPCO samples together with a third component, that according to the preceding discussion could be PSCI, DPCDO or a mixture of them. Better separations were obtained on polyamide sheets, from which it was concluded that the commer-

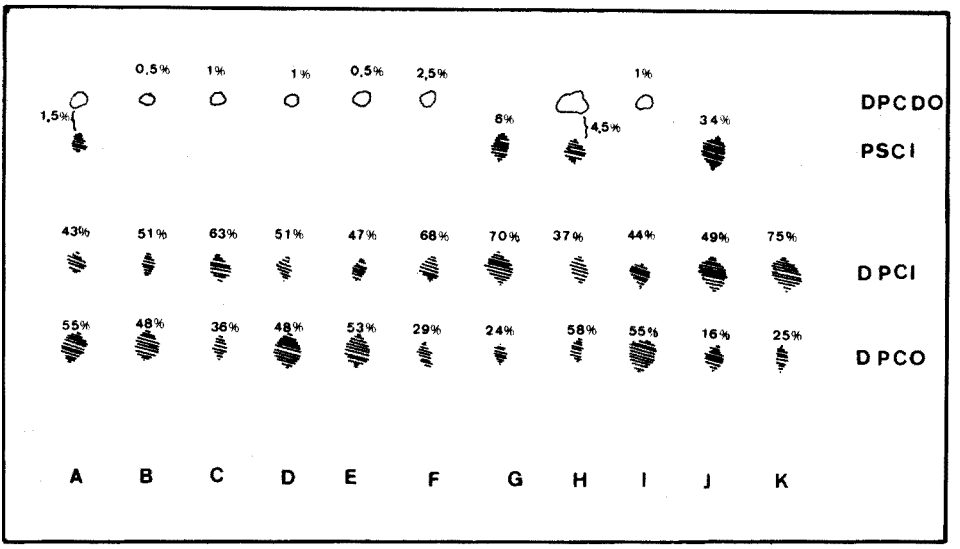

Fig. 1. Thin-layer chromatograms of samples A–K on polyamide 11.

cial DPCO reagents are mixtures of up to six compounds, two of which—only visible after irradiation and present as traces—could not be identified. In addition to the main components, DPCI and DPCO, the presence of PSCI and DPCDO was confirmed; the relative amounts of the components varied very considerably in the different commercial samples (Fig. 1). The trace components, with $hR_F \simeq 10$–20 are not indicated in this Figure and will be not further discussed. The DPCDO spots, when present, fluoresced on irradiation with u.v. light of 366 nm; the fluorescence, according to Da Silva *et al.*, is probably due to the formation of 2,2′-diphenylene-5-oxytetrazolium betaine[8].

The sequence of the hR_F values on silica gel sheets (Table I), with slightly acidic surface properties, can easily be understood from the pK_a of the different components as the more acidic DPCO ($K_a = 10^{-8}$) will migrate much faster than the other more basic compounds. On the polyamide sheets, the sequence of the hR_F values is reversed, because of the basic properties of the polyamide surface (Table I).

Since the identification of the PSCI and the DPCDO spot could not be done at this stage of the analysis, it was necessary to separate the fraction on a preparative

TABLE I

hR_F VALUES OBTAINED

On silica gel, eluted with solvent system A	*On polyamide 11, eluted with solvent system B*
PSCI 10	DPCO 32
DPCI 15	DPCI 50
DPCO 55	PSCI 73
	DPCDO 85 (fluorescing)

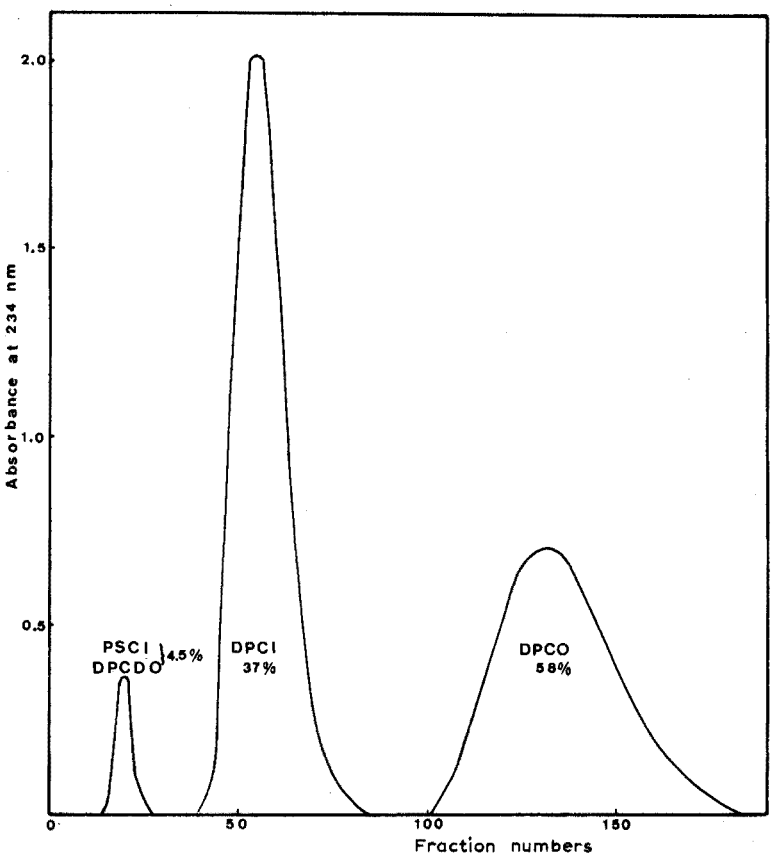

Fig. 2. Elution pattern of sample H on an analytical column (Polyamide 6) monitored at 234 nm.

scale. Liquid column chromatography (l.s.c.) and, as polyamide-11 powder was not available in column quality, polyamide-6-CC was used for all the column investigations.

Preliminary separations, however, on an analytical column showed that the results on l.s.c. were not identical with the t.l.c. data. For the different commercial products, only three elution peaks were obtained on separation by l.s.c. monitored at 234 nm, even for products for which on t.l.c. sheets four spots were located (Fig. 2). The reasons for these differences between the elution patterns could be the different quality of polyamide powder, used in t.l.c. and l.s.c. separations, as well as the more fundamental differences in experimental conditions between the two techniques.

Although DPCDO and PSCI could not be separated by l.s.c. on polyamide-6, the composition of fraction 1 could be determined by comparison of the mass spectrum of this fraction residue with the mass spectra of the pure PSCI and DPCDO (Figs. 3 and 4). The identification was based on the most characteristic ion peaks for PSCI, with molecular ion peak 151 and fragment peaks 107 and 108. and for DPCDO, with molecular ion peak 238 and fragment peaks 210 and 105. In this way, it could be concluded that the first l.s.c. fraction of the different DPCO

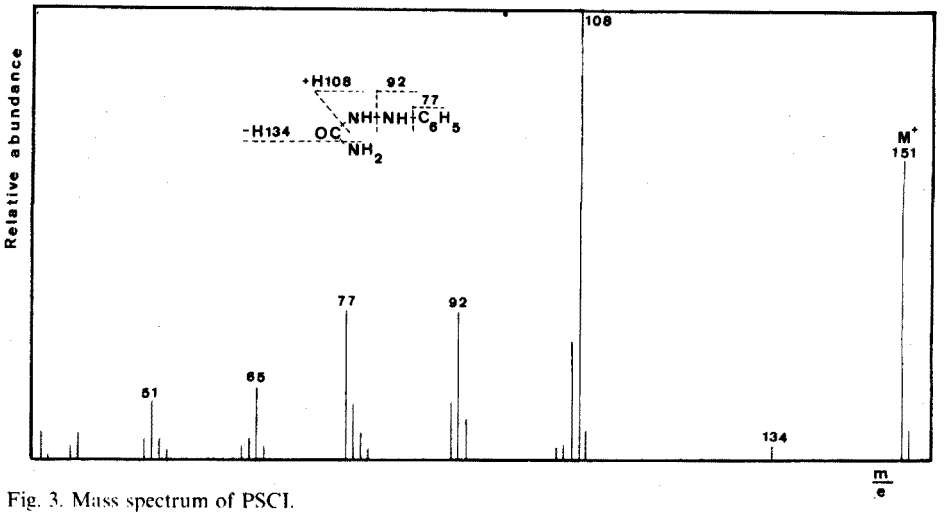

Fig. 3. Mass spectrum of PSCI.

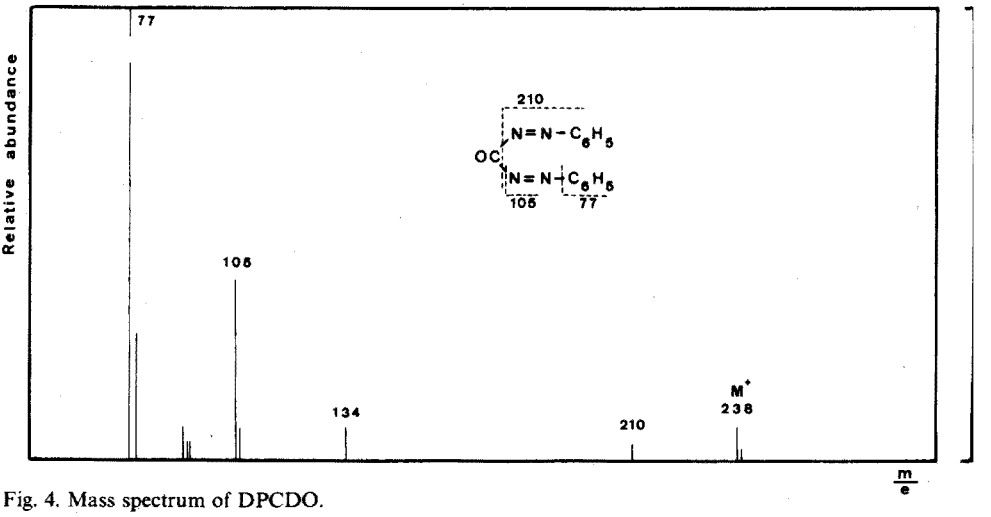

Fig. 4. Mass spectrum of DPCDO.

reagents, is either pure PSCI or pure DPCDO or a mixture of both. These results confirmed the results of the t.l.c. experiments, as illustrated in Fig. 1.

Once the composition of fraction 1 was known, the relative quantitative determination of the elution chromatograms was possible, in as far as fraction 1 was pure. When fraction 1 was a mixture of PSCI and DPCDO, the relative amount of the total mixture against the two other fractions could be estimated, because of the small difference in the molar absorptivities of the two components at 234 nm ($\varepsilon^{234}_{PSCI} = 11{,}000$; $\varepsilon^{234}_{DPCDO} = 11{,}600$; Fig. 5).

Evaluation was done by determining the peak area of the different fractions of the elution chromatogram. These peak areas were referred to the PSCI peak and then corrected for their differences in molar absorptivities at 234 nm (Table II).

The molar absorptivities of PSCI and DPCI had been formerly determined[1];

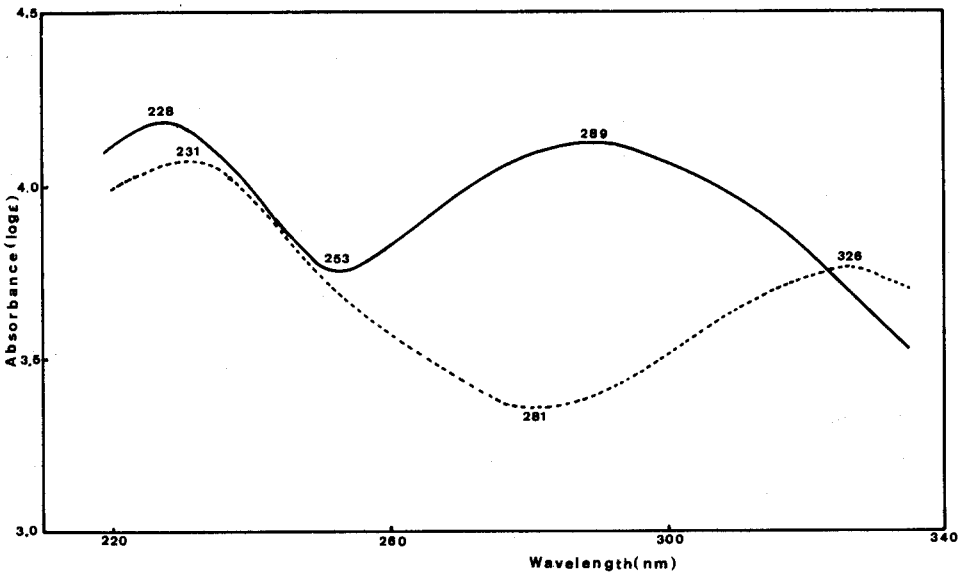

Fig. 5. The ultraviolet spectra (in methanol) of diphenylcarbazone (solid line) and diphenylcarbadiazone (dotted line).

TABLE II

THE RELATIVE AMOUNTS (IN %) OF THE DIFFERENT COMPONENTS IN DPCO REAGENTS

	Source										
	A	*B*	*C*	*D*	*E*	*F*	*G*	*H*	*I*	*J*	*K*
DPCI	43	51	63	51	47	68	70	37	44	49	75
DPCO	55	48	36	48	53	29	24	58	55	16	25
DPCDO		0.5	1	1	0.5	2.5			1		
PSCI							6			34	0
DPCDO+ PSCI	1.5							4.5			

the value for DPCDO was obtained by u.v. spectrometry of the same sample as that used for the determination of the mass spectrum and the value for DPCO by u.v. spectrometry of a thrice chromatographed sample (Fig. 5).

CONCLUSIONS

The DPCO reagents which are commercially available, are not only mixtures of DPCO and DPCI, as described by Krumholz and Krumholz[2] in 1937, but also contain PSCI and DPCDO in varying concentrations. This was clearly proved by chromatography and mass spectra data.

The quantitative estimations of DPCO and DPCI do not confirm the findings of Da Silva *et al.*, who reported in 1964 that under conditions of mild oxidation the

reaction stops at a 1:1 intermolecular compound, leaving exactly one half of the DPCI unoxidized, although the possibility of the existence of hydrogen bonds between the two compounds has not been refuted by the present work.

The authors thank Prof. H. Vanderhaeghe for mass-spectrometer facilities in the Laboratory of Pharmaceutical Chemistry at Leuven and Dr. G. Janssen for recording and interpreting the mass spectra.

SUMMARY

Nine different, commercially available, samples of diphenylcarbazone were examined by thin-layer and liquid column chromatography. From all of them, 3–4 components were isolated by elution chromatography and identified by mass spectrometry. The relative amounts of diphenylcarbazide, diphenylcarbazone, phenylsemicarbazide and diphenylcarbadiazone were evaluated from the peak areas of the elution pattern at 234 nm. The amount of diphenylcarbazone varied very considerably from sample to sample; there was no stoichiometric relationship between the carbazone and carbazide.

RÉSUMÉ

Des essais chromatographiques sur couche mince et sur colonne ont été mis au point pour contrôler et analyser le réactif diphénylcarbazone. Neuf échantillons commerciaux de différentes origines ont été examinés, contenant tous de trois à quatre composants, isolés par chromatographie sur colonne et identifiés par spectrométrie de masse. Les quantités relatives de diphénylcarbazide, diphénylcarbazone, phénylsemicarbazide et diphénylcarbadiazone ont été évaluées par détermination de la surface des pics d'élution à 234 nm. Ces déterminations permettent de constater que la quantité de diphénylcarbazone varie considérablement d'un réactif à l'autre; on a pu conclure qu'il n'existe pas de relation stoechiométrique entre diphénylcarbazone et diphénylcarbazide, comme d'autres auteurs le signalent.

ZUSAMMENFASSUNG

Mittels Dünnschicht- und Säulenchromatographie wurden neun verschiedene Handelsproben von Diphenylcarbazon untersucht. Diese enthielten drie bis vier Bestandteile, die durch Säulenchromatographie isoliert und massenspektrometrisch identifiziert werden konnten. Die relativen Mengen von Diphenylcarbazid, Diphenylcarbazon, Phenylsemicarbazid und Diphenylcarbadiazon wurden aus den Flächen des Elutionschromatogramms berechnet. Der Behalt von Diphenylcarbazon variierte stark von Probe zu Probe; ein stöchiometrisches Verhältnis zwischen dem Carbazon und dem Carbazid bestand nicht.

REFERENCES

1 G. Willems, R. Lontie and W. Seth-Paul, *Anal. Chim. Acta*, 51 (1970) 544.
2 P. Krumholz and E. Krumholz, *Monatsh.*, 70 (1937) 431.

3 M. Bose, *Anal. Chim. Acta*, 10 (1954) 201.
4 J. J. Da Silva, J. C. Calado and M. L. De Moura, *Talanta*, 11 (1964) 983.
5 P. Krumholz and H. Watzek, *Monatsh.*, 70 (1937) 437.
6 Heller, *Liebigs Ann. Chem.*, 263 (1891) 274.
7 E. Bamberger, R. Padova and E. Ormerod, *Liebigs Ann. Chem.*, 446 (1926) 260.
8 J. J. De Silva, J. C. Calado and M. L. De Moura, *Rev. Port. Quim.*, VI (1964) 22.

Analytica Chimica Acta, 68 (1974) 119–130

ION-EXCHANGE FOAM CHROMATOGRAPHY

PART II. RAPID SEPARATIONS ON HETEROGENEOUS CATION-EXCHANGE FOAMS*

T. BRAUN and A. B. FARAG

Institute of Inorganic and Analytical Chemistry, L. Eötvös University, P.O. Box 123, 1443 Budapest (Hungary)

(Received 6th July 1973)

During the last few years, there has been considerable interest[2,3] in preparing ion-exchange materials with reduced solid-phase mass transport in order to increase the rate of exchange processes. It has been realized[4] that the application of very small resin beads, which have a low resistance to mass transport, allows a rapid equilibrium with the mobile phase. However, it is necessary to employ forced flow to attain reasonable flow-rates in column operations. The speed and efficiency of ion-exchange separations have been greatly increased by the development[2,5] of packings which consist of a thin layer of ion-exchange resin coated on the surface of a solid-core support (pellicular ion exchangers). This type of resin has been shown to be extremely useful in reducing solid-phase mass transport resistances and thus accelerating the exchange processes. However, the capacity of these pellicular resins is extremely low, and chromatographic systems based on these materials are limited to very small amounts of solute. The preparation of a superficially sulphonated, highly cross-linked exchange resin on styrene–divinylbenzene base has also been described[3,6]. Again, the application of these resins allowed the exchange equilibrium to be attained rapidly, but their capacities are several orders of magnitude smaller than that of common exchange resins.

In a recent paper[1] various methods have been tested for the preparation of homogeneous and heterogeneous ion-exchange foams. Homogeneous ion-exchange foams were prepared by introducing ion-exchange groups on previously prepared phenol–formaldehyde, polyurethane and polyethylene foams. Heterogeneous ion-exchange foams were prepared by foaming a fine powder of a commercially available cation exchanger with the precursors of open-cell polyether-type polyurethane foam. Preliminary investigations[1] on heterogeneous ion-exchange foams showed that the kinetics of the exchange processes is fast and the capacity is quite suitable.

In previous work[7–10] on "foam chromatography", *i.e.* the application of foams as chromatographic column fillings, the hydrodynamic properties and the kinetics of partition on foam-packed chromatographic columns proved to be extremely favourable. It was decided to investigate the applicability of the recently

* For Part I see ref. 1.

described flexible ion-exchange foams in quick column separations. The kinetics of the exchange processes and the selectivity of foam ion exchanger were studied in comparison with the normal ion-exchange beads.

EXPERIMENTAL

Reagents and materials

All reagents used were of analytical grade unless otherwise specified. Copper, zinc and cadmium solutions were prepared by dissolving the sulphate salts in water. Iron and calcium chloride solutions were prepared by dissolving the chloride salts in 0.03 *M* hydrochloric acid and distilled water, respectively.

Polyurethane–Varion KS heterogeneous ion-exchange foam was prepared as previously described[1]. The foam material contained 40% (w/w) cation exchanger. The ion-exchange resin used was the powdered Varion KS sulphonated polystyrene cation exchanger of 0.3–0.5 mm particle original diameter (Nitrokémia, Füzfögyártelep, Füzfö, Hungary).

Apparatus

Columns. Glass columns of 15 mm diameter and 15 cm long were used. A separating funnel was fitted at the top of the column as a reservoir of the eluting solution.

Counter. For activity measurement, a NaI(Tl) detector and an energy-selective counting device (type NK-107/B, Gamma, Budapest, Hungary) were employed.

Column preparation

The polyurethane–Varion KS heterogeneous ion-exchange foam (cubes of about 5 mm edge) was washed several times with water and allowed to stand with it overnight. The water was poured off and the foam material was shaken 3 times with 3 *M* hydrochloric acid solution. The foam material was washed with a large portion of water, and after decantation, it was shaken with 1 *M* sodium hydroxide solution for 3 h and again washed several times with water. Finally, the foam material was shaken with 2 *M* hydrochloric acid solution to change it to the H^+-form, and then washed with distilled water. The water-wetted foam exchanger was packed in the column by the procedure previously developed[8].

Experiments at controlled temperatures were done with water-jacketed columns.

Distribution ratios

The distribution ratios were determined for 5 mg of the elements in 50 ml of solution and 0.2 g of resin beads or foam in the H-form which had been dried at 80° in a drying oven. After equilibration for 6 h at room temperature in a mechanical shaker, the ion-exchange beads or foams were separated from the aqueous phase by filtration and the amount of the elements on the beads or foam were determined by suitable analytical methods. From the results, the distribution ratios

$$D = \frac{\text{amount of element in resin}}{\text{amount of element in solution}} \cdot \frac{\text{ml of solution}}{\text{g of dry resin}}$$

were calculated.

Determination of the rate of exchange of copper(II) by ion-exchange foam

In 15 stoppered flasks of 25-ml capacity, 5-ml portions of water were added to 0.1 g of washed, dry foam. The flasks were shaken at room temperature in a mechanical shaker for 4 h, and then 5 ml of ^{64}Cu-labelled copper sulphate solution (1 mg Cu^{2+} ml^{-1}) were added to each flask. The flasks were then shaken for different times (1–90 min) and copper(II) was determined in the aqueous phase by measuring the radioactivity of 2 ml of each solution.

Elution of copper(II) by hydroxyammonium chloride

Copper(II) sulphate solution (1 ml of a 5 mg Cu^{2+} ml^{-1} solution) was used as the feed. Sorption took place at a flow-rate of 2 ml min^{-1} and then the column was washed with 20 ml of distilled water. A 0.5 *M* hydroxyammonium chloride solution was used to elute copper at flow-rates of 2–10 ml min^{-1}.

Separation of cadmium, zinc, iron and calcium

The feed solution contained 1 ml of cadmium sulphate (5 mg Cd^{2+} ml^{-1}), 0.5 ml of zinc sulphate (10 mg Zn^{2+} ml^{-1}), 1 ml of iron(III) chloride (5 mg Fe^{3+} ml^{-1}) and 1 ml of calcium chloride (5 mg Ca^{2+} ml^{-1}) solutions. The mixture was allowed to pass through the foam ion-exchange column (bed height *ca.* 12 cm, 5 g of dry foam) at a flow-rate of 2 ml min^{-1} and the column was then washed with 20 ml of distilled water. The elements were then eluted in the following sequence: 200 ml of 0.2 *M* hydrochloric acid in 40% ethanol for cadmium(II), 150 ml of 0.2 *M* hydrochloric acid in 80% ethanol for zinc(II), 150 ml of 1.0 *M* hydrochloric acid in 80% ethanol for iron(III), and 150 ml of 2.0 *M* hydrochloric acid in 20% ethanol for calcium.

Analytical methods

All metal ions were titrated with 0.01 *M* EDTA solution in the presence of an appropriate indicator. Copper when present in trace amounts was measured radiometrically.

RESULTS AND DISCUSSION

Although the results obtained by applying columns packed with pellicular resins[2,5], in which a solid core is surrounded by a thin film of cross-linked ion-exchange material, and with superficially sulphonated resins[3,6] are very promising, yet the low capacity of these resins remains a serious limitation. Many investigators, *e.g.* Pinfold and Karger[4], have shown that the exchange processes on finely pulverized ion exchangers proceed substantially faster than the processes on bigger beads of the same composition. As previously mentioned[1], the use of fine grains causes difficulties even in the "batch technique", since they form colloidal suspensions. An acceptable solution for this problem was found by the

successful preparation of heterogeneous ion-exchange foams in which finely ground commercial ion-exchange resin was built into a polyurethane foam matrix of an open-cell polyether type. The mechanical properties of this ion-exchange foam were found[1] to be the same as those of foam containing no ion-exchange resin. Furthermore, the distribution of the exchanger grains was proved[1] to be uniform.

Several questions have to be answered before this ion-exchange foam can be used for analytical purposes: (1) should the ion-exchange foam be homogeneously packed to produce sharp break-through curves?; (2) will the ion-exchange process be fast enough to permit the application of high flow-rates?; (3) will the selectivity of the ion exchanger be affected?; and (4) does the swelling of the foam support limit the application of foam ion exchanger in water-miscible organic solvents?

In order to answer these and other questions, two separation models were investigated in detail. The first model was the separation of copper(II) by aqueous hydroxyammonium chloride solution[11].

Break-through capacity

Previous studies[8–10] on foam chromatography showed that the vacuum technique of packing was the most suitable for foam column packing. One of the advantages of this method is that it allows the application of a high flow-rate simply by gravity flow. This method of column packing was therefore used again.

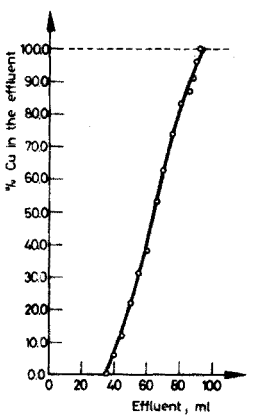

Fig. 1. Break-through capacity curve of copper(II) on cation-exchange foam. Foam weight, 1 g; feed: copper sulphate, 1 mg Cu^{2+} ml^{-1}; flow-rate, 1 ml min^{-1} at room temperature. Total capacity of the exchange foam, 1.8 meq. g^{-1}.

The break-through capacity of a column packed with 1 g of cation-exchange foam was determined by passing copper(II) sulphate solution (1 mg Cu^{2+} ml^{-1}) through the column at a 1 ml min^{-1} flow-rate. A plot of percent copper in the effluent *vs.* effluent volume is shown in Fig. 1. The sharp slope of the curve indicates that the column is homogeneously packed and also that the exchange equilibrium of copper(II) on the ion-exchange foam is attained rapidly.

The rate of sorption of copper(II) by ion-exchange foam

The rate of sorption of copper(II) by the ion-exchange foam is fast. The half-life of equilibrium sorption, calculated from the curve of Fig. 2, is 0.6 min. It is clear from the curves that sorption of copper(II) takes place in one step, *i.e.* gel diffusion is not the rate-controlling step as in the case of common ion-exchange beads. The two-step sorption previously reported on ion-exchange foams[1] was probably due to the use of coarser ion-exchange powder in foam preparation.

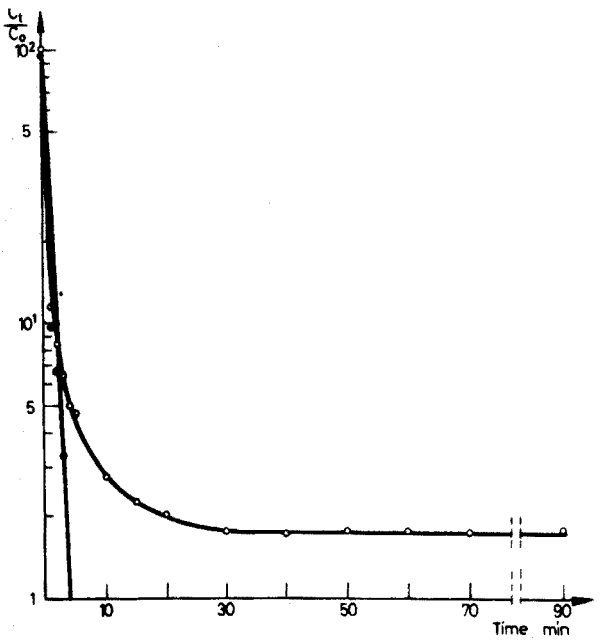

Fig. 2. Rate of sorption of copper(II) on ion-exchange foam at room temperature, [Cu^{2+}]. 5 mg.

It is interesting to note that the half-life of equilibrium sorption on the present ion-exchange foam is exactly the same as that obtained[3] in the case of the first rapid step on surface-sulphonated pearl polymer. However, the capacity of the proposed ion-exchange foam is much higher than that of the superficially sulphonated resin. These results suggest the application of ion-exchange foam for rapid separations in column operation.

The effect of flow-rate on the elution of copper(II) by 0.5 M hydroxyammonium chloride solution

Flow-rates ranging between 2 and 10 ml min^{-1} were applied at 50°. The elution curves are shown in Fig. 3. A slight increase in peak width with increased flow-rate occurs but the elution of copper is quantitative even at flow-rates as high as 10 ml min^{-1}. These results agree well with the previously discussed kinetic results obtained in batch experiments.

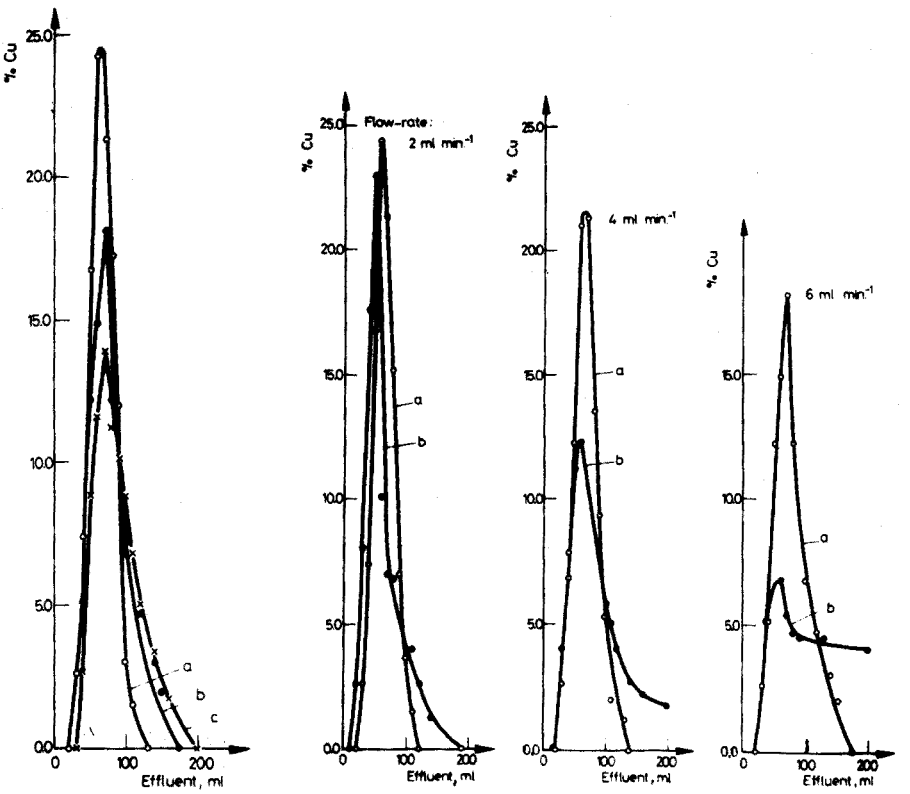

Fig. 3. Effect of flow-rate on the elution of copper(II) with 0.5 *M* hydroxyammonium chloride solution from a foam column of 12-cm bed height at 50°. (a) At 2 ml min^{-1}; (b) at 6 ml min^{-1}; (c) at 10 ml min^{-1}.

Fig. 4. Effect of flow-rate on the elution of copper(II) with 0.5 *M* hydroxyammonium chloride solution at 50°. (a) Ion-exchange foam column; (b) ion-exchange bead column.

A comparison between the elution of copper(II) on ion-exchange resin beads (Varion KS) and on ion-exchange foam columns was also carried out. Figure 4 shows the elution curves obtained at 2, 4 and 6 ml min^{-1} for columns packed with resin beads and foam under otherwise identical experimental conditions. The elution of copper(II) from the bead columns is greatly affected by flow-rate and quantitative elution is obtained only at a flow-rate of 2 ml min^{-1}.

Worth mentioning is that complete retention and elution of microgram quantities of copper(II) is possible on foam-filled columns. Figure 5 shows the elution curve obtained for 0.6 μg of ^{64}Cu spiked copper at 50° with a flow-rate of 2 ml min^{-1}.

Comparative selectivity of cation-exchange foams and beads in HCl–ethanol mixtures

A systematic investigation was next undertaken to determine the selectivity of the cation-exchange foam in comparison with the ion-exchange beads (Varion KS). In order to carry out this study, initial experiments were conducted to

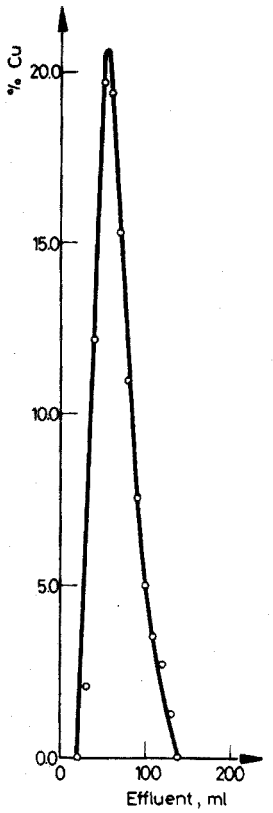

Fig. 5. Elution of microgram amount of copper(II) (0.6 μg) with 0.5 *M* hydroxyammonium chloride on a foam column of 12-cm bed height at 50° with a 2 ml min^{-1} flow-rate.

determine the distribution ratios of a set of elements with the conventional cation-exchange beads and the cation-exchange foam. The cation-exchange distribution ratios of cadmium(II), zinc(II), iron(III) and calcium(II) were measured in a wide range of hydrochloric acid–ethanol mixtures. The curves of Fig. 6 represent plots of the distribution ratios as a function of hydrochloric acid concentration in the absence and presence of ethanol at different concentrations. The set of curves in Fig. 7 show plots of the distribution ratios *vs.* ethanol concentration at various hydrochloric acid strengths. As may be seen from these figures, hydrochloric acid and ethanol have more or less the same general effect on the distribution ratios of the elements tested. However, the results obtained for the distribution ratios on the foam are generally shifted to slightly lower values. As is evident from the curves, the selectivity seems to be about the same as that of the original cation-exchange beads. This was further confirmed by the results obtained for the separation of a synthetic mixture of cadmium, zinc, iron and calcium on foam columns. It was found that these metal ions are eluted by hydrochloric acid–ethanol mixtures in the same order as that reported by Strelow *et al.*[12] for AG 50W-X8 sulphonated polystyrene cation-exchange resin (100–200 or 200–400 mesh particle size). Cadmium(II) was eluted with 0.2 *M* hydrochloric

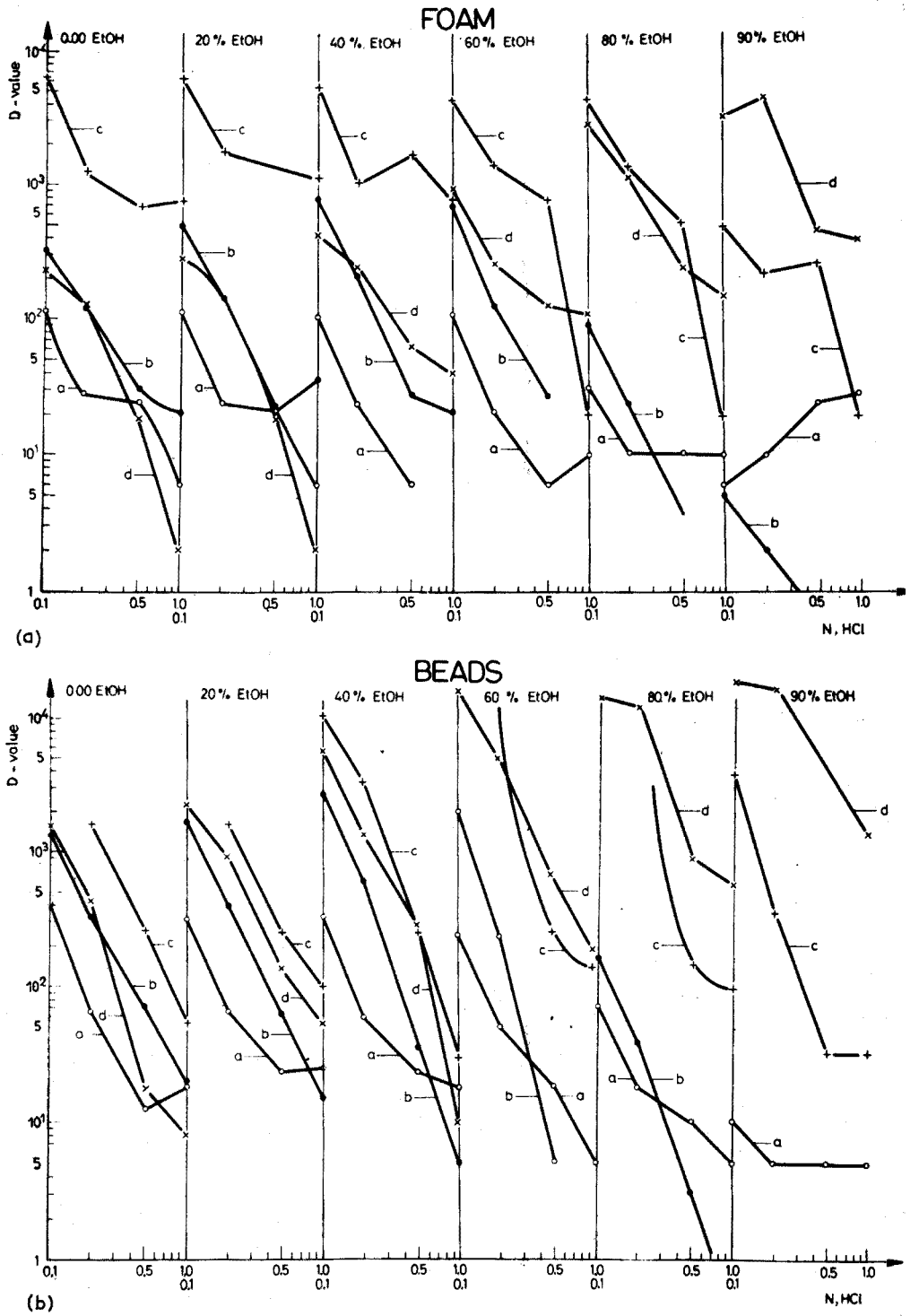

Fig. 6. Cadmium, zinc, iron and copper distribution ratios *vs.* hydrochloric acid concentration at different ethanol concentrations, for foam and bead columns. (a) Cd^{2+}; (b) Zn^{2+}; (c) Fe^{3+}; (d)

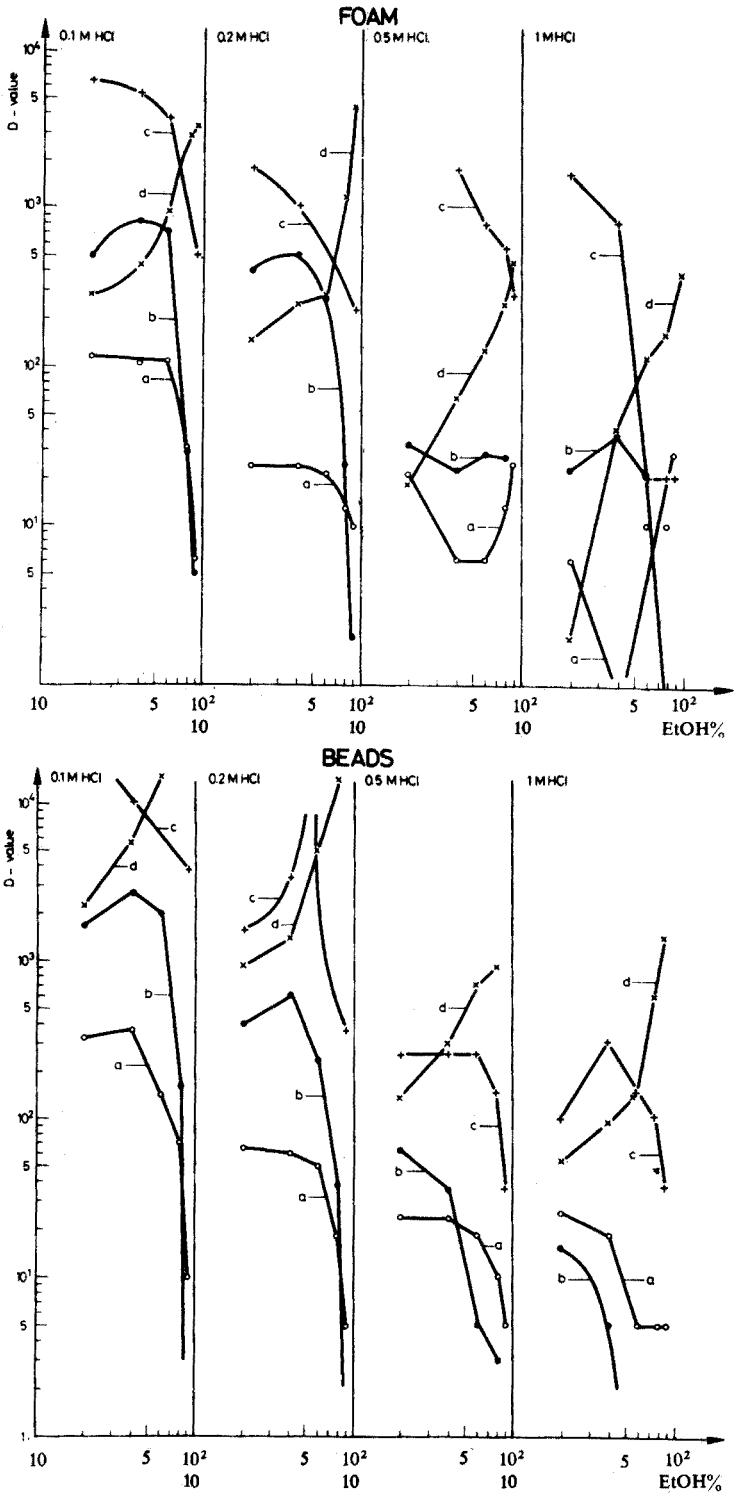

g. 7. Cadmium, zinc, iron and copper distribution ratios *vs.* ethyl alcohol concentration at various drochloric acid strengths for foam and bead columns. (a) Cd^{2+}; (b) Zn^{2+}; (c) Fe^{3+}; (d) Ca^{2+}.

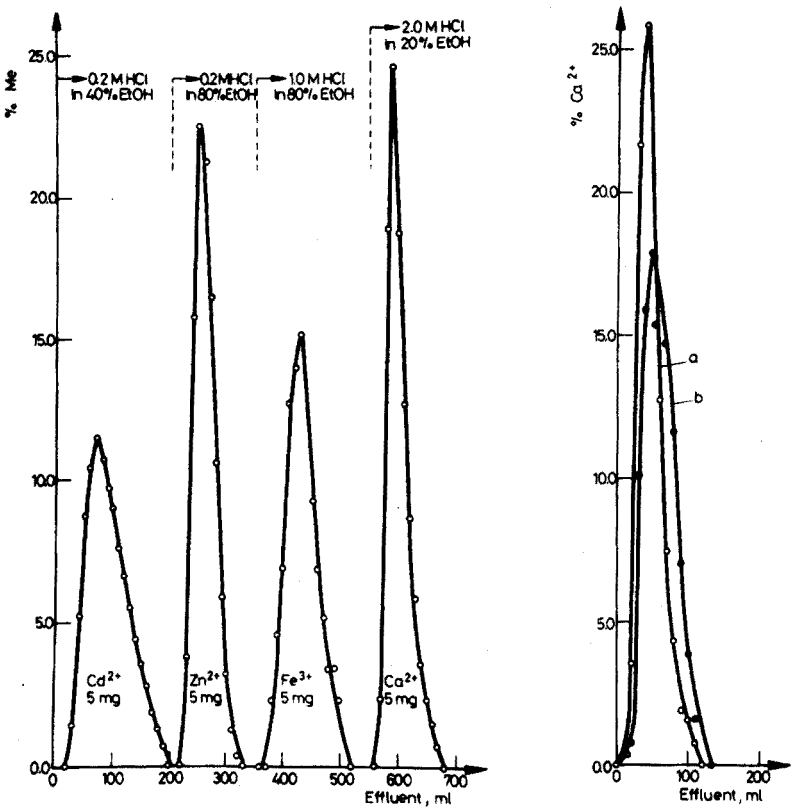

Fig. 8. Elution curve for Cd(II)–Zn(II)–Fe(III)–Ca(II) mixture on a cation-exchange foam column of 12-cm bed height at room temperature.

Fig. 9. Elution curves for calcium(II) with 3 *M* hydrochloric acid in 20% ethanol solution. (a) Ion-exchange foam column at a flow-rate of 10–12 ml min^{-1}; (b) ion-exchange bead column at a flow-rate of 2 ml min^{-1}.

acid in 40% ethanol, zinc(II) with 0.2 *M* hydrochloric acid in 80% ethanol, iron(III) with 1.0 *M* hydrochloric acid in 80% ethanol, and calcium with 2.0 *M* hydrochloric acid in 20% ethanol (Fig. 8). The elution of these elements was quantitative at room temperature with flow-rates of 3–7 ml min^{-1}.

It is worth mentioning that calcium(II) was quantitatively eluted from foam columns with 3 *M* hydrochloric acid in 20% ethanol at a flow-rate of 10–12 ml min^{-1} (Fig. 9). It was found that the elution curve of calcium at this relatively high flow-rate is sharper than the elution curve obtained with the conventional cation-exchange bead column (Varion KS, 0.3–0.5 mm diameter) at a flow-rate of 2 ml min^{-1}, under otherwise the same experimental conditions (Fig. 9). As is obvious from these results, cation-exchange foam columns seem to work more efficiently than the common cation-exchange bead columns in water-miscible organic solvents also.

CONCLUSIONS

The results of this investigation indicate that cation-exchange foam can be homogeneously packed in columns by the previously developed[8] vacuum method of packing. The kinetic processes on the finely grained cation exchanger supported on the polyurethane foam are extremely fast and are not affected by the foaming process. Gel-diffusion has no part in the exchange equilibrium. The selectivity of the cation-exchange foam is similar to that of the original ion-exchange beads. The application of cation-exchange foam columns for separations in aqueous solutions and water-miscible organic solvents seems to have advantages over both conventional ion-exchange and superficially coated[2,5] or sulphonated[3] exchange resins.

One of the most obvious advantages of the cation-exchange foam is its reasonable capacity and high efficiency. There are no special requirements for sample size; amounts of sample which are commonly used in conventional ion-exchange bead columns can be successfully separated on foam columns.

Work is in progress on the preparation of anion-exchange foams and their application for quick separation.

Grateful acknowledgement is made to Dr. K. Kádár, Mr. O. Békeffy and the North Hungarian Chemical Works, Sajóbábony, Hungary for the preparation of the heterogeneous ion-exchange foams used in this work.

SUMMARY

The possibility of using polyurethane–Varion KS heterogeneous cation-exchange foam for rapid separations in aqueous and alcoholic solutions was investigated. The exchange equilibria on the ion-exchange foam were attained rapidly and the break-through capacity of columns packed with the foam material was quite acceptable. Relatively high flow-rates could be applied without any appreciable loss in column performance. With foam columns, microgram and milligram amounts of copper could be retained and eluted quantitatively with hydroxyammonium chloride solution. The overall capacity of the examined ion-exchange foams was about 40% of the original capacity of beads. Cation-exchange distribution coefficients of cadmium(II), zinc(II), iron(III) and calcium-(II) were determined for foam material and conventional bead exchanger; the selectivity of both was about the same.

RÉSUMÉ

On examine les possibilités d'utilisation de l'échangeur de cations, hétérogène mousse polyuréthane–Varion KS, pour des séparations rapides dans des solutions aqueuses et alcooliques. L'équilibre d'échange est atteint trés vite. A l'aide des colonnes de mousse, des quantités de cuivre, de l'ordre du micro- et du milligramme peuvent être retenues et éluées quantitativement au moyen d'une solution de chlorhydrate d'hydroxylammonium. On examine également la capacité de ces mousses, de même que leur sélectivité.

ZUSAMMENFASSUNG

Die Anwendbarkeit von heterogenem Polyurethan-Kationenaustauscher-Schaum (Varion KS) für schnelle Trennungen in wässrigen und alkoholischen Lösungen wurde untersucht. Die Austauschgleichgewichte am Ionenaustauscher-Schaum stellten sich schnell ein, und die Durchbruch-Kapazität der mit dem Schaummaterial gefüllten Säulen war annehmbar. Relativ hohe Fliessgeschwindigkeiten konnten ohne Verminderung der Säulenleistung angewendet werden. Mit Schaumsäulen konnten Mikrogramm- und Milligramm-Mengen von Kupfer zurückgehalten und mit Hydroxylammoniumchlorid-Lösung quantitativ eluiert werden. Die Gesamt-Kapazität der untersuchten Ionenaustauscher-Schäume war etwa 40% der ursprünglichen Kapazität von Perlen. Die Kationenaustausch-Verteilungskoeffizienten von Cadmium(II), Zink(II), Eisen(III) und Calcium(II) wurden für Schaum-Material und für konventionellen Perlen-Austauscher bestimmt; die Selektivität von beiden war etwa dieselbe.

REFERENCES

1 Part I. T. Braun, O. Békeffy, I. Haklits, K. Kádár and G. Majoros, *Anal. Chim. Acta*, 64 (1973) 45.
2 J. J. Kirkland, *J. Chromatogr. Sci.*, 7 (1969) 361.
3 M. Skafi and K. H. Lieser, *Z. Anal. Chem.*, 249 (1970) 182.
4 T. A. Pinfold and B. L. Karger, *Separ. Sci.*, 5 (1970) 183.
5 G. G. Horvath, B. A. Preiss and S. R. Lipsky, *Anal. Chem.*, 39 (1967) 1422.
6 M. Skafi and K. H.-Lieser, *Z. Anal. Chem.*, 250 (1970) 306; 251 (1970) 177.
7 T. Braun and A. B. Farag, *Talanta*, 19 (1972) 828.
8 T. Braun and A. B. Farag, *Anal. Chim. Acta*, 61 (1972) 265.
9 T. Braun, É. Huszár and L. Bakos, *Anal. Chim. Acta*, 64 (1973) 77.
10 T. Braun, A. B. Farag and A. Klimes-Szmik, *Anal. Chim. Acta*, 64 (1973) 71.
11 Y. Shigetomi, R. Arimoto and T. Nagahota, *Talanta*, 19 (1972) 1210.
12 F. W. E. Strelow, C. R. Van Zyl and C. J. C. Bothma, *Anal. Chim. Acta*, 45 (1969) 81.

Analytica Chimica Acta, 68 (1974) 131–136

ISOLEMENT DU GROUPE DES TERRES RARES DE L'APATITE PAR L'ACIDE DI-(2-ETHYHEXYL)PHOSPHORIQUE (HDEHP)

I. ROELANDTS

Laboratoire de Géologie, Pétrologie et Géochimie, Université de Liège, Liège (Belgique)

G. DUYCKAERTS

Laboratoires de Chimie Analytique, Université de Liège, Liège (Belgique)

(Reçu le 25 juin 1973)

Depuis que Peppard *et al.*[1] proposèrent en 1957 l'extraction des lanthanides par l'acide di-(2-éthylhexyl)phosphorique (HDEHP), de nombreux travaux ont été effectués[2–17], la plupart avec des éléments en dose traceur et des concentrations en acide relativement faibles. Dans ces conditions, la distribution est proportionnelle à $(HDEHP/H^+)^3$.

Lorsque la concentration en acide augmente, l'extraction passe par un minimum qui se situe aux environs de 7 *M* pour HCl ou HNO_3 et 8 *M* pour H_2SO_4.

Nous avons observé que pour des acidités situées au delà du minimum, le facteur de séparation devient très faible et que l'extraction semble par conséquent basée sur un phénomène nouveau.

Nous avons cherché à utiliser l'extraction par HDEHP pour isoler le groupe des Terres Rares contenues dans les apatites en vue de leur analyse par radioactivation; comme la mise en solution des apatites exige des acidités élevées, nous avons examiné les courbes d'extraction des lanthanides aux fortes acidités.

Cette publication décrit la méthode à laquelle nous sommes arrivés.

CONDITIONS OPÉRATOIRES

L'HDEHP utilisé (BDH* no. 28135) a été purifié selon la méthode décrite par Peppard *et al.*[1].

Une solution (10 ml) d'acide de molarité connue contenant le radioélément dont l'activité a été mesurée et 10 ml de HDEHP à 25% en volume (25 ml HDEHP dilué à 100 ml par du cyclohexane) sont introduits successivement dans des tubes à centrifugation en pyrex préalablement traités au moyen de méthylphényldichlorosilane et munis de rodages normalisés. Les tubes sont agités manuellement pendant 5 min (la cinétique d'échange est très rapide[1]). On effectue 2 prélèvements de 4 ml de la phase aqueuse dans des capsules en pyrex et on évapore à sec sur plaque chauffante.

Les émetteurs β et γ sont mesurés au moyen d'un compteur à flux gazeux

* L'analyse du lot non purifié a donné les caractéristiques suivantes (laboratoire BDH); densité: 0.9736; indice de réfraction: 1.4438; pureté: 98.4%.

à fenêtre mince (Tracerlab). Toutes nos expériences ont été réalisées en double, à température ambiante et les valeurs moyennes sont reportées.

Coefficient de distribution et pourcentage d'extraction

Le coefficient de distribution, E, de l'élément étudié est défini par le rapport

$$E = \frac{\text{Concentration totale de l'élément dans la phase organique}}{\text{Concentration totale de l'élément dans la phase aqueuse}}$$

$$= \frac{\text{activité/ml phase organique}}{\text{activité/ml phase aqueuse}}$$

Le pourcentage d'extraction, P, peut être calculé à partir de E

$$P = 100\, E/\left(E + \frac{\text{volume phase organique}}{\text{volume phase aqueuse}}\right)$$

Dans le cas de volumes égaux, $P = 100\, E/(E+1)$

RÉSULTATS ET DISCUSSION

Une étude préalable de divers diluants a été menée pour le système HDEHP 1.5 *M*–HCl variable. Parmi la gamme: chloroforme, toluène, tétrachlorure de car-

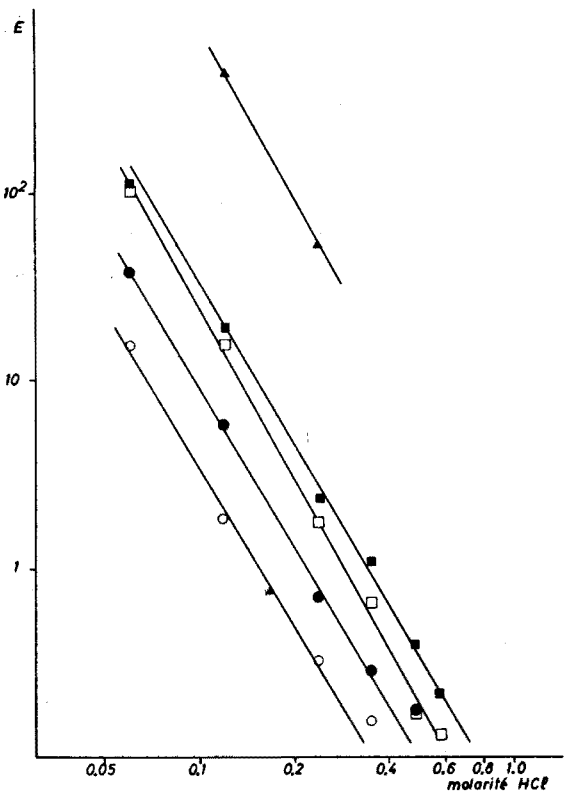

Fig. 1. Variation du coefficient de distribution du ^{141}Ce avec la concentration en HCl dans différents solvants. HDEHP 1.5 *M*. Diluants: (○) chloroforme; (●) toluène; (□) di-n-butyléther; (■) tétrachlorure de carbone; (▲) cyclohexane.

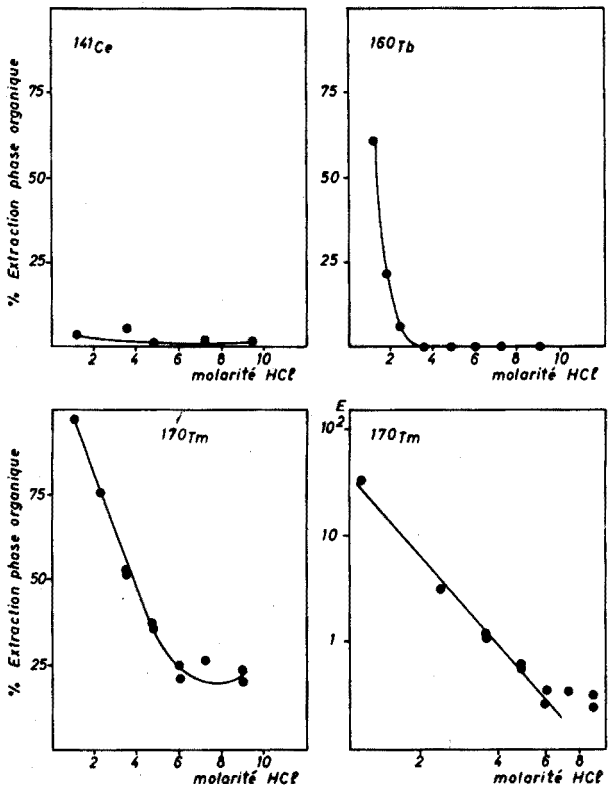

Fig. 2. Influence de la concentration en HCl sur l'extraction des Terres Rares. HDEHP (0.75 *M*) dans le cyclohexane.

bone, di-n-butyléther, cyclohexane, ce dernier s'est révélé supérieur aux autres diluants ce qui a justifié son emploi ultérieur.

L'influence de la nature du diluant est représentée sur la Fig. 1.

Nous avons constaté expérimentalement une pente de 3, prévisible, pour les droites $E = f\,M(\text{HDEHP})$ dans le domaine 0.2–0.75 *M* HDEHP.

L'extraction des Terres Rares par le système HDEHP 1.5 *M*–heptane–HCl a fait l'objet, tout récemment, d'un rapport de Gusmini et Nonnenmacher[16]. Cette étude a été reprise pour le système HDEHP 0.75 *M*–cyclohexane–HCl. Nos résultats illustrés dans la Fig. 2 rejoignent les conclusions de Gusmini Nonnenmacher: il est impossible d'extraire, en phase organique, la totalité du groupe des Terres Rares de l'apatite, la mise en solution du minéral réclame une acidité en acide chlorhydrique supérieure à 2 *M*. A cette concentration, la majorité des Terres Rares légères se retrouvent pratiquement dans la phase aqueuse donc non séparées du calcium et des phosphates.

Bien que les coefficients de distribution en milieu nitrique soient supérieurs à ceux obtenus en milieu chlorhydrique, l'emploi de cet acide n'offre guère de possibilité d'isolement du groupe des Terres Rares de la matrice minéralogique; nous nous sommes proposés dès lors d'étudier l'acide perchlorique.

De l'examen de la Fig. 3, on peut admettre qu'en milieu modérément

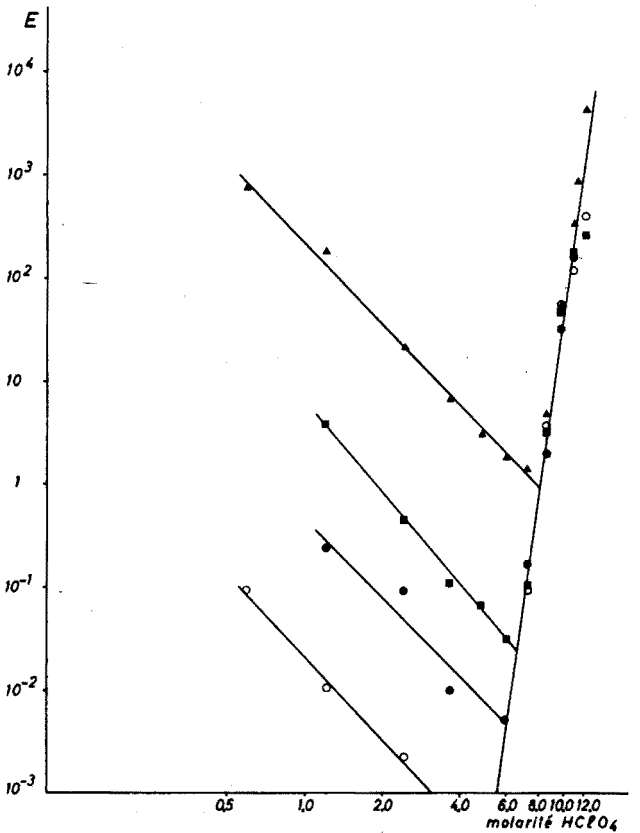

Fig. 3. Variation du coefficient de distribution des Terres Rares avec la concentration en $HClO_4$ HDEHP (0.75 *M*) dans le cyclohexane. (○) ^{141}Ce; (●) ^{147}Nd; (■) ^{160}Tb; (▲) ^{170}Tm.

concentré en acide perchlorique, l'extraction est contrôlée par le mécanisme du type chélation pure. L'espèce extraite en phase organique est un composé moléculaire; en phase aqueuse, elle est plus ou moins ionisée. Dans ces conditions, l'extraction est inversément proportionnelle à la 3ème puissance de la concentration en ions H^+.

L'extraction en phase organique passe par un minimum pour une concentration en acide perchlorique située aux environs de 4–6 *M*.

Au-delà de cette zone, l'extraction en phase organique augmente avec la concentration en acide perchlorique; il semble donc qu'un nouveau mécanisme, du type association par paire d'ions sans doute, gouverne l'extraction. La pente de la droite $E = f\,M(HClO_4)$, en échelle logarithmique, est de $+18$.

Une étude systématique des variations du pourcentage d'extraction et du coefficient de distribution des divers constituants de l'apatite a été entreprise, dans le système HDEHP 0.75 *M*–cyclohexane–$HClO_4$ variable.

Nous avons rassemblé dans le Tableau I l'ensemble des observations résultant de nos expériences.

L'examen des droites $P = fM(HCl)$ (Fig. 2) montre que dans le système HDEHP 0.75 *M*–cyclohexane, la majorité des éléments des terres rares est totalement

TABLEAU I

ISOLEMENT DES TERRES RARES PAR LE SYSTÈME HDEHP 0.75 *M*–CYCLOHEXANE–$HClO_4$ 12 *M*

Elément	*% Extraction phase organique*	*% Extraction phase aqueuse*
Ce^{3+}	100	—
Nd^{3+}	100	—
Tb^{3+}	100	—
Tm^{3+}	100	—
Na^{+}	—	100
Rb^{+}	—	100
Ca^{2+}	4	96
Sr^{2+}	—	100
Ba^{2+}	—	100
Al^{3+}	—	100
Fe^{3+}	~100	—
PO_4^{3-}	—	100

extraite en phase chlorhydrique 9 *M*; seul de 4 terres rares étudiées, le thulium fait exception: le pourcentage d'extraction du thulium en phase aqueuse n'atteint que 80%. Il est cependant possible d'obtenir un meilleur rendement d'extraction en phase aqueuse en diluant la phase organique par du cyclohexane pur et d'ajuster au même volume la phase aqueuse.

Mode opératoire

Le mode opératoire préconisé pour l'isolement du groupe des Terres Rares de l'apatite est le suivant: 100 mg d'apatite irradiée sont mis en solution par 10 ml d'acide perchlorique 12 *M*. Le groupe des Terres Rares est quantitativement extrait par 10 ml d'une solution HDEHP 0.75 *M* diluée dans du cyclohexane. Les phases sont séparées par centrifugation. Après un lavage par 10 ml d'acide perchlorique 12 *M*, la phase organique, décantée et centrifugée, est diluée par 20 ml de cyclohexane et agitée pendant 5 min avec 30 ml d'acide chlorhydrique 9 *M*. La phase aqueuse, décantée et centrifugée, contient le groupe des Terres Rares séparées du calcium et des phosphates.

RÉSUMÉ

L'extraction des Terres Rares par l'acide di-(2-éthylhexyl)phosphorique (HDEHP)–cyclohexane–acide perchlorique (1–12 *M*) est étudiée. Pour des molarités modérées en acide perchlorique (1–6 *M*), le coefficient de distribution, *E*, est inversément proportionnel à la 3ème puissance de la concentration en acide dans la phase aqueuse. Cependant, pour des acidités plus élevées, la pente des droites est de +18. En milieu perchlorique 12 *M*, les Terres Rares sont extraites de l'apatite quantitativement et sélectivement en phase organique. La réextraction en phase aqueuse s'effectue en milieu chlorhydrique 9 *M*.

SUMMARY

The liquid–liquid extraction of rare-earth elements (REE) by 0.75 *M* di-(2-ethylhexyl)phosphoric acid (HDEHP) in cyclohexane from perchloric acid (1–12 *M*) has been investigated. At moderate perchloric acid molarities (1–6 *M*), the distribution coefficient, *E*, has an inverse third-power dependency upon the acid concentration in the aqueous phase. However, at higher perchloric acid concentrations, the slope of the resulting curve is about +18, which means a change in the extraction mechanism. In 12 *M* perchloric acid medium, REE are quantitatively and selectively extracted from apatite minerals, in the organic phase. In order to strip out all the lanthanides, back-extractions were carried out with 9 *M* hydrochloric acid solutions.

ZUSAMMENFASSUNG

Die Extraktion der "Seltenen Erden" in Gegenwart von Di-2-Äthylhexylphosphorsäure (HDEHP)–Cyclohexan–Perchlorsäure (1–12 *M*) wurde untersucht. Im Falle $HClO_4$ 1–6 *M*, hat der Verteilungskoeffizient, *E*, den Wert-3. Für höhere $HClO_4$ Molaritäten hat die Steigung im linearen Bereich der Funktion $E = f(\log[HClO_4])$ den Wert +18.

BIBLIOGRAPHIE

1 D. F. Peppard, G. W. Mason, J. L. Maier et W. J. Driscoll, *J. Inorg. Nucl. Chem.*, 4 (1957) 334.
2 D. F. Peppard, G. W. Mason et S. W. Moline, *J. Inorg. Nucl. Chem.*, 5 (1957) 141.
3 D. F. Peppard, G. W. Mason, W. J. Driscoll et R. J. Sironen, *J. Inorg. Nucl. Chem.*, 7 (1958) 276.
4 D. F. Peppard, E. P. Horwitz et G. W. Mason, *J. Inorg. Nucl. Chem.*, 24 (1962) 429.
5 D. F. Peppard, in Le Roy Eyring, *Progress in the Science and Technology of Rare Earth*, Pergamon Press, Oxford, 1964, p. 89.
6 G. W. Mason, S. Lewey et D. F. Peppard, *J. Inorg. Nucl. Chem.*, 26 (1964) 2271.
7 C. F. Baes, R. A. Zingaro et C. F. Coleman, *J. Phys. Chem.*, 62 (1958) 129.
8 C. A. Blake, C. F. Baes, K. B. Brown et C. F. Coleman, *Proc. 2nd Int. Conf. Peaceful Uses At. Energy*, 28 (1958) 289.
9 K. Kimura, *Bull. Chem. Soc. Jap.*, 33 (1960) 1038.
10 K. Kimura, *Bull. Chem. Soc. Jap.*, 34 (1961) 63.
11 J. J. McCrown et R. P. Larsen, *Anal. Chem.*, 33 (1961) 1003.
12 T. B. Pierce et P. F. Peck, *Analyst*, 88 (1963) 217.
13 C. Dubuquoy, R. Guillaumont et G. Boussières, *Radiochim. Acta*, 8 (1967) 49.
14 T. Goto, *J. Inorg. Nucl. Chem.*, 30 (1968) 3305.
15 T. Harada et M. Smutz, *J. Inorg. Nucl. Chem.*, 32 (1970) 649.
16 S. Gusmini et R. Nonnenmacher, *CEA-R-4004-1970.*
17 O. B. Michelsen et M. Smutz, *AED-CONF-1971-070-012.*

Analytica Chimica Acta, 68 (1974) 137–142

COMPLEXIMETRIC BACK-TITRATIONS OF TRACES OF INDIUM

TH. J. M. POUW, G. DEN BOEF, U. HANNEMA, J. M. VAN DER MEER and S. Q. J. ZONNEVELD

Laboratory for Analytical Chemistry, University of Amsterdam, Nieuwe Achtergracht 166, Amsterdam (The Netherlands)

(Received 11th June 1973)

Indium(III) reacts slowly with EDTA to give a very stable complex. Because it reacts slowly, back-titrations are necessary in titrimetric procedures; and as the indium(III)–EDTA complex is very stable, back-titrations of traces of indium are possible.

In order to achieve a selective determination of indium the pH of the titration solution should be kept low. A perchloric acid medium of pH 1.3 appeared to be suitable. At this pH the conditional stability constant of the indium(III)–EDTA complex is $10^{10.3}$. Few other metal ions react with EDTA under these conditions.

During this investigation, two linear indication methods were used, *viz.* photometry and amperometry. In general, the condition for a suitable titration, based on the complexation reaction, is that $K'c$, the product of the conditional stability constant of the chelate and the concentration of the metal ion to be determined, should be at least 10^2 when linear indication methods are used. This would lead to a lower limit of determination of 10^{-8} M for indium(III) at pH 1.3. However, the indication method may and does lead to a somewhat higher concentration limit.

The selection of a suitable metal ion for the back-titration is very important. For this metal, the condition $K'c \geqslant 10^2$ is also required. Furthermore, the back-titrant should react instantaneously with EDTA at very low concentrations, and some suitable indication of the end-point of the back-titration must be available. Trivalent bismuth meets all these requirements. The conditional stability constant of the bismuth(III)–EDTA complex at pH 1.3 calculated from current handbooks is 10^8, but there is evidence that this value is slightly larger in perchloric acid medium. Thus bismuth(III) meets the stability requirement. Moreover, it reacts very quickly with EDTA at very low concentrations, and at least two good methods of end-point detection are possible.

PHOTOMETRIC INDICATION

A photometric indication method was based on the absorption by the bismuth(III)–EDTA chelate in the ultraviolet at 260 nm[1]. Very few other chelates absorb at this wavelength. The molar absorptivity of the bismuth(III)–EDTA chelate at 260 nm is about 10.000 l cm^{-1} $mole^{-1}$. In general, a change in absorbance of 0.1 is sufficient for a suitable photometric titration curve; if the cell has an optical path length of 5 cm, this leads to a lower limit of determination of $2 \cdot 10^{-6}$

M for the determination of EDTA with bismuth(III). This limit is somewhat higher than the limit set by the stability constant of the bismuth(III)–EDTA chelate.

This indication method for the back-titration of metal ions such as indium(III) depends on the fact that the conditional stability constant of bismuth–EDTA is smaller than the corresponding constant of the metal ion to be determined. Metal ions forming less stable chelates with EDTA than does bismuth(III) do not interfere when this indication method is used.

The determinations with photometric end-point detection were carried out by coulometric titration with bismuth(III) generated from bismuth amalgam in a 30-ml cell as described previously[2]. The electrogeneration of trace amounts of bismuth(III) is possible with 100% current efficiency when the amalgam is protected cathodically during the interruptions of the generation current[2].

As EDTA was added in a 100% excess with respect to indium(III) the limit of determination for indium(III), set by the Zeiss PMQ spectrophotometer, was about $2 \cdot 10^{-6}$ *M*, which corresponds to about 5 μg of indium(III) in a 30-ml cell.

Procedure

Place 30 ml of a perchloric acid solution (pH 1.3), containing about 5 μg of indium(III) in the titration cell of the spectrophotometer, which contains bismuth amalgam for the generation of the titrant; add 0.1 ml of 10^{-3} *M* EDTA, which corresponds to a 100% excess with respect to indium(III). Carry out the titration coulometrically with photometric end-point detection ($\lambda = 260$ nm) in a nitrogen atmosphere, as mentioned in the previous paper[2].

The generation current for 5 μg of indium(III) is 0.25 mA. The cathodic protection potential of the amalgam is −0.6 V *vs.* S.C.E.

TABLE I

DETERMINATION OF INDIUM(III) IN THE PRESENCE OF OTHER METAL IONS
(5.65 μg In(III) taken in each case)

Other metal ion	*Amount other metal / Amount indium (w/w)*	*In found (μg)*	*Error (%)*
Ba(II)	3000	5.54	−2.0
Mg(II)	500	5.44	−3.7
Ca(II)	1000	5.49	−2.8
Mn(II)	2000	5.49	−2.8
Zn(II)	300	5.60	−0.9
Al(III)	150	5.77	+2.0
Cd(II)	100	5.71	+1.1
Pb(II)	20	5.84	+3.3
Co(II)	12	5.98	+5.8
Co(II)	6	5.34	−5.4
Ni(II)	6	5.51	−2.5
Tl(I)	4	5.70	+0.9
Cr(III)	10	5.84	+3.0
Ga(III)	1	5.70	+0.9
Fe(III)	2	5.96	+5.6

Results

In the absence of other metal ions, the determination of 5 μg of indium(III) appeared to be possible with a standard deviation of 2.8%. No systematic error was observed.

The influence of the presence of other metal ions was thoroughly investigated. It can be expected that only those metal ions interfere which have a larger conditional stability constant with EDTA than has bismuth(III), because they are not displaced by the titrant from their complexes. However, in practice, kinetic factors may cause interference of other metal ions, *e.g.* nickel(II), or non-interference of metal ions expected to interfere, *e.g.* chromium(III). Table I summarizes the results of the determination of 5 μg of indium(III) in the presence of other metal ions. In general, the maximum amounts of these metal ions are mentioned which do not interfere.

As the lower limit of determination is set by the photometric indication method, another indication method was tried in order to lower this limit and to exploit completely the possibilities offered by the reaction between bismuth(III) and EDTA.

AMPEROMETRIC INDICATION

In previous communications[3,4] the principle has been described of an amperometric complex formation titration, with utilizes the anodic wave shown by the free ligand at a rotating mercury electrode. Determinations at the 10^{-7} *M* level were possible.

This indication method leads, in the case of back-titrations of indium(III) or other metal ions, to an L-shaped curve, by setting the potential of the indicator electrode at a value where mercury oxidizes from the electrode in the presence of EDTA but not in its absence. When using this indication method, the condition for the photometric indication that $K_{BiEDTA} < K_{InEDTA}$ is no longer required. On the other hand, every metal ion complexing with EDTA under the experimental conditions interferes, as the indicator electrode does not register the displacement of metal ions forming weaker complexes with the ligand than does bismuth(III). Therefore, although it results in a lower limit of determination, this method is less selective.

Instrumentation

The titration cell had a volume of 10 ml. It was connected by means of a fritted glass disc to a second compartment, provided with a saturated calomel electrode. Both compartments were filled with the same supporting electrolyte.

The titration cell was provided with a rotating mercury electrode, rotating at 250 r.p.m. In earlier work[3,4] an amalgamated gold electrode was used. In more recent work, a mercury coated platinum wire electrode, as described by Neeb[5], appeared to give a better response over a longer period of time. A PAR model 171 polarograph (Princeton Applied Research) supplied the voltage for the cell and also served for the measurement of the current.

The titrations were carried out by adding the titrant solution from a 0.5-ml Metrohm microburette (type E 457).

Coupling of the coulometric generation of bismuth(III) with this amperometric indication method has not been accomplished yet.

Procedure

Dissolve a sample containing 0.1–1 μg of indium(III) (1–10 nmole) in 10 ml of a 0.1 *M* perchloric acid solution of pH 1.9, and place the solution in the cell; add EDTA (2–12 nmole). Titrate the excess of EDTA with 10^{-4} or $4 \cdot 10^{-4}$ *M* bismuth(III); the potential of the indicator electrode was taken as +0.32 V *vs.* S.C.E.

As the concentrations were smaller (10^{-7} *M*) than in the case of the photometric indication method, the pH was made slightly higher in order to obtain sharp breaks in the titration curves.

Results

The results for determinations in the absence of other metal ions are given in Table II. The interferences of other ions were only investigated for those ions which were expected to interfere seriously under the experimental conditions. Large amounts of chloride, sulphate and nitrate must be avoided because the weak complexes of these ions with bismuth(III) and mercury(II) seriously affect the sharpness of the titration curve at this concentration level at pH 1.9.

The influence of some metal ions on the determination of 0.115 μg of indium(III) is presented in Table III. Iron(III) and gallium(III) interfered, obviously

TABLE II

DETERMINATION OF INDIUM(III) IN THE ABSENCE OF OTHER METAL IONS

In(III) (μg)		*Error (%)*	*s (%) (no. of detns.)*
Taken	*Found*		
0.861	0.867	+0.7	4.9(6)
0.574	0.588	+2.4	5.7(6)
0.287	0.294	+2.2	5.7(7)
0.115	0.121	+5.2	6.3(8)

TAPLE III

DETERMINATION OF INDIUM(III) IN THE PRESENCE OF OTHER METAL IONS

(0.115 μg In(III) taken in each case)

Other metal ion	*Amount other metal / Amount indium (w/w)*	*In(III) found (μg)*	*Error (%)*	*s (%) (no. of detns.)*
Tl(I)	4	0.118	+2.6	3.0(4)
Ni(II)	5	0.119	+3.4	4.2(4)
Zn(II)	30	0.114	−1.0	8.2(4)
Cr(III)	50	0.112	−3.4	5.0(4)
Co(II)	500	0.124	+7.8	3.7(4)

because of the high conditional stability constants of their complexes with EDTA. Chromium(III), although it also has a large conditional stability constant, obviously does not interfere because of the low rate of the reaction between chromium(III) and EDTA.

DISCUSSION

Compleximetric back-titrations involving bismuth(III) as the back-titrant are obviously very useful for the titrations of traces of metal ions which react slowly with EDTA. For those metal ions forming very stable complexes with EDTA, selective determinations are possible by working at rather low pH values (pH 1–2). Some other examples such as the determination of chromium(III) will be discussed later.

SUMMARY

Indium(III) has been determined in the microgram range by compleximetric back-titration with EDTA, bismuth(III) serving as the back-titrant. About 5 μg of indium(III) can be determined by means of a spectrophotometric indication method, the absorbance of the bismuth(III)–EDTA complex being measured at 260 nm. Smaller amounts of indium, down to 0.1 μg, can be determined by amperometric indication of EDTA at a rotating mercury electrode. A good selectivity is obtained by working at pH values between 1 and 2.

RÉSUMÉ

On a dosé l'indium(III) dans le domaine de microgramme par titrage en retour complexométrique avec EDTA, en faisant usage du Bi(III) comme titrant. L'indication spectrophotométrique par l'adsorption du chélate Bi(III)–EDTA à 260 nm permet le dosage de 5 μg In(III). L'indication ampérometrique de l'agent complexant avec une électrode indicatrice à mercure tournante permet le dosage de 0.1 μg In(III). La sélectivité est bonne quand le dosage est excecuté dans un milieu assez acide de pH 1 à 2.

ZUSAMMENFASSUNG

Indium(III) wurde im Mikrogrammbereich bestimmt durch komplexometrische Rücktitration mit ÄDTA unter Verwendung von Bi(III) als Titrant. Bei Anwendung einer photometrischen Endpunktsbestimmung, wobei die Absorption vom Bi(III)–ÄDTA-Komplex bei 260 nm benutzt wurde, erwies sich die Bestimmung von 5 μg In(III) als möglich. Eine niedrigere Bestimmungsgrenze (0.1 μg In(III)) wurde erzielt durch amperometrische Indizierung von ÄDTA an einer rotierenden Quecksilberelektrode. Die Selektivität ist gut, wenn die Bestimmungen bei niedrigen pH-Werten (1–2) durchgeführt werden.

REFERENCES

1 G. den Boef, W. E. van der Linden and S. Beijer, *Mikrochim. Acta*, (1971) 761.

2 Th. J. M. Pouw, G. den Boef and U. Hannema, *Anal. Chim. Acta*, 67 (1973) 000.
3 F. Freese and G. den Boef, *Talanta*, 13 (1966) 865.
4 F. Freese, H. J. Jasper and G. den Boef, *Talanta*, 17 (1970) 1945.
5 R. Neeb, *Inverse Polarographie und Voltammetrie*, Verlag Chemie, Weinheim, 1969, pp. 98–100.

Analytica Chimica Acta, 68 (1973) 143–154

DETERMINATION OF THE COMPOSITION AND THE STABILITY CONSTANTS OF COMPLEXES OF MERCURY(II) WITH AMINO ACIDS

W. E. VAN DER LINDEN and C. BEERS

Laboratory for Analytical Chemistry, University of Amsterdam, Nieuwe Achtergracht 125, Amsterdam (The Netherlands)

Received 19th March 1973)

A knowledge of the interaction between metal ions and amino acids is of possible significance for the understanding of the biological action of these metals. Although much knowledge is available about the complex formation between some transition metals and amino acids, little work has been done on the complexation of mercury(II)[1,2]. Apart from a more thorough investigation of the complex formation of mercury(II) with histidine[3] and cysteine[4], the only information found in the literature is that 1:2 complexes are formed, especially at higher pH values. Some values of the corresponding stability constants have been reported[5–8].

The present paper deals with the complexes of mercury(II) with all the twenty amino acids that are important in protein synthesis. The complex formation was studied in aqueous solutions at pH values varying from 2.7 to 8.5. In this pH region, almost all amino acids are present mainly as the single protonated form HL ($L^- = R\text{–}CNH_2\text{–}COO^-$), the proton being attached to the α-amino group. A few amino acids occur as the H_2L or H_2L^+ forms over the whole pH range used; this is true for tyrosine, cysteine and lysine where the protons of the phenolic group, the sulphhydryl group and the protonated amino-endgroup, respectively, are not released. For these amino acids, the method outlined hereafter will be applicable if the ligand is taken as $HL^{(-)}$ (*i.e.* $H^{(+)}R\text{–}CNH_2\text{–}COO^-$) instead of L^-. The amino acids histidine, aspartic acid and glutamic acid, occur in the single protonated form at higher pH values; but especially histidine, and to a lesser extent both other compounds, will become doubly protonated on decreasing pH.

Although Stricks and Kolthoff[4] mention the formation of polynuclear mercury(II)–cysteine complexes, the existence of polynuclear complexes in the present experiments is very unlikely, because a large excess of ligand was used in all experiments. The following species are to be expected in solutions containing mercury(II) and amino acids: ML, MLH, ML(OH), $ML(OH)_2$, ML_2, ML_2H, ML_2H_2, $ML_2(OH)$ and $ML_2(OH)_2$ if the maximum number of hydroxo groups in a complex is limited to 2. A complex MLH_2 is very improbable, as the protonation is in fact a protonation of the ligand.

The principal experimental data used were the potentials of a mercury/mercury(II) electrode as a function of pH. All amino acids were present in the solution in at least a ten- to twentyfold excess with respect to mercury. The pH of the solutions was changed by addition of sodium hydroxide or nitric acid. The simultaneous measurement of both the concentration of the metal ion and the pH

simplifies the determination of the complex compositions and the calculation of the corresponding stability constants, and allows a rather straightforward treatment. The method applied resembles that presented by Ringbom and Harju[9]. Although the method is very easy to apply, no claim can be laid on the utmost accuracy. However, an accuracy to within the first decimal in the logarithm suffices for most analytical work.

THEORY

Notation

In the subsequent treatment, the following notation is used.

C_X = total concentration of species X

[X] = actual concentration of X

$$\beta_{M_mL_nX_p} = \frac{[M_mL_nX_p]}{[M]^m[L]^n[X]^p} \tag{1}$$

$$K^{X\,ML_n}_{ML_nX} = \frac{[ML_nX]}{[ML_n][X]} \tag{2}$$

$$\alpha_{M(OH)} = 1 + \sum_{m=1}^{M}\sum_{q=1}^{Q} m\beta_{M_m(OH)_q}[M]^{m-1}[OH]^q \tag{3}$$

$$\alpha_{L(H)} = 1 + \sum_{p=1}^{P} \beta_{H_pL}[H]^p \tag{4}$$

$$\alpha_{M(L)} = 1 + \sum_{m=1}^{M}\sum_{n=1}^{N}\sum_{p=0}^{P}\sum_{q=0}^{Q} m\beta_{M_mL_nH_p(OH)_q}[M]^{m-1}[L]^n[H]^p[OH]^q \tag{5}$$

Development

When the expected species, as mentioned in the introduction, are formed in the pH region 2.7–8.5, the following holds:

$$\frac{C_M}{[M]} = \alpha_{M(L)} + \alpha_{M(OH)} - 1$$

or

$$\alpha_{M(L)} = \frac{C_M}{[M]} - \alpha_{M(OH)} + 1 \tag{6}$$

For the total ligand concentration we can write:

$$C_L = [L] + \sum_{n=1}^{N}\sum_{p=0}^{P}\sum_{q=0}^{Q} n[ML_nH_p(OH)_q] + \sum_{p=1}^{P}[H_pL] \tag{7}$$

If $C_L \gg C_M$, the fraction of the ligand concentration that is complexed by the metal can be neglected and only the protonated forms of the ligand have to be considered. For all uncomplexed amino acids for which the single protonated form of the ligand is the predominant species in solution, we can write:

$$\frac{C_L}{[L]} = \alpha_{L(H)} \simeq 1 + \beta_{HL}[H] \simeq \beta_{HL}[H]$$

$$\rightarrow [H] = \frac{\alpha_{L(H)}}{\beta_{HL}} = \frac{C_L}{[L]} \frac{1}{\beta_{HL}} \tag{8}$$

If irrelevant species are omitted, combination of eqns. (5) and (8), and arrangement in order of increasing value of the exponent of [L] yields:

$$\alpha_{M(L)} = \{1 + \beta_{MLH} \frac{C_L}{\beta_{HL}} + \beta_{ML_2H_2} \frac{C_L^2}{\beta_{HL}^2}\} + \{\beta_{ML} + \beta_{ML_2H} \frac{C_L}{\beta_{HL}}\} [L] +$$
$$+ \{\beta_{ML_2} + \beta_{ML(OH)} \frac{K_w \beta_{HL}}{C_L}\} [L]^2 + \{\beta_{ML(OH)_2} \frac{K_w^2 \beta_{HL}^2}{C_L^2} +$$
$$+ \beta_{ML_2(OH)} \frac{K_w \beta_{HL}}{C_L}\} [L]^3 + \beta_{ML_2(OH)_2} \frac{K_w^2 \beta_{HL}^2}{C_L^2} [L]^4 \tag{9}$$

Method

[M] can be calculated from the readings of the mercury-electrode potentials by applying Nernst's law. The value of $\alpha_{M(L)}$ is then obtained from eqn. (6). The measured pH values were used to determine [L] by means of eqn. (8).

Over the total pH region, $\alpha_{M(L)}$ and [L] will vary by several orders of magnitude, hence it is advisable first to make a graph of log $\alpha_{M(L)}$ as a function of log[L]. This graph will give valuable information about species which can be excluded in further calculations. For example, the fact that log $\alpha_{M(L)}$ *vs.* log[L] curves coincide for different values of C_L will be an indication that all species, which are responsible for the introduction of the factor C_L in eqn. (9), are of minor or no importance, *i.e.* all species containing protons or hydroxo groups may be considered as insignificant. The slope of the curve at a certain log[L]-value will give some information about which species are likely to predominate at that value of [L], and which species may be excluded. If, for instance, a maximum slope of 2 is found, it can be concluded that $ML(OH)_2$, $ML_2(OH)$ and $ML_2(OH)_2$ do not occur.

If no dependence on C_L is noticeable and a maximum value of the slope of 2 is observed, only ML and ML_2 need be considered. This is the case for most amino acids studied. Equation (9) then reduces to:

$$\alpha_{M(L)} = 1 + \beta_{ML}[L] + \beta_{ML_2}[L]^2 \tag{10}$$

or

$$\frac{\alpha_{M(L)} - 1}{[L]} = \beta_{ML} + \beta_{ML_2}[L] \tag{11}$$

A plot of the left-hand side of eqn. (11) *vs.* [L] will yield a straight line with an intercept of β_{ML} and a slope of β_{ML_2}. Generally, the log $\alpha_{M(L)}$ *vs.* log[L] curve will show two distinct straight lines with slopes of 1 and 2, respectively, connected by a curved part. Obviously ML and ML_2, respectively, predominate in separate regions and the following equations hold:

$$\frac{d \log \alpha_{M(L)}}{d \log [L]} = 1 \rightarrow \log \alpha_{M(L)} = \log \beta_{ML} + \log [L] \quad (12)$$

$$\frac{d \log \alpha_{M(L)}}{d \log [L]} = 2 \rightarrow \log \alpha_{M(L)} = \log \beta_{ML_2} + 2 \log [L] \quad (13)$$

This procedure makes it possible to obtain very quickly a first approximation of the values β_{ML} and β_{ML_2}. By introducing small variations in the values of both constants, a best fit of calculated and experimental curves can be obtained in 2–4 calculations.

EXPERIMENTAL

Chemicals

All amino acids were used in the purest form available (mostly from Ajinomoto Co., Inc.; 100%), all of them being in the L-form; 0.1 *M* stock solutions were made. Where necessary, sodium hydroxide was used to bring the compounds in solution. A 0.1 *M* mercury(II) stock solution was prepared by dissolving doubly distilled mercury in (1+1) nitric acid. The concentration of this solution was checked by titration with a standardized TRIEN solution. In all experiments sodium nitrate was added to bring the ionic strength to 0.1 at the start. Because of the titration technique used, a variation of the ionic strength between 0.1 and 0.12 had to be accepted.

Instrumental

Potential differences between the mercury electrode and a SCE were measured with a Radiometer PHM4c compensation pH meter; pH measurements were made with a Radiometer expanded scale pH meter. The pH was varied by addition of sodium hydroxide or nitric acid from a piston-type buret. In the calculations carried out with he aid of a EL X-8 computer, a correction was made for dilution. The temperature was kept at 25°.

RESULTS

The applicability of a mercury electrode for measurements of the mercury(II) concentration (activity) might be questionable, because of the disproportionation reaction $Hg^0 + Hg^{2+} \rightleftarrows Hg_2^{2+}$ that may take place. In fact, this reaction did affect the calibration of the electrode with mercury(II) solutions of known concentrations in the absence of complexing agents; the potential readings were too low to correspond with Nernst's law for the reaction $Hg^{2+} + 2e \rightleftarrows Hg^0$. However, if mercury(II) forms complexes of sufficient stability, the divalent state is stabilized, and the disproportionation reaction can be neglected. In that case, the application of the Nernst equation $E = E^0_{Hg^{2+},Hg} + RT/2F \ln [Hg^{2+}]$ is justified; this was proved by application of the method to the determinaton of known stability constants of mercury(II) complexes with ligands like DTPA, CDTA and EGTA. The values of the constants obtained for these complexes were in agreement with those obtained by other methods.

TABLE I

LOGARITHMIC VALUES OF THE STABILITY CONSTANTS

No.	*Amino acid*	$K_{HL}^{H,L}$ [a]	$K_{H_2L}^{H,HL}$ [a]	$K_{H_3L}^{H,H_2L}$ [a]	$K_{ML}^{M,L}$	$K_{ML_2}^{L,ML}$	β_{ML_2}
1	Alanine	9.80	2.50		12.4	7.2	19.6
2	Arginine	9.21	2.19		11.5	7.3	18.8
3	Asparagine	8.85	2.14		11.4	7.2	18.6
4	Glycine	9.68	2.44		12.2	7.0	19.2
5	Glutamine	9.16[b]	2.27[b]		11.5	7.2	18.7
6	Leucine	9.62	2.37		11.9	7.6	19.5
7	Iso-leucine	9.66[b]	2.40[b]		12.4	7.4	19.8
8	Phenylalanine	9.18	2.21		12.4	7.2	19.6
9	Proline	10.52	2.02		12.2	7.9	20.1
10	Serine	9.13	2.21		11.7	7.4	19.1
11	Threonine	8.86	2.24		11.7	7.0	18.7
12	Tryptophan	9.43	2.39		13.9	7.5	21.4
13	Valine	9.59	2.38		11.7	7.2	18.9
14	Lysine	10.72	9.18	2.18	11.3[c]	7.4[c]	18.7[c]
15	Tyrosine	10.16	9.11	2.34	12.3[c]	7.2[c]	19.5[c]
16	Cysteine	10.55	8.48	1.96	—	—	39.4[c]
17	Aspartic acid	9.62	3.70	1.94	13.2	6.8[d]	20.0
18	Glutamic acid	9.54	4.21	2.39	12.8	6.4[e]	19.2
19	Histidine	9.16	6.00	1.79	—	—	21.6[f]
20	Methionine	9.13	2.26		12.8	6.7	19.5[g]

[a] Taken from refs. 1 and 2.

[b] Present experimental values.

[c] These constants correspond to $K_{ML}^{M,L}(M+HL\rightleftarrows MHL)$, $K_{ML_2}^{L,ML}(MHL+HL\rightleftarrows M(HL)_2)$, $\beta_{ML_2}(M+2HL\rightleftarrows M(HL)_2)$.

[d] $K_{MLH}^{H,ML}=3.0$.

[e] $K_{MLH}^{H,ML}=3.6$.

[f] $K_{ML_2H}^{H,ML_2}=6.2$; $K_{ML_2H_2}^{H,ML_2H}=5.8$.

[g] $\beta_{ML_2H_2}=27.3$; $\beta_{ML_2H}=24.6$.

The amino acids 1–13 (Table I) showed no irregularities. For all these compounds, no concentration-dependence was observed and the log $\alpha_{M(L)}$ *vs.* log[L] curves indicated a maximum metal-to-ligand ratio of 1:2. Calculations based on the plot of $(\alpha_{M(L)}-1)/[L]$ as a function of [L], and the plot of log $\alpha_{M(L)}$ *vs.* log[L], yielded the same results to within the first decimal of the logarithm. A typical log $\alpha_{M(L)}$ *vs.* log[L] curve is shown in Fig. 1. For tyrosine, lysine and cysteine, the log $\alpha_{M(L)}$ *vs.* log[L] curve was shifted to larger values of log $\alpha_{M(L)}$ over the whole pH region, when the ligand concentration was increased (Fig. 2). This immediately provides proof that all complexes contain at least one proton. Evidently, this is the proton of the end OH group, the NH_3^+ group and the α-NH_3^+ group respectively. When a plot of log $\alpha_{M(L)}$ *vs.* log[HL] was made, the curves for different ligand concentrations coincided (Fig. 3), and the stability constants of the complex-formation reactions $M+n\,HL\rightleftarrows M(HL)_n$ could be evaluated as described above.

Glutamic acid and aspartic acid showed a small deviation in the lower pH region, the log $\alpha_{M(L)}$ values being somewhat increased in comparison to the values that are to be expected if only ML complexes are formed. This deviation can be

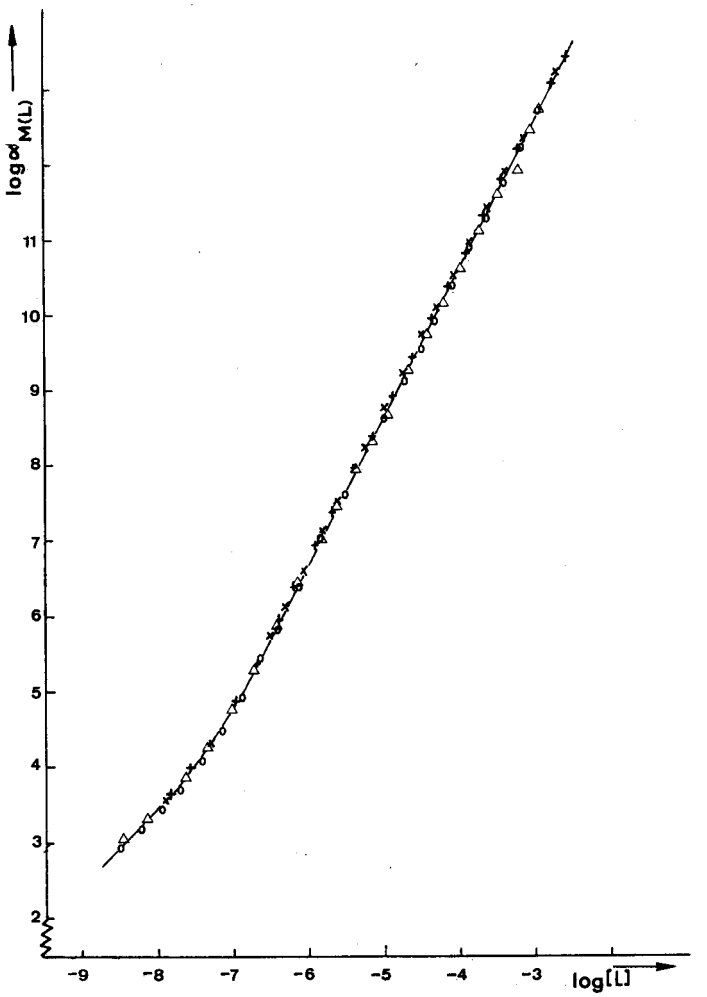

Fig. 1. Log $\alpha_{M(L)}$ as a function of log[L] for asparagine. $c_{Hg^{2+}} = 10^{-3}$ M; (○, △), $C_L = 10^{-2}$ M; (+, ×), $C_L = 2 \cdot 10^{-2}$ M.

attributed to the protonation of the second carboxylate group that plays no role in the chelation. As this occurs in the pH region where no ML_2 complexes are formed, the equation for $\alpha_{M(L)}$ becomes:

$$\alpha_{M(L)} = 1 + \beta_{ML}[L] + \beta_{MLH}[L][H] \tag{14}$$

or

$$\frac{\alpha_{M(L)} - 1}{[L]} = \beta_{ML} + \beta_{MLH}[H] \tag{15}$$

At lower pH values, a straight line was obtained for the plot of the left-hand side of eqn. (15) *vs.* [H]. The intercept yielded the value of β_{ML} and the slope the value of β_{MLH}.

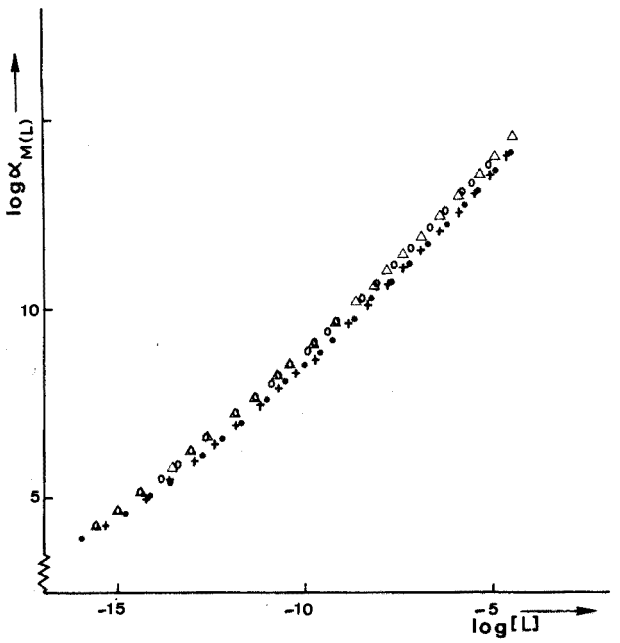

Fig. 2. Log $\alpha_{M(L)}$ as a function of log[L] for tyrosine. $c_{Hg^{2+}} = 10^{-3}$ M; (●, +), $C_L = 10^{-2}$ M; (△, ○), $C_L = 2 \cdot 10^{-2}$ M.

The greatest deviations were found for histidine and methionine. Both showed an increased value of $\alpha_{M(L)}$ below pH 5 as well as a significant dependence on the concentration (Figs. 4 and 5). At higher values of the pH, obviously ML_2 is formed in both cases.

There is, however, also a distinct difference between histidine and methionine based on the molecular structure. For histidine, a protonation of the second nitrogen atom in the imidazole ring is to be expected whereas for methionine no protonation can take place if the amino carboxylate group is involved in the chelation of mercury. Below pH 5 histidine is mainly present as H_2L^+, as can be calculated from the acid constants, thus

$$[H] = \left\{ \frac{C_L}{\beta_{H_2L}[L]} \right\}^{\frac{1}{2}} \tag{16}$$

If only ML and ML_2, and their protonated forms, are considered, we can write:

$$\alpha_{M(L)} = 1 + \beta_{ML}[L] + \beta_{ML_2}[L]^2 + \beta_{MLH}[L][H] + \\ + \beta_{ML_2H}[L]^2[H] + \beta_{ML_2H_2}[L]^2[H]^2$$

or substituting eqn. (16):

$$\alpha_{M(L)} = 1 + \beta_{ML}[L] + \beta_{ML_2}[L]^2 + \beta_{MLH}[L]^{\frac{1}{2}} \left\{ \frac{C_L}{\beta_{H_2L}} \right\}^{\frac{1}{2}} + \\ \beta_{ML_2H}[L]^{\frac{1}{2}} \left\{ \frac{C_L}{\beta_{H_2L}} \right\}^{\frac{1}{2}} + \beta_{ML_2H_2}[L] \frac{C_L}{\beta_{H_2L}} \tag{17}$$

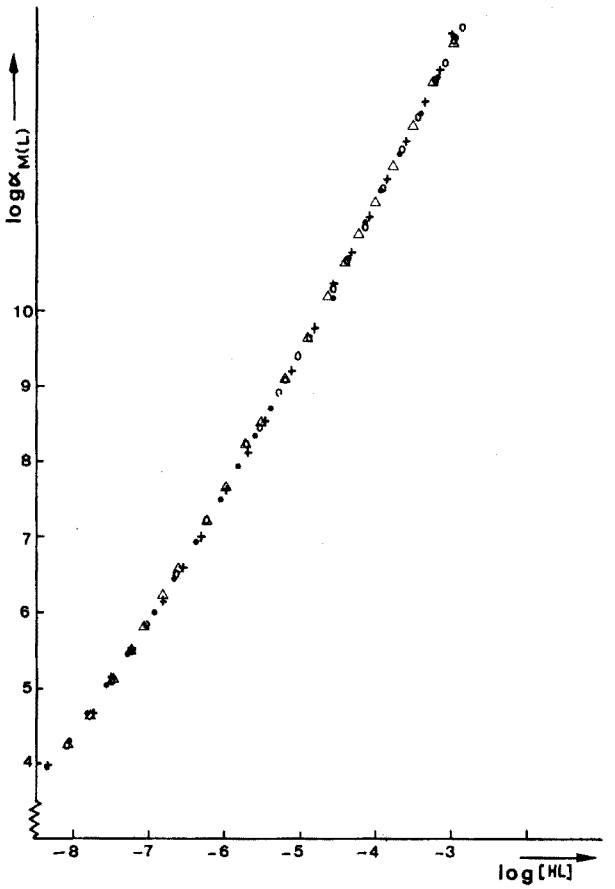

Fig. 3. Log $\alpha_{M(L)}$ as a function of log[HL] for tyrosine. $C_{Hg^{2+}} = 10^{-3}$ M; (●, +), $C_L = 10^{-2}$ M; (△, ○), $C_L = 2 \cdot 10^{-2}$ M.

A plot of $\alpha_{M(L)}$ *vs.* [L] at lower values of [L] yielded a straight line through the origin. Thus in eqn. (17) the presence of MLH, ML_2 and ML_2H can be exluded, which leads to:

$$\alpha_{M(L)} = \left\{ \beta_{ML} + \beta_{ML_2H_2} \frac{C_L}{\beta_{H_2L}} \right\} [L] = \gamma [L] \tag{18}$$

or

$$\beta_{ML_2H_2} = \gamma \frac{\beta_{H_2L}}{C_L} - \frac{\beta_{H_2L}}{C_L} \beta_{ML} \tag{19}$$

For different ligand concentrations the same value of $\gamma\beta_{H_2L}/C_L$ was found, and it was apparent that in all cases protonated complexes occurred, hence it was concluded that the last term in eqn. (19) could be neglected and that ML was not present. The fact that ML_2H is not detectable at lower pH values does not mean that this species not exist. Above pH 7, histidine splits off one proton and is predominantly present as HL in solution. If ML_2H exists the following equation holds:

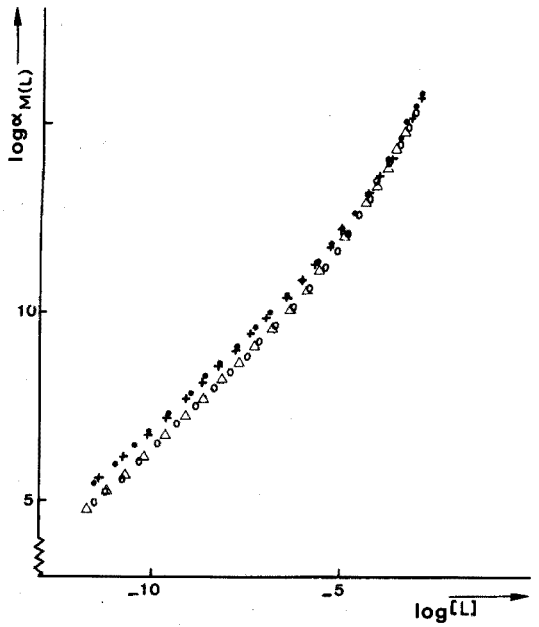

Fig. 4. Log $\alpha_{M(L)}$ as a function of log [L] for histidine. $C_{Hg^{2+}} = 10^{-3}$ M; (○, △), $C_L = 10^{-2}$ M; (●, +), $C_L = 2 \cdot 10^{-2}$ M

$$\alpha_{M(L)} = 1 + \beta_{ML_2}[L]^2 + \beta_{ML_2H}[L]^2[H] + \beta_{ML_2H_2}[L]^2[H]^2$$

or substituting $[H] = \dfrac{C_L}{[L]\beta_{HL}}$:

$$\alpha_{M(L)} = 1 + \beta_{ML_2}[L]^2 + \beta_{ML_2H}[L]\frac{C_L}{\beta_{HL}} + \beta_{ML_2H_2}\frac{C_L^2}{\beta_{HL}^2} \qquad (20)$$

As the plot of $(\alpha_{M(L)} - 1)/[L]$ *vs.* [L] gives a straight line, the existence of ML_2H_2 can obviously be neglected at the higher pH values. The intercept gives the value of $\beta_{ML_2H}(C_L/\beta_{HL})$, and the slope yields the value of β_{ML_2}. The values thus obtained for ML_2, ML_2H and ML_2H_2 agree favourably with those found by Brooks and Davidson[3].

The same approach was used for methionine. In this case too, species ML_2, ML_2H and ML_2H_2 seem to be present as well as ML. To prove the correctness of our method, the method suggested by Ringbom and Harju[9] was also applied to the case of methionine. The same results were obtained.

DISCUSSION

All amino acids with the exception of histidine, methionine and cysteine have almost the same values of β_{ML} and β_{ML_2}. This suggests that the same groups in the amino acids are responsible for the chelation. Evidently, the chelation takes place by the amino-carboxylate group with a simultaneous abstraction of the proton on the α-amino group. The oxygen atom of the phenolic group of tyrosine and the

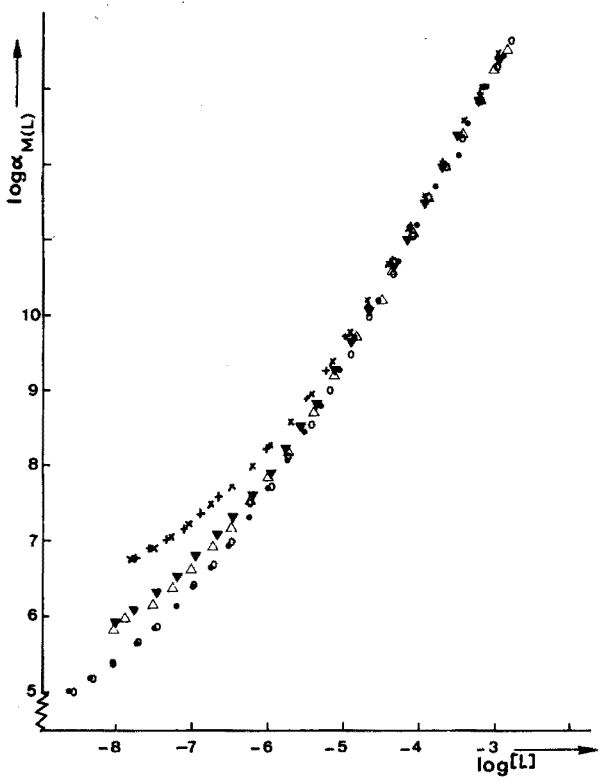

Fig. 5. Log $\alpha_{M(L)}$ as a function of log [L] for methionine. $C_{Hg^{2+}} = 10^{-3}$ M; (○, ●), $C_L = 10^{-2}$ M; (▼, △), $C_L = 2 \cdot 10^{-2}$ M; (×, +), $C_L = 5 \cdot 10^{-2}$ M.

nitrogen atom of the amino-endgroup in lysine do not participate in the complex formation and remain protonated in the pH region 2.7–8.5. The second carboxylate group of glutamic acid or aspartic acid plays no part in the chelation, and can become protonated at lower pH values. The basicity of the carboxylate group is somewhat diminished in comparison to the uncomplexed state.

Brooks and Davidson[3] and Toropova and Azizov[7] have pointed out that the different behaviour of histidine can be explained by the assumption that complex formation takes place mainly through the nitrogen atom in the imidazole ring and the α-amino group. At lower pH values, the other nitrogen atom in the imidazole will become protonated. The values of the protonation constants show that the basicity of this nitrogen atom is hardly influenced by complex formation.

The very large value of $\beta_{ML_2H_2}$ for cysteine must be attributed to a different type of complex formation. Evidently the sulphhydryl group is the important group and complex formation takes place with a simultaneous abstraction of the proton. The protons in the ML_2H_2 complex are obviously the protons on the α-amino groups, which then play no role in the complex formation. This is in disagreement with the suggestion of Lenz and Martell[8], who claim that both the sulphur atom and the α-amino group participate in this complex formation. However, if both the sulphur atom and the α-amino group are bound to the same mercury ion, yielding

a terdentate ligand, the protons cannot be accommodated. In the proposed scheme, the α-amino group would remain available for complex formation of other mercury ions, leading to M_2L_2 and even M_3L_2 complexes, as found by Stricks and Kolthoff[4]. Such complexes were not detected in the present work because an excess of ligand was always present.

The strong protonation of methionine complexes is difficult to understand. If chelation takes place through the α-amino-carboxylate group protonation becomes impossible. A rather speculative explanation might be that in more acidic solutions, complex formation takes place with the sulphur atom. On increasing the pH the chelation is gradually taken over by the α-amino-carboxylate group leading to a normal value of β_{ML_2}.

The authors are grateful to Mr. J. Fraanje for doing most of the experimental work.

SUMMARY

The complex formation of mercury(II) with twenty of the most important amino acids has been investigated, and the corresponding stability constants are reported. Calculations are based on simultaneous pH and pM measurements of solutions containing the amino acid in excess with respect to mercury. It is shown that most amino acids form mononuclear monoligand complexes as well as mononuclear biligand complexes. A different behaviour is observed for histidine and methionine, for which the complexes become strongly protonated at lower pH values.

RÉSUMÉ

Une étude est effectuée sur la formation de complexes du mercure(II) avec vingt des plus importants acides aminés; on indique les constantes de stabilité correspondantes. Les calculs sont basés sur des mesures simultanées de pH et pM de solutions contenant l'acide aminé en excès, par rapport au mercure. On constate que la plupart des acides aminés forment des complexes mononucléaires, monoligand ou mononucléaire biligand. L'histidine et la méthionine se comportent différemment; les complexes deviennent fortement protonés à des pH plus bas.

ZUSAMMENFASSUNG

Die Komplexbildung zwischen Quecksilber(II) und zwanzig der wichtigsten Aminosäuren wurde untersucht; die korrespondierenden Bildungskonstanten wurden berechnet. Die Berechnungen beruhen auf gleichzeitigen pH- und pM-Messungen von Lösungen, die die Aminosäure im Überschuss enthalten im Vergleich zu Quecksilber. Es wurde gezeigt, dass die Aminosäuren in wässrigen Lösungen einkernige Komplexe bilden mit ein und zwei Aminosäure-Molekülen. Ein abweichendes Verhalten wurde beobachtet bei Histidin und Methionin, bei denen die Komplexe stark protoniert werden.

REFERENCES

1 L. G. Sillén and A. E. Martell, *Stability Constants of Metal-ion Complexes*, The Chemical Society, Spec. Publ. No. 17, London, 1964.
2 L. G. Sillén and A. E. Martell, *Stability Constants of Metal-ion Complexes, Suppl. No. 1*, The Chemical Society, Spec. Publ. No. 25, 1972.
3 Ph. Brooks and N. Davidson, *J. Amer. Chem. Soc.*, 82 (1960) 2118.
4 W. Stricks and I. M. Kolthoff, *J. Amer. Chem. Soc.*, 75 (1953) 5673.
5 D. J. Perkins, *Biochem. J.*, 51 (1952) 487.
6 D. J. Perkins, *Biochem. J.*, 55 (1953) 649.
7 V. F. Toropova and Yu. M. Azizov, *Russ. J. Inorg. Chem.*, 11 (1966) 288.
8 G. R. Lenz and A. E. Martell, *Biochemistry*, 3 (1964) 745.
9 A. Ringbom and L. Harju, *Anal. Chim. Acta*, 59 (1972) 33.

Analytica Chimica Acta, 68 (1974) 155–160

DIRECT POTENTIOMETRIC DETERMINATION OF CALCIUM IN WATERS WITH A CONSTANT COMPLEXATION BUFFER

ADAM HULANICKI and MAREK TROJANOWICZ

Institute of Fundamental Problems in Chemistry, University of Warsaw, Warsaw (Poland)

(Received 10th May 1973)

The potentiometric determination of calcium with ion-selective electrodes has attracted much attention, although several other techniques (*e.g.* flame emission or absorption spectrometry) offer convenient determinations of total calcium content. The main advantage of direct potentiometry is that it gives the activity of free calcium ions, which is of primary importance, for example, in biomedical research. Several attempts have been made to correlate the measurement to the total calcium content. Such procedures need relatively simple equipment and can be easily automated, which is important for routine analysis or constant on-line monitoring. The varying compositions of the samples encountered in natural products introduces difficulties, but procedures have been developed for analysis of sea water[1], tap water[2] or soil extracts[3].

The main difficulties of such determinations are the limited selectivity of the calcium electrode (which is influenced by other cations *e.g.* magnesium or sodium), the effect of variable ionic strength, and the presence of ions which may complex calcium, *e.g.* hydrogencarbonate and sulphate. The influence of all those parameters has been reported previously, but the practical problems of overcoming them in analysis of waters have not been solved.

The potential of the calcium-sensitive electrode in the normal working range is given by the equation:

$$E = E^0 + \frac{RT}{nF} \ln\left[\frac{f_{Ca^{2+}}}{\alpha_{Ca^{2+}}} c_{Ca^{2+}} + \Sigma K_i \left(\frac{f_i}{\alpha_i} c_i\right)^{2/n}\right] \quad (1)$$

where $c_{Ca^{2+}}$ and c_i are the total concentrations of calcium and interfering ion of charge n, respectively; $f_{Ca^{2+}}$ and f_i are the activity coefficients of the corresponding ions; $\alpha_{Ca^{2+}}$ and α_i are the side-reacton coefficients (reciprocal of mole fraction of free ions); and K_i is the selectivity coefficient of the i-ion.

The constancy of $f_{Ca^{2+}}$, $\alpha_{Ca^{2+}}$, E^0 and of the last term in eqn. (1) is the necessary condition to obtain meaningful results for total calcium content by means of a calibration curve. A search for conditions under which this is fulfilled, is described in this paper. A constant complexation buffer containing potassium nitrate, ammonia–ammonium chloride buffer, iminodiacetate and acetylacetone was found to give greatly improved results.

EXPERIMENTAL

Equipment

The Orion calcium-selective liquid ion-exchanger electrode (Orion 92-20) was

used with a saturated calomel electrode (Radiometer K 401). The potential was measured with a Radiometer pH meter pHM 26. The pH was checked with a Radelkis OP-206 pH meter.

Reagents

Ethyleneglycol-bis(β-aminoethylether)-N,N,N',N'-tetraacetic acid, tetramethylammonium salt [$(Me_4N)_4EGTA$]. A 0.01 *M* solution was prepared by dissolution of the free acid in tetramethylammonium hydroxide solution. The acid (Schuchardt) was purified by precipitation with hydrochloric acid from the salt solution in the presence of a small amount of nickel chloride. This solution, and a 0.01 *M* EDTA solution, were standardized against dried zinc oxide with Eriochrome Black T as indicator.

Calcium nitrate solution, 0.1 M. Solutions in water and in 0.2 *M* potassium nitrate were prepared and standardized potentiometrically with the silver electrode[4].

All reagents were of analytical grade. The water was double-distilled in quartz apparatus. All solutions were stored in polyethylene vessels.

Constant Complexation Buffer (CCB). 40.4 g of potassium nitrate, 3.6 g of disodium iminodiacetate, 160 ml of aqueous 0.5 *M* acetylacetone solution, 2 ml of 10 *M* ammonia and 1.07 g of ammonium chloride were dissolved in water and diluted to 1 l.

Preparation of calibration curve

Dilute 100 ml (or more) of CCB solution with distilled water in a beaker. Insert both electrodes, which have previously been well rinsed with this solution. Wait for a steady potential reading in the solution stirred magnetically. Then add calcium nitrate in appropriate increments and take the potential readings about 2 min after each addition. Plot the potential *versus* negative logarithm of calcium concentration expressing the concentration as molarity or in p.p.m.

Determination of calcium in water

Deaerate the samples by bubbling nitrogen through the solutions for 10–15 min at room temperature. Take 3–5 samples, each 50 ml, and dilute them (1 + 1) with the CCB solution. Insert the electrodes and measure the potential after 3 min in stirred solutions. Repeat the series of measurements with the same solutions, waiting 2 min for attainment of the steady potential value. This second series should be taken as the basis for the calcium determination. Between measurements neither rinse the calcium electrode nor dry it. All measurements should be taken at the same ($\pm 0.5°$) temperature.

RESULTS AND DISCUSSION

To establish the optimal experimental conditions, various parameters were investigated. In all series, the working curves were prepared by addition of standard calcium nitrate solution to distilled water or to solutions which contained the same amounts of reagents as were added to the analysed samples. The accuracy of all results was evaluated on the basis of titrimetric results with tetramethylammonium–EGTA as titrant with the calcium indicator electrode[5], and with Na_2EDTA as

titrant with calcon as visual indicator[6].

When the only preparation of the samples consisted of adjustment to pH 9 with tetramethylammonium hydroxide, the results were on average 25% low with a scatter of about 35%. This is undoubtedly the result of complexation of calcium in samples by hydrogencarbonate and sulphate, the former being present in varying amounts because of absorption of carbon dioxide during sample preparation and measurement.

To reduce those unfavourable effects several measurements were performed with the addition of ammonium buffer pH 9.0. Some improvement was also expected from the use of a solution for calibration which simulates the average composition of water (20 mg $Mg\,l^{-1}$, 60 mg $Na\,l^{-1}$, 60 mg $SO_4\,l^{-1}$, 80 mg $Cl\,l^{-1}$). In both cases, without and with addition of potassium nitrate for stabilization of ionic strength, the results were 35–45% high, with a large scatter. This large positive error and poor precision can be attributed to a variable and high α_{Ca} coefficient in the solution used for calibration. No improvement of results was obtained when the samples were acidified to pH 2 with hydrochloric acid before addition of buffer. Also without effect were experiments in which the preliminary treatment of the sample consisted of passing it through the anion-exchanger Amberlite IRA 400 (chloride form). Accidental errors in this procedure were the highest, approaching 40%.

A significant improvement was attained when an additional complexing agent was added; suitable complexing agents must be stronger in action than ligands present in samples, but not sufficiently strong to depress the free calcium ion activity to the vicinity of the limit of electrode sensitivity. A suitable effect was obtained with iminodiacetic acid at a total concentration of 10^{-2} *M*. The stability constant of the calcium complex[7] β is $10^{2.6}$; this causes an approximately three-fold decrease of the calcium activity, but a nearly Nernstian working curve was still obtained. In the presence of iminodiacetate an average error of only +6.5% was obtained in a series of 20 measurements, the largest scatter being 10%. Such results correspond to untreated samples, whereas the above-mentioned preliminary treatments increase the accuracy and precision. Some experimental results are given in Table I.

All results in the systems mentioned are sensitive to the presence of magnesium, which increases the results in varying degrees, which are not strictly related to the amount of interfering ion. This may be attributed at least partly to changes in the selectivity coefficient K_{MgCa} at various stages in the electrode life, so that it is necessary to decrease the final term of eqn. (1). The amounts of magnesium found in waters (5–50 mg l^{-1}) may cause positive errors up to several tens percent. To eliminate this effect, acetylacetone was added; acetylacetone complexes magnesium but has practically no effect on calcium[7]. The results in Table II indicate that even up to 100 mg of magnesium has no influence on the determination of calcium. The final composition of the Constant Complexation Buffer (CCB) selected is as follows: 0.4 *M* KNO_3, 0.02 *M* IDA, 0.04 *M* AcAc, 0.02 *M* NH_3, and 0.02 *M* NH_4Cl. This mixture gives pH 9.1 and an ionic strength of *ca.* 0.5. To all samples this CCB solution is added in a (1+1) ratio. The errors of the results usually do not exceed 4%, which can be considered sufficient for general experimental conditions, which potential deviations of ± 0.3 mV correspond to *ca.* 3 mg $Ca\,l^{-1}$.

TABLE I

DIFFERENT BUFFERING SOLUTION FOR DETERMINATION OF CALCIUM IN WATER

(Results are the average of two parallel determinations)

Sample composition ($mg\ l^{-1}$)	*Buffer components*	*Found Ca* ($mg\ l^{-1}$)	*Error* (%)
76.4 Ca	$KNO_3 + NH_3/NH_4Cl$	122.5	+60
72.0 Ca		92.6	+29
68.3 Ca		99.1	+45
94.4 Ca	KNO_3 + IDA	105.6	+12
91.3 Ca		98.4	+7.8
91.3 Ca, 24 Mg		105.7	+16
91.3 Ca, 48 Mg		111.6	+22
94.4 Ca, 48 Mg		110.5	+17
94.4 Ca, 96 Mg		118.4	+27
91.6 Ca	NH_3/NH_4Cl + IDA	109.4	+19
91.6 Ca, 48 Mg		120.8	+32
91.6 Ca, 96 Mg		139.2	+52
87.7 Ca	$KNO_3 + NH_3/NH_4Cl$	91.8	+4.7
76.4 Ca	+ IDA	83.6	+9.5
68.3 Ca		72.0	+5.4

TABLE II

DETERMINATION OF CALCIUM BY DIRECT POTENTIOMETRY IN THE PRESENCE OF CCB

Sample composition ($mg\ l^{-1}$)	*Ca content found* ($mg\ Ca\ l^{-1}$)		*Error* (%)	
94.4 Ca	98.4;	100.8	+4.2;	+6.8
74.3 Ca	73.8;	76.4	−0.7;	+2.8
	76.4;	76.4	+2.8;	+2.8
90.0 Ca	93.0;	93.0	+3.5;	+3.5
	94.0;	94.0	+4.5;	+4.5
94.7 Ca	94.0;	96.2	−0.7;	+1.6
	98.4;	98.4	+3.9;	+3.9
175.5 Ca	165.6;	165.6	−6.0;	−6.0
	Standard deviation $n=9$ $s=1.76$ mg		Average accuracy error +2.0	
94.7 Ca; 24 Mg	97.9;	97.9	+3.6;	+3.6
48 Mg	97.4;	97.4	+2.9;	+2.9
96 Mg	98.7;	96.4	+4.2;	+1.8
230 Na	95.7;	95.7	+1.1;	+1.1
300 Na_2SO_4	93.0;	90.9	−1.8;	−4.0

In the studied range—20–800 mg Ca l^{-1}, *i.e.*, $-\log[Ca^{2+}]=2$ to 3.6—the working curve is linear. However, it must be remembered that such promising results may be obtained only when sufficient attention is paid to details such as

constant depth of immersion of electrodes, constant stirring, constant temperature and good grounding and screening of electrical equipment.

This study was made as part of a cooperative project with the Institute of Water Economics, Warsaw (Instytut Gospodarki Wodnej), which financially supported this research.

SUMMARY

The effect of the composition of solutions in the direct potentiometric determination of total calcium content with an Orion calcium-selective electrode was investigated. In order to obtain accurate results for water samples, it is necessary to add ammonium buffer (0.02 *M*) to maintain constant pH, potassium nitrate (0.4 *M*) for constant ionic strength, iminodiacetic acid (0.02 *M*) for constant complexation of calcium, and acetylacetone (0.04 *M*) to mask magnesium. In the presence of the proposed Constant Complexation Buffer (CCB), the results are accurate to within a few percent in the range 20–800 mg Ca l^{-1}.

RÉSUMÉ

Une étude est effectuée sur l'influence de la composition des solutions, lors du dosage potentiométrique direct du calcium total, au moyen d'une électrode sélective calcium-Orion. Pour obtenir des résultats précis lors de l'analyse de l'eau, il est nécessaire d'ajouter: un tampon ammonium (0.02 *M*) pour maintenir le pH constant, du nitrate de potassium (0.4 *M*) pour une force ionique constante, de l'acide iminodiacétique (0.02 *M*) pour une complexation constante du calcium et de l'acétylacétone (0.04 *M*) pour masquer le magnésium. Les résultats sont alors précis, à quelques pour cent près, pour des concentrations allant de 20 à 800 mg Ca l^{-1}.

ZUSAMMENFASSUNG

Der Einfluss der Zusammensetzung von Lösungen bei der direkten potentiometrischen Bestimmung des Gesamt-Calcium-Gehaltes mittels einer calcium-selektiven Orion-Elektrode wurde untersucht. Um für Wasserproben genaue Ergebnisse zu erzielen, ist es notwendig, Ammoniumpuffer (0.02 *M*) für einen konstanten pH-Wert, Kaliumnitrat (0.4 *M*) für konstante Ionenstärke, Iminodiessigsäure (0.02 *M*) für konstante Komplexierung von Calcium und Acetylaceton (0.04 *M*) zur Maskierung von Magnesium hinzuzufügen. In Gegenwart des vorgeschlagenen konstanten Komplexierungs-Puffers waren die Ergebnisse im Bereich 20–800 mg Ca l^{-1} innerhalb weniger Prozent genau.

REFERENCES

1 M. E. Thompson and J. W. Ross, Jr., *Science*, 154 (1966) 1643.
2 J. B. Andelman, *J. Water Pollut. Control Fed.*, 40 (1968) 1844.
3 E. A. Woolson, J. H. Axley and P. C. Kearney, *Soil Sci.*, 109 (1970) 279.

4 W. Kemula, A. Hulanicki and M. Trojanowicz, *Chem. Anal. (Warsaw)*, 14 (1969) 481.
5 A. Hulanicki and M. Trojanowicz, *Chem. Anal. (Warsaw)*, 18 (1973) 235.
6 J. Gelo, *Przegl. Papier.*, 25 (1969) 109.
7 A. Ringbom, *Complexation in Analytical Chemistry*, Interscience, New York, 1963.

Analytica Chimica Acta, 68 (1973) 161–175

NOUVELLE METHODE DE DOSAGE AUTOMATIQUE DE SUBSTANCES OXYDANTES OU RÉDUCTRICES PAR POTENTIOMÉTRIE DIFFÉRENTIELLE

PARTIE II. MISE AU POINT MANUELLE DU DOSAGE DU LACTOSE*

J. O. BOSSET et B. BLANC

Station Fédérale de Recherches Laitières, CH-3097 Liebefeld-Berne (Switzerland)

E. PLATTNER

Institut de Génie Chimique, Ecole Polytechnique Fédérale, CH-1025 Lausanne (Switzerland)

(Reçu le 18 mai 1973)

Pour automatiser le dosage du lactose dans un lait entier frais, on dispose —généralement après certaines opérations préliminaires (déprotéinisation)—de plusieurs critères analytiques: réactions de coloration avec des produits de condensation (furfural et dérivés)[1] ou avec des enzymes spécifiques[2], indice de réfraction[3], pouvoir rotatoire[4], pouvoir réducteur, etc. Si l'on retient ce dernier critère, très classique du reste, il existe à nouveau un choix important de méthodes[5–7], mais dont quelques-unes seulement se prêtent à l'analyse automatique dite "à flux continu"[8]. Il faut en effet écarter toutes celles qui font appel à la volumétrie, à la gravimétrie ou à toute autre opération typiquement discontinue. Il reste un très important groupe, celui des déterminations photométriques (colorimétriques, spectrophotométriques, etc.)[9,10].

Quelle que soit la substance à doser, on constate de façon générale la suprématie de ce type de mesure dans l'analyse à flux continu. Si, pour le lactose, la colorimétrie fait montre d'indéniables qualités (réponse proportionnelle à la concentration dans le domaine de Lambert–Beer, relative précision, reproductibilité et simplicité de la méthode), elle présente également certains désavantages: les solutions doivent être limpides, l'équipement doit comporter un photomètre à compensation partielle ou totale (double faisceau), etc. D'autres critères analytiques encore peu exploités jusqu'ici semblent prometteurs, vu leur simplicité et le coût modique des appareils requis; tel est le cas de la potentiométrie différentielle.

Les bases théoriques de cette nouvelle méthode ont été élaborées précédemment[11] pour le cas tout à fait général du dosage d'un réducteur quelconque (r*; o*) par un oxydant dont le couple rédox (o; r) soit défini et réversible, où:

o = forme oxydée de l'oxydant r = forme réduite de l'oxydant	liqueur "titrante" ou réactif
o* = forme oxydée du réducteur r* = forme réduite du réducteur	liqueur "titrée"

* Extrait d'une thèse de doctorat prochainement publiée sous la direction des Prof. B. Blanc et E. Plattner.

Le dosage cérimétrique des glucides[12–15], particulièrement du lactose—vu la lenteur de la cinétique d'oxydoréduction—est un exemple d'application idéal de potentiométrie différentielle, puisqu'il n'est pas nécessaire d'attendre que la réaction soit terminée. Cette étude permet de vérifier également la validité de la théorie proposée[11].

On trouve dans la littérature un certain nombre de publications proposant de doser quantitativement les sucres par réduction du cérium(IV)[16–23], mais toujours par titration conventionnelle complète (point d'équivalence). Dans cette étude d'un dosage direct, on étudiera en discontinu les paramètres principaux déjà définis (concentration en réactif, temps et température de la réaction) dans l'optique d'une transposition directe à l'analyse automatique en flux continu (type "Auto-Analyzer®" de Technicon).

THÉORIE ET PRINCIPE DE LA MÉTHODE

Dans le lait de vache frais, on ne trouve pratiquement qu'un seul glucide, le lactose, un diholoside réducteur (4-0-*β*-*d*-galactopyranosyle-*d*-glucopyranose). Les autres glucides n'existant qu'en quantités minimes (*ca.* 2% de l'ensemble des sucres), il est possible d'utiliser pour le doser en grandes séries des méthodes qui ne lui sont pas forcément spécifiques. Sa grande solubilité dans l'eau (216 g l^{-1} à 25°) fait qu'il se trouve entièrement dissous dans le lait. Son faible poids moléculaire (360.3 sous forme monohydratée) et ses très faibles dimensions permettent de le séparer facilement et de plusieurs manières—notamment par dialyse—des autres composés principaux du lait (protéines) qui peuvent interférer lors de son dosage.

La méthode proposée est basée sur la mesure potentiométrique du "pouvoir réducteur" de ce glucide. Il en résulte qu'elle est applicable de manière générale à tous les autres glucides "réducteurs", mais ne peut les différencier. Par "pouvoir réducteur", il ne faut pas seulement considérer celui de leur fonction carbonyle, mais également celui de leurs fonctions hydroxyles, puisque l'oxydant choisi pour cette méthode, le sulfate cérique, est capable d'oxyder complétement la molécule en acide formique et en anhydride carbonique.

L'oxydation du lactose étant irréversible, il n'est pas possible de suivre son évolution par la mesure directe du potentiel d'oxydoréduction du couple fictif "lactose oxydé/lactose réduit". Par contre, dans un système formé de lactose (réducteur) et de cérium(IV) (oxydant), il est aisé de suivre l'évolution de cette oxydation en déterminant la variation de la concentration de l'oxydant engagé, par la mesure au cours du temps du potentiel rédox du couple réversible Ce^{4+}/Ce^{3+}. La réaction globale d'oxydoréduction de ce système est vraisemblablement la suivante[24]:

$$C_{12}H_{22}O_{11} + 13\ H_2O - 26\ e^- \rightarrow 11\ HCOOH + CO_2 + 26\ H^+ \quad (1)$$

$$26\ Ce^{4+} + 26\ e^- \rightarrow 26\ Ce^{3+} \quad (2)$$

L'oxydation globale définie par l'éqn. (1) ne peut se réaliser en une seule étape, mais est l'aboutissement d'une importante chaîne d'oxydations partielles. Il est éventuellement possible d'en imaginer quelques-unes par analogie avec ce que l'on trouve dans la littérature pour d'autres oxydants[25]. Si l'on considère le cas du glucose, en tant que sous-unité de structure du lactose, on a pu identifier les réactions "ménagées" suivantes: avec l'eau de brome à température ordinaire, on

obtient un monoacide aldonique, l'acide *d*-gluconique; avec l'acide nitrique ($d = 1.31$) à froid, un monoacide cétoaldonique, l'acide céto-5-*d*-gluconique; avec le même acide ($d = 1.2$) à chaud, un diacide, l'acide *d*-saccharique, etc.

En outre, d'autres facteurs jouent un rôle important dans ce processus d'oxydoréduction, notamment le pH. Si H^+ n'apparaît pas dans le couple rédox Ce^{4+}/Ce^{3+}, il intervient par contre de façon extrêmement complexe dans le mécanisme même de l'oxydation du lactose, ce qu'indique déjà l'éqn. (1). Une publication traitant la cinétique d'une oxydation pourtant beaucoup plus simple, celle de l'acétone par le sulfacte cérique en milieu sulfurique[26], ne mentionne pas moins de 6 étapes dépendant du pH. Ce dernier influence encore les nombreux équilibres et produits de solubilité des divers composés engagés ou formés.

En l'absence même de tout agent oxydant, le lactose donne lieu à toute une série de réactions en milieu acide, surtout à chaud[27]. D'abord, il est hydrolysé en deux monoholosides, le *d*-glucose et le *d*-galactose. A leur tour, ces hexoses se transforment en 5-hydroxyméthylfurfurol. Une exposition plus longue aux acides chauds conduit ensuite à la formation d'acides lévulique et formique, ou à la formation de produits de condensation insolubles de couleurs sombres, connus sous le nom d'acides humiques.

Puisque la réaction globale fait appel à une chaîne d'oxydations partielles consécutives, on en déduit que le nombre d'équivalents de réducteur, ψ, que fournit une mole de lactose varie continuellement pendant le temps de réaction et doit s'écrire:

$$\Delta r^{*\,i}_{\ j} = \Delta(\psi[\text{ose}])^i_j \qquad (3)$$

où $\Delta r^{*\,i}_{\ j}$ est la consommation de la forme réduite du réducteur pendant le laps de temps considéré (instant *i*–instant *j*).

Si la réaction est complète selon l'éqn. (1), $\psi = 26$.

MODE OPÉRATOIRE ET APPAREILLAGE

Le mode opératoire consiste à injecter rapidement au temps *i* (choisi comme origine du temps) un volume donné d'une solution de lactose de concentration connue $[\text{ose}]_i$ dans un volume donné d'un mélange de sulfates cérique et céreux de concentrations initiales $[Ce^{4+}]_i$ et $[Ce^{3+}]_i$, dissous dans l'acide sulfurique 0.5 *M* (dans tous les essais qui suivent, la concentration en sulfate céreux, à l'origine, est donnée par la teneur usuelle ou "impureté" du réactif pro analysi utilisé). La Figure 1 indique comment évolue le potentiel d'oxydoréduction $E_{\text{rédox}}$ de ce couple en fonction du temps de réaction *t* (*j* est un point quelconque où est supposée se situer la seconde électrode de mesure dans un système en flux continu). Si la réaction est terminée, $j \equiv f$.

Les essais ont été réalisés au moyen d'un équipement Metrohm: un potentiographe E 436, équipé d'un réducteur de vitesse d'enregistrement US-320-18, et d'une cellule EA 880 T-20 ml, montée sur l'agitateur magnétique correspondant et couplée à un thermostat à circulation Lauda WB20D. Le $\Delta E_{\text{rédox}} = E_{\text{rédox}} - E_{\text{réf}}$ est mesuré par une électrode combinée (Pt–Ag/AgCl) EA 217, supportant des températures supérieures à 60°, sous atmosphère inerte (N_2) injectée par un barboteur EA 649. La température est contrôlée par un thermomètre EA 623.

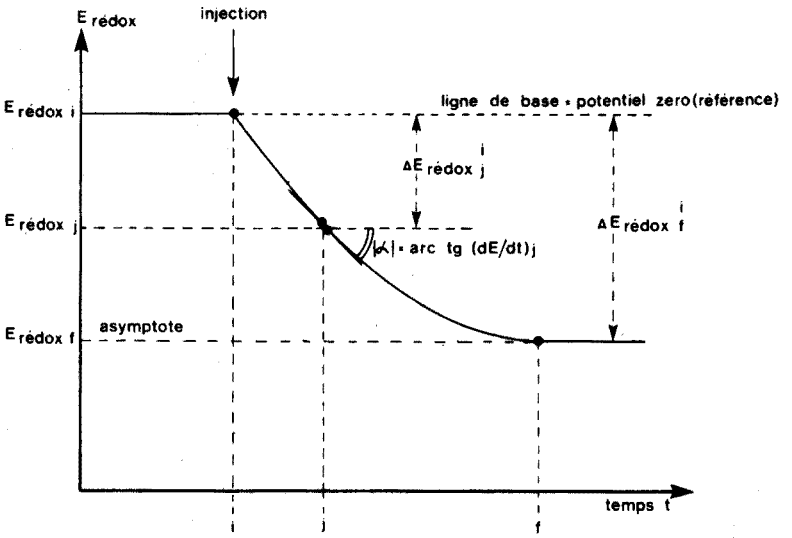

Fig. 1. Evolution du potentiel d'oxydoréduction $E_{\text{rédox}}$ du couple Ce^{4+}/Ce^{3+} en fonction du temps de réaction t avec le lactose.

Afin d'éviter toute interférence éventuelle due à quelque autre substance réductrice, la mise au point de cette méthode a été opérée avec des solutions aqueuses ne contenant que du lactose.

Produits utilisés étaient lactose (monohydraté, LAB de Merck, art. 7660), sulfate cérique (tétrahydraté, p.A. de Merck, Art. 2274), et acide sulfurique (p.A. de Merck, Art. 731) dilué à 0.5 *M*.

RÉSULTATS EXPÉRIMENTAUX ET INTERPRÉTATION

Détermination du rapport Ce^{3+}/Ce^{4+} pour le réactif utilisé

La teneur en "impureté" (forme réduite de l'oxydant), définie comme le rapport $K = r_i/o_i = [Ce^{3+}]_i/[Ce^{4+}]_i$ du réactif utilisé, a été déterminée par la mesure du potentiel rédox (relation de Nernst) du réactif seul:

$$E_{\text{rédox}\,i} = E_{0\,\text{rédox}} + (RT/F)\ln(o_i/r_i) = E_{0\,\text{rédox}} - (RT/F)\cdot\ln K \qquad (4)$$

Une mesure supplémentaire, avec la même électrode combinée, effectuée dans une solution équimolaire en forme oxydée et réduite ($o_i = r_i$), permet d'éliminer par différence le potentiel rédox normal E_0 et le potentiel de référence $E_{réf}$. La différence de potentiel existant entre ces deux mesures devient alors:

$$\Delta E = (RT/F)\ln(o_i/r_i) = 59.2\cdot\log_{10}([Ce^{4+}]_i/[Ce^{3+}]_i) = 126.5\ (\text{mV}) \qquad (5)$$

(Calcul effectué pour $T = 25°$; moyenne de 9 mesures; valeurs extrêmes obtenues: $121\ (\text{mV}) < \Delta E < 132\ (\text{mV})$.)

Il est alors possible de déduire la valeur de K:

$$K = [Ce^{3+}]_i/[Ce^{4+}]_i = -\text{antilog}_{10}(126.5/59.2) = 7.3\cdot 10^{-3} \qquad (6)$$

(valeurs extrêmes: $6\cdot 10^{-3} < K < 9\cdot 10^{-3}$)

Influence de la concentration du réactif et du temps de réaction

La vérification expérimentale du développement théorique mentionné[11] a été effectuée comme suit: à une température fixée à 85°, on injecte 1 ml d'une solution de lactose à 5 g l^{-1}, soit 14 méq l^{-1} si l'on considère l'oxydation comme complète pour $\psi = 26$, dans 25 ml de solution sulfurique (0.5 *M*) de Ce^{4+} dont la concentration est échelonnée pour les différents essais entre $4 \cdot 10^{-2}$ et $5 \cdot 10^{+2}$ mmol l^{-1} (ou méq l^{-1}).

Le potentiographe est réglé comme suit: compensation = 1200 mV; zéro électrique = flottant; expansion d'échelle = 1 mV mm^{-1}; vitesse d'enregistrement = 5 (*ca.* 16.5 mm min^{-1}). Les graphes des Figs. 2 et 3 montrent l'évolution du potentiel rédox $E_{rédox}$ en fonction:

du temps de réaction pour diverses concentrations en $[Ce^{4+}]_i$ (Fig. 2);

de la concentration en oxydant engagé $[Ce^{4+}]_i$ pour différents temps de mesure *j* (Fig. 3).

Puisque c'est la mesure différentielle $\Delta E_{rédox}{}_j^i$ que l'on recherche, on admettra arbitrairement, pour chacun des graphes, que $E_{rédox\,i} \equiv 0$ (translations du système d'axes). Le tracé de l'enregistreur correspondant à cette dernière valeur de $E_{rédox}$ définit la "ligne de base" du graphe.

Comme l'indiqué dans l'étude théorique[11], l'étude de la concentration du réactif se ramène à l'étude du quotient:

$$Q = o_i/\Delta r^*{}_j^i = [Ce^{4+}]_i/\Delta(\psi[ose])_j^i$$

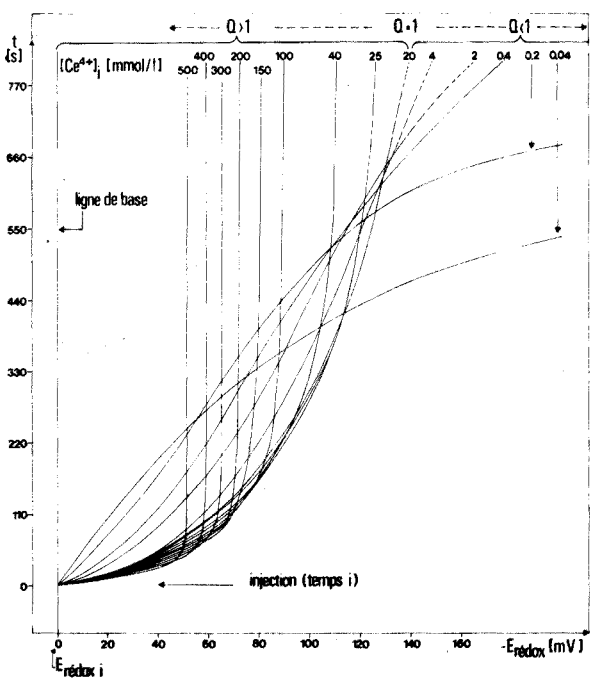

Fig. 2. Influence du temps de réaction *t* sur le potentiel $E_{rédox}$ pour diverses concentrations initiales de l'oxydant $[Ce^{4+}]_i$ (85°).

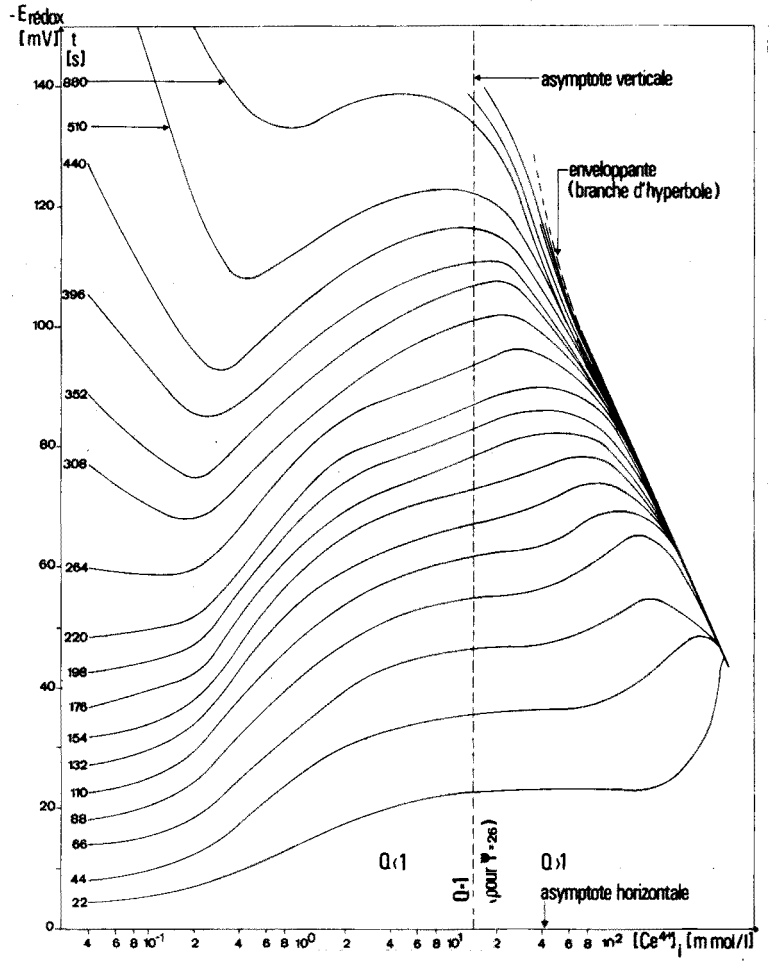

Fig. 3. Influence de la concentration initiale de l'oxydant $[Ce^{4+}]_i$ sur le potentiel $E_{rédox}$ pour différents temps de réaction t (85°).

c'est à dire du rapport entre l'oxydant engagé et la consommation du réducteur entre les instants i et j. Pour simplifier la discussion, on utilisera par la suite le terme de "réactif" pour désigner l'oxydant (Ce^{4+}) avec sa teneur en "impureté" (Ce^{3+}).

La forme générale des divers graphes de la Fig. 2 amène à la conclusion suivante, en accord avec la théorie.

Lorsque $Q > 1$, les graphes de $E_{rédox}$ en fonction du temps—après un tracé initial décrivant un point anguleux au moment de l'injection du lactose—s'infléchissent progressivement en tendant asymptotiquement vers l'équilibre (f). Ce dernier est atteint d'autant plus rapidement (*cf.* les pentes des tangentes peu après l'injection $[dE/dt]_j$) et avec un $\Delta E_{rédox\,j}^{\,i}$ d'autant plus petit que Q est grand.

Lorsque $Q < 1$, ces mêmes graphes présentent des formes totalement différentes. Si le début de la courbe peut rappeler celui obtenu pour $Q > 1$, à concavité tournée vers les potentiels positifs croissants (excès momentané, apparent), ces

graphes passent ensuite par un point d'inflexion, leur concavité étant tournée—en fin de réaction—du côté opposé. La dérive de $E_{\text{rédox}}$ vers les potentiels négatifs est d'autant plus grande et plus rapide que $Q \to 0$. Il n'y a plus de stabilisation possible, le couple Ce^{4+}/Ce^{3+} n'étant plus défini.

Lorsque $Q = 1$, le graphe présente une allure intermédiaire. Ce qui a été vu pour l'un et l'autre cas précédents doit encore être vrai "à la limite" (excès ou défaut de réactif tendant vers un). Il faudrait théoriquement un temps infini pour atteindre l'équilibre ($f = \infty$).

En conclusion, il est nécessaire de travailler avec $Q > 1$, afin que $E_{\text{rédox}}$ soit contrôlé par le couple Ce^{4+}/Ce^{3+}; cet excès ne doit cependant pas être trop gros pour éviter une inutile perte de sensibilité de la méthode, $\Delta E_{\text{rédox}}{}^{i}_{f} \to 0$ lorsque $[Ce^{4+}]_i \to \infty$. En ce qui concerne le temps de réaction, il faut le choisir aussi grand que possible, $\Delta E_{\text{rédox}}{}^{i}_{j}$ croissant lorsque $j \to f$.

La forme générale des divers graphes de la Fig. 3, montrant l'évolution de $E_{\text{rédox}}$ en fonction de $[Ce^{4+}]_i$ engagé, à divers instants de la réaction (courbes isochrones), permet de confirmer et compléter les informations précédentes.

Lorsque $j \to f$, le faisceau des courbes isochrones tend vers une courbe limite, son enveloppante. Ce lieu géométrique des $E_{\text{rédox}\,f}$ ou $\Delta E_{\text{rédox}}{}^{i}_{f}$ n'est autre que l'une des branches de l'hyperbole définie par la relation théorique[11]:

$$\Delta E_{\text{rédox}}{}^{i}_{f} = \frac{RT}{F} \cdot \ln \frac{KQ+1}{KQ-\mathrm{K}} \tag{8}$$

L'autre branche de l'hyperbole n'a pas de signification physique. L'asymptote verticale correspond à $Q = 1$, l'asymptote horizontale, à $Q = \infty$.

Chaque courbe isochrone montre un maximum et un minimum, dus à la compétition de deux effets opposés. Pour le maximum, il s'agit de la compétition existant entre la vitesse de réaction (d'autant plus grande que $Q \to \infty$) et la sensibilité ou $\Delta E_{\text{rédox}}{}^{i}_{j}$ (d'autant plus faible que $Q \to \infty$). Pour le minimum, il s'agit de celle existant entre la vitesse de réaction (idem) et la vitesse de disparition du Ce^{4+} (d'autant plus grande que $Q \to 0$). Tous les minima se situent donc en dessous de la stoechiométrie ($Q = 1$). Lorsque $j \to f$, le lieu géométrique des minima et celui des maxima converge vers le point à l'infini de l'asymptote verticale que définit la réaction stoechiométrique ($\Delta E_{\text{rédox}}{}^{i}_{j} \to \infty$ quand $j \to f = \infty$).

Dans un certain domaine de concentration en $[Ce^{4+}]_i$ ($Q > 1$), on remarque que $E_{\text{rédox}\,f}$ (ou $\Delta E_{\text{rédox}}{}^{i}_{f}$) est inversément proportionnel, à une constante additive près, au logarithme de la concentration du réactif pour une quantité donnée de lactose. Inversément, pour des concentrations initiales en Ce^{4+} et Ce^{3+} constantes, le $\Delta E_{\text{rédox}}{}^{i}_{f}$ sera proportionnel à une constante additive près, à $\ln(\psi[\text{ose}])$. Ce point sera repris plus loin. Ainsi se trouve confirmée la relation établie au cours de l'étude théorique[11]:

$$\Delta E_{\text{rédox}}{}^{i}_{j} = K^{\text{II}} \ln \Delta r^{*}{}^{i}_{j} + K^{\text{III}} \tag{9}$$

Pour $[Ce^{4+}]_i > 50$ mmol l^{-1}, il faut néanmoins signaler, après un certain temps de réaction, la formation d'un précipité jaune, ce qui indique que l'un des produits de solubilité a été dépassé; cela peut expliquer la différence existant entre les $\Delta E_{\text{rédox}}{}^{i}_{j}$ mesurés et ceux que l'on trouve par le calcul.

Au-dessous d'une certaine valeur de Q, l'approximation proposée (identification de l'hyperbole à une droite sur un certain segment) n'est plus possible, l'écart existant entre la valeur exacte et la valeur approchée devenant trop important. C'est le "seuil supérieur de linéarité" (trop de lactose engagé pour l'oxydant présent).

N.B. La fonction $E_{\text{rédox}} = f(t)$ est monotone décroissante, toujours négative, puisqu'il s'agit d'une réduction de Ce^{4+}, dont le potentiel de référence est celui du réactif initial, identiquement nul par définition ($E_{\text{rédox}\,i} \equiv 0$).

Influence de la température

Sur la base de l'essai précédent, l'influence de la température T a été étudiée de la manière suivante: 1 ml d'une solution de lactose à 5 g l^{-1} (0.5%) est injecté dans 25 ml d'une solution 20 mmol l^{-1} de sulfate cérique en milieu sulfurique 0.5 *M*. L'essai est répété à diverses températures comprises entre 20° et 90°. Le potentiographe est réglé comme précédemment. Les résultats obtenus sont présentés par les graphes de la Fig. 4.

En convenant à nouveau de considérer chaque ligne de base comme potentiel de référence, c'est à dire chaque $E_{\text{rédox}\,i} \equiv 0$, quel que soit son potentiel absolu, on

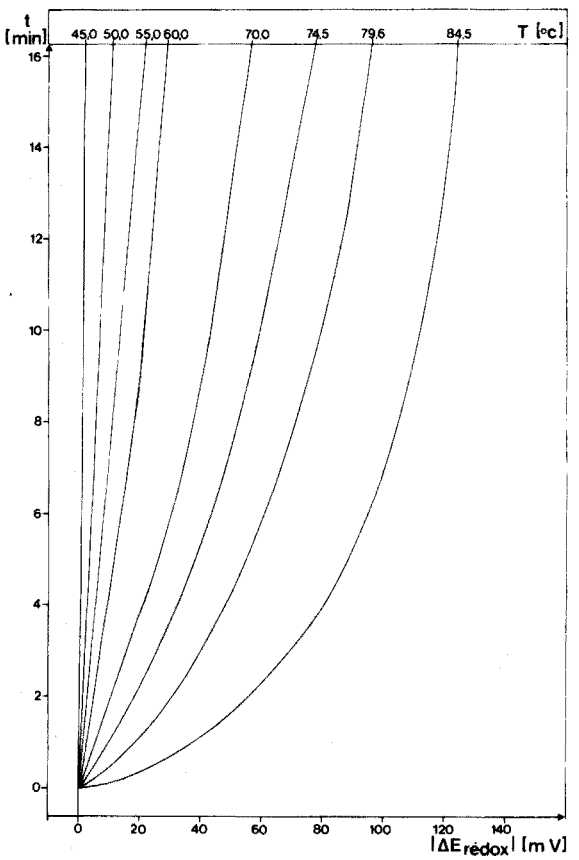

Fig. 4. Influence du temps de réaction t sur $\Delta E_{\text{rédox}}$ pour différentes températures T ($[Ce^{4+}]_i = 20$ mmol l^{-1}).

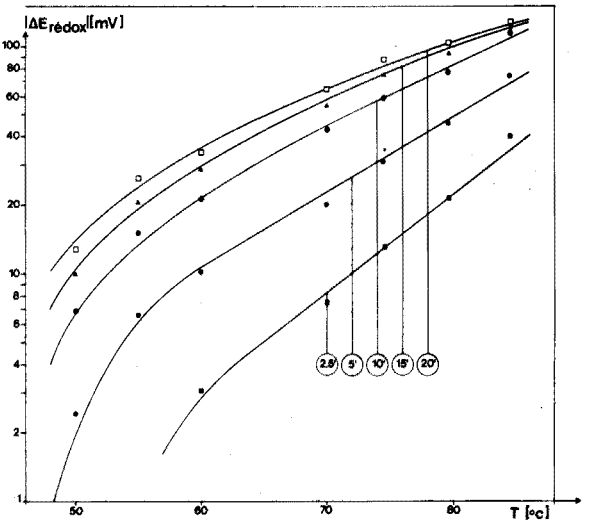

Fig. 5. Influence de la température de réaction T sur la différence de potentiel $\Delta E_{\text{rédox}}$ mesurée entre le début de la réaction et l'instant j (à savoir: $t = 2.5$, 5, 10, 15 et 20 min).

remarque que la température augmente considérablement le signal $|\Delta E_{\text{rédox}}{}^{i}_{j}|$ ou $|E_{\text{rédox}\,j}|$ obtenu, ce que prévoyait la théorie. Au-dessous de 40°, la réaction n'a pratiquement pas lieu. Au-dessus de 55° environ, $E_{\text{rédox}}$ varie à peu près exponentiellement avec la température, comme le montre la Fig. 5 (énergie d'activation minimale pour que la première réaction rédox au moins puisse se produire).

Essai d'application: courbe d'étalonnage

Sur la base des données acquises, un essai d'application a été effectué sous la forme d'une courbe d'étalonnage: à 25 ml d'une solution de sulfate cérique en milieu sulfurique 0.5 M, on ajoute rapidement 1 ml d'une solution de lactose dont la concentration varie, pour les divers essais, de 10^{-1} à 10^{1} g l^{-1}. Les conditions expérimentales retenues sont: $T = 85°$; $[Ce^{4+}]_i = 20$ mmol l^{-1}; $K = 7.3 \cdot 10^{-3}$; $[Ce^{4+}]_i \cong 0.15$ mmol l^{-1}. Le potentiographe est réglé comme avant, sauf pour la vitesse d'enregistrement qui est un peu plus rapide (voir Fig. 6a). Les résultats obtenus pour les temps $j = 45$, 90, 135 et 180 s (t_f non atteint) sont représentés par les graphes de la Fig. 6b.

Reprenant ces valeurs, le Tableau I analyse dans quel domaine de concentration en lactose et dans quelle mesure (coefficient de corrélation) la relation (9) est vérifiée par l'expérience.

L'expérience confirme la proportionnalité existant dans un certain domaine de concentration, entre la différence des potentiels rédox de la solution à deux instants donnés de la même réaction et le logarithme de la teneur en réducteur (lactose) de l'échantillon. Comme prévu théoriquement, il existe aussi pour des concentrations données en Ce^{4+} et en Ce^{3+}, un "seuil inférieur de linéarité" (trop peu de lactose engagé pour le réactif présent), au-dessous duquel l'approximation proposée n'est plus valable.

On constate en effet que lorsque $[ose] \to 0$, c'est à dire que $\ln[ose] \to -\infty$,

$|\Delta E_{\text{rédox}}| \to 0$ (asymptote horizontale) et non vers $-\infty$, ce qui serait le cas si la proportionnalité n'était pas bornée inférieurement (*cf.* Fig. 6b).

En ce qui concerne la double inégalité:

$$r_i \ll \Delta r^{*i}_j \ll o_i \text{ (réf. 1), c'est à dire } [Ce^{3+}]_i \ll \Delta(\psi[\text{ose}])^i_j \ll [Ce^{4+}]_i \qquad (10)$$

il est extrêmement difficile de déterminer dans quelle mesure cette dernière est respectée, le coefficient ψ étant inconnu ($\psi < 26$, puisque f n'est pas atteint).

TABLEAU 1

VÉRIFICATION DE LA VALIDITÉ DE LA RELATION APPROCHÉE[a]:

$\Delta E_{\text{rédox}}{}^i_j = K^{II} \ln \Delta r^{*i}_j + K^{III}$

Domaine de concentration en lactose considéré		*Valeur de j (s)*	*Droite de régression*			
(g l^{-1})[b]	*(mmol l^{-1})*[c]		K^{II}	K^{III}	R[d]	N[e]
2.0[f]–10.0	0.21–1.07	45	18.30	−33.49	0.99322	10
1.5[f]–10.0	0.16–1.07	90	23.09	−34.03	0.99745	11
1.0[f]–10.0	0.11–1.07	135	25.43	−30.07	0.99871	12
0.5[f]–10.0	0.05–1.07	180	26.16	−22.05	0.99837	13

[a] Conditions: $T = 85°$; $[Ce^{4+}]_i = 20$ mmol l^{-1}; $[Ce^{3+}]_i = 0.15$ mmol l^{-1}.
[b] Concentration de la solution de lactose *injectée*, exprimée en g l^{-1} (sans tenir compte du volume du réactif).
[c] Concentration de la solution *finale* en lactose, exprimée en mmol l^{-1} (en tenant compte du volume total, mais pas du coefficient ψ).
[d] R = coefficient de corrélation.
[e] N = nombre de points considérés dans le calcul (population statistique).
[f] Seuil inférieur du domaine de proportionnalité étudié.

Le Tableau 1 et la Fig. 6 confirment numériquement ce que les essais antérieurs ont déjà indiqué, notamment qu'il est intéressant d'attendre que la réaction soit aussi complète que possible, puisque lorsque $j \to f$, on observe:

un accroissement de la sensibilité analytique (les pentes K^{II} des droites de régression croissent avec le temps);

un abaissement du "seuil inférieur de linéarité", c'est à dire de la concentration minimum nécessaire en lactose, sans pour autant diminuer la qualité de cette proportionnalité (le coefficient de corrélation R tend vers 1 avec le temps). La raison en est vraisemblablement la suivante: puisque le coefficient ψ augmente avec le temps, la grandeur $\Delta(\psi[\text{ose}])^i_j$ croît pendant la réaction; la première inégalité de la relation (10) ($r_i \ll \Delta r^{*i}_j$) n'en est que mieux respectée;

une diminution de l'erreur relative entachant la mesure de $\Delta E_{\text{rédox}}{}^i_j$ pour une valeur de j donnée, les diverses courbes tendant asymptotiquement vers leur valeur définitive.

Spécificité de la méthode

Toutes les substances capables de réduire le cérium(IV) dans les conditions

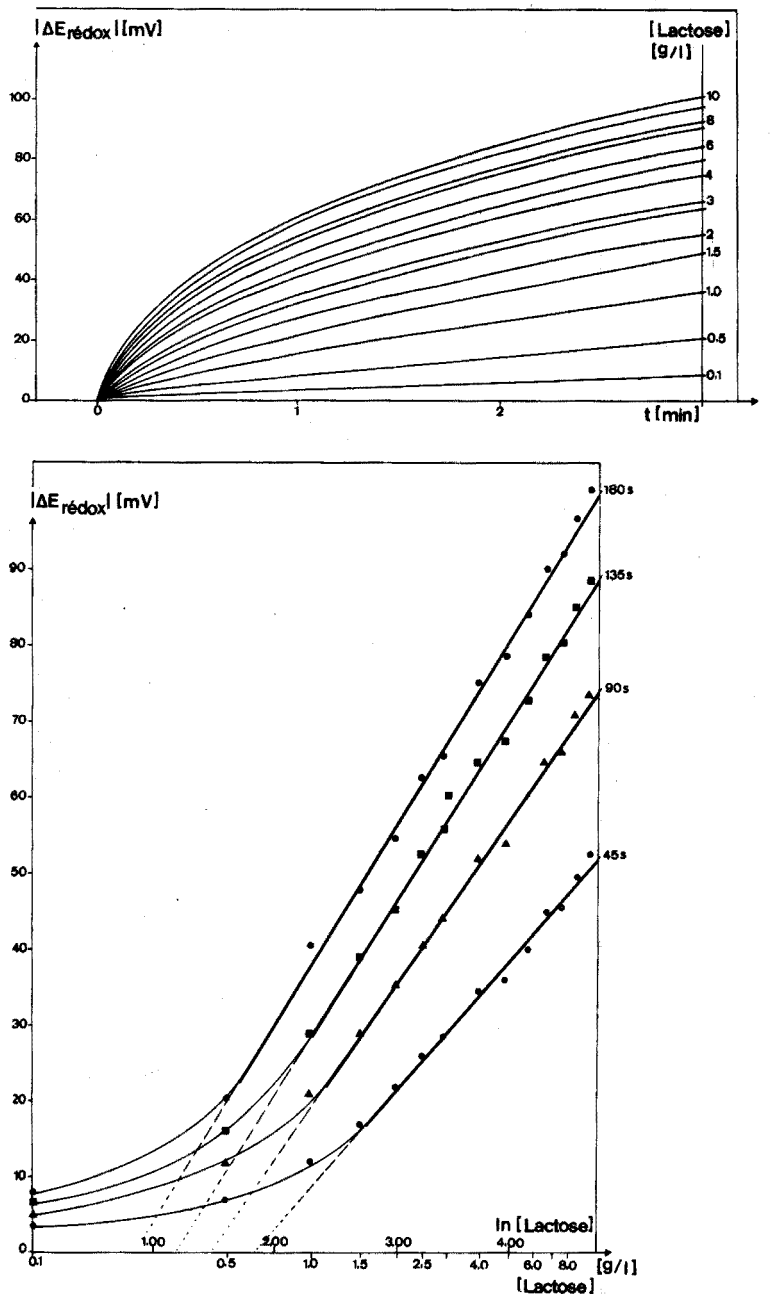

Fig. 6 (a) et (b). Variation de $\Delta E_{rédox}$ en fonction du temps de réaction et de la concentration en lactose.

choisies vont réagir. La méthode n'est donc pas spécifique et nécessite l'élimination préliminaire de ces dernières. Dans le lait, seules les protéines gênent effectivement le dosage du lactose par cette méthode, puisque leurs fonctions –SH, –S–S– et –OH

principalement réagissent. Les essais préliminaires ont montré qu'il s'agit surtout des restes cystyles, cystéyles, méthionyles, hydroxyprolyles, séryles, thréonyles et tyrosyles. Dans un analyseur à flux continu, on peut les éliminer par une simple dialyse. La matière grasse du lait devrait aussi intervenir, mais les réactions obtenues sont peu caractéristiques (lentes et faibles)[16].

Pour être rigoureux, il faut encore mentionner les réactions rédox qui peuvent se produire avec les halogénures, les vitamines C et E, etc. Mais la concentration de ces éléments mineurs dans le lait de vache est suffisamment faible comparativement à celle du lactose pour qu'on puisse la négliger ou la considérer comme constante quant à son effet sur le $\Delta E_{\text{rédox}}$.

Conclusion

La potentiométrie différentielle s'avère être une méthode intéressante pour la détermination quantitative du lactose. Le modèle mathématique proposé dans l'étude théorique[11] semble être entièrement vérifié par l'expérience, bien que la valeur du coefficient ψ ne soit qu'imparfaitement connue en raison de son évolution constante au cours de la réaction. Le $\Delta E_{\text{rédox}}{}^{i}_{j}$, mesuré entre deux *instants* donnés dans la méthode manuelle, sera mesuré entre deux *points* donnés du système automatique à flux continu. Les essais de mise au point de la méthode, réalisés sur des solutions ne contenant que du lactose, permettent de fixer la valeur des principaux paramètres définis:

$K = r_i/o_i = [Ce^{3+}]_i/[Ce^{4+}]_i$: aussi faible que possible, non nulle: la valeur de K du produit utilisé est suffisante ($K = 0.007$);

T = température de la réaction: aussi élevée que possible (85° à 95° pour des raisons pratiques);

Δt = intervalle de temps entre les mesures initiale et finale ou temps de réaction: aussi grand que possible, même si la cinétique décroît avec t (5–10 min);

$Q = o_i/\Delta r^{*i}_{j} = [Ce^{4+}]_i/\Delta(\psi[\text{lactose}]^{i}_{j} > 1$: un accroissement de Q augmente la cinétique, mais diminue la sensibilité. Comme l'indique le développement théorique[11], la qualité de l'approximation proposée (courbe hyperbolique ≅ courbe linéaire sur un certain segment) est également fonction de Q; Q est encore limité par les produits de solubilité des divers constituants présents.

Les essais complémentaires ont montré que les protéines réagissent également; il est donc nécessaire de les éliminer au préalable: manuellement, par une déprotéinisation classique à l'acide trichloroacétique, ou en flux continu, par une dialyse.

Remarques. La mise au point de cette nouvelle méthode a été réalisée au moyen d'un potentiographe pour des raisons de commodité; il n'est pourtant pas nécessaire de posséder un instrument de cette classe: n'importe quel bon pH-mètre ou potentiomètre couplé à un enregistreur suffit.

Destinée à être automatisée, cette méthode n'a pas fait l'objet de tests statistiques particuliers au niveau de l'expérimentation manuelle. Un essai de reproductibilité a néanmoins montré que sur 11 déterminations d'un même échantillon, seules les deux premières s'écartent de plus de $\pm 2\%$ relatifs de la valeur moyenne. On peut en conclure que la méthode est très reproductible, mais que le mode d'injection de l'échantillon joue un rôle capital.

Le cérium(IV) étant jaune et le cérium(III), incolore[28], on pourrait utiliser

la même réaction d'oxydoréduction pour doser le lactose par une colorimétrie classique en flux continu.

Le choix de l'oxydant à engager est dicté par plusieurs raisons, dont les principales sont la réversibilité (forme oxydée⇄forme réduite), le pouvoir oxydant ($E_{0\,\text{rédox}}$ élevé), la stabilité (non volatil et stable à l'air), la solubilité et la pureté (K). Le cérium présente en outre l'avantage de n'avoir que deux degrés d'oxydation (sous forme ionique) bien définis[28].

Autres possibilités d'utilisation de la méthode

Le champ d'application de cette nouvelle méthode ne paraît pas se limiter à la seule détermination quantitative du lactose. En supprimant la dialyse prévue pour l'analyse en flux continu et choisissant une température de réaction un peu moins élevée pour empêcher tout à fait la matière grasse de réagir, on peut garder la même méthode pour doser directement la teneur en solides non gras ("non-fat-solids") du lait entier frais, comme l'indiquent certains travaux analogues[29,30], mais recourant aux titrations manuelles conventionnelles.

Dans un domaine voisin, celui de la chimie clinique, la méthode proposée devrait également permettre le dosage automatique des glucides (réducteurs) du sérum sanguin, en adoptant d'autres concentrations.

RÉSUMÉ

Le présent travail propose une nouvelle méthode de dosage cérimétrique du lactose dans le lait entier frais. Dans des conditions de réaction bien définies et reproductibles, on considère les rapports de concentrations Ce(IV)/Ce(III) à deux instants donnés de la même réaction d'oxydoréduction. L'expérience montre que, dans un certain domaine de concentration, la différence des potentiels de Nernst correspondants est proportionnelle, à une constante additive près, au logarithme de la concentration en lactose présent. Les divers paramètres caractérisant cette réaction (température, temps, pH, rapport des concentrations) sont étudiés systématiquement dans le but de les optimiser. Les résultats expérimentaux obtenus confirment le modèle théorique général proposé antérieurement pour les dosages par potentiométrie différentielle. Après dialyse en flux continu, la méthode est applicable directement à l'analyse automatique en flux continu.

SUMMARY

A new cerimetric method is proposed for the determination of lactose in whole fresh milk. Under well defined and reproducible reaction conditions, the Ce(IV)/Ce(III) concentration ratio is considered at two given instants of the same redox reaction. In a given concentration range, the difference in the corresponding Nernst potential is proportional (plus a fixed constant) to the logarithm of the lactose concentration. The various parameters characterising the reaction (temperature, time, pH, concentration ratio) are systematically studied in order to establish optimal conditions. The experimental results obtained confirm the general theoretical model proposed earlier for measurement of substances by differential potentiometry.

After dialysis in continuous flow, the method is directly applicable to automatic continuous flow analysis.

ZUSAMMENFASSUNG

Es wird eine neue cerimetrische Methode zur quantitativen Lactosebestimmung in frischer Vollmilch beschrieben. Das Prinzip der Methode beruht auf der Ermittlung des Ce(IV)/Ce(III)-Konzentrationsverhältnisses an zwei bestimmten Punkten der Redoxreaktion, die unter genau definierten und reproduzierbaren Bedingungen abläuft. Die durchgeführten Versuche haben gezeigt, dass die Differenz der zwei entsprechenden Nernstpotentiale in einem gewissen Konzentrationsbereich bis auf eine zu addierende Konstante, dem Logarithmus der Lactosekonzentration procortional ist. Die Reaktionsparameter (Temperatur, Zeit, pH, Konzentrationsverhältnisse) wurden im Hinblick auf die Ermittlung optimaler Bedingungen systematisch untersucht. Die experimentellen Ergebnisse bestätigen unsere früher vorgeschlagen theoretischen Modellvorstellungen über die Reaktionsabläufe bei der Differential-Potentiometrie. Die beschriebene Methode kann, wenn ein kontinuierlich arbeitendes Dialyse-System vorgeschaltet wird, direkt für Durchfluss-Analysenautomaten verwendet werden.

BIBLIOGRAPHIE

1 A. J. Lawrence, *Aust. J. Dairy Technol.*, 23 (2) (1968) 103.
2 G. Kurz et K. Wallenfels, dans H. U. Bergmeyer, *Methoden der enzymatischen Analyse*, Bd. II, Verlag Chemie, Weinheim, 1970, p. 1147–1151.
3 A. Beckel, *Z. Unters. Lebensm.*, 64 (1932) 130.
4 *Methods of Analysis of the A.O.A.C.*, 1960, Official method no. 15026.
5 K. G. Sloman, A. K. Foltz et J. A. Yeranstan, *Anal. Chem.*, 41 (5) (1969) 66R.
6 *International Standard FIL-IDF 28*, 1964.
7 *Schweiz, Lebensmittelbuch*, Bd. I, 5. Aufl., 1964, pp. 559–570.
8 K. W. Fuller, *Technicon Symposia, Automation in Analytical Chemistry, 1966*, Vol. II, 1966, pp. 57–61.
9 A. Conneta, L. Stookey et H. Zehnder, *Technicon Int. Congr. on Advances in Automated Analysis, 1970*, Vol. II, 1970, pp. 81–85.
10 L. Velluz, *Pratique de l'Analyse Organique Colorimétrique*, Masson, Paris, 1966, pp. 213–216.
11 J. Bosset, B. Blanc et E. Plattner, *Anal. Chim. Acta*, 67 (1973) 403.
12 P. Pascal, *Traité de Chimie Minérale*, Tome VIII, Masson, Paris, 1933, pp. 188–191.
13 G. Lejeune, *J. Chim. Phys.*, 24 (1927) 482.
14 A. K. Goard et E. K. Rideal, *Proc. Roy. Soc. A*, 105 (1924) 135.
15 G. Birstein et M. Blumental, *Bull. Soc. Chim. Fr.*, 11 (1944) 573.
16 T. L. Lunder, *Lait*, 50 (498) (1970) 483.
17 A. H. Best, A. H. Peterson et H. M. Sell, *Ind. Eng. Chem.*, 14 (2) (1942) 145.
18 R. Vanossi et R. Ferramola, *An. Soc. Cient. Argent.*, 121 (1936) 59.
19 W. Z. Hassid, *Ind. Eng. Chem., Anal. Ed.*, 9 (1937) 228.
20 C. S. Sudheendranath, D. Sethu Rao et C. P. Anantakrishnan, *Indian J. Dairy Sci.*, 14 (1963) 41.
21 D. Sethu Rao, C. S. Sudheendranath, D. S. Krishna Rao, M. Bhimasena Rao et C. P. Anantakrishnan, *Indian J. Dairy Sci.*, 17 (1964) 91.
22 A. A. Forist et J. C. Speck, *Anal. Chem.*, 27 (1955) 1166.
23 G. F. Smith and F. R. Duke, *Ind. Eng. Chem., Anal. Ed.*, 13 (1941) 558; 15 (1943) 120.
24 N. N. Sharma, *Anal. Chim. Acta*, 14 (1956) 423; *Z. Anal. Chem.*, 154 (1957) 340.
25 V. Hasenfratz et M. Frerejacque, dans V. Grignard, G. Dupont et R. Locquin, *Traité de Chimie Organique, Vol. VIII*, Masson, Paris, 1938, pp. 241–243, 262 et 519.
26 J. Shorter et C. Hinshelwood, *J. Chem. Soc. (London)*, (1950) 3276, 3425.

27 H. L. Greenhaus, A. M. Feibush et L. Gordon, *Anal. Chem.*, 29 (10) (1957) 1531.
28 E. Wadsworth, F. R. Duke et C. A. Goetz, *Anal. Chem.*, 29 (12) (1957) 1824.
29 D. Sethu Rao, C. S. Sudheendranath, S. Krishna Rao, M. Bhimasena Rao et C. P. Ananiakrishnan, *Indian J. Dairy Sci.*, 18 (1965) 31.
30 A. G. Leggatt, *Can. Dairy and Ice-Cream J.*, 33 (4) (1954) 36, 70.

Analytica Chimica Acta, 68 (1974) 177–184

AN ENZYME-COUPLED CYANIDE SOLID-STATE ELECTRODE

M. MASCINI and A. LIBERTI
Istituto Chimica Analitica, Università degli Studi, Roma (Italy)
(Received 4th May 1973)

The coupling of enzymes immobilized in artifical membranes has broadened the field of application of ion-selective electrodes, and various analytical determinations have been developed. Urea has been assayed with an ammonium ion-selective electrode coupled with urease immobilized in a polyacrylamide membrane[1]; l-and d-amino acid assay has been done with an ammonium electrode coupled with l- and d-aminoacid oxidase[2,3]; and penicillins have been determined with a pH glass electrode coupled with penicillin-β-lactamase[4].

Recently, Llenado and Rechnitz[5] described the determination of amygdalin with a cyanide solid-state electrode coupled with β-glucosidase immobilized in a polyacrylamide membrane. Thus when the enzyme-coupled membrane electrode is exposed to aqueous solutions of amygdalin, the immobilized β-glucosidase catalyzes the hydrolysis of amygdalin at the surface of the electrode according to

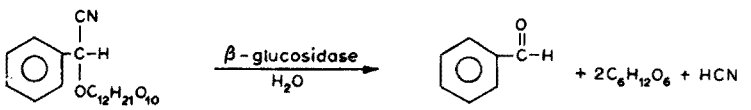

The cyanide ion produced stoichiometrically from the amygdalin in the solution, determines the electrode potential of the cyanide membrane electrode.

The preparation of such coupled electrodes is, however, rather complicated and an unskilled analyst may meet some difficulty. Moreover, these electrodes require a fairly long response time to attain equilibrium (15 min for a 10^{-2} *M* amygdalin solution and 30 min for 10^{-4} *M*). In this paper, a new arrangement for such electrodes is described; a simplified procedure for the determination of amygdalin has been developed.

The preparation of the electrode is quite simple and can be realized with a cyanide-sensitive electrode just before use, if for each electrode a very small amount of enzyme (about 1 mg) is used. The electrode in the selected working conditions has a fast response time (1–3 min) and its lifetime under continuous operation is about one week. The improved characteristics are obtained by spreading the enzyme on the membrane surface of the electrode; the enzyme is then immobilized with a thin dialysis paper stretched by means of a rubber ring.

It was shown that a cyanide electrode is an indicator for cyanide not only in alkaline solution but also in a solution at pH 7 though in such a medium undissociated acid is the predominant species. At pH 7, the enzyme activity is much higher than in the alkaline range, which was used previously,

and consequently the response time and other electrode characteristics are improved. Operating conditions of the enzyme coupled with the cyanide electrode, in terms of pH, enzyme concentration, dialysis paper thickness, etc. in static and dynamic conditions have been evaluated.

EXPERIMENTAL

A cyanide electrode SensIon, Mod 201-I (Amel, Milano, Italy) was used; this is composed of a heterogeneous membrane of silver iodide and polythene moulded to a polythene tube[6]. The reference electrode was a saturated calomel electrode. E.m.f. measurements were made with a Beckman Research pH meter, and the response time was recorded with an Amel potentiometer chart recorder.

β-Glucosidase enzyme (Sigma), amygdalin (BDH) and dialysis paper (20-μm thickness; Arthur H. Thomas Co.) were obtained commercially.

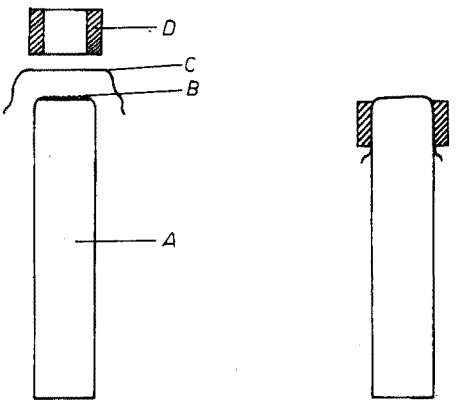

Fig. 1. Preparation of amygdalin electrode. (A) Electrode body; the angles of the section with the membrane have been rounded; (B) 1 mg of enzyme with about 1 μl of water spread directly on the surface; (C) dialysis paper 20 μm thick; (D) rubber ring.

Preparation of the enzyme electrode.

About 1 mg of β-glucosidase is mixed with a little (a few microlitres) of distilled water; the viscous paste obtained is spread with a spatula on the surface of electrode in a thin layer. A piece of dialysis paper is placed over this layer to entrap the enzyme, and is fixed by means of a rubber ring that stretches the dialysis paper over the electrode surface (Fig. 1). The electrode coupled with a reference electrode is placed in the amygdalin solution.

The solutions were prepared by dissolving the proper amount of amygdalin in distilled water; they were buffered at pH 7 with a phosphate buffer and at pH 10 with a borate buffer. The solutions were magnetically stirred during measurements (see Results).

RESULTS

Substrate concentration and pH effect

Figure 2 shows the effect of substrate concentration (10^{-1}–10^{-4} *M*

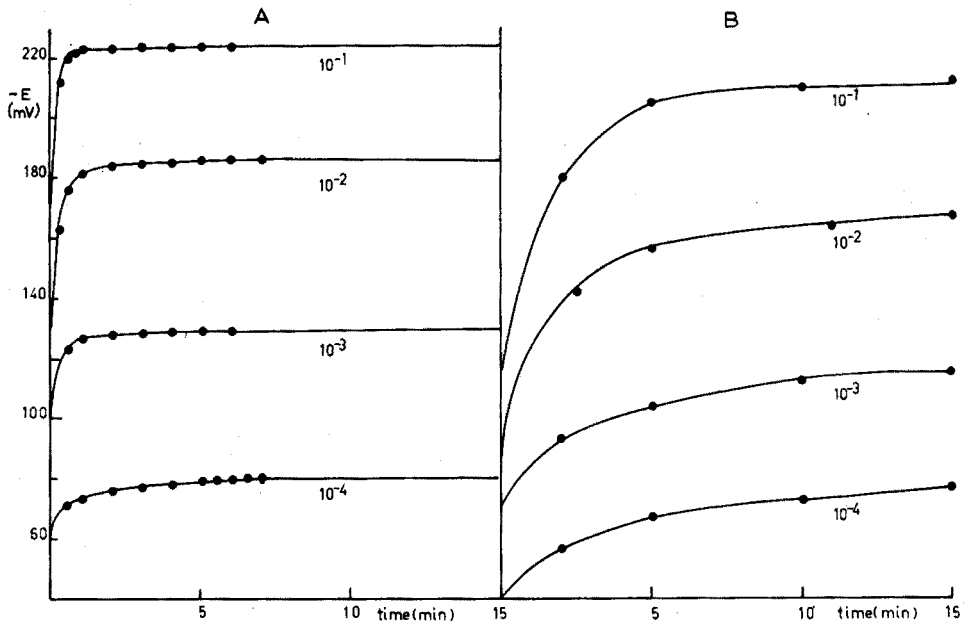

Fig. 2. Amygdalin response-time curves for an electrode containing 1 mg of β-glucosidase immobilized by a dialysis paper. (A) At pH 7. (B) At pH 10.

amygdalin) on the response time of the enzyme electrode at pH 7 and at pH 10. The pH affects the response of electrode: equilibrium is reached more rapidly at pH 7 than at pH 10, a faster response being obtained in more concentrated solution.

In Fig. 3, the calibration curves of the amygdalin electrode (equilibrium potential values *versus* amygdalin concentration) are plotted at pH 7 and 10. On the same diagram, the calibration curves of the same electrode *versus* total cyanide concentration at the same pH values are also given. The slope of the electrode potential *vs.* cyanide concentration plots at both pH values is close to the Nernst value (57 mV per decade). The potential value at pH 10 is higher than that measured at pH 7, because of the effect of the ionization constant of hydrocyanic acid.

The response of the electrode to amygdalin is linear but the slope is 47 mV per decade concentration at pH 10, and 53 mV at pH 7. For the same amygdalin concentration a more negative potential value is obtained at pH 7; this behavior is the reverse of that exbihited by the cyanide electrode, and can be attributed to a higher cyanide concentration reaching the electrode surface.

Effect of amount of enzyme

Figure 4 shows how the amount of enzyme spread on the surface of the electrode affects the equilibrium value. Experiments were carried out in solutions at pH 7 and 10 with a constant concentration of amygdalin (10^{-2} *M*). At pH 7, the electrode response is not significantly affected by the amount of β-glucosidase used, the same value being obtained with 0.1 mg or 5 mg. However, at pH 10,

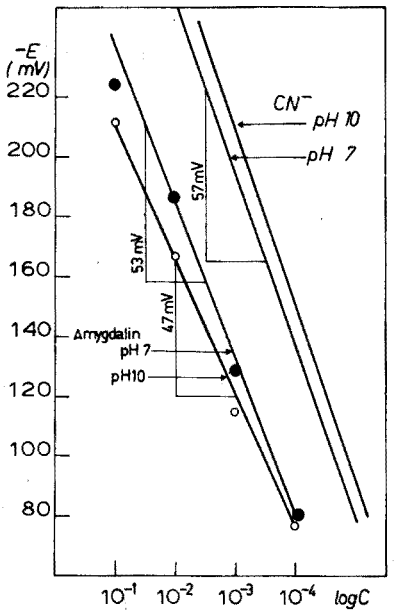

Fig. 3. Amygdalin and cyanide calibration curves at pH 7 and 10.

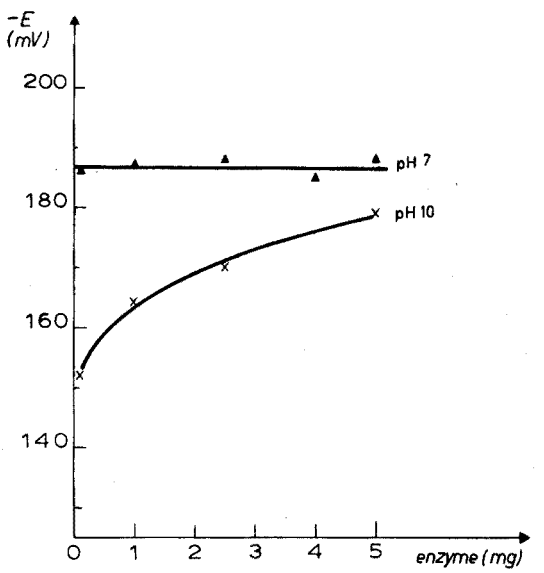

Fig. 4. Effect of amount of enzyme spread on electrode surface at pH 7 and 10. [Amygdalin] = 10^{-2} *M*.

the equilibrium value is strongly dependent upon the amount of enzyme.

The effect of the amount of enzyme (0.1–5 mg) on the response time at pH 7 is shown in Fig. 5; a constant amygdalin concentration of 10^{-2} *M* was used. Equilibrium was achieved more rapidly when a small amount (up to about

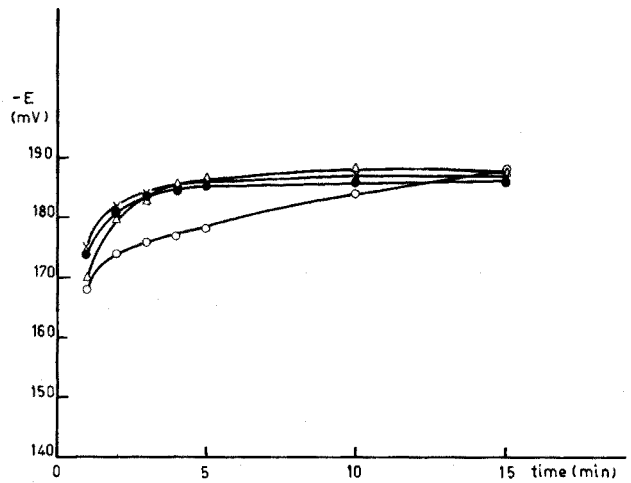

Fig. 5. Response-time curves with different amounts of enzyme. pH 7; [Amygdalin] = 10^{-2} *M*. (●) 0.1 mg enzyme; (×) 1 mg enzyme; (△) 2.5 mg enzyme; (○) 5 mg enzyme.

2.5 mg) of enzyme was used. This effect was not observed at pH 10; in this case, a larger amount of enzyme always caused a higher response rate.

Stirring of the solution and thickness of dialysis paper

Magnetic stirring of the solution affects the electrode response with regard to both the response time and the equilibrium potential (Fig. 6). Stirring speed is expressed in arbitrary units; the higher the speed, the lower the potential measured until a constant value is reached. All measurements in this work, except the experiments of Fig. 6, were made at high stirring speeds, as more reproducible potentials were obtained.

Electrodes with various thicknesses of dialysis membrane were prepared (20–80 μm); Fig. 7 shows how response time and equilibrium values are altered by varying the thickness of the membrane. Membranes of constant thickness must be used in order to obtain reproducible results.

Reproducibility of electrode response

The behaviour of the enzyme electrode *versus* amygdalin concentration was followed over a period of time (Table I). Measurements were obtained on different days during one week: the response-time characteristics do not change appreciably during this time.

DISCUSSION

This research shows a number of improvements over the method developed by Llenado and Rechnitz. The electrode can be prepared by any unskilled operator, and a much smaller amount of enzyme is required. The electrode lifetime is much longer as the enzyme is not leached continuously from the solution. The electrode is rugged and as easy to handle as most membrane ion-selective electrodes.

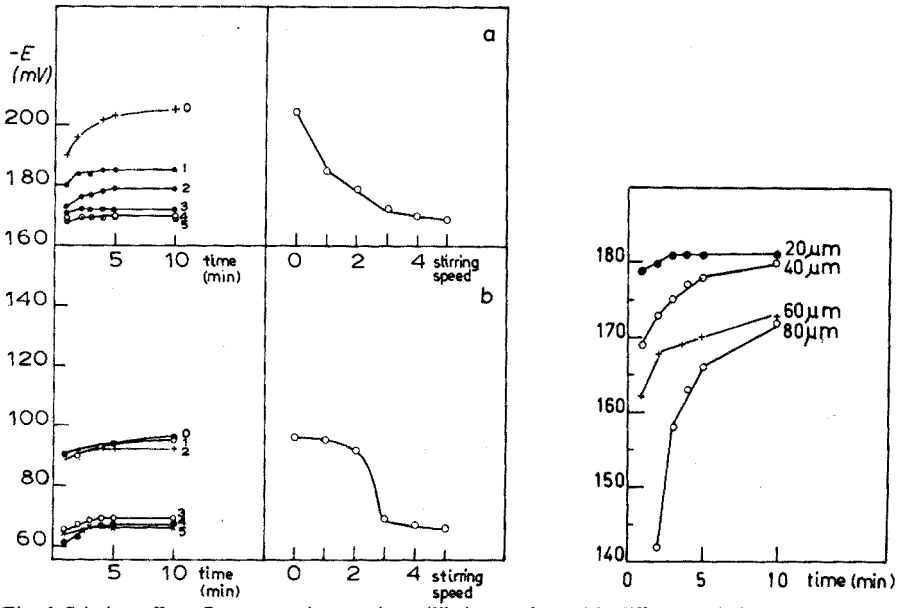

Fig. 6. Stirring effect. Response time and equilibrium value with different stirring speed. The number 0 corresponds to unstirred solutions and numbers 1–5 to increasing stirring speed and are arbitrary numbers. [Amygdalin] = (a) 10^{-2} *M*, (b) 10^{-4} *M*; enzyme amount = 1 mg.

Fig. 7. Effect of thickness of dialysis paper on response time and on equilibrium values. [Amygdalin] = 10^{-2} *M*; enzyme amount = 1 mg.

TABLE I

REPRODUCIBILITY OF RESPONSE-TIME CURVE

Amygdalin concn.	10^{-4} *M*				10^{-3} *M*				10^{-2} *M*			
Time (min) / *Trial*	*1*	*2*	*3*	*5*	*1*	*2*	*3*	*5*	*1*	*2*	*3*	*5*
1	51	59	63	67	108	114	117	119	171	176	178	179
2	48	53	56	61	104	113	116	118	172	174	176	177
3	52	58	59	60	104	112	114	116	173	175	175	176
4					100	111	114	118	173	176	177	177
5	57	60	62	63	112	114	116	118	173	176	176	177
6	54	57	60	61	103	112	116	119	173	176	177	178
7	57	60	62	64	109	116	118	119	173	176	177	178
8	57	61	63	64	100	111	115	118	171	175	176	177
9					100	109	113	117	174	176	178	179

A point of interest is the selected pH to assay amygdalin solutions; it is well known that in the pH range 5–8, the activity of β-glucosidase has the largest value. It has been shown[7] that a cyanide electrode has a rather high sensitivity in this pH range; by coupling the electrode with immobilized β-glucosidase at this pH, one obtains a better performance than in the alkaline range.

The response of the electrode is determined by the diffusion of amygdalin through the dialysis paper, its decomposition in the presence of β-glucosidase to form hydrogen cyanide, and the reaction between cyanide and the silver iodide of the membrane to yield the electrode potential. Though the electrode mechanism is rather complicated, it was found (Fig. 5) that a steady-state equilibrium independent of the amount of enzyme is obtained at pH 7; definitely, a higher activity is exhibited by β-glucosidase at this pH.

The dependence of the steady state, responsible for the electrode potential, on stirring can be attributed to the increased diffusion rate of hydrocyanic acid from the immobilized enzyme through the membrane in the solution, so that the amount reaching the electrode surface is decreased. However, the use of a thicker dialysis paper and of a larger amount of enzyme (>2 mg) yields a slower response time and a lower steady-state equilibrium concentration (Figs. 5 and 7). Both effects influence the diffusion process of amygdalin through the dialysis membrane, and it seems that the concentration of amygdalin inside the membrane is lowered by a thicker membrane and consequently the potential value is also decreased.

Conclusion

The steady-state equilibrium concentration at pH 7 depends on the stirring of the solution and the thickness of the membrane whereas at pH 10, it is also dependent on the enzyme amount. The response time of the electrode depends on all three factors.

The best operational conditions for a β-glucosidase-coupled cyanide electrode were found by working at pH 7, by stirring the solution at a reasonably constant high speed by using a thin dialysis membrane, and by spreading about 1 mg of enzyme on the electrode surface. Electrodes prepared and used in this way yield very satisfactory results and are suitable for routine analysis as well as in automatic equipment to assay amygdalin. The procedure developed should be applicable to any other enzyme electrode.

SUMMARY

A simplified amygdalin electrode prepared by coupling β-glucosidase with a heterogeneous membrane cyanide electrode is described. The electrode is prepared by spreading the enzyme straight on to the membrane surface and covering it with a thin dialysis paper. Operational conditions have been evaluated and the assay of amygdalin at pH 7 is described. The electrodes have a rapid response time and can be used continuously for about a week.

RÉSUMÉ

On décrit une nouvelle électrode amygdaline simplifiée par couplage de β-glucosidase avec une électrode cyanure à membrane hétérogène. L'électrode est préparée par un spray d'enzyme sur la surface de la membrane, en la couvrant avec un papier de dialyse mince. Les conditions opérationnelles ont été évaluées; on décrit un essai d'amygdaline à pH 7. Ces électrodes ont un temps de réponse rapide et peuvent être utilisées sans interruption pendant environ une semaine.

ZUSAMMENFASSUNG

Es wird eine vereinfachte Amygdalin-Elektrode beschrieben, bei der β-Glucosidase mit einer heterogenen Membran-Cyanidelektrode gekoppelt wird. Die Elektrode wird hergestellt, indem das Enzym auf der Membranoberfläche aufgebracht und mit einem dünnen Dialysepapier abgedeckt wird. Die Arbeitsbedingungen wurden ausgearbeitet, und die Bestimmung von Amygdalin bei pH 7 wird beschrieben. Die Elektroden sprechen schnell an und können ununterbrochen etwa eine Woche lang benutzt werden.

REFERENCES

1 G. G. Guilbault and J. G. Montalvo, Jr., *J. Amer. Chem. Soc.*, 92 (1970) 2533.
2 G. G. Guilbault and E. Hrabankova, *Anal. Chem.*, 42 (1970) 1779.
3 G. G. Guilbault and E. Hrabankova, *Anal. Chim. Acta*, 56 (1971) 285.
4 G. J. Papariello, A. K. Mukherji and C. M. Shearer, *Analytical Symposium, Atlantic City, N.Y., Nov. 2, 1972.*
5 R. A. Llenado and G. A. Rechnitz, *Anal. Chem.*, 43 (1971) 1457.
6 M. Mascini and A. Liberti, *Anal. Chim. Acta*, 47 (1969) 339; 51 (1970) 231.
7 M. Mascini, *Anal. Chem.*, 45 (1973) 614.

Analytica Chimica Acta, 68 (1974) 185–196

STUDY OF THE BEHAVIOUR OF SOLID-STATE MEMBRANE ELECTRODES

PART I. ROLE OF VARIOUS FACTORS ON THE LIMITS OF SENSITIVITY OF CHLORIDE AND FLUORIDE ELECTRODES

N. PARTHASARATHY, J. BUFFLE and D. MONNIER

Department of Inorganic and Analytical Chemistry, University of Geneva, Geneva (Switzerland)

(Received 14th May 1973)

Most of the solid-state electrodes (for copper, lead, halides, etc.) exhibit Nernstian behaviour over a fairly large range of concentration[1–4]. However, for all these electrodes the relation $E = f(\log c)$ diverges from linearity, and the potential tends to become independent of c for very low concentrations of the ion under investigation. Several hypotheses have been put forward in an attempt to explain this behaviour. Those most frequently cited for the fluoride and chloride electrodes are:

(a) solubility of the membrane[5–12];

(b) presence of impurities of the ion under investigation in the background electrolyte[5–7,13];

(c) adsorption of test ions on the walls of the containers[14].

However, no systematic study confirming these hypotheses has so far been carried out. At times, in certain specific cases, it is essential to know the exact nature of the phenomena which limit the sensitivity of the electrode, for instance, in the direct determination of solubility products of inorganic compounds[15].

EXPERIMENTAL

Apparatus

The behaviour of Beckman fluoride electrode 39600, Beckman fluoride combination electrode 39650, Orion fluoride electrode 94-09 A, and Beckman chloride electrode 39604 was studied.

The membrane of the fluoride electrodes is made of lanthanum fluoride single crystal doped with europium(II), whereas the chloride electrode is made of compressed precipitate of silver chloride.

The reference electrode used with the fluoride electrodes was Metrohm fiber-junction calomel electrode (EA 404), except for Beckman combination electrode. In the case of the chloride electrode, a Metrohm mercury(I) sulfate/2 M Na_2SO_4 reference electrode was used.

All the measurements were made by stirring the solution with a magnetic bar at $25° \pm 0.1°$. A Metrohm digital pH meter E-500 with a precision of ± 0.1 mV coupled with a Metrohm recorder E-478 was used for measurements of potential.

An atomic absorption spectrophotometer (Unicam SP-90) was used for the determination of silver(I).

Hewlett-Packard and CDC 3800 computers were used for calculations.

Fluoride electrode

Reagents. Sodium nitrate (Merck pro anal.), potassium nitrate (Merck, pro anal.), and Metrohm standard sodium fluoride solution (0.1 *M*) were used. All the fluoride solutions were prepared by successive dilution of this standard solution with demineralized water, and were stored in polyethylene bottles. Fluoride solutions over the range 10^{-6}–10^{-8} *M* had to be prepared at the time of measurement. Indeed, for dilute solutions, it was found that the concentration of fluoride decreased with time, probably owing to the adsorption of fluoride ions on the walls of the container.

Total ionic strength buffer (TISAB) was prepared by dissolving 80 g of sodium nitrate and 28 ml of glacial acetic acid in about 250 ml of demineralized water. The solution was adjusted to pH 5.5 with 5 *M* sodium hydroxide solution. The resulting solution was diluted to 500 ml in a volumetric flask with demineralized water.

Procedure. 10 ml of TISAB and 10 ml of the fluoride solution under investigation were pipetted into a polyethylene beaker. Potential *versus* time was recorded by immersing the fluoride and the reference electrodes in the solutions. The readings were taken once a stable value of potential had been attained. This procedure was repeated for concentration of fluoride between 10^{-2} and 10^{-8} *M*.

Chloride electrode

Reagents. Potassium nitrate (Merck pro anal.), potassium chloride (Merck pro anal.) and silver nitrate (Merck pro anal.) were used; a 1 *M* solution of potassium nitrate was prepared. A stock solution of 0.1 *M* potassium chloride was prepared and solutions in the range 10^{-2}–10^{-6} *M* were obtained by successive dilution with demineralized water.

Procedure. 10 ml of 1 *M* potassium nitrate and 10 ml of the chloride solution under investigation were pipetted into a polyethylene beaker and the pH was adjusted to *ca.* 5.0 with nitric acid. The chloride and reference electrodes were dipped in the solution and the steady value of the potential was measured as described for fluoride determination. The above procedure was repeated for concentrations of chloride ranging from 10^{-2} to 10^{-6} *M*.

The same procedure was used with silver solutions.

ROLE OF THE SOLUBILITY OF THE MEMBRANE ON THE RESPONSE OF THE ELECTRODE

Theory

The response of anion-selective electrodes can be written in the general form:

$$E = E^0 + E_j - s \cdot \log(\gamma_A \cdot c_A)$$

where E^0, E_j, c_A, γ_A, and s are the standard potential with respect to the reference electrode used, the junction potential between the reference electrode and sample solution, the concentration of the anion A under investigation (F^- or Cl^-), its

activity coefficient, and the slope usually close to 2.303 RT/zF (where these symbols have their usual significance), respectively. If the measurements are made at constant ionic strength, then E will depend directly on concentration and can be expressed as follows:

$$E = E' - s \cdot \log c_A \tag{1}$$

where

$$E' = E^0 + E_j - s \cdot \log \gamma_A = \text{constant}$$

or, if the test ion is a cation with concentration c_M, then:

$$E = E' + s \cdot \log c_M \tag{1'}$$

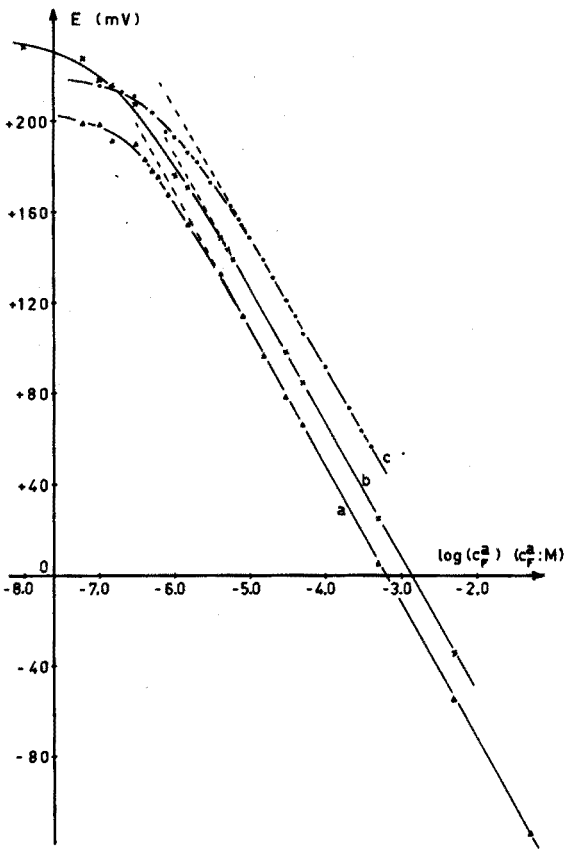

Fig. 1. Calibration curves for fluoride electrodes Beckman 39600 (curve c), Beckman 39650 (curve a) Orion 94-09A (curve b). The values of E' and s, obtained by least-squares fit are:

Curve	*E' (mV)*	*s (mV)*
a	−193.9	60.3
b	−170.3	59.2
c	−137.8	57.2

The concentration c_A is the sum of two concentration terms: the concentration of the anion added (c_A^a) and that coming from the dissolution of the electrode crystal, c_A^d. Hence we have:

$$c_A = c_A^a + c_A^d \tag{2}$$

For a crystal of type $A_{z_M}M_{z_A}$, where A^{-z_A} and M^{+z_M} are the anion and cation, respectively, and z_A and z_M their respective number of charges, the solubility product is given by:

$$(c_A)^{z_M} \cdot (c_M)^{z_A} = K_{sp}/[(\gamma_A)^{z_M} \cdot (\gamma_M)^{z_A}] \tag{3}$$

If the number of positive and negative charges which come into the solution by dissolution are equal, then one has:

$$(c_A^d/z_M) = (c_M/z_A) \tag{4}$$

Combining eqns. (2)–(4), one obtains:

$$c_A = c_A^a + \frac{z_M}{z_A} \cdot \frac{(K_{sp})^{1/z_A}}{\gamma_M \cdot (\gamma_A)^{z_M/z_A}} \cdot \frac{1}{(c_A)^{z_M/z_A}} \tag{5}$$

If c_A^a is large, then the second term in eqn. (5) can be neglected. Then this equation becomes: $c_A = c_A^a$ and eqn. (1) would be valid even if c_A were replaced by c_A^a. However, this is no longer the case when c_A^a is very small.

By putting $c_A = c_A^a$ in eqn. (1), it was found experimentally that this relation was obeyed up to a concentration of $5 \cdot 10^{-6}$ M for all the fluoride electrodes (Fig. 1). The limit for chloride electrode was found to be about 10^{-4} M (Fig. 2) when silver(I) as well as chloride were used as potential-determining ions. These results are in good agreement with published data[2–4].

It is possible to verify whether the deviation of the experimental curve from linearity is really and solely due to the dissolution of the electrode membrane. Indeed, from eqn. (5), for low values of c_A^a, we can compute Δc_A, where:

$$\Delta c_A = c_A - c_A^a = \frac{z_M}{z_A} \cdot \frac{(K_{sp})^{1/z_A}}{\gamma_M \cdot (\gamma_A)^{z_M/z_A}} \cdot \frac{1}{(c_A)^{z_M/z_A}} \tag{6}$$

Thus a plot of Δc_A against $1/(c_A)^{z_M/z_A}$ should give a straight line passing through the origin. From the slope it would be possible to compute the solubility product at the ionic strength used. If the electrode is sensitive to cation M, and if the measurements are made in solutions containing a concentration c_M^a of added ions, then eqn. (6) becomes:

$$\Delta c_M = c_M - c_M^a = \frac{z_A}{z_M} \cdot \frac{(K_{sp})^{1/z_M}}{\gamma_A \cdot (\gamma_M)^{z_A/z_M}} \cdot \frac{1}{(c_M)^{z_A/z_M}} \tag{7}$$

Δc_A and c_A can be calculated from the calibration curve since E' and s (eqn. 1) can be computed by least-squares fit for high values of c_A^a. Then, by using these parameters, measured potentials corresponding to c_A, and (eqn. 1), it is possible to compute values of c_A corresponding to low values of c_A^a.

Sources of errors

Since the experiments conducted to verify the above hypothesis have to be

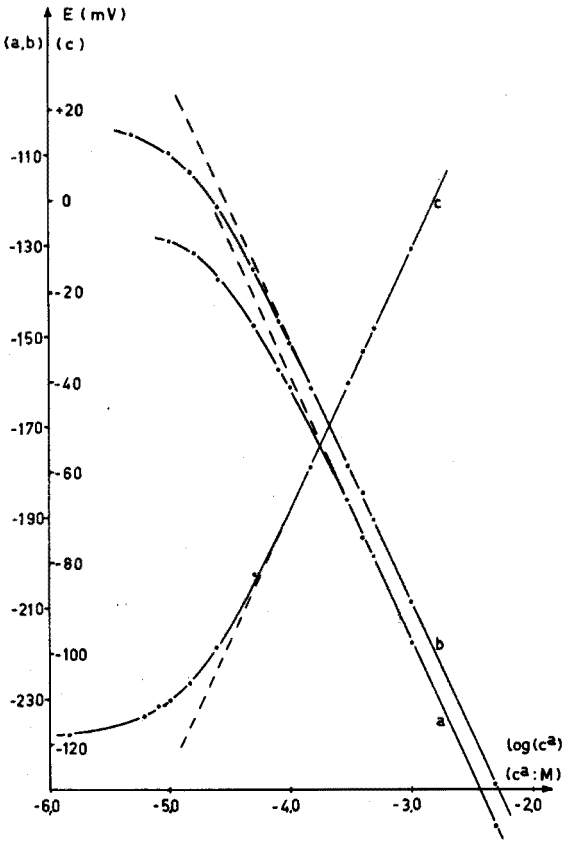

Fig. 2. Calibration curves for chloride electrode, using Cl^- (curve a, b) or Ag^+ (curve c) as potential-determining ion. The values for E', s obtained by least-squares fit are:

Curve	*E' (mV)*	*s (mV)*	*Ionic strength*
a	−394.4	59.0	0.5 *M*
b	−382.7	58.2	10^{-2} *M*
c	+165.0	58.4	10^{-2} *M*

carried out in the concentration range where the errors made in measurements may be high, it is necessary to estimate the order of magnitude of these errors.

c_A is calculated from the expression:

$$c_A = \exp[-2.303 \cdot (E - E')/s] \tag{8}$$

or:

$$c_A = \exp[-2.303 \cdot (E - E')/(s + \Delta s)] \cdot \exp[2.303 \cdot \Delta E'/(s + \Delta s)] \tag{9}$$

if values $(s + \Delta s)$ and $(E' + \Delta E')$ are used instead of s and E', respectively, Δs and $\Delta E'$ being the respective errors. Because of these errors, a systematic error in c_A will be introduced, corresponding to the difference between eqns. (8) and (9).

Table I gives the values of Δs and $\Delta E'$ for ten calibration curves

TABLE I

VALUES OF Δs AND $\Delta E'$ FOR FLUORIDE ELECTRODES OBTAINED BY LINEAR REGRESSION ANALYSIS WITH 95% PROBABILITY

Calibration curve	*Number of points*	*Concentration range (M)*	*ΔE' (mV)*	
I	9	$5\cdot10^{-5}$–10^{-6}	2.7	0.52
II	8	$5\cdot10^{-2}$–$4\cdot10^{-6}$	1.2	0.29
III	12	$5\cdot10^{-2}$–10^{-5}	1.1	0.29
IV	7	$5\cdot10^{-2}$–$3\cdot10^{-5}$	0.2	0.06
V	7	$5\cdot10^{-3}$–$4\cdot10^{-6}$	1.9	0.43
VI	10	$4\cdot10^{-4}$–10^{-5}	4.6	1.07
VII	7	$5\cdot10^{-3}$–$6\cdot10^{-6}$	5.4	1.25
VIII	7	$5\cdot10^{-4}$–$6\cdot10^{-6}$	1.8	0.41
IX	10	10^{-4}–$3\cdot10^{-6}$	2.4	0.51
X	6	10^{-4}–$5\cdot10^{-6}$	2.8	0.62

obtained with fluoride electrodes. It is seen that, for 95% probability, the mean values of Δs and $\Delta E'$ are 0.5 mV and 2.4 mV respectively. By means of eqns. (8) and (9), it is possible to compute the maximum values of the systematic errors on c_A, caused by these two parameters; these were found to be 6% and 7%, respectively.

Therefore it is absolutely essential to determine E' and s for each set of measurements in order to minimize as much as possible the errors arising from the above-mentioned parameters.

The statistical error in c_A, $e(c_A)$, is given by[16]:

$$[e(c_A)]/c_A = 2.303\cdot[e(E)]/s \qquad (10)$$

where $e(E)$ is the statistical error in the measured potential (*ca.* 0.1 mV).

It was found that, with dilute fluoride solutions, there was a systematic error in c_A^a, probably caused by adsorption of A on the walls of the container. However, by performing experiments systematically, the latter errors could be eliminated by using freshly prepared solutions.

The estimated statistical error in preparing a solution of concentration c_A^a is about 1.5% for 10^{-5} M solutions and about 2% for 10^{-7} M solutions. Finally, as Δc_A is given by:

$$\Delta c_A = c_A - c_A^a$$

the statistical error in c_A is given by:

$$[e(\Delta c_A)]^2 = [e(c_A)]^2 + [e(c_A^a)]^2 \qquad (11)$$

By using eqns. (10) and (11) with the values cited above for $e(c_A^a)/c_A^a$ and $e(c_A)/c_A$, and considering that $c_A > c_A^a$, one obtains:

$$e(\Delta c_A) < 0.02\cdot c_A \quad \text{for} \quad 10^{-4}\ M > c_A > 10^{-6}\ M$$

$$e(\Delta c_A) < 0.025\cdot c_A \quad \text{for} \quad 10^{-6}\ M > c_A > 10^{-8}\ M$$

Results with chloride electrode

In this case, $z_M = z_A = 1$. From Fig. 3 (curve a) it is seen that the relation

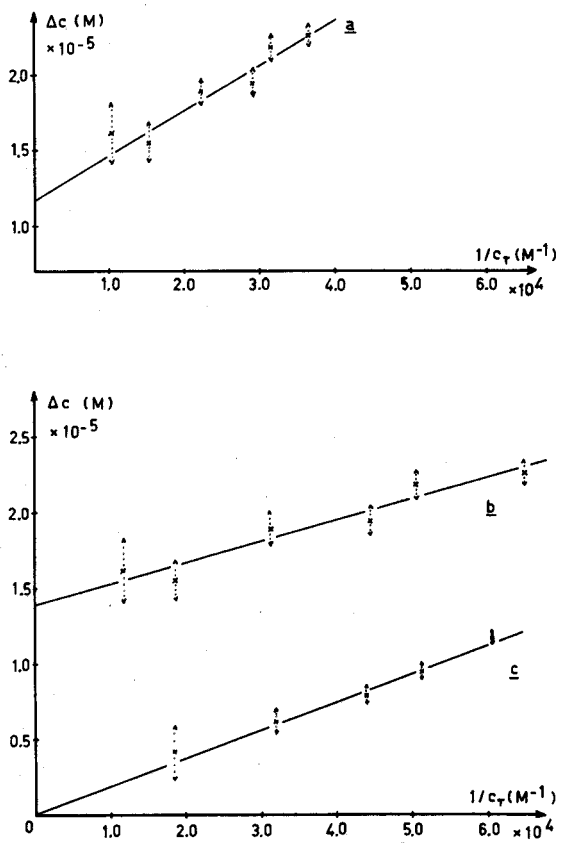

Fig. 3. Curves $\Delta c = f(1/c_T)$ obtained with chloride Beckman electrode, by using chloride as potential-determining ion. <.....> estimated error

Curve	*Values on the abscissa*	*Electrolyte*	*Slope*	*Intercept on the ordinate*
a	$1/c_T$	0.5 *M* $NaNO_3$	$(3.0\pm0.4)\cdot10^{-10}$	$(1.2\pm0.4)\cdot10^{-5}$
b	$1/c_T - 1.2\cdot10^{-5})$	0.5 *M* $NaNO_3$	$(1.3\pm0.6)\cdot10^{-10}$	$(1.4\pm0.4)\cdot10^{-5}$
c	$1/c_T$	10^{-2} *M* $NaNO_3$	$(1.9\pm0.4)\cdot10^{-10}$	0

Fisher coefficients corresponding to the hypothesis slope = 0 and intercept on the ordinate = 0, with 95% probability, are as follows:

Curve	*Fisher coefficients*		
	Calculated for slope	*Calculated for intercept on the ordinate*	*Theoretical*
a	37.32	58.8	7.71
b	34.79	141.85	7.71
c	188.29	0.005	10.13

TABLE II

DETERMINATION OF SOLUBILITY OF THE CRYSTAL BY MEASURING THE CONCENTRATION OF DISSOLVED SILVER(I) BY ATOMIC ABSORPTION SPECTROMETRY

c^a_{Cl} (M)	c_{Cl} (M)	c_{Ag} (M)	$c_{Cl} \cdot c_{Ag}$	$(c_{Cl} - 1.2 \cdot 10^{-5}) \cdot c_{Ag}$
$4.85 \cdot 10^{-6}$	$2.7 \cdot 10^{-5}$	$5.0 \cdot 10^{-6}$	$1.4 \cdot 10^{-10}$	$7.7 \cdot 10^{-11}$*
$1.0 \cdot 10^{-5}$	$3.2 \cdot 10^{-5}$	$3.9 \cdot 10^{-6}$	$1.2 \cdot 10^{-10}$	$7.7 \cdot 10^{-11}$
$1.5 \cdot 10^{-5}$	$3.4 \cdot 10^{-5}$	$3.2 \cdot 10^{-6}$	$1.1 \cdot 10^{-10}$	$7.1 \cdot 10^{-11}$
$2.5 \cdot 10^{-5}$	$4.4 \cdot 10^{-5}$	$3.4 \cdot 10^{-6}$	$1.5 \cdot 10^{-10}$	$1.1 \cdot 10^{-10}$

$\Delta c_{Cl} = f(1/c_{Cl})$, calculated from the results of Fig. 2a, is indeed linear, but the line does not pass through the origin. This could be due either to the presence of impurities of chloride in the solution, or to nitrate interference. However, the slope of the line enables one to estimate the apparent solubility product. By weighting the results of Fig. 3 (curve a) by means of eqns. (10) and (11), linear regression analysis gave the following values:

$$\text{slope} = (3.0 \pm 0.4) \cdot 10^{-10}; \text{ intercept on the ordinate} = (1.2 \pm 0.4) \cdot 10^{-5}\ M.$$

An attempt was made to verify the part played by the dissolution of the electrode by determining the concentration of silver(I) in the solutions which had previously been used to construct the calibration curve (Fig. 2, curve a). Atomic absorption spectrometry was used for the determination of c_{Ag}.

Table II shows these results, as well as the corresponding values of c^a_{Cl}, c_{Cl} and $c_{Cl} \cdot c_{Ag}$. This product is the solubility product of silver chloride, if one assumes that the constant term obtained by extrapolation of curve a (Fig. 3) is fully due to impurities of chloride in the background electrolyte. If this constant term is fully attributed to interference of nitrate, the solubility product of the crystal is given by $(c_{Cl} - 1.2 \cdot 10^{-5}) \cdot c_{Ag}$. As can be seen from Table II, the mean values obtained for the solubility product in the two cases ($1.3 \cdot 10^{-10}$ and $0.8 \cdot 10^{-10}$, respectively) are close to the value $1.8 \cdot 10^{-10}$ cited in the literature[17].

Results with fluoride electrodes

Table III gives the values of c^a_F, c_F and Δc_F calculated from Fig. 1 for the three fluoride electrodes used. It can be seen that Δc_F is practically independent of c_F, whereas the apparent solubility product calculated by eqn. (5) varies regularly with c^a_F (see column 4 of Table III). Hence the process of solubility alone would not explain adequately the behaviour of fluoride electrodes.

ROLE OF IMPURITIES OR INTERFERING IONS

When an ion-selective electrode sensitive to an ion A is immersed in a solution containing that ion, the concentration of this ion includes, apart from the concentration c^d_A arising from dissolution of the crystal and concentration of the sample c^a_A, an amount of impurities A, c^i_A, present in the reagents. Furthermore, a background electrolyte with concentration c_E is normally added to the solution of A, the ions of which may influence the response of the electrode depending on

TABLE III

VALUES OF Δc_F FOR VARIOUS FLUORIDE ELECTRODES

c_F^a (M)	c_F (M)	Δc_F (M)	Apparent solubility product (from eqn. 5)
Beckman electrode 39600			
$3.00 \cdot 10^{-6}$	$3.63 \cdot 10^{-6}$	$6.3 \cdot 10^{-7}$	$1.0 \cdot 10^{-23}$
$2.00 \cdot 10^{-6}$	$2.54 \cdot 10^{-6}$	$5.4 \cdot 10^{-7}$	$2.9 \cdot 10^{-24}$
$1.50 \cdot 10^{-6}$	$2.14 \cdot 10^{-6}$	$6.4 \cdot 10^{-7}$	$1.7 \cdot 10^{-24}$
$1.00 \cdot 10^{-6}$	$1.62 \cdot 10^{-6}$	$6.2 \cdot 10^{-7}$	$8.8 \cdot 10^{-25}$
$7.50 \cdot 10^{-7}$	$1.44 \cdot 10^{-6}$	$6.9 \cdot 10^{-7}$	$4.8 \cdot 10^{-25}$
$3.00 \cdot 10^{-7}$	$7.96 \cdot 10^{-7}$	$5.0 \cdot 10^{-7}$	$8.3 \cdot 10^{-26}$
$2.00 \cdot 10^{-7}$	$7.24 \cdot 10^{-7}$	$5.2 \cdot 10^{-7}$	$6.6 \cdot 10^{-26}$
$1.00 \cdot 10^{-7}$	$6.33 \cdot 10^{-7}$	$5.3 \cdot 10^{-7}$	$4.5 \cdot 10^{-26}$
Beckman combination electrode 39650			
$1.50 \cdot 10^{-6}$	$1.66 \cdot 10^{-6}$	$1.6 \cdot 10^{-7}$	$2.4 \cdot 10^{-25}$
$8.00 \cdot 10^{-7}$	$9.85 \cdot 10^{-7}$	$1.9 \cdot 10^{-7}$	$5.9 \cdot 10^{-26}$
$6.00 \cdot 10^{-7}$	$7.20 \cdot 10^{-7}$	$1.2 \cdot 10^{-7}$	$1.5 \cdot 10^{-26}$
$5.00 \cdot 10^{-7}$	$6.62 \cdot 10^{-7}$	$1.6 \cdot 10^{-7}$	$1.6 \cdot 10^{-26}$
$4.00 \cdot 10^{-7}$	$5.50 \cdot 10^{-7}$	$1.5 \cdot 10^{-7}$	$8.3 \cdot 10^{-27}$
$3.00 \cdot 10^{-7}$	$4.27 \cdot 10^{-7}$	$1.3 \cdot 10^{-7}$	$3.3 \cdot 10^{-27}$
$1.50 \cdot 10^{-7}$	$4.05 \cdot 10^{-7}$	$2.6 \cdot 10^{-7}$	$5.6 \cdot 10^{-27}$
$1.00 \cdot 10^{-7}$	$3.00 \cdot 10^{-7}$	$2.0 \cdot 10^{-7}$	$1.8 \cdot 10^{-27}$
$6.00 \cdot 10^{-8}$	$2.98 \cdot 10^{-7}$	$2.4 \cdot 10^{-7}$	$2.1 \cdot 10^{-27}$
Orion electrode 94-09 A			
$3.00 \cdot 10^{-7}$	$4.25 \cdot 10^{-7}$	$1.3 \cdot 10^{-7}$	$3.2 \cdot 10^{-27}$
$1.50 \cdot 10^{-7}$	$3.00 \cdot 10^{-7}$	$1.5 \cdot 10^{-7}$	$1.4 \cdot 10^{-27}$
$1.00 \cdot 10^{-7}$	$2.80 \cdot 10^{-7}$	$1.8 \cdot 10^{-7}$	$1.3 \cdot 10^{-27}$
$6.00 \cdot 10^{-8}$	$1.90 \cdot 10^{-7}$	$1.3 \cdot 10^{-7}$	$2.8 \cdot 10^{-28}$
$1.00 \cdot 10^{-8}$	$1.50 \cdot 10^{-7}$	$1.4 \cdot 10^{-7}$	$1.7 \cdot 10^{-28}$

the selectivity constant K. The Nernst equation can then be written as:

$$E = E' - s \cdot \log(c_A^a + c_A^d + c_A^i + K \cdot c_E) \tag{12}$$

The total concentration of A is now given by:

$$c_A = c_A^a + c_A^d + c_A^i$$

Hence, by taking into account eqns. (3) and (4):

$$\Delta c_A = c_A - c_A^a = c_A^i + \frac{z_M}{z_A} \cdot \frac{(K_{sp})^{1/z_A}}{\gamma_M \cdot (\gamma_A)^{z_M/z_A}} \cdot \frac{1}{(c_A)^{z_M/z_A}} \tag{13}$$

But the potential measurements and eqn. (12) only enable us to calculate c_T defined as:

$$c_T = c_A^a + c_A^d + c_A^i + K \cdot c_E$$

Hence we have:

$$\Delta c_T = c_T - c_A^a = c_A^i + K \cdot c_E + \frac{z_M}{z_A} \cdot \frac{(K_{sp})^{1/z_A}}{\gamma_M \cdot (\gamma_A)^{z_M/z_A}} \cdot \frac{1}{(c_T - K \cdot c_E)^{z_M/z_A}}$$

If $K \cdot c_E$ is small compared to c_T, it is apparent that the relation $\Delta c_T = f(1/(c_T)^{z_M/z_A})$ will give a line of slope equal to the solubility product and intercept on the ordinate equal to c_A^i. If $K \cdot c_E$ is fairly large, in theory this relation would not be linear. But, taking into account the inaccuracies in the measurements, this nonlinearity is not noticeable as can be seen in Fig. 3 (curves a and b). Curve b was obtained by supposing that the intercept on the Y axis in curve a was fully due to the $K \cdot c_E$ term and using the value of the latter ($K \cdot c_E = 1.2 \cdot 10^{-5}$ M) for plotting the graph Δc_T against $1/(c_T - K \cdot c_E)$. It is seen that in both cases (curves a and b), the relationships appear to be linear. $K_{sp}/\gamma_{Cl} \cdot \gamma_{Ag}$ calculated from curve b gave a value of $(1.3 \pm 0.6) \cdot 10^{-10}$.

In order to verify the fact that the line does not pass through the origin because of either impurities or interference of nitrate ion present in the solution, the measurements corresponding to Fig. 3 (curves a and b) were repeated but with 10^{-2} M potassium nitrate as background electrolyte (Fig. 3, curve c). Under these conditons, the quantities of the interfering ions and the chloride impurities in the supporting electrolyte were diminished by a factor of 50. From regression analysis carried out for the results of Fig. 3 (curve c), it is seen that the intercept on the Y axis is not significantly different from zero. Hence the effect of interference or impurities effectively can play an important role on the response of the chloride electrode in the low concentration range of chloride.

From regression analysis carried out for the results of Fig. 3 (curve c), the value of $K_{sp}/\gamma_{Cl} \cdot \gamma_{Ag}$ was found to be: $(1.9 \pm 0.4) \cdot 10^{-10}$, which is in good agreement with the value given in the literature at this ionic strength. Moreover, the value of the solubility product of silver chloride does not seem to change significantly with ionic strength[17].

It should be emphasised that these experiments do not allow a decision about which of the two terms c_A^i or $K \cdot c_E$ predominates over the other. However, some observations seem to indicate that the interfering effect is the more important phenomenon.

It was also verified that solubility is the principal factor which determines the limit of sensitivity of the electrode, by carrying out experiments with the chloride electrode and silver(I) as the test ion. The curve in Fig. 4 was obtained from the results of Fig. 2 (curve c). It can be seen that eqn. (14) is satisfied. As in the case of Fig. 3 the effect of impurities and interfering ions is negligible at 10^{-2} M ionic strength. The value of $K_{sp}/\gamma_{Cl} \cdot \gamma_{Ag}$, obtained from the slope, was found to be: $K_{sp}/\gamma_{Cl} \cdot \gamma_{Ag} = (1.9 \pm 0.4) \cdot 10^{-10}$. This is in good agreement with that obtained from Fig. 3c.

It should be noted that the value of $K_{sp}/\gamma_{Cl} \cdot \gamma_{Ag}$ can also be obtained from E'_{Ag} and E'_{Cl}, corresponding to the values obtained from calibration curves of silver(I) and chloride, respectively[11,18]. It can be shown that:

$$\log(K_{sp}/\gamma_{Cl} \cdot \gamma_{Ag}) = -(E'_{Ag} - E'_{Cl})/s$$

The value of $K_{sp}/\gamma_{Cl} \cdot \gamma_{Ag}$ by this method, was found to be: $K_{sp}/\gamma_{Cl} \cdot \gamma_{Ag} = (4 \pm 2) \cdot 10^{-10}$ which is obviously not very accurate, because the errors in E' are relatively large.

In addition to this, the drift in the value of E' with time willl also give rise to errors in K_{sp} values. Another drawback of this method is that no indication whatsoever of the effect of interfering ions or impurities would be obtained.

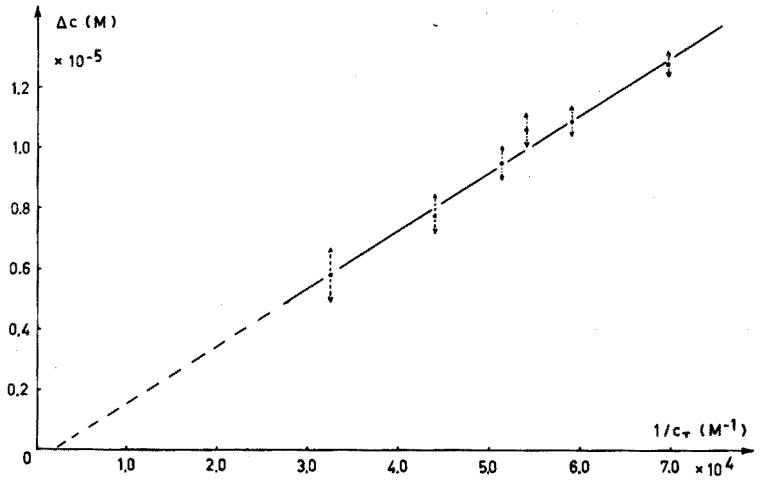

Fig. 4 Curves $\Delta c = f(1/c_T)$ obtained with Beckman chloride electrode with Ag^+ as potential-determining ion. <.....> estimated error. Electrolyte, 10^{-2} *M* $NaNO_3$. Slope $= (1.9 \pm 0.4) \cdot 10^{-10}$; intercept on the ordinate is not significantly different from zero. Fisher coefficients (see Fig. 3) are as follows: theoretical value = 7.71, calculated value for slope = 172.76, calculated value for intercept on the ordinate = 0.001.

It seems that the results obtained with fluoride electrode (Table III) can be explained as being due to the same effects as described above. Indeed, the constant values obtained for Δc_A seem to indicate that the role played by solubility in eqn. (13) is negligible in comparison with c_A^i or $K \cdot c_E$. Several authors have put forward this hypothesis[6,19]. However, the behaviour of the fluoride electrode in several other experiments cannot solely be explained in terms of c_A^i and $K \cdot c_E$. In particular, from these experiments, it appears that the part played by the adsorption of fluoride ions on the electrode surface cannot be neglected. These results will be described in another article.

The authors wish to thank Beckman Instrument Inc. and Orion Research Inc. for providing them with the Fluoride and Chloride electrodes.

SUMMARY

A study of the behaviour of the chloride-selective electrode in the concentration range below the linear response region, has shown that the nonlinearity is principally due to three factors: the solubility of the membrane, the concentration of chloride impurities and the interference of ions of the background electrolyte or other impurities. Similar studies with fluoride electrodes have shown that, in addition to these factors, other parameters also play an important role.

RÉSUMÉ

L'étude du comportement de l'électrode au chlorure, dans le domaine de concentration où la relation linéaire entre le potentiel et le logarithme de la concentration n'est plus vérifiée, a montré que cette non linéarité est due essentielle-

ment à trois facteurs: la solubilité de la membrane, la concentration des impuretés de chlorure et l'interférence des ions de l'électrolyte. Des études semblables effectuées avec l'électrode au fluorure ont montré que, en plus des facteurs mentionnés ci-dessus, d'autres paramètres jouent probablement un rôle important.

ZUSAMMENFASSUNG

Eine Untersuchung des Verhaltens der chlorid-selektiven Elektrode bei Konzentration unterhalb des linearen Ansprechbereiches zeigte, dass die Nichtlinearität grundsätzlich auf drei Faktoren zurückzuführen ist: die Löslichkeit der Membran, die Konzentration von Chlorid-Verunreinigungen und die Störung der Ionen des Hintergrund-Elektrolyten oder anderer Verunreinigungen. Ähnliche Untersuchungen mit Fluoridelektroden ergaben, dass zusätzlich zu diesen Faktoren auch andere Parameter eine wichtige Rolle spielen.

REFERENCES

1 M. R. Frant and J. W. Ross, *Science*, 154 (1966) 2553.
2 J. W. Ross, *Ion Selective Electrodes*, N.B.S. Spec. Publ. no. 314, 1969, Ch. II, p. 57.
3 *Guide to Selective Ion Electrode Measurements*, Beckman Inc.
4 *Analytical Guide to Specific Ion Electrodes*, Orion Research, October 1971.
5 J. J. Lingane, *Anal. Chem.*, 39 (1967) 881.
6 E. W. Bauman, *Anal. Chim. Acta*, 54 (1971) 189.
7 J. Ruzicka and C. G. Lamm, *Anal. Chim. Acta*, 54 (1971) 1.
8 J. Buffle, N. Parthasarathy and D. Monnier, *Anal. Chim. Acta*, 59 (1972) 427.
9 E. Pungor, K. Toth and J. Havas, *Mikrochim. Acta*, (1966) 689.
10 A. K. Covington, *Ion Selective Electrodes*, N.B.S. Spec. Publ. no. 314, 1969, Ch. III, p. 97.
11 E. Pungor, K. Toth and J. Havas, *Acta Chim. Acad. Sci. Hung.*, 58 (1968) 16.
12 R. P. Buck, *Anal. Chem.*, 40 (1968) 1432.
13 E. Mesmer, *Anal. Chem.*, 40 (1968) 443.
14 R. Durst and B. T. Duhart, *Anal. Chem.*, 42 (1970) 1002.
15 N. Parthasarathy, J. Buffle, J.-C. Landry, C. Birraux, J. F. Monn, M. C. Arrigo and W. Haerdi, *Chimia*, 27 (1973) 368.
16 J. Buffle, N. Parthasarathy and D. Monnier, *Chimia*, 25 (1971) 223.
17 L. G. Sillen and A. E. Martell, *Stability Constants*, Spec. Publ. no. 17, The Chemical Society, London, 1964.
18 J. Bagg and G. A. Rechnitz, *Anal. Chem.*, 45 (1973) 271.
19 J. N. Butler, Ion Selective Electrodes, N.B.S. Spec. Publ. no. 314, 1969, Ch. V, p. 143.

Analytica Chimica Acta, 68 (1974) 197–202

AUTOMAT ZUR KOHLENSTOFFBESTIMMUNG IN URAN- UND PLUTONIUM-CARBIDEN

W. BARTSCHER und D. PEL

Europäisches Institut für Transurane, 75-Karlsruhe (Bundesrepublik Deutschland)

(Eingegangen den 27 Mai 1973)

Wegen der besseren Wärmeleitfähigkeit und höheren Dichte der Carbide, Nitride und Carbonitride von Uran und Plutonium gegenüber deren Oxiden wendet sich das Interesse der Reaktorindustrie in steigendem Masse diesen Verbindungen zu. Da wesentliche Eigenschaften dieser Kernbrennstoffe, wie Kompatibilität mit dem Hüllenmaterial, Schwellverhalten und Phasenstabilität in starkem Masse vom Kohlenstoffgehalt abhängen, ergibt sich für das Kernbrennstofflaboratorium eine zunehmende Nachfrage nach exakten Kohlenstoffbestimmungen. Um dieser Nachfrage gerecht zu werden, bedarf es einer schnellen, hinreichend genauen und leicht automatisierbaren Methode. Die als Absolutmethode vielfach bevorzugte Gravimetrie[1,2] zeichnet sich zwar durch hohe Genauigkeit aus, ist aber ausserordentlich zeitraubend. Die manometrische Methode[3] steht der gravimetrischen an Genauigkeit kaum nach, liegt aber mit einem Zeitbedarf von 20 Minuten pro Bestimmung immer noch unzumutbar hoch. In einer Vergleichsstudie der existierenden Verfahren[1] erscheinen die auf der Messung der elektrischen Leitfähigkeit, der thermischen Leitfähigkeit und der Coulometrie beruhenden als die schnellsten, aber auch ungenauesten. Allerdings wurden bei diesem Vergleich Geräte benutzt, die für eine Bestimmung von Kohlenstoffspuren im Stahl konstruiert waren. Wie Malissa[4] zeigte, lassen sich mit einer Variante des auf der Messung der elektrischen Leitfähigkeit beruhenden Analysators, die für höhere Kohlenstoffgehalte konzipiert ist, Genauigkeiten erreichen, die den Anforderungen der organischen Elementaranalyse genügen. Wir haben ein speziell für die Carbidanalyse ausgelegtes Modell benutzt (Carmhomat 6ADG, H. Wösthoff oHG, Bochum) und es durch Verbindung mit einem Hochfrequenzofen und Geräten zur digitalen Datenausgabe zu einer weitgehend automatisierten Anordnung ausgebaut.

Prinzip

Das Probenmaterial wird in einem hochfrequent beheizten Platintiegel im Sauerstoffstrom verbrannt. Im Analysator wird das Kohlendioxid in Natronlauge absorbiert und durch Messung der elektrischen Leitfähigkeitsänderung dieser Natronlauge bestimmt. Wegen der begrenzten Stabilität der Natronlauge ist das Verfahren eichbedürftig. Als Eichsubstanz hat sich Wolframcarbid, dessen Kohlenstoffgehalt gravimetrisch ermittelt wurde, sehr gut bewährt. Der Analysator ist mit einem Ferngeberpotentiometer ausgerüstet, welches—nach Einspeisung mit einer konstanten Gleichspannung—der Leitfähigkeitsänderung proportionale Ausgangsspannungen liefert. Diese werden von einem Digitalvoltmeter gemessen. Die am

Ausgang dieses Instrumentes im BCD-Code parallel anliegenden Daten werden in einem Datenkonverter seriell in den ASC II-Fernschreibcode umgewandelt, auf einer Fernschreibmaschine ausgeschrieben und gleichzeitig auf Lochband gestanzt. Der zeitliche Ablauf der Bestimmung wird von einer Steuerungseinheit gelenkt. Die Waageablesungen werden von Hand über die Fernschreibmaschine eingegeben. Die Berechnung der Analysenresultate und der zugehörigen Standardabweichungen sowie das Ausfüllen der Analysenprotokolle erfolgt über eine Datenverarbeitungsanlage.

BESCHREIBUNG DER ANORDNUNG

Abb. 1 zeigt das Fliessbild der Anlage. Der zur Verbrennung benutzte Hochfrequenzofen (Philips, Modell PH 1095/01) ist zur Fernbedienung eingerichtet. Die Probe (0.1–0.159) befindet sich in einem sauerstoffdurchströmten Quarzrohr im Innern der Anregungsspule. Wegen der ungenügenden elektrischen Leitfähigkeit des Probematerials wird ein Platintiegel (Höhe: 10 mm, Durchmesser: 12 mm, Wandstärke: 0.5 mm) als Suszeptor benutzt. Die Anregungsbedingungen werden so eingestellt, dass der Tiegel eine Temperatur von 1250° erreicht. Aus Sicherheitsgründen befindet sich der Ofen im Handschuhkasten. Zur Abscheidung radioaktiven Staubes durchlaufen die Verbrennungsgase vor dem Verlassen des Handschuhkastens ein elektrostatisches Filter (Fa. H. Wösthoff oHG, Bochum, Typ EF 10) sowie ein Glasfrittenfilter (Porosität 4). In einem Kupferoxidofen wird eventuell gebildetes Kohlenmonoxid bei 600° nachverbrannt. Die Gase treten dann in den Analysator ein. Ein mittels einer Gasmischpumpe abgemessenes Aliquot der Gase gelangt in die Messzelle, in der die bei der Absorption des Kohlendioxids auftretenden Änderung der elektrischen Leitfähigkeit von Natronlauge gegenüber unverbrauchter Lauge gemessen wird[5]. Anstelle der vorgesehenen 0.1 *M* Natronlauge wurde 0.05 *M* Natronlauge verwendet. Damit wurde eine Steigerung der Empfindlichkeit auf das Doppelte erreicht, ohne dass sich das Absorptionsvermögen oder der Linearitätsbereich der Leitwertkurve wesentlich veränderten[6].

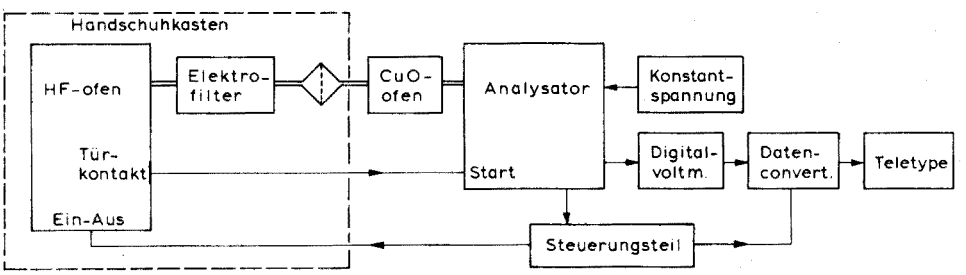

Abb. 1. Fliessbild der Anlage.

Das Ferngeberpotentiometer des Analysators wird mit einer Spannung von 1 V gespeist. Diese wird einer 3 Volt-Konstantspannungsquelle (Fa. J. Duckert, München) über einem niederohmigen Spannungsteiler entnommen. Die Ausgangsspannung des Ferngeberpotentiometers wird mit einem $4\frac{1}{2}$-stelligen Digitalvoltmeter mit BCD-Ausgang (Weston Instruments, Inc., Modell 1294) gemessen. Nach einem

vom Steuerungsteil erteilten Auslöseimpuls erfolgt die serielle Umwandlung der BCD-Daten in den ASC II-Code in einem Datenconverter mit Wortzähler (Fa. Elektronik-Service GmbH, Frankfurt/M.) und das Ausschreiben der Daten auf einer Fernschreibmaschine mit Lochstreifenstanzer (Teletype Corp., Modell ASR 33 TAC). Die Wägedaten und alphanumerischen Probeindizierungen werden von Hand über die gleiche Fernschreibmaschine eingegeben.

Der Analysator ist mit einer Beschickungsautomatik ausgerüstet. Nach Betätigen eines Kontaktes erfolgt selbstätig das Ablassen der verbrauchten Absorptionslösung sowie das Spülen und Neubeschicken der Messzelle. Nach einer Wartezeit von einer Minute, die zur Homogenisierung und Temperatureinstellung der Messlösung erforderlich ist, zeigt das Aufleuchten einer Kontrollampe die Messbereitschaft des Gerätes an. Es wurde nun der Startkontakt der Beschickungsautomatik mit einem Türkontakt am Hochfrequenzofen verbunden, so dass mit dem Öffnen des Ofens zum Probenwechsel die Neubeschickung der Messzelle erfolgt. Parallel zur Kontrollampe wurde ein Relais angeschlossen, das mit dem Aufleuchten der Lampe die Steuerungseinheit in Betrieb setzt. Diese steuert nun die weitere Programmabfolge.

Zwei Minuten nach dem Einschalten der Steuerungseinheit wird der Anfangswert des Digitalvoltmeters abgelesen. Fünf Sekunden später wird der Hochfrequenzofen eingeschaltet. Nach einer Verbrennungszeit von 5 Minuten wird der Ofen abgeschaltet und 2 Minuten später der Endwert am Digitalvoltmeter abgelesen. Sodann wird das Programm angehalten, um es mit dem Öffnen des Ofens und dem Erlöschen der Kontrollampe in seine Ausgangsstellung zurückspringen zu lassen.

Abb. 2 zeigt den logischen Schaltplan des Steuerungsteils. Zum Aufbau wurden integrierte digitale Bausteine verwendet.

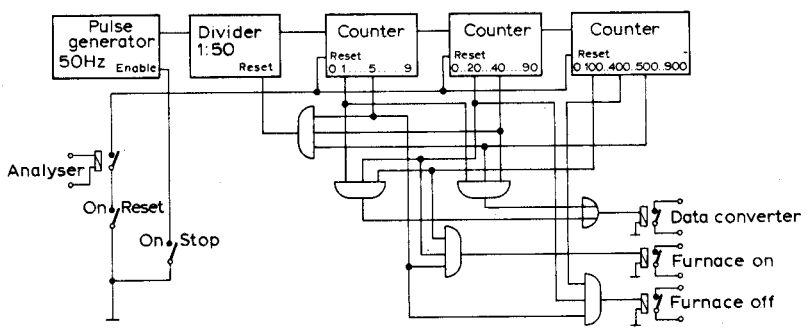

Abb. 2. Logischer Schaltplan des Steuerungsteils.

Auswertung

Die Auswertung der Lochstreifen erfolgt auf einer IBM-1130-Datenverarbeitungsanlage (8K). Die Eingangsdaten umfassen die alphanumerischen Probeindizierungen für Eich- und Analysenproben, die Wägedaten und die Spannungswerte. Um eine Neuindizierung aller numerischen Daten zu vermeiden, müssen die Eingabe der Probeindizes und der Wägedaten sowie die Verbrennungen in gleicher Reihenfolge erfolgen. Die Zuordnung kann dann durch die Datenverarbeitungsanlage erfolgen. Zur Unterscheidung der verschiedenen Eingangsdaten werden alle

Probeindizes durch ein besonderes Zeichen (in unserem Falle ein E) angeführt. Das zweite Zeichen dient der Unterscheidung der Indizes von Eichproben und Analysenproben, geordnet nach Klienten. Wägeresultate und Spannungswerte unterscheiden sich durch ihre Stellenzahl. Während die Spannungswerte stets vierstellig sind, sind die Wägedaten fünf- und mehrstellig.

Im Verlauf des Auswertungsprogramms werden zunächst die eingelesenen Daten nach Probeindizes, Wägeresultaten und Spannungswerten geordnet. Sodann wird aus den Eichwerten der Eichfaktor und seine Standardabweichung errechnet. Mittels dieser Werte wird für die Analysenproben der Kohlenstoffgehalt und dessen Standardabweichung ermittelt. Dabei wird zur Berechnung der Standardabweichung der mittlere Fehler der Methode (10 μg Kohlenstoff), der mittlere Fehler der Einwaage für zwei Wägungen auf einer normalen Analysenwaage (0.14 mg) sowie die Unsicherheit der Eichung (Standardabweichung des Eichfaktors dividiert durch die Wurzel aus der Anzahl der Eichungen) nach dem Fehlerfortpflanzungsgesetz berücksichtigt. Schliesslich werden die Resultate nach Klienten geordnet mit den zugehörigen Probeindizes ausgegeben. Wegen der Schwierigkeiten bei der Verarbeitung alphanumerischer Daten musste das Programm in IDEAL-FORTRAN geschrieben werden.

DISKUSSION

Normalerweise werden zur Kohlenstoffbestimmung widerstandsbeheizte Röhrenöfen bevorzugt. Bei der Verwendung im Handschuhkasten bereitet es jedoch Schwierigkeiten, die von diesen Öfen abgegebene Wärme abzuführen. Zudem stellen die auch bei guter Isolierung stets heissen Stirnflächen der Öfen eine Gefahr für die Handschuhe dar. Wir haben daher einen Hochfrequenzofen, der nur während der Verbrennungszeit von 5 Minuten eine geringe Energie (etwa 500 W) abstrahlt, benutzt.

Die Verbrennung liess sich in den meist benutzten Keramiktiegeln, die mit 1 g Kupfer als Wärmeüberträger beschickt waren, nur schwer unter Kontrolle bringen. Ein weiteres Problem bereitete die Wiedergewinnung des Spaltmaterials aus der geschmolzenen Keramikmasse. Durch Verwendung von Platintiegeln konnten bei konstanter Anregungsenergie reproduzierbare Temperaturen erreicht werden, wodurch eine Automatisierung mit einfachen Mitteln erst ermöglicht wurde. Durch Nachverbrennen der Rückstände zuvor nach obiger Methode untersuchter Uranoxid-Kohlenstoff-Gemische, Wolframcarbide und Urancarbide im Keramiktiegel wurden Restkohlenstoffgehalte zwischen 9 und 47 p.p.m. ermittelt, also Werte, die normalerweise vernachlässigbar sind.

Die Standardabweichung des Verfahrens wurde durch jeweils 5–10 Bestimmungen an vier verschiedenen Urancarbid- und zwei Wolframcarbidproben ermittelt. Während die Standardabweichung von 5 Proben bei 10 μg lag, betrug die einer Urancarbidprobe 20 μg. Der Unterschied war auf dem 99%-Niveau signifikant. Die Werte dieser Probe wurden daher ausgeschlossen und aus den restlichen eine Standardabweichung des Verfahrens von 9.8 μg Kohlenstoff mit 38 Freiheitsgraden berechnet.

Innerhalb einer Ringuntersuchung[7] wurden zwei Urancarbidproben mit 4.5 bzw. 4.8% Kohlenstoff in sieben verschiedenen Laboratorien untersucht. In zwei

Laboratorien wurde die Verbrennung in Hochfrequenzöfen, in den übrigen in Widerstandsöfen durchgeführt. Zur Bestimmung wurden coulometrische, volumetrische, gravimetrische und konduktometrische Verfahren benutzt. Bei einer mittleren Streuung der Mittelwerte der einzelnen Laboratorien von 0.02% um den gemeinsamen Mittelwert weichen unsere Werte um −0.005% bzw. +0.001% vom gemeinsamen Mittelwert ab.

Die Gesamtdauer der Bestimmung beträgt 11 Minuten. Da die Einführung der Probe in das Verbrennungsrohr dabei die einzige von Hand auszuführende Tätigkeit darstellt, bleibt genügend Zeit zur Ausführung der Einwaage, so dass an einem achtstündigen Arbeitstag bis zu 40 Bestimmungen durchgeführt werden können. Eine weitere Erleichterung—wenn auch kein Zeitgewinn—wäre durch die Verwendung einer Waage mit elektronischer Datenausgabe zu erreichen.

ZUSAMMENFASSUNG

Es wird eine Anordnung beschrieben, mit der—unter weitgehender Verwendung handelsüblicher Bausteine—die Kohlenstoffbestimmung in Uran- und Plutonium-Carbiden automatisch durchgeführt wird. Die eigentliche Bestimmung erfolgt durch Absorption des bei der Verbrennung des Kohlenstoffs gebildeten Kohlendioxids in Natronlauge und Messung der Änderung der elektrischen Leitfähigkeit. Der Anfangs- und Endleitfähigkeit proportionale Daten, die Einwaagen sowie die Probekennzeichen werden auf Lochband gespeichert und daraus die Analysenresultate und Analysenprotokolle mittels einer elektronischen Datenverarbeitungsanlage erstellt. Die Standardabweichung des Verfahrens beträgt 10 μg Kohlenstoff bei einer oberen Erfassungsgrenze des Analysators von 10 mg. Der Zeitbedarf für eine Bestimmung beträgt 11 Minuten.

SUMMARY

Instrumentation, consisting largely of commercial components, is described for the automatic determination of carbon in uranium and plutonium carbides. For the determination, the sample is burned in oxygen and the change in electric conductivity of a sodium hydroxide solution during the absorption of the formed carbon dioxide is measured. Voltage values corresponding to the initial and final conductivity, the weights and the sample identification are stored on paper tape for final computer evaluation. The standard deviation of the method is 10 μg of carbon, and the maximum capacity is 10 mg of carbon. The time demand for one determination is 11 min.

RÉSUMÉ

On décrit un appareillage pour doser automatiquement le carbone dans des carbures d'uranium et de plutonium. Cet appareillage a été construit surtout d'éléments commerciaux. Le dosage proprement dit est effectué par combustion de l'échantillon dans l'oxygène et la mesure du changement de la conductivité électrique d'une solution d'hydroxide de sodium pendant l'absorption du dioxide de carbone. Les valeurs digitales correspondant à la conductivité initiale et finale, les poids et les

dénominations des échantillons sont stockés sur bande perforee pour une évaluation finale par ordinateur. L'écart-type de la méthode est 10 μg, et la capacité maximale est 10 mg de carbone. La durée d'un dosage est de 11 min.

LITERATUR

1 G. Serrini and J. Collin, *Anal. Chim. Acta*, 32 (1965) 148.
2 F. Lievens, A. Lecocq und M. Constant, *Z. Anal. Chem.*, 247 (1969) 171.
3 D. Crossley und E. Foster, *AERE-R 4359*, 1963.
4 H. Malissa, *Mikrochim. Acta*, (1960) 127; s.a. W. Stuck, *Mikrochim. Acta*, (1960) 421.
5 W. Schmidts und W. Bartscher, *Z. Anal. Chem.*, 181 (1961) 54.
6 W. Bartscher und W. Schmidts, *Z. Anal. Chem.*, 203 (1964) 168.
7 *Bericht AIKEM-KAR-10*, Alkem GmbH, Wolfgang b. Hanau, 1972.

Analytica Chimica Acta, 68 (1974) 203–204

SHORT COMMUNICATION

Detection of various α-substituted ketones via chemiluminescence of 5-amino-2,3-dihydro-1,4-phthalazinedione

HARVEY W. YUROW and SAMUEL SASS
Chemical Laboratory, Edgewood Arsenal, Md. 21010 (U.S.A.)
(Received 9th March 1973)

The chemiluminescence of 5-amino-2,3-dihydro-1,4-phthalazinedione (luminol), which was reported for the first time in 1928[1], requires the presence of a strong base, an oxidant such as hydrogen peroxide, and a catalyst. The most commonly used catalysts are iron complexes such as potassium hexacyanoferrate(III) or hemin[2], copper–ammonia complexes and various other metal compounds[3]. Little work has been reported on the detection of organic compounds by the luminol reaction.

A number of organic compounds are reported to react with hydrogen peroxide in basic solution, including: α,β-unsaturated carbonyl compounds, quinones, 1,2-diketones, α-ketoacids, mercaptans, aldehydes and nitriles[4]. In some instances unstable peroxy intermediates are formed. If these intermediates are of sufficient stability and have appreciable oxidizing power then they may induce the chemiluminescence of luminol.

Experimental

Reagents. The 5-amino-2,3-dihydro-1,4-phthalazinedione (Aldrich, 97%) was prepared as an 0.002 *M* solution in 0.20 *M* sodium hydroxide. The hydrogen peroxide was prepared fresh daily from Mallinckrodt 30% reagent grade material, diluted 1+99 with water containing 0.002 *M* tetrasodium ethylenediaminetetracetate, and stored in a dark bottle. The organic compounds tested were commercial materials in the purest grades available, with the exception of hydroxypyruvic aldehyde which was synthesized from 1,3-dihydroxy-2-propanone[5]. These compounds were prepared as aqueous solutions for testing.

Equipment. Relative light intensities were measured with the Aminco-Bowman spectrofluorometer. To facilitate measurements of rapid reactions, the handle of the cell compartment cover-plate was removed to allow insertion of hypodermic syringe needles into a 1-ml microcell.

Procedure. A 0.2-ml sample (1.0 mg ml^{-1}) was introduced into the cell. The time-base mode was started at an emission wavelength of 410 nm, and 0.2-ml volumes each of luminol and hydrogen peroxide were introduced simultaneously into the cell. The relative light intensities were measured and corrected for molecular weight differences among the various compounds. Results as given in Table I are for duplicate determinations.

TABLE I

CHEMILUMINESCENCE INDUCED IN LUMINOL BY VARIOUS ORGANIC COMPOUNDS

Compound	*Relative intensity*	*Compound*	*Relative intensity*
2,3-Butanedione	1700	Hydroxypyruvic aldehyde	160
2,3-Pentanedione	2700	Pyruvic acid	0
2,3-Hexanedione	2800	Phenyl glyoxal	5800
4-Methyl-1,2-cyclohexanedione	15	Glyceraldehyde	20
1,4-Dibromo-2,3-butanedione	190	1,3-Dihydroxy-2-propanone	400
1-Phenyl-1,2-propanedione	3400	3-Hydroxy-2-butanone	75
2,4-Pentanedione	0	4-Hydroxy-3-methyl-2-butanone	0
Glyoxal	100	Cyclobutanone	670
Pyruvic aldehyde	280	Cyclopentanone	0

Results and discussion

The results for the various compounds tested are given in Table I.

The reaction has applicability as a spot test in a 10×75 mm test tube. With one drop each of luminol and peroxide, amounts of 2,3-butanedione of the order of 5 μg in 0.05 ml solution were detected.

Positive tests are given by various ketones substituted in the α-position by a group that increases the fractional positive charge on the carbonyl group such as carbonyl oxygen or hydroxyl. The 1,2-diketones such as 2,3-butanedione are known to react with strongly nucleophilic hydroperoxide anion to form unstable hydroperoxy compounds of the type

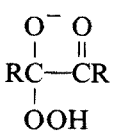

which decompose to give acids[6]. These hydroperoxides are sufficiently strong oxidants to produce chemiluminescence in luminol.

The test is capable of distinguishing comparable amounts of a number of closely related compounds, *e.g.* 1,3-dihydroxy-2-propanone and glyceraldehyde, 3-hydroxy-2-butanone and 4-hydroxy-3-methyl-2-butanone, 2,3-hexanedione and 4-methyl-1,2-cyclohexanedione, and cyclobutanone and cyclopentanone. The failure of the test for pyruvic acid as compared to pyruvic aldehyde may be related to the assumed dinegative charge on the hydroperoxide intermediate for the former.

REFERENCES

1 H. O. Albrecht, *Z. Phys. Chem.*, A136 (1928) 321.
2 W. Specht, *Angew. Chem.*, 50 (1937) 155.
3 W. R. Seitz, W. W. Suydam and D. M. Hercules, *Anal. Chem.*, 44 (1972) 957.
4 J. G. Wallace, *Hydrogen Peroxide in Organic Chemistry*, DuPont, Wilmington, Del., 1962, pp. 31–47.
5 W. E. Evans, Jr., C. J. Carr and J. C. Krantz, Jr., *J. Amer. Chem. Soc.*, 60 (1938) 1628.
6 C. A. Bunton, *Nature*, 163 (1949) 444.

Analytica Chimica Acta, 68 (1974) 205–206

SHORT COMMUNICATION

The temperature-dependence of fluorescence as an aid to the identification of oxybarbiturates

L. A. KING, J. N. MILLER and D. THORBURN BURNS

Department of Chemistry, Loughborough University of Technology, Loughborough LE11 3TU

J. W. BRIDGES

Department of Biochemistry, University of Surrey, Guildford (England)

(Received 30th April 1973)

A recent publication described the determination of oxybarbiturates by means of their low-temperature luminescence[1]. It was shown that, in certain cases, the luminescence spectra and phosphorescence lifetimes could provide information on the identity of an unknown barbiturate. The present communication describes a further procedure, which facilitates the characterization of certain barbiturates by making use of the temperature-dependence of their fluorescence.

Experimental

Fluorescence intensity measurements were made with a Baird-Atomic SF100E spectrofluorimeter (Baird-Atomic Ltd., Braintree, Essex) fitted with a Bryans Model 2700 recorder (Bryans Ltd., Mitcham, Surrey). The excitation and emission monochromators were set at 260 nm and 430 nm, respectively, and the slits adjusted to give an overall resolution of 32 nm. The spectrofluorimeter cell housing was modified to accomodate a silica Dewar flask with an unsilvered stem. (A similar arrangement is used in phosphorimetry.) A silica sample tube (i.d. 2 mm, wall thickness 1 mm) was located centrally in the Dewar stem together with an ordinary mercury thermometer (0–110°). The Dewar was filled with distilled water heated to *ca.* 350° K, and the fluorescence intensity of each sample was observed as it cooled slowly. The sample tube itself was used as a stirrer between measurements, to ensure a uniform temperature in the Dewar, and samples were protected from incident light as much as possible.

Phenobarbitone (5-phenyl-5-ethylbarbituric acid), barbitone (5,5-diethylbarbituric acid), seconal (5-allyl-5-(1′methylbutyl)barbituric acid), amylobarbitone (5-ethyl-5-(3′methylbutyl)barbituric acid), butabarbitone (5-ethyl-5-sec-butylbarbituric acid), and pentabarbitone (5-ethyl-5-(1′methylbutylbarbituric acid) were examined in concentrations of *ca.* 30 μg ml^{-1} in aqueous 0.1 *M* sodium hydroxide.

Results and discussion

The relationship between temperature (T) and fluorescence intensity (I_f) for three oxybarbiturates is shown in Fig. 1. The logarithmic ordinate used was found

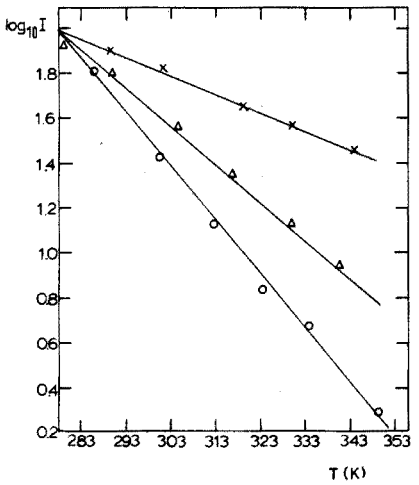

Fig. 1. The fluorescence of phenobarbitone (×), seconal (△) and barbitone (○) as a function of temperature. The data have been adjusted to give similar fluorescence intensities at 278°K. The straight lines represent the best fit by least-squares analysis. Each point is the mean of three determinations.

to produce linear plots over the limited temperature range studied. Attempts to fit the data to the theoretically derived expression[2] $(1/(I_f)-1)=A\cdot e^{-E/RT}$, where A and E are constants, were unsuccessful. Phenobarbitone, seconal and barbitone can be readily distinguished from one another, but amylobarbitone, butabarbitone and pentabarbitone show a similar temperature-dependence to that of barbitone. The other luminescence properties of the last four compounds are also very similar, whereas those of seconal and phenobarbitone show further differences. Both have lower quantum yields of fluorescence at room temperature, and phenobarbitone is the only one of the barbiturates studied here which exhibits appreciable phosphorescence at 77°K[3,4].

In favourable cases, measurements of fluorescence intensity at only two different temperatures might be sufficient to obtain a provisional identification of a barbiturate, and the principle may be applicable to other classes of compound. Since C-5 dialkylbarbiturates change in fluorescent intensity by *ca.* 2% per degree at 298 K, careful attention to temperature control is clearly desirable in quantitative work.

REFERENCES

1 L. A. Gifford, W. P. Hayes, L. A. King, J. N. Miller, D. Thorburn Burns and J. W. Bridges, *Anal. Chim. Acta*, 62 (1972) 214.
2 E. J. Bowen and J. Sahu, *J. Phys. Chem.*, 63 (1959) 4.
3 C. I. Miles and G. H. Schenk, *Anal. Chem.*, 45 (1973) 130.
4 L. A. Gifford, W. P. Hayes, L. A. King, J. N. Miller, D. Thorburn Burns and J. W. Bridges, *Anal. Chem.*, in press.

Analytica Chimica Acta, 68 (1974) 207–211

SHORT COMMUNICATION

Determination of nanogram quantities of mercury in sea water

JÓN ÓLAFSSON
Marine Research Institute, Skúlagata 4, Reykjavík (Iceland)
(Received 8th May 1973)

The mercury concentrations that have been reported for sea water[1–11] cover the whole range from 0.5 to 364 ng l^{-1}, excluding the values from the contaminated Minamata Bay[12]. Many of the recent values have been obtained by neutron activation analysis[2–5], but spectrophotometric determination on a dithizone extract[6–8] or cold mercury vapour[9–11] has also been employed. Despite the very high sensitivity of the flameless atomic absorption technique, large sample volumes have been required in order to determine mercury in sea water. As a preliminary concentration step for such measurements, workers have used both dithizone extraction[10] and tin(II) chloride reduction followed by volatilization of the mercury into an absorbing solution[9].

Mercury may be collected from a gas stream by amalgamation on a noble metal[13,14]. This permits interfering substances to be vented out of the analytical system before flameless atomic absorption measurement. The amalgamation can also serve as a concentration technique. Elemental gold[14] has been used to collect mercury pyrolyzed from geological or biological samples.

This communication describes a flameless atomic absorption procedure coupled to amalgamation on gold, which is presently used for the determination of nanogram quantities of mercury in samples from North Atlantic waters.

Experimental

Apparatus. A Varian Techtron AA5 atomic absorption spectrophotometer was used. The burner was replaced with a platform holding, between two spring clips, a silica cell of 100 mm optical path length. Instrumental settings were as follows: hollow-cathode lamp current, 3 mA; wavelength, 253.7 nm; slit width, 100 μm; and scale expansion $\times 4$. The spectrophotometer was equipped with a Varian A-25 strip-chart recorder, which was used at a rate of 2 cm min^{-1}.

Mercury collector. About 20 g of gold foil (0.06 mm thick) was cut into *ca.* 5×2 mm pieces which were bent U-shaped, washed in concentrated nitric acid and deionized water, dried and packed into a silica tube to form a *ca.* 9-cm layer held in position with a silica wool plug at the outlet end. The tube (10 mm i.d. and 12 cm long) had inlet and outlet arms (6 mm i.d.), which were 6 and 12 cm long, respectively. The body of the tube was closely wound with *ca.* 1.5 m of 5.4 ohm m^{-1} resistance wire, connected to an ammeter and a variable transformer. The

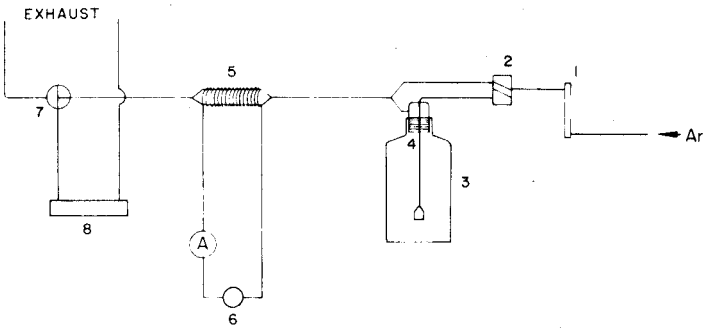

Fig. 1. Schematic diagram of apparatus. (1) Flowmeter, (2) double-bore stopcock, (3) reduction vessel, 500-ml Pyrex bottle with ground 24/29 neck, (4) Drechsel head with 24/29 joint and fritted glass distribution tube, (5) mercury collector, (6) variable transformer, (7) Teflon T-bore stopcock, (8) optical cell.

apparatus was connected up as shown in Fig. 1, all connections being made of 6-mm i.d. P.T.F.E. tubing. The flow of argon carrier gas was checked by means of a calibrated flowmeter.

Reagents. The nitric acid was selected *pro analysi* grade of low mercury content or acid redistilled from a silica still.

A 20% (w/v) solution of tin(II) chloride in 2 *M* hydrochloric acid was aerated for 30 min before use, to remove mercury traces.

Mercury standards. A stock solution (100 μg Hg ml^{-1}) was prepared by dissolving 0.1354 g of Specpure mercury(II) chloride (Johnson-Matthey Ltd) in 1 *M* nitric acid and diluting to 1 l. An intermediate standard was prepared by diluting 5 ml of the stock solution to 500 ml with 1 *M* nitric acid. For the working standard (20 ng Hg ml^{-1}), 5 ml of the intermediate standard was diluted to 250 ml with 1 *M* nitric acid.

Results and discussion

Reduction and amalgamation. Early results showed that after inorganic mercury salts in deionized water had been reduced with tin(II) chloride, the mercury vapour could be collected from a stream of argon (1 l min^{-1}) by amalgamation with gold. Moreover, the mercury could be completely released from the gold by heating and thence carried with a stream of argon into the optical cell for measurement. However, when this procedure was applied to sea water spiked with mercury, low and irreproducible recoveries were found. This was remedied by greatly reducing the argon flow rate and simultaneously increasing the time of aeration. At fast argon flow rates, droplets of sea water are carried over to the mercury collector, and their chloride content greatly reduces the extent of amalgamation.

The rate of recovery of 20 ng of mercury from 450 ml of sea water was investigated at an argon flow of 140 ml min^{-1}, which was intermittently interrupted, and the mercury accumulated on the collector was determined as outlined above. About 50% recovery was achieved after 7 min, but total recovery required an aeration time of 35 min. Similar rates of recovery were found for deionized water. The aeration time for 100% recovery depends on sample size; thus it takes 25 min to recover all mercury from a 150-ml sea water sample in a 250-ml

reduction vessel, and 15 min with a 50-ml sample in a 100-ml vessel.

Release and measurement. The mercury in 450 ml of sea water amounts to only a few, or at most, a few tens, of nanograms, which must all be present simultaneously in the absorption cell if maximal sensitivity is to be attained. This is possible only if one knows how the distribution of mercury vapour in the argon stream after release is affected by the flow rate of argon and the heating rate of the mercury collector. The temperature of the argon emerging from the collector (measured by inserting a thermocouple into the silica tube) was found to be about 320° after a time of heating corresponding to mercury release. The temperature of release of mercury from gilded quartz is about 300°[14].

Thermal expansion of the argon gas means that the flow through the absorption cell at maximal absorbance will be about twice the value read on the flowmeter which is calibrated at room temperature. With this in mind, a careful study was made of the shape and height of absorbance peaks (chart speed 20 cm min^{-1}) obtained by releasing 20 ng of mercury from the collector at: (1) argon flow settings from 100 to 450 ml min^{-1} (Fig. 2); and (2) with current from 2 to 4 A applied to the collector tube. This showed that at argon flow rates between 150 and 240 ml min^{-1} and with a current of 3 A or more, the mercury was released fast enough from the gold for all its vapour to be present in the absorption cell at the moment of maximal absorbance. A current of 3.6 A and an argon flow of 180 ml min^{-1} produces an absorbance peak similar to curve 2 in Fig. 2 after *ca.* 34 s of heating, and ensures long life of the silica tubing.

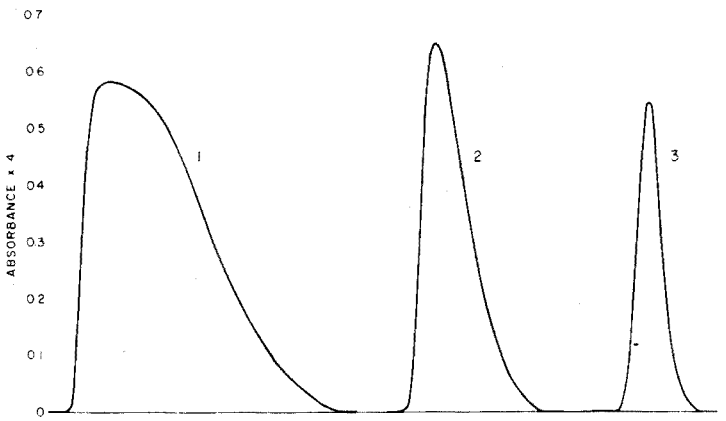

Fig. 2. Effect of varying the argon flow on the absorbance produced by 20 ng of mercury. Chart speed 20 cm min^{-1}. (1) 100 ml Ar min^{-1}, (2) 220 ml Ar min^{-1}, (3) 450 ml Ar min^{-1}.

Recommended procedure

Draw the sea water sample from the water bottle on board ship into a 500-ml Pyrex glass bottle containing 9 ml of concentrated nitric acid and marked at 450 ml. After reaching the laboratory, add 15 ml of the 20% tin(II) chloride solution down the inner wall of the flask. Quickly connect the flask to the Drechsel head (Fig. 1) and start an argon flow of 140 ml min^{-1} through the sample and past the absorption cell. After 40 min, turn stopcock 2 to let the argon bypass the sample, and about 30 s later turn the T-bore stopcock 7 to divert the argon flow into the

absorption cell. Adjust the argon flow to 180 ml min^{-1}, zero the spectrophotometer, apply a current of 3.6 A to the collector tube, start the recorder and, after the absorbance has reached a maximum, turn off the current and allow the tube to cool for a short while before the next analysis.

Blank. As the sample is not transferred between containers after collection, the risk of contamination is slight. The only probable source of blank is the nitric acid used for acidification; acid of low mercury content should be selected after applying the above method to variable amounts of the acid in deionized water.

Calibration. The method is calibrated by adding aliquots of the working standard to 450 ml of acidified sea water which is of very low mercury content on account of having been stored at its natural pH in a polyethylene container. A linear relationship was found between mercury and absorbance in the range 0–24.0 ng of mercury in the sample.

TABLE I

MERCURY IN SEA WATER AT STATION B4/73-90

(63°07'N, 19°54'W)

Depth (m)	*Hg (ng l^{-1})*
0	13.0, 13.6
400	18.6
600	18.7
800	10.5
1000	10.2, 9.77

Application

Table I shows the results for sea water samples collected off the south coast of Iceland during a cruise of R/V Bjarni Saemundsson. These values compare well with other recent results for N.E. Atlantic Ocean water[8]. Seven replicate determinations on coastal sea water (Faxa Bay, S.W. Iceland) gave a mean concentration of 12.9 ng Hg l^{-1}, with a standard deviation of 0.60. The values represent total mercury as the sample was unfiltered; inhomogeneities in the sample may have influenced the results and hence increased the standard deviation. Besides sea water, the method has been applied to other natural waters such as rain and ground water.

On the premise that all the mercury vapour is present in the cell at the moment of maximal absorbance, the molar absorptivity for mercury vapour in argon can be calculated; the value found was $\varepsilon = 5.0 \cdot 10^6$ l $mole^{-1}$ cm^{-1}, which is comparable to $\varepsilon = 4.1 \cdot 10^6$ l $mole^{-1}$ cm^{-1} reported for mercury vapour in dry air[15]. Sensitivity (for 1% absorbance) was 0.47 ng.

Several substances have been reported to interfere with the reduction and aeration of mercury[16,17], iodide and bromide producing the greatest interference. Theitechnique proposed has been used to recover 20 ng of mercury from sea water and distilled water, but no difference in response was found.

This work was partly supported by the Ministry of Industry.

REFERENCES

1 A. Stock and F. Cucuel, *Naturwiss.*, 22 (1934) 390.
2 D. F. Robertson, L. A. Rancitelli, J. C. Langford and R. W. Perkins, *Baseline Studies of Pollutants in the Marine Environment*, Brookhaven National Laboratory, 1972, p. 231.
3 H. V. Weiss and T. E. Crozier, *Anal. Chim. Acta*, 58 (1972) 231.
4 P. M. Williams and H. V. Weiss, *J. Fish. Res. Board Can.*, 30 (1973) 293.
5 H. V. Weiss, S. Yamamoto, T. E. Crozier and J. H. Mathewson, *Environ. Sci. Techn.*, 6 (1972) 645.
6 K. Hosohara, *J. Chem. Soc. Jap., Pure Chem. Sect.*, 82 (1961) 1107.
7 J. D. Burton and T. M. Leatherland, *Nature*, 231 (1971) 440.
8 T. M. Leatherland, J. D. Burton, M. J. McCartney and F. Culkin, *Nature*, 232 (1971) 112.
9 G. Topping and J. M. Pirie, *Anal. Chim. Acta*, 62 (1972) 200.
10 R. Chester, D. Gardner, J. P. Riley and J. Stoner, *Mar. Pollut. Bull.*, 4 (1973) 28.
11 R. A. Carr, J. B. Hoover and P. E. Wilkniss, *Deep-Sea Res.*, 19 (1972) 747.
12 K. Hosohara, H. Kozuma, K. Hawasaki and T. Tsuruta, *J. Chem. Soc. Jap., Pure Chem. Sect.*, 82 (1961) 1479.
13 V. I. Muscat, T. J. Vickers and A. Andren, *Anal. Chem.*, 44 (1972) 218.
14 See, *e.g.*, J. Marinenko, I. May and J. H. Dinnin, *U. S. Geol. Surv. Prof. Pap.*, 800 B (1972) B151.
15 J. F. Uthe, F. A. J. Armstrong and M. P. Stainton, *J. Fish. Res. Board Can.*, 27 (1970) 805.
16 G. Lindstedt, *Analyst*, 95 (1970) 264.
17 S. H. Omang, *Anal. Chim. Acta*, 63 (1973) 247.

Analytica Chimica Acta, 68 (1974) 212–216

SHORT COMMUNICATION

Spectroscopic determination of atomization efficiency ($CuCl \rightarrow Cu + Cl$) in an air–hydrogen flame

KUNIYUKI KITAGAWA, MASAAKI YANAGISAWA and TSUGIO TAKEUCHI

Department of Synthetic Chemistry, Faculty of Engineering, Nagoya University, Chikusaku, Nagoya (Japan)

(Received 28th March 1973)

Observations on the behavior of species in flames are of interest in analysing interferences in atomic emission or absorption spectrometry, and some papers[1,2] on measurements of atomization efficiency (β-values) have been published. In a previous paper[3], the degree of ionization of manganese atoms in a microwave-excited plasma torch was determined by comparison of ionic and atomic lines. The advantage of this method is that no assumption of reaction equilibrium is required, only local thermal equilibrium being necessary. In the present work, an equation for this method of determining the β-value was derived. In the experimental work, a solution of copper(II) chloride was sprayed into an air–hydrogen flame supported by a Beckman burner, and two atomic copper lines and a CuCl line consisting of many rotational lines were observed.

Calculation

The temperature was measured by the well known two-lines method; two atomic copper lines which are of different upper-state energies were used:

$$T = E_1 - E_2/\ln(R_2/R_1) + \ln(\lambda_2 g_1 A_1 p/\lambda_1 g_2 A_2) \quad (1)$$

where T is the temperature in °K, E_1 and E_2 are the upper energies, R_1 and R_2 the responses measured, λ_1 and λ_2 the wavelengths, g_1 and g_2 the statistical weights, A_1 and A_2 the Einstein transition probabilities for emission, and p is the factor for the response of the photomultiplier.

As in the previous treatment for the degree of ionization[3], the ratio of the copper and CuCl emissions can be expressed as follows:

$$pR_{Cu}/R_{CuCl} = \frac{\beta\lambda_{CuCl}Q(T)_{CuCl}g_{Cu}A_{Cu}}{(1-\beta)\lambda_{Cu}Q(T)_{Cu}g_{CuCl}A_{CuCl}} \exp\left(\frac{E_{CuCl}-E_{Cu}}{kT}\right) \quad (2)$$

where $Q(T)$ is the partition function. $Q(T)_{CuCl}$ is expressed as a product $q_v(T)q_e(T)$ for the line including all rotational lines, which constitute the P- and R-branches. The vibrational and electronic partition functions are written as follows, respectively:

$$q_v(T) = e^{-hc\omega_0/2kT}/1 - e^{-hc\omega_0/kT} \quad (3)$$

$$q_e = \sum_j g_j \exp(-E_j/kT) \quad (4)$$

where h is Planck's constant, c the light velocity, ω_0 the wave number of the fundamental vibration, and E_j the energy of state j. $q_e(T)$ was calculated, on the assumption that $g_j = 1$, from Table I, and $Q(T)_{Cu}$ was taken from the results of De Galan *et al.*[4]. For $g_{CuCl}A_{CuCl}$, an approximate calculation for Σ–Σ and 0–0 transitions was carried out:

$$g_{CuCl}A_{CuCl} = \frac{64\pi^4}{3h\lambda_{CuCl}^3}\mu_e^2\left(\int\psi_{v=0}^2\,dx\right)^2$$

where the second term is unitary. The electronic transition moment μ_e was calculated, without regard to the overlapping integral $\mu_e = eab\,r_e$, where e is the electron charge, and a and b are coefficients in the wave function of the ground-state CuCl:

$$\psi_{CuCl}^0 = a\phi_{Cu} + b\phi_{Cl} \tag{5}$$

and without regard to the overlapping integral, $a^2 + b^2 = 1$. Furthermore, in order to estimate a and b, use was made of the Pauling's electronegativities of copper and chlorine. The charge on the copper atom $q_{Cu} \approx \int 2\psi_{CuCl}^{0^2}\,dv \approx 2a^2$. q_{Cu} may be expressed in terms of the electronegativities χ_{Cl} and χ_{Cu} as follows:

$$q_{Cu} = e[1 - \exp\{-(\chi_{Cl} - \chi_{Cu})^2/4\}] \tag{6}$$

The results estimated were as follows:
$q_{Cu} = -q_{Cl} = 0.26e$, $a = 0.608$, $b = 0.794$ and $\mu_e = 2.51 \cdot 10^{-35}$ in c.g.s. with $r_e = 2.16$ Å.

Lines observed

The copper lines observed were those which had different upper energies; the observed CuCl emission line was a Σ–Σ transition with $v = v' = 0$. These are asterisked in Table I.[5,6]

TABLE I

LINES PROPERTIES

Cu I			*CuCl emission*			
λ (nm)	E (cm^{-1})	gA ($10^8\ s^{-1}$)	$\lambda_{0,0}$ (nm)	E (cm^{-1})	ω_e (cm^{-1})	*Transition*
327.4*	0–30535	1.9	395.8	0–25282	383	F–$^1\Sigma(X)$
249.2*	0–40114	0.31	433.4*	0–23077	406	$^1\Sigma$–$^1\Sigma(X)$
282.4	11203–46598	3.1	435.5	0–22973	395	$^1\pi$–$^1\Sigma(X)$
296.1	11203–44963	0.97	484.8	0–20635	399	C–$^1\Sigma(X)$
261.8	11303–49383	4.3	488.3	0–20488	401	B–$^1\Sigma(X)$
			526.4	0–19001	410	A–$^1\Sigma(X)$

With all values of constants inserted, eqn. (2) can be written as follows:

$$\beta = 1 - 1/1 + 0.66\,\frac{R_{Cu,327.4}}{R_{CuCl,433.4}}\,f(T) \tag{7}$$

with the modified eqn. (1)

$$T = 13{,}807/\ln(R_{327.4}/R_{249.2}) - 1.897\,. \tag{8}$$

where

$$f(T) = \frac{2.598e^{-0.2999/T'}}{1-e^{-0.5998/T'}} \frac{q_e(T')}{Q_{Cu}(T')} \exp(-11.02/T')$$

and

$$T' = T/1{,}000. \tag{9}$$

According to the result of De Galan *et al.*[4]

$$Q_{Cu}(T') = 2.1905 - 1.938 \cdot 10^{-1} T' + 5.1491 \cdot 10^{-2} T'^2 - 1.4419 \cdot 10^{-3} T'^3$$

and

$$q_e(T') = 1 + \exp(-36.37/T') + \exp(-33.20/T') + \exp(-33.05/T') + \exp(-29.69/T') + \exp(-29.48/T') + \exp(-27.34/T'),$$

which was derived directly from the definition with Table I on the assumption that $g_j = 1$.

Experimental

A Nippon Jarrell-Ash AA-1E atomic absorption and flame emission spectrometer was fitted with a Beckman-type burner and the response was recorded on a Hitachi QPD-54 recorder.

A 0.095 *M* copper solution was prepared by dissolving copper(II) chloride (analytical grade) in deionized water.

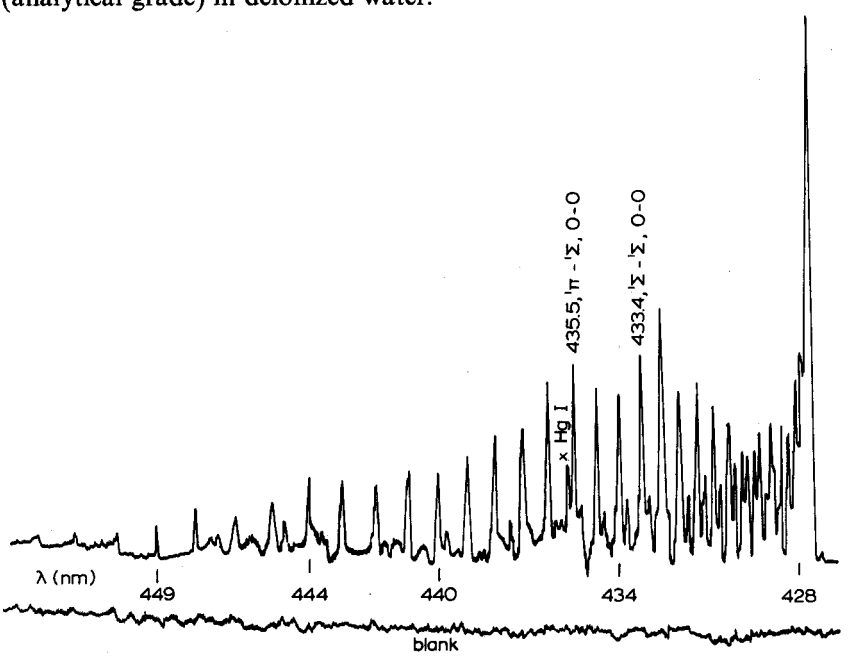

Fig. 1. Spectrum of CuCl. Slit width, 50 μm; air, 3 l min^{-1}; hydrogen, 15 l min^{-1}; aspirating rate, 0.40 mmol min^{-1}.

The solution was introduced at a rate of 2.82 ml min^{-1}, and the resultant emission lines of Cu I and CuCl were observed through a rectangular slit situated in front of the slit of the monochromator, the width of which was 50 μm.

Results and discussion

The observed spectrum of the CuCl emission is shown in Fig. 1; the Cu I 327.4-nm line was much more intense than the Cu I 249.2-nm and CuCl 433.4-nm emission. The voltage applied to the photomultiplier for the measurement at 327.4 nm was 440 V, and 740 V for the others. The plot $\ln(\lambda pR/gA)$ *versus* E/k for correcting the photomultiplier sensitivity for the applied voltage, by means of radiation from a copper hollow-cathode lamp (5 mA current), is shown in Fig. 2, the correction factor was found to be $e^{7.68}$, and the excitation temperature of copper atoms was found to be 3,000 °K in the hollow-cathode lamp. The intensity profiles above the burner nozzle for the Cu I lines and the CuCl emission are shown in Fig. 3; the results computed for temperature and β-value, by means of eqns. (7) and (8), are shown in Fig. 4.

The β-value was found to be 70–90% in the temperature range of 1,700–2,200 °K. The high excitation temperature did not cause high β-values, which suggests that atoms obtain energy after dissociation, and that the excitation

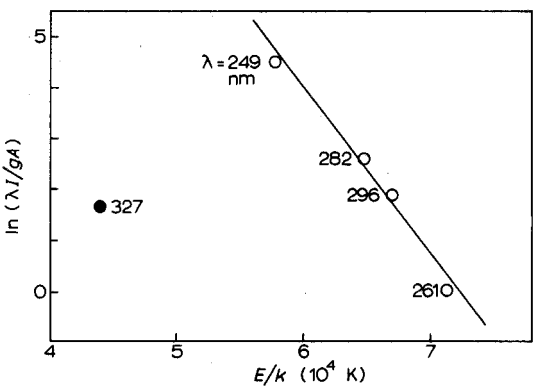

Fig. 2. Plot of ln $(\lambda I/gA)$ *vs.* E/k. Current for hollow-cathode lamp, 5 mA.

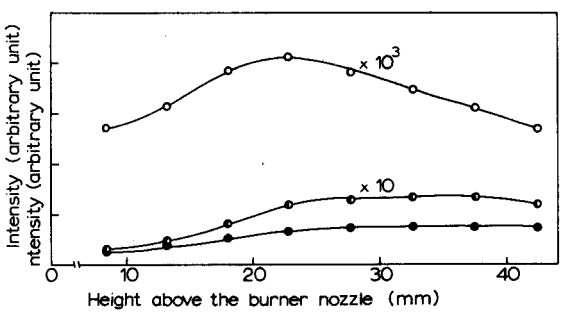

Fig. 3. Intensity profiles above the burner nozzle for CuI and CuCl emission. Air, 3 l min^{-1}; hydrogen, 9 l min^{-1}. (○) CuI, 327.4 nm; (◐) CuCl, 433.4 nm; (●) CuI, 249.2 nm.

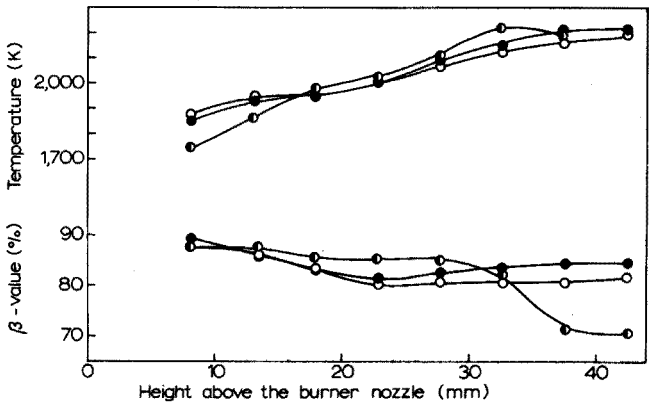

Fig. 4. Excitation temperature of copper atoms and β-value calculated. Flow rate of hydrogen: (◐) 6 l min^{-1}, (●) 9 l min^{-1}, (○) 12 l min^{-1}; air, 3 l min^{-1} throughout.

temperature is not necessarily consistent with translational, vibrational or rotational phenomena in the diffusion flame.

The β-value measured in this work may be different from the current, which is usually determined as an atomization efficiency and would be somewhat lower than the value obtained here. This method, however, is valid for most experimental purposes, with an advantage that no reaction equilibrium is assumed.

REFERENCES

1 L. De Galan and J. D. Winefordner, *J. Quant. Spectrosc. Transfer*, 7 (1967) 251.
2 S. R. Koityohann and E. E. Pickett, *Spectrochim. Acta*, 26B (1970) 349.
3 K. Kitagawa and T. Takeuchi, *Anal. Chim. Acta*, 60 (1972) 309.
4 L. De Galan, R. Smith and J. D. Winefordner, *Spectrochim. Acta*, 23B (1968) 521.
5 C. H. Corliss and W. R. Bozman, *NBS Monogr h 53*, 1962.
6 G. Herzberg, *Molecular Spectra and Molecular Structure. I*, D. Van Nostrand, New York, 1950.

Analytica Chimica Acta, 68 (1974) 217–221

SHORT COMMUNICATION

A spectrophotometric method for the determination of traces of nitrate. Application to water analysis

B. NAWRATIL, M. MARCANTONATOS and D. MONNIER
Department of Inorganic and Analytical Chemistry, University of Geneva, Geneva (Switzerland)
(Received 28th June 1973)

Numerous colorimetric methods have been proposed for the determination of micro amounts of nitrate. Many of them require the nitration, in concentrated sulfuric acid, of aromatic compounds such as xylenols[1–3], chromotropic[4–6] and phenoldisulfonic[7,8] acids, toluene[9] and fluorescein[10], while others are based either on the oxidation of compounds such as diphenylbenzidine[11], diphenylaminesulfonic acid[12,13] and strychnidine[14], or on the reduction of nitrate to nitrite and formation of coloured diazo compounds[15–17]. Sensitive spectrophotometric techniques based on brucine[18–21] and aminopyrene[22] have also been reported.

In the present communication, a colorimetric determination of traces of nitrate is proposed, based on the reaction reported by Meyer[23,24] between nitric acid and bianthronyl ([9,9′-bianthracene]-9,9′-hydro-10,10′-dione) in 96% sulfuric acid. This method is characterized by high sensitivity and good reproducibility, without the need for heating or extraction, necessary to several of the methods cited above; the selectivity is good enough for a direct determination of nitrate in natural waters.

Bianthronyl (I) reacts with nitrate in sulfuric acid (96%) to give a red coloured intermediate compound; it was shown that in subsequent steps this yields anthraquinone(III) (Fig. 1).

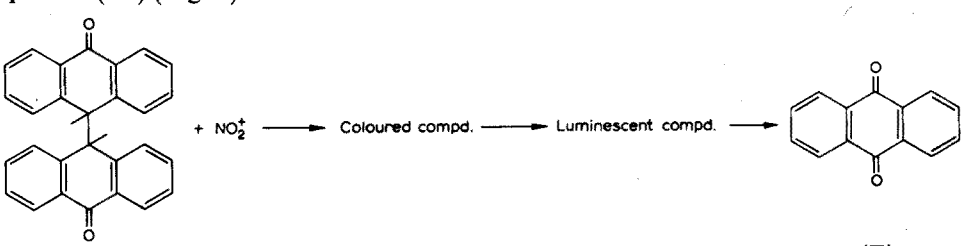

(I) (II) (III)

The intermediate compound (II) which constitutes the basis of the proposed method goes through a maximum stationary concentration within 3–5 min, as evidenced by its absorption at 500 nm *versus* time (Fig. 2).

The mechanism of this reaction is currently being investigated.

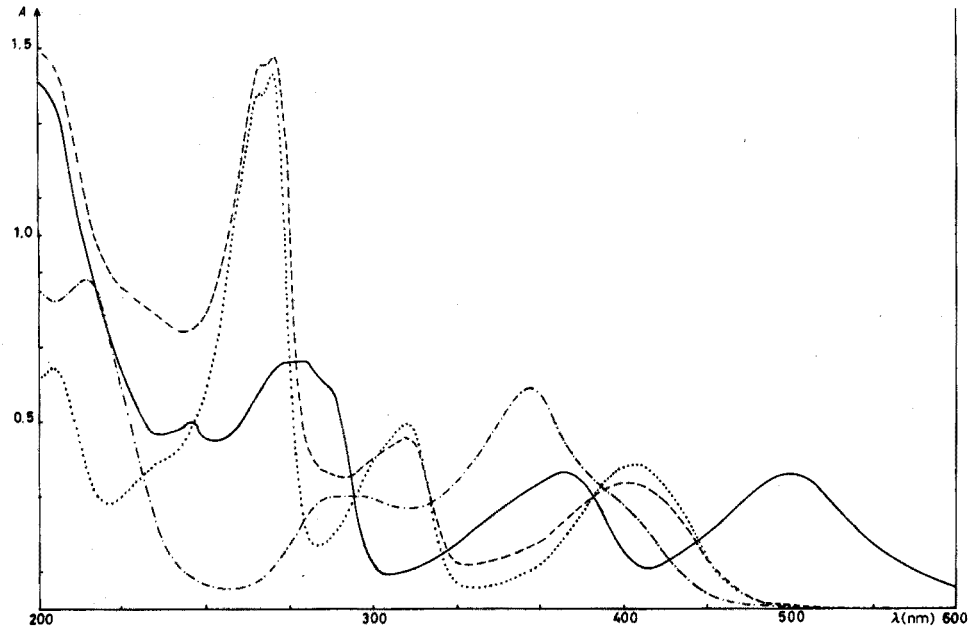

Fig. 1. Spectral evolution of nitrate–bianthronyl reaction in sulfuric acid (96%). Reagent (I) alone (–·–·–); intermediate compound (II) (——); end-product (– – –); anthraquinone (· · · · · ·). [Bianthronyl] = $2 \cdot 10^{-5}$ *M*; $[NO_3^-] = 10^{-3}$ *M*; [anthraquinone] = $4 \cdot 10^{-5}$ *M*.

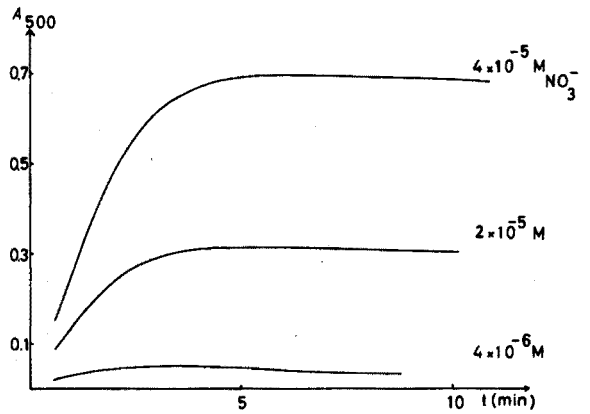

Fig. 2. Absorbance *versus* time curves for the intermediate compound (II) at 500 nm. [Bianthronyl] = $8 \cdot 10^{-4}$ *M*.

Experimental

Spectra and calibration curves were recorded on a Unicam SP800 spectrophotometer with 1-cm quartz cells.

Aqueous samples were evaporated in pyrex crucibles (5-cm diameter) which were treated previously by boiling water, chloroform, acetone and tridistilled water in that order.

Bianthronyl (Aldrich) was recrystallized from a chloroform–hexane mixture

(1+1) with activated charcoal (m.p. 245°). It was observed that whereas the unrecrystallized bianthronyl solutions in sulfuric acid are stable at the most for 1 h, the stability of the solutions of the recrystallized compound extends to several hours.

Sulfuric acid (Merck G.R.) 96%, determined by conductimetry[25,26], was used throughout. Solutions of potassium nitrate were prepared with Merck G.R. reagent recrystallized from water. Sulfuric acid solutions of antimony(III)[6] were prepared by heating 0.5 g of antimony powder (Fluka, puriss. 99.9999%) in aqueous sulfuric acid (95% v/v) until no more sulfur dioxide fumes were evolved. The precipitate of antimony sulfate that may be formed can be dissolved by heating the solution.

Analytical procedure. Evaporate the neutral (pH 6–8) water sample (5 ml) to dryness on a steam bath in a Pyrex crucible. Dissolve the residue in 4.5 ml of sulfuric acid at room temperature in a dry atmosphere. The time for total dissolution is about 20 min. If chloride ion is present, dissolve in a mixture of 3.5 ml of sulfuric acid and 1.0 ml of the sulfuric solution of antimony[6] (5 g l^{-1}). After addition of 0.5 ml of the sulfuric solution of bianthronyl ($8 \cdot 10^{-3}$ *M*), record the absorbance at 500 nm *versus* a blank solution containing only the reagents. The maximum value is attained in 3–5 min.

Prepare the calibration curve by treating aqueous nitrate solutions (0.248–2.48 μg NO_3^- ml^{-1}) as described above (Fig. 3).

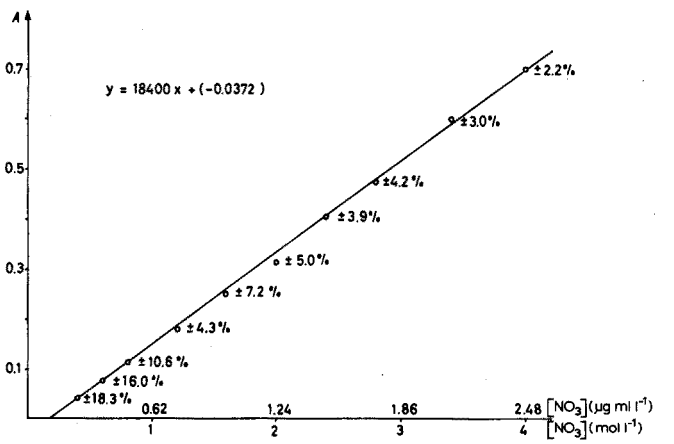

Fig. 3. Calibration curve (l=1 cm).

Interference of foreign ions

Interference by foreign ions was checked by determining nitrate in the presence of known concentrations of other ions which are commonly encountered in natural waters. The chosen foreign ion concentrations were at least in a ten-fold excess of the permitted concentrations in drinking water. As seen in Table I, only iron interferes; chloride ion in a large excess interferes also, giving lower results. Nitrite ion above 0.2 mg l^{-1} speeds up the reaction without affecting the results.

Determination of nitrate in original water samples

The present method was applied to the determination of the nitrate content

TABLE I

INTERFERENCE OF FOREIGN IONS
(NO_3^- added: 1.24 mg l^{-1})

Ions investigated	*mg l^{-1}*	*NO_3^- found (mg l^{-1})*	*Ions investigated*	*mg l^{-1}*	*NO_3^- found (mg l^{-1})*
Al^{3+}	2	1.23	Se^{4+}	0.2	1.22
NH_4^+	1	1.21	Sr^{2+}	2	1.23
Ag^+	2	1.24	V^{5+}	0.06	1.26
Cd^{2+}	0.5	1.28	Zn^{2+}	7	1.24
Co^{2+}	1	1.25	F^-	10	1.25
Cr^{6+}	0.2	1.24	Br^-	0.1	1.20
Cu^{2+}	5	1.28	Cl^-	7	1.24
Fe^{2+}	2	1.00	Cl^-	70	0.85
Fe^{3+}	2	1.00	Cl^-	200	<0.4
Hg^{2+}	0.03	1.24	NO_2^-	0.02	1.24
Mn^{2+}	1	1.25	SO_4^{2-}	200	1.24
Mg^{2+}	10	1.24	PO_4^{3-}	2	1.25
Pb^{2+}	0.7	1.26			

in water samples originating from Lake Geneva before and after purification. The determinations were done by the internal and external standard methods.

The results are in fairly good agreement with those obtained by the phenoldisulfonic acid method (Table II).

TABLE II

DETERMINATION OF NITRATE IN WATER

	Bianthronyl method (p.p.m. NO_3^-)[a]	*Phenoldisulfonic acid method (p.p.m. NO_3^-)*
Before purification	1.31±0.05	1.50
	1.40±0.02	1.46
	1.48±0.03	1.59
After purification	1.45±0.03	1.46
	1.55±0.04	1.59
	1.54±0.03	1.51
Drinking water	1.59±0.05	—
	1.77±0.03	—

[a] Mean value for 1-, 2-, 3-, and 5-ml water samples.

REFERENCES

1 H. Barnes, *Analyst*, 75 (1950) 388.
2 A. M. Harthey and R. I. Asai, *Anal. Chem.*, 35 (1963) 1207 and 1214.
3 W. W. Andrews, *Analyst*, 89 (1964) 730.
4 Ph. W. West and P. Sarma, *Mikrochim. Acta*, 4 (1957) 506.
5 Ph. W. West and G. L. Lyles, *Anal. Chim. Acta*, 23 (1960) 227.
6 Ph. W. West and J. P. Ramachandran, *Anal. Chim. Acta*, 35 (1966) 317.

7 M. J. Taras, *Anal. Chem.*, 22 (1950) 1020.
8 C. M. Johnson and A. Ulrich, *Anal. Chem.*, 22 (1950) 1526.
9 M. K. Bhatty and A. Townshend, *Anal. Chim. Acta*, 56 (1971) 55.
10 H. P. Axelrod, J. Bonelli and J. P. Lodge, *Anal. Chim. Acta*, 51 (1970) 21.
11 H. Riehm, *Z. Anal. Chem.*, 81 (1930) 353 and 439.
12 I. M. Kolthoff and G. E. Napone, *J. Amer. Chem. Soc.*, 55 (1933) 1448.
13 A. G. Roberts, *Anal. Chem.*, 21 (1949) 813.
14 P. D. Westland and R. R. Langford, *Anal. Chem.*, 28 (1956) 1996.
15 B. F. Salzmann, *Anal. Chem.*, 26 (1954) 1949.
16 J. W. Chow and M. S. Johnstone, *Anal. Chim. Acta*, 27 (1962) 441.
17 C. R. Sawicki, *Anal. Lett.*, 4 (1971) 761.
18 B. Wolf, *Anal. Lett.*, 16 (1944) 446.
19 Ch. Noll, *Anal. Lett.*, 17 (1945) 426.
20 F. L. Fischer, E. R. Ibert and N. F. Beckman, *Anal. Lett.*, 30 (1958) 1972.
21 D. Jenkins and L. Medsker, *Anal. Lett.*, 36 (1964) 610.
22 E. Sawicki, H. Johnson and T. W. Stanley, *Anal. Chem.*, 35 (1963) 1934.
23 H. Meyer, *Ber.*, 42 (1909) 143.
24 H. Meyer, *Monatsh. Chem.*, 30 (1909) 165.
25 R. J. Gillespie and S. Wasif, *J. Chem. Soc.*, (1953) 204.
26 R. J. Gillespie, J. V. Oubridge and C. Solomons, *J. Chem. Soc.*, (1957) 1804.

Analytica Chimica Acta, 68 (1974) 222–225

SHORT COMMUNICATION

Spectrophotometric determination of thorium with chromeazurol S and cetyltrimethylammonium bromide

B. EVTIMOVA

Department of Analytical Chemistry, University of Sofia, Sofia 26 (Bulgaria)

(Received 20th June 1973)

In studies of the highly sensitive reactions between some polyvalent metal ions, chromeazurol S and cetyltrimethylammonium bromide[1], it was found that thorium also forms a pure blue complex in aqueous solution. Despite the excellent reaction of thorium with arsenazo(III)[2], an investigation of the properties of this ternary, water-soluble thorium complex seemed worthwhile because of its very high molar absorptivity (over 10^5). Shijo and Takeuchi[3] have reported the formation of an analogous complex in an aqueous pyridine medium. Since very sensitive reactions are important in trace analysis, this communication suggests a new possibility to determine thorium spectrophotometrically in a normal aqueous solution.

Experimental

Reagents. A 10^{-2} *M* thorium nitrate solution was standardized compleximetrically with the CuEDTA–PAN system as indicator in solutions buffered with sodium acetate. Solutions of lower concentration were prepared by dilution with 10^{-2} *M* nitric acid.

Aqueous 10^{-3} or 10^{-4} *M* chromeazurol S (E. Merck) solutions were prepared.

A $2 \cdot 10^{-3}$ *M* cetyltrimethylammonium bromide (CTAB; E. Merck) solution was prepared by warming 0.0728 g of the reagent in 100 ml of distilled water. A $2 \cdot 10^{-4}$ *M* solution was used as required.

Acetic acid (0.5 *M*) and sodium acetate (0.5 *M*) were used to prepare buffer solutions by pH-meter control.

Apparatus. A VSU-1 universal spectrophotometer, a Specord UV-VIS recording spectrophotometer and a pH-meter L. Seibold, type GLD, were employed.

Absorption spectra

The effect of addition of CTAB to the thorium–chromeazurol S system is shown in Fig. 1. There is a very large increase in the reaction sensitivity accompanied by a bathochromic shift of about 80 nm. The absorbance of the reagent is very small, thus promoting excellent analytical conditions. Detailed measurements showed that the ternary complex thorium–chromeazurol S–CTAB

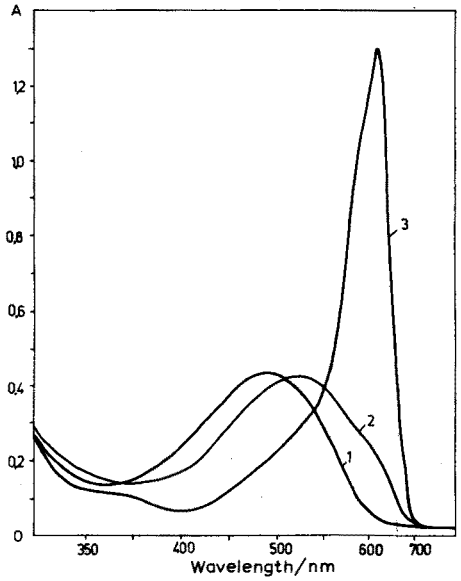

Fig. 1. Absorption spectra of thorium–chromeazurol S–cetyltrimethylammonium bromide system. pH 4.5; 2-cm cell. (1) $2 \cdot 10^{-5}$ *M* CAS; (2) $2 \cdot 10^{-5}$ *M* CAS and $4 \cdot 10^{-6}$ *M* thorium; (3) $2 \cdot 10^{-5}$ *M* CAS, $4 \cdot 10^{-6}$ *M* thorium and $8 \cdot 10^{-5}$ *M* CTAB.

has a wavelength maximum at 635 nm, whereas that of the thorium–chromeazurol S complex is at 554 nm[4].

Study of the optimal conditions for complex formation

The effect of pH on the absorption of ternary complex was studied at 635 nm with solutions containing 1 ml of $1.025 \cdot 10^{-4}$ *M* thorium, 5 ml of 10^{-4} *M* chromeazurol S and 10 ml of $2 \cdot 10^{-4}$ *M* CTAB diluted in 25-ml volumetric flasks. Maximal absorbance was achieved in the pH range 4–6, the absorbance decreasing gradually outside these limits. A pH 4.5 (acetate) buffer was chosen for all further work.

The effect of chromeazurol S concentration was studied with solutions containing 1 ml of $1.025 \cdot 10^{-4}$ *M* thorium, 10 ml of $2 \cdot 10^{-4}$ *M* CTAB and 0.5 ml of acetate buffer (pH 4.5) in 25-ml volumetric flasks. The absorbances were measured at 635 nm and 610 nm (see below) against a reagent blank. The maximal colour intensity was obtained with a 5-fold molar excess of chromeazurol S (Fig. 2).

The effect of varying CTAB concentration was established by measuring the absorbance of solutions containing 1 ml of $1.025 \cdot 10^{-4}$ *M* thorium, 5 ml of 10^{-4} *M* chromeazurol S and 0.5 ml of acetate buffer (pH 4.5) in 25-ml volumetric flasks; 1–11 ml of $2 \cdot 10^{-4}$ *M* CTAB were used. Whether absorbances were measured at 610 nm or 635 nm, they reached a plateau value above a 13-fold molar excess of CTAB. In all later experiments, a larger excess of CTAB (20-fold) was used.

Full colour development required at least 45 min, when absorbance was measured at 635 nm, or 10 min for measurement at 610 nm, and then remained

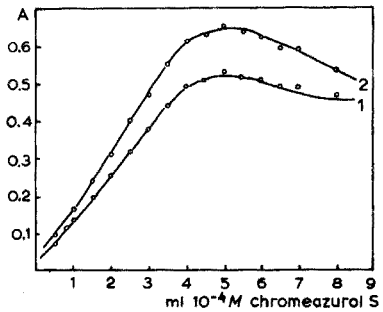

Fig. 2. Variation of absorbance with chromeazurol S concentration. (1) 610 nm, 1-cm cell; (2) 635 nm, 1-cm cell.

constant. The order of addition of reagents was unimportant. Measurements of the absorbance when the pH of the solutions was adjusted with sodium hydroxide instead of acetate buffer showed that the latter (regardless of the amount present) had no effect.

Beer's law

In preparing the calibration graph, it was necessary to investigate the reaction in detail, because of some influence of the molar ratio of reagent to metal on the shift of the wavelength of maximal absorbance. An increase of the chromeazurol S and CTAB concentrations (taken in the ratio 1:4) compared to thorium moved the maximum wavelength to shorter wavelengths and caused some decrease in the sensitivity. It was found that Beer's law was obeyed in a small concentration interval (0.09–0.47 μg Th ml^{-1}), when 0.5 ml of 10^{-3} *M* chromeazurol S, 1 ml of $2 \cdot 10^{-3}$ *M* CTAB and 0.5 ml of buffer pH 4.5 were added to the standard thorium solution in 25-ml volumetric flasks, and the absorbances were measured at 635 nm in a 1-cm cell. For higher thorium concentrations, the absorbance increased more rapidly with concentration, hence these points lay on another straight line with a higher slope. This behaviour can be attributed to different metal:ligand ratios at different thorium concentrations. For a ratio thorium:chromeazurol S:CTAB of 1:5:20, Beer's law was obeyed in the concentration range 0.09–1.14 μg Th ml^{-1} at 635 nm (1-cm cell); the molar absorptivity was $1.46 \cdot 10^5$.

When the calibration graph was prepared with 0.5 ml of 10^{-3} *M* chromeazurol S and 1 ml of $2 \cdot 10^{-3}$ *M* CTAB, and absorbances were measured at 610 nm in 1-cm cells, Beer's law was again followed for thorium concentrations of 0.09–1.14 μg ml^{-1}, but the molar absorptivity was $1.18 \cdot 10^5$. According to Sandell, the sensitivity of the reaction was 0.00196 μg Th cm^{-2}. Therefore, the spectrophotometric determination of thorium proposed here can be applied successfully in trace analysis.

Interference study

Several foreign ions were investigated for their effect in solutions containing 12 μg of thorium, 0.5 ml of 10^{-3} *M* chromeazurol S, 1 ml of $2 \cdot 10^{-3}$ *M* CTAB, and 0.5 ml of buffer pH 4.5 in 25-ml volumetric flasks. Table I lists the

TABLE I

TOLERANCE FOR DIVERSE IONS

Ion	*Tolerance (μg)*	*Ion*	*Tolerance (μg)*	*Ion*	*Tolerance (μg)*
Ti(IV)	7.2	In(III)	34.5	Ce(III)	250
Y(III)	450	La(III)	695	Mg(II)	1200
Ca(II)	2000	Mn(II)	2750	Ni(II)	2940
Co(II)	2940	Zn(II)	3270	Cd(II)	5610
Pb(II)	10360				

results obtained; concentrations of titanium and indium greater than those given interfere, but for the other elements, the amounts mentioned represent the largest amounts tested.

Serious interferences were caused by U(VI), Cu(II), Ga(III), Fe(III) and Al(III); only a 1:10 metal-to-thorium molar ratio could be tolerated. A preliminary separation of thorium would be necessary in most cases when these metal ions are present.

REFERENCES

1 B. Evtimova and D. Nonova, *Anal. Chim. Acta*, 67 (1973) 107.
2 S. B. Savvin, *Dokl. Akad. Nauk USSR*, 127 (1959) 1231; V. F. Lukianov, S. B. Savvin and I. V. Nikolskaia, *Zavod. Lab.*, 25 (1959) 1155.
3 Y. Shijo and T. Takeuchi, *Anal. Abstr.*, 19 (1970) 2956.
4 R. Ishida, *Anal. Abstr.*, 14 (1967) 3893.

Analytica Chimica Acta, 68 (1974) 226–230

SHORT COMMUNICATION

Chemical determination of copper, copper(I) and copper(II) in a borate glass

S. BANERJEE* and A. PAUL
Department of Glass Technology, University of Sheffield, Sheffield (England)
(Received 7th April 1973)

Simple spectrophotometric and titrimetric methods have been developed for estimating all the three common oxidation states of copper, namely, Cu^0, Cu^+ and Cu^{2+}, in a sodium borate glass.

Determination of total copper

Copper(II) forms an intense blue colour with cuprizone reagent (bis-cyclohexanoneoxalyldihydrazone) in a slightly ammoniacal medium[1]. If too much ammonia is present, the colour intensity diminishes and the method gives erroneous results.

Standard copper solution. Dissolve electrolytic copper powder in nitric acid and dilute the solution to a concentration of 50 μg ml^{-1}.

Cuprizone reagent. Dissolve 0.20 g of cuprizone in 20 ml of hot (1+1) methanol–water, and dilute to 200 ml with water.

Procedure. Transfer appropriate aliquots of the standard copper solution to 50-ml volumetric flasks to give concentrations of 1, 2, 3, 4 and 5 μg copper per ml in the final solution. Add 2 ml of (1+4) hydrochloric acid, 2 ml of (1+4) nitric acid and 5 ml of (1+3) ammonia solutions, followed by 10 ml of cuprizone reagent. Dilute to the mark with distilled water. Prepare a blank solution similarly. After 15 min, measure the absorbance of the blue solution (Spekker absorptiometer) in a 1-cm cell using H503 and 606 filters. The calibration curve so prepared was linear, and was shown to be unaffected by constituents of the base glass (0.20 g of blank glass powder was added in some solutions).

For total copper in the glass, weigh about 0.20 g of finely powdered glass and dissolve in 2 ml of (1+4) hydrochloric acid, 2 ml of (1+4) nitric acid, and 6 ml of water over a hot plate. Then transfer the solution directly to a 50-ml volumetric flask or dilute further depending upon the concentration of total copper. Develop and measure the colour as described above. Calculate the concentration of copper in the glass from the calibration curve. Some experimental results are given in Table I.

Determination of copper(I)

Copper(I) was determined by oxidation with cerium(IV) sulfate using ferroin

* Present address: General Refractories Co. Research Laboratories, Baltimore, MD., U.S.A.

TABLE I

ESTIMATION OF TOTAL COPPER IN A 30 $Na_2O \cdot 70\ B_2O_3$ GLASS MELTED WITH 0.20 wt.% COPPER OXIDE

Weight of glass taken (g)	*Total copper determined (μg)*	*mg total copper/ g glass taken*	s_r *(%)*
0.050	79.6	1.592	
0.050	80.1	1.602	
0.100	160.3	1.603	4.2
0.100	159.8	1.598	
0.150	239.8	1.599	
0.150	240.4	1.603	

as indicator, after addition of iron(III), the iron(II) produced being titrated. The difference between the titration value with the blank glass (*i.e.* a base glass melted without copper) and the test glass gave the volume consumed by copper(I).

Copper(I) oxide powder. For standardization of the method, GPR-quality copper(I) oxide was used. On analysis (by dissolving in iron(III) sulfate solution followed by titration of the iron(II) produced), this powder was found to contain 95.6% Cu_2O. This powder (50 mg) was mixed with 25 g of powdered base glass thoroughly in an agate mortar, and weighed portions of this mixture were used.

Procedure. To a 100-ml conical flask, add 2 ml of iron(III) sulfate solution (0.01 *M* in 0.75 *M* sulfuric acid) and 10 ml of cerium(IV) sulfate solution (0.002 *M* in 0.75 *M* sulfuric acid). Accurately weigh 1.000 g of the mixture of copper(I) oxide and glass powder, and add to the flask. Swirl the flask, add 25 ml of 0.75 *M* sulfuric acid, and shake until all the glass particles dissolve. Add 1 ml of (1+49) concentrated ferroin solution (B.D.H.) and titrate with 0.005 *M* iron(II) ammonium sulfate solution in 0.75 *M* sulfuric acid until the colour just turns red. Apply the same procedure to 1.00 g of blank glass. The difference in titration values from the blank glass gives the copper(I) equivalent of iron(II). The results for standardization of the method on 1-g samples gave an average of 1.782 mg of copper(I) with a standard deviation of 0.017 mg (4 determinations).

Interference of metallic copper

Metallic copper in finely powdered form may dissolve in cold dilute sulfuric acid, particularly in the presence of oxidizing agents[2]. The copper particles in copper ruby glasses are expected to be very small (20-nm diam.). Since no such fine copper particles free of oxygen could be made, the present investigation was made with electrolytic copper powder (–200 mesh); even on these particles a layer of oxide film could be seen under a microscope. Five 100-ml conical flasks were charged with 10 mg of copper powder along with 1.000 g of the above mixture of Cu_2O and blank glass powder, and this was treated with iron(III), cerium(IV) and sulfuric acid solutions as described above. After different lengths of time, the contents of the flasks were titrated with the 0.005 *M* iron(II) solution to the ferroin end-point. The average result found was 1.97 mg of copper(I) ($s = 0.022$ mg), and the results did not vary with time during the period 15–90 min; however, the

results were higher than those obtained in the absence of metallic copper. In another series of experiments, different amounts of copper powder were taken with 1 g of Cu_2O–glass mixture, and the total copper(I) was determined. The results (Table II) showed that the excess copper(I) estimated per mg of copper powder was constant. The high results obtained in the first series may be accounted for by considering the solubility of the fine film of copper(I) oxide on the surface of neutral copper particles.

TABLE II

ESTIMATION OF Cu^+ IN PRESENCE OF VARYING AMOUNTS OF NEUTRAL COPPER WITH CERIC SULPHATE SOLUTION

Copper powder taken (mg)	*Volume of equiv. 0.005 M iron(II) (ml)*	*Total Cu^+ calculated (mg)*	*Excess Cu^+ (mg)/Cu (mg)*
–	5.60	1.78	–
5.0	5.89	1.87	0.018
10.0	6.21	1.97	0.017
15.0	6.56	2.08	0.020
20.0	6.83	2.17	0.020
20.0[a]	1.24	0.39	0.020

[a] No Cu_2O–glass mixture was added.

Determination of copper(I) and metallic copper

Method with cerium(IV) solution. Metallic copper is not soluble in 0.75 *M* sulfuric acid in the cold, but can be dissolved by heating with a small amount of silver sulfate solution in the presence of a known excess of cerium(IV) solution. This gives the combined value for Cu^0 and Cu^+. The Cu^0 is calculated by subtracting the value for Cu^+ from this combined value.

To obtain a mixture for testing, 10 g of blank glass powder was mixed thoroughly with 11.5 mg of Cu_2O and 10 mg of electrolytic copper powder (–200 mesh) in an agate mortar. All other reagents were same as used in the determination of copper(I).

Procedure. Place 2 ml of iron(III) solution (0.01 *M*), 10 ml of cerium(IV) solution (0.002 *M*) and 1 ml of aqueous silver sulfate solution (0.25 wt.%) in each of two conical flasks. Weigh 1.00 g of blank glass into one of the flasks, and in the other flask 1.000 g of the mixture of glass, Cu_2O and metallic copper powder. Shake to distribute the glass uniformly, add 25 ml of 0.75 *M* sulfuric acid solution, swirl, and leave on a hot water bath for 30 min. Cool, add 1 ml of ferroin solution to each flask, and then titrate with iron(II) solution (0.005 *M*) as before. The difference in the titration value of the two flasks gives the volume consumed jointly by metallic copper and Cu_2O. The results are calculated as copper(I) from which the individual quantities can be calculated if the total copper concentration is known. The results for standardization of the method gave an average copper(I) equivalent value of 2.84 mg (s = 0.05 mg; 4 determinations).

Method with iodine monochloride[3,4]. This method involves the oxidation of

copper(I), and copper(0) to copper(II) by iodine monochloride. The liberated iodine is then titrated back to iodine monochloride with iodate.

Iodine monochloride solution. Dissolve 10 g of Analar potassium iodide and 6.44 g of Analar potassium iodate in 100 ml of 9 *M* hydrochloric acid (Analar). Then add 2 ml of carbon tetrachloride and shake vigorously. Add dilute iodate solution to bleach the organic layer. Dilute 5 ml of this concentrated solution to 100 ml with 9 *M* hydrochloric acid.

Procedure. In a 25-ml measuring cylinder place 20 ml of 6 *M* hydrochloric acid and add 2 ml of diluted ICl solution and 2 ml of carbon tetrachloride. Use 0.50 g of the glass mixture, as for the method with cerium(IV), accurately weighed into a ground-glass stoppered tube which had been cleaned and dried previously. Add the solution from the measuring cylinder and add another 20 ml of 6 *M* hydrochloric acid. Cover the glass stopper with a small amount of vacuum grease. Shake well for 15 min during which time the glass dissolved completely. Titrate the liberated iodine with standard 0.002 *M* potassium iodate solution. The results for standardization gave an average copper(I) equivalent value of 1.44 mg (s = 0.04 mg; 4 determinations). The results obtained by this method agreed fairly well with those of the cerium(IV) method for the determination of $(Cu^0 + Cu^+)$.

Determination of a mixture of Cu^0, Cu^+ and Cu^{2+} in a glass

In a glass containing Cu^0, Cu^+ and Cu^{2+}, total copper and $(Cu^0 + Cu^+)$ were determined as described above; copper(II) was calculated from the difference. An indirect check of the consistency of the results was made by determining the absorptivity of copper(II) at the absorption peak around 800 nm. The results are shown in Table III. The absorptivity of copper(II) was calculated from

$$\varepsilon = (63.54/X \cdot \rho) \cdot (\text{absorbance}/t)$$

where ε = absorptivity (l mole^{-1} cm^{-1}), X = mg Cu^{2+} per g of glass (calculated from the results), ρ = density of the glass (g cm^{-3}), and t = thickness of the glass specimen (cm).

TABLE III

DETERMINATION OF ABSORPTIVITY OF COPPER(II) AT 800 nm IN $30Na_2O \cdot 70B_2O_3$ GLASSES

Glass number	*Total copper (wt.%)*	*Cu^+ (wt.%) by cerium(IV) method*	*Absorptivity at 800 nm (l mole^{-1} cm^{-1})*
1	0.475	0.086	32.9
2	0.517	0.091	32.6
3	0.470	0.087	32.7
4	0.321	0.118	32.5
5	0.763	0.229	32.8
6	0.645	0.201	32.9

Thus any inconsistency in the chemical determination would have been reflected in the absorptivity reported.

REFERENCES

1 A. I. Vogel, *Quantitative Inorganic Analysis*, Longmans, London, 3rd Ed., 1961, p. 802.
2 J. N. Fuchs, *Philos. Mag.*, 3rd Ser., 18 (1841) 91.
3 A. I. Vogel, *Quantitative Inorganic Analysis*, Longmans, London, 3rd Ed., 1961, p. 381.
4 A. Paul, *Glass Technol.*, 6 (1965) 22.

Analytica Chimica Acta, 68 (1974) 231–236

SHORT COMMUNICATION

Determination of the total amount of volatile, but slightly soluble, organic materials dissolved in water from oil and oil products

JIRI POLAK and BENJAMIN C.-Y. LU
Department of Chemical Engineering, University of Ottawa, Ottawa, Ontario (Canada)
(Received 19th April 1973)

The aim of this study was to develop a fast reliable method for determining the total amount of volatile but slightly soluble organic materials in water, in order to establish the extent of contamination of water by oil and oil products in emergencies such as oil spills. Such a method should not involve too many operation steps, so that possible changes in the dissolved materials are minimized, and should require relatively small samples.

Few gas-chromatographic methods have been reported for dissolved hydrocarbons and oil products in water. A water sample may be injected directly into a gas chromatograph equipped with a flame-ionization detector; water is not detected, but interfering peaks prevent the evaluation of the hydrocarbon content[1]. These peaks are present even when pure water is tested. Two modifications have been described to overcome this difficulty: either the carrier gas was saturated with steam, the method being successful for determining hydrocarbons up to isobutane[2], or a pre-column absorber was used to remove the water without absorbing the organic compounds[3,4]. However, there remains a danger of absorbing traces of high-boiling compounds on the desiccant.

The other group of methods involves extraction of the dissolved organic materials with a solvent such as iso-octane[4], pentane[5], n-heptane[6] or nitrobenzene[1]; a sample of the solvent layer is than injected into a gas chromatograph for analysis and identification. However, because an excess of solvent is present, the base-line is generally unstable and the sensitivity is low, so that large water samples (1–2 l) are frequently used. In some cases, the low-boiling extracting solvent is partially evaporated before the analysis[5,7] with the possible loss of the low-boiling fraction of the dissolved materials. The dissolved materials may contain polar compounds which may remain in the water layer and so escape detection. The selection of a suitable solvent also poses a problem. If a low-boiling solvent is used, any organic materials with elution times close to this solvent will not be detected, because their small peaks will be hidden in the large solvent peak; this error can be serious because the low-boiling components are usually the more soluble ones. On the other hand, if a high-boiling solvent is used, the analysis of the sample will take longer and some of the high-boiling components may escape detection.

Another method involves successive gas-chromatographic analyses after repeated equilibrations of a hydrocarbon-free carrier gas (*e.g.* helium) with an aqueous sample containing dissolved hydrocarbons[8]. Gas-chromatographic data on the successive equilibrium gas phases are simply added, or plotted and extrapolated to the hydrocarbon concentration in the original aqueous sample.

All the available methods are intended to determine the dissolved hydrocarbons individually, and are unsuitable for rapid screening of samples.

The method proposed here combines some of the features of the earlier methods, but is relatively fast and is suitable for determining the total amount of the dissolved materials. It takes about one hour to analyze one sample. For dilute samples, and samples containing more volatile components, even less time is required. The amount of sample taken is only 15 ml. Although a lower amount was still adequate, no attempt was made to determine the minimal amount of the sample needed.

Experimental

Apparatus and procedure. The arrangement of the apparatus is shown in Fig. 1. There are two 15-ml hypo-vials (B_1 and B_2), which are connected in parallel to the helium carrier gas stream. The helium flow is controlled by four valves (V_1 to V_4). Hypo-vial B_1 is filled with distilled water and hypo-vial B_2 with the sample to be analyzed. A flame-ionization detector of a Hewlett-Packard gas chromatograph model 5750B was used, with the complete apparatus placed in the gas chromatograph oven space.

During the analysis, a stream of the carrier gas is first bubbled through B_1, with V_3 and V_4 closed, and then introduced into the flame-ionization detector. In this step, the carrier gas is partially saturated with water vapor, and stable base-line conditions for the detector can be established. The hypo-vial B_2 is then filled with the sample, weighed and connected to the system. The carrier gas is now switched to pass through B_2 by (i) opening V_3, (ii) opening V_4 and closing V_2 simultaneously, and (iii) closing V_1. When the carrier gas bubbles through the sample, a portion of the dissolved materials is carried into the detector for analysis.

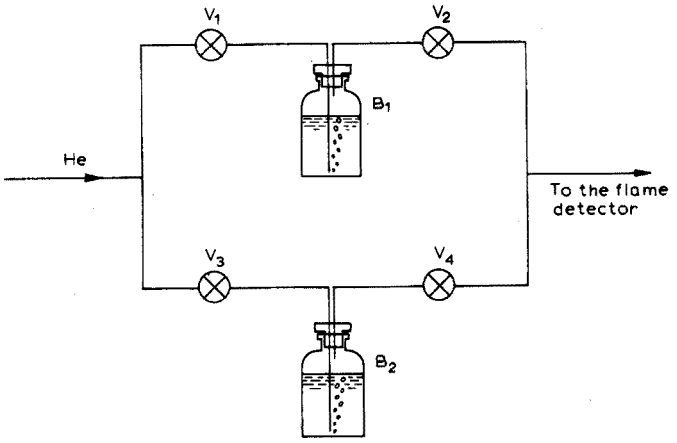

Fig. 1. Arrangement of apparatus.

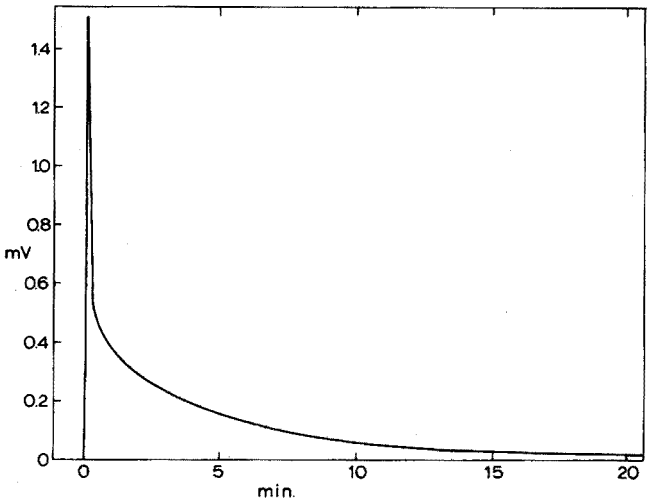

Fig. 2. A typical flame-ionization detector response to the presence of organic materials in sample.

A typical detector response is shown in Fig. 2. A sharp surge appears initially, but tapers off and approaches zero exponentially as the dissolved materials are gradually depleted by the carrier gas from the solution.

The operating conditions of the detector used were as follows: helium flow rate, 40 ml min^{-1}; hydrogen flow rate, 25 ml min^{-1}; air flow rate, 500 ml min^{-1}; detector temperature, 205°; range, 10^3. A Hewlett-Packard model 3373B electronic digital integrator was used with an integrator attenuation of 10 and with a maximal sensitivity setting.

Method of calculation. Along the exponential curve of Fig. 2, the change of vapor concentration (c_v) with time (θ), may be expressed as a function of the liquid concentration (c_l) by means of the following equation

$$dc_v/d\theta = -k_1 c_l \tag{1}$$

The quantity k_1 depends on the properties of the dissolved materials, the relative and absolute amounts of the materials, and other factors such as temperature. The partition coefficient c_v/c_l may be assumed to be constant, and expressed by k_2, when the concentration of the materials present is low. Hence, if q is written for k_1/k_2, we have

$$dc_v/d\theta = -qc_v \quad \text{or} \quad d \ln c_v = -q\,d\theta$$

and

$$c_{v_\theta} = c_{v_\theta} \exp(-q\theta) \tag{2}$$

In eqn. (2), θ^0 refers to the initial time, which is conveniently but arbitrarily chosen somewhere on the exponential curve and considered as zero time; θ refers to the time interval relative to θ^0. Hence $c_{v_{\theta^0}}$ and c_{v_θ} refer to the vapor concentrations at times θ^0 and θ, respectively. The area under the curve (Fig. 2) was integrated and printed out at intervals of about 5 min for 1 h. The total area under the curve for this period is therefore known. However, at the end of this period,

organic materials remain in the aqueous sample, for the detector response, in general, has not yet reached zero. The area under the curve from θ^0 to θ is obtained from eqn. (2):

$$A = \int_{\theta^0=0}^{\theta} c_v \mathrm{d}\theta = -(c_{v_{\theta^0}}/q)[\exp(-q\theta)-1]$$
$$= a[\exp(b\theta)-1] \quad (3)$$

in which A represents the area, and a and b are coefficients which are evaluated from the integrator readings for the exponential curve by a least-squares method. Because coefficient b must be negative, owing to the trend of the curve, the area under the curve from θ^0 to $\theta \rightarrow \infty$ can be represented by

$$\lim_{\theta \rightarrow \infty} A = -a$$

The sum of this area together with the area evaluated by the integrator from the beginning of the detector response to θ^0, represents the total area under the curve, which is proportional to the total amount of the organic materials present in the sample. For samples with low concentrations of organic materials, the curve reaches the base-line well before 60 min, and the total area count is then taken without using the extrapolation procedure.

In order to evaluate the absolute amount of the organic materials present in the sample, a detector response factor is required. This factor may be obtained by calibrating with samples saturated with known organic materials.

Results

Determination of the detector response factor. The detector response factor was obtained by calibrating with water samples saturated with n-hexane and with benzene at 25°. Solubilities of these pure substances in water were previously determined by an extraction method. The response factors for these solutions varied within $\pm 6.4\%$. It should be mentioned that this factor may vary with the organic substances used, and for the compounds present in oil, is believed to be within $\pm 5\%$[3,9,10]. The overall uncertainty of the proposed method is therefore about $\pm 10\%$ for concentrations above 0.1 p.p.m. The value of the response factor used here was $1.80 \cdot 10^{-6}$ g mV^{-1} s^{-1}.

Solubility of No. 2 fuel oil in water. The applicability of the proposed method was tested on water extracts of No. 2 fuel oil (Imperial Oil of Canada). About 350 ml of the oil was poured into a closed vessel (i.d. 15 cm) containing 3 l of distilled water. A stirrer, which rotated at about 2 r.p.m., could be adjusted so that its blade was always at the oil–water interface. The stirring was provided to regenerate the interface layer so that polar molecules would not be concentrated at the interface. The whole vessel was placed in a water thermostat at $25 \pm 0.01°$. Water samples were taken from the bottom layer directly into 15-ml hypo-vials through a stainless steel capillary with its upper end positioned 10 cm from the interface.

The oil–water system was allowed to equilibrate for 5 days. Samples were then taken for several days. The results obtained are listed in Table I. The mean value of the volatile material is 9.74 ± 0.53 p.p.m. (by weight).

TABLE I

RESULTS OF SOLUBILITY OF NO. 2 FUEL OIL IN WATER AT 25°

Days of contact	5.17	6.21	7.00	8.00	9.08	9.15	9.19
Volatile organic material (p.p.m.)	9.42	9.14	9.80	9.04	9.86	10.46	10.44

TABLE II

READINGS OF THE DIGITAL INTEGRATOR

Reading No.	*Elapsed time (min)*	*Area (mV s)*	*Total area (mV s)*
1	17.39	7080	7080
2	22.13	204.9	7285
3	25.98	122.5	7407
4	32.09	155.4	7563
5	36.07	83.1	7646
6	40.64	81.7	7728
7	45.22	70.3	7798
8	50.50	71.2	7869
9	55.01	51.8	7921
10	60.38	52.8	7974
11	194.54[a]	275.1	8249

[a] The signal reached the base-line.

Sample calculation. The proposed calculation method is illustrated here for the run after 8 days of contact (Table I). The experimentally obtained values of the area under the response curve of the flame-ionization detector are given in Table II. The coefficients a and b of eqn. (3), evaluated by a least-squares method from readings 8–10, were: $a = -499.9$ mV s, and $b = -0.02871$ min^{-1}. In this calculation, $\theta^0 = 45.22$ min. The area from this time to $\theta \rightarrow \infty$ is given by $A = -a = 500$ mV s. The total area under the complete detector response curve is therefore $7798 + 500 = 8298$ mV s. This area can be compared with the experimental value of 8249 mV s, obtained after 194.54 min when the signal reached the base-line. The difference is 0.59%, indicating the usefulness of the proposed method of calculation. With the detector response factor obtained, the area of 8298 mV s corresponded to $1.49 \cdot 10^{-4}$ g of organic materials in the sample. The total weight of this sample was 16.4903 g, hence the concentration was 9.04 p.p.m.

It should be mentioned that the reproducibility of the method may be improved by frequent calibration of the detector. Furthermore, for water samples having small contents of organic materials or those containing very volatile components, the signal of the detector reaches the base-line much sooner than 1 h, so that no extrapolation is needed. For example, it took only about 30 min to remove n-hexane from an aqueous solution containing 6 p.p.m. of n-hexane under the conditions described. Attempts to speed up analyses for less volatile components by heating the samples failed because of flame instability.

The authors are indebted to the National Research Council of Canada for financial support.

REFERENCES

1 R. Jeltes and R. Veldink, *J. Chromatogr.*, 27 (1967) 242.
2 D. N. Saraf and P. A. Witherspoon, *Science*, 142 (1963) 955.
3 C. McAuliffe, *J. Phys. Chem.*, 70 (1966) 1267.
4 W. M. Zarrella, R. J. Mousseau, N. D. Coggeshall, M. S. Norris and G. J. Schrayer, *Geochim. Cosmochim. Acta*, 31 (1967) 1155.
5 D. B. Boylan and B. W. Tripp, *Nature*, 230 (1971) 44.
6 A. Demayo, *Tech. Bull. No. 32*, Inland Waters Branch, Department of Energy, Mines and Resources, Ottawa, 1970.
7 C. McAuliffe, *Chem. Geol.*, 4 (1969) 225.
8 C. McAuliffe, *Chem. Tech.*, Jan. (1971) 46.
9 J. C. Sternberg, W. S. Gallaway and D. T. L. Jones, in N. Brenner, J. E. Callen and M. D. Weiss, *Gas Chromatography*, Academic Press, New York, 1962, p. 231.
10 L. Szepesy, *Gas Chromatography*, Iliffe Books, London, 1970, p. 148.

Analytica Chimica Acta, 68 (1974) 237–242

SHORT COMMUNICATION

Solvent extraction of uranium(VI) with trioctylphosphine oxide in the presence of fatty acids

M. KONSTANTINOVA
Higher Institute of Chemical Technology, Sofia 54 (Bulgaria)
St. MAREVA and N. JORDANOV
Institute of General and Inorganic Chemistry, Bulgarian Academy of Sciences, Sofia 13 (Bulgaria)
(Received 15th May 1973)

It was shown in a previous paper[1] that, depending on the pH value of the medium, aromatic carboxylic acids have different effects on the extraction of uranium(VI) with trioctylphosphine oxide (TOPO)—antagonistic up to pH 1.8 and synergic at higher pH values. A linear dependence was established between the extent of synergic enhancement and the strength of the acids.

The present paper describes a study of the influence of fatty acids on the extraction of uranium(VI) with solutions of TOPO in different diluents. The following representatives of the homologous series of fatty acids were used: valeric acid $CH_3(CH_2)_3COOH$, capric acid $CH_3(CH_2)_8COOH$, pentadecanoic acid $CH_3(CH_2)_{13}COOH$, palmitic acid $CH_3(CH_2)_{14}COOH$, and margaric acid $CH_3(CH_2)_{15}COOH$. There are no data about the strength of these acids (above C_9) in aqueous solution, because of their limited solubility. All the acids below C_9, except formic acid, are weak and have similar dissociation constants—from 4.72 for acetic acid to 4.95 for pelargonic acid. The effect of chain length on the acid strength is negligible. Possibly, the last representatives of the homologous series have a similar strength[2].

Fatty acids diluted with organic diluents have been used for the extraction of many elements including uranium(VI)[3–11]. It could be expected that they would act synergically on the extraction of uranium(VI) with TOPO.

Experimental

The trioctylphosphine oxide was purified as described previously[1]. The diluents—carbon tetrachloride, cyclohexane and benzene—were purified and fraction-distilled by the usual methods[12]. The fatty acids were recrystallized from alcoholic solutions; their purity was checked by melting points and by gas chromatography. The impurities of corresponding unsaturated analogues did not exceed 2%.

Mixtures of $2 \cdot 10^{-2}$ *M* TOPO and $1 \cdot 10^{-2}$ *M* acid in the diluents mentioned above were used for extraction. An uranyl nitrate solution in 0.01 *M* nitric acid was used. Uranium(VI) (1 mg) was extracted at different pH values. Equal

volumes of aqueous and organic phases (10 ml) were shaken at 200 r.p.m. until equilibrium was attained (10 min). The two phases were separated by centrifugation. The distribution coefficients were found by determining uranium photometrically with arsenazo III[13] in an aliquot of the aqueous phase and in the back-extract.

Results and discussion

Table I shows the distribution coefficient D of uranium in extraction with carbon tetrachloride solutions of TOPO or of TOPO and fatty acids at different pH values of the aqueous phase.

TABLE I

EXTRACTION OF URANIUM(VI) WITH CARBON TETRACHLORIDE SOLUTIONS

($2 \cdot 10^{-2}$ *M* TOPO and mixtures of $2 \cdot 10^{-2}$ *M* TOPO and $1 \cdot 10^{-2}$ *M* fatty acid)

Extractant / *pH aq. phase*	*Distribution coefficient D*							
	1.03	*1.90*	*2.75*	*3.65*	*4.40*	*5.00*	*5.30*	*5.70*
TOPO	14.0	0.7	0.2	0.2	0.12	0.1	—	—
TOPO–valeric acid	6.7	0.5	0.6	3.3	6.7	19.2	35.5	78
TOPO–capric acid	5.6	0.5	0.5	4.2	7.4	24.5	61.5	600
TOPO–pentadecanoic acid	5.7	0.5	0.6	3.8	6.5	20.4	57.8	700
TOPO–palmitic acid	5.6	0.5	0.6	3.4	7.0	22.6	58.0	700
TOPO–margaric acid	5.6	0.5	0.6	3.4	6.6	20.7	59.1	700

There are two regions of action of the acids on the distribution of uranium—antagonistic up to pH 1.9 and synergic above pH 1.9. The synergic effect S ($S = D_{\text{TOPO+acid}}/D_{\text{TOPO}}$) for the investigated fatty acids is of the same order and rises as the pH values of the aqueous phase increase. The dependence log S *vs.* pH was found to be linear for all acids up to pH 5 (Fig. 1). These results confirm that the acids are similar in strength and that the chain length does not alter the synergic effect for this pH region. The dependence log S *vs.* pH above pH 5 is linear only for valeric acid; presumably, the extraction mechanism in the presence of valeric acid remains unchanged for all pH values. The synergic effect in the presence of the other four acids (Fig. 1, pH 5.30–5.70) increases to the same degree. The rise is very sharp between pH 5.3 and 5.7, where D changes from 60 to 700, while D_U for valeric acid only doubles from 35 to 78. The difference between the influence of the valeric acid and the other acids is probably due to some different mechanism of extraction connected with the state of uranium above pH 5 and the chain length, distribution and dimerization of the acids.

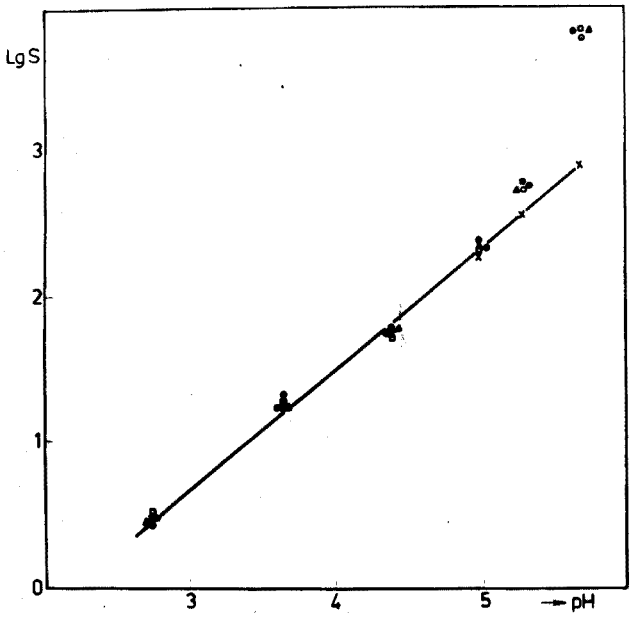

Fig. 1. Variation of log S with pH for mixtures of $2 \cdot 10^{-2}$ M TOPO and $1 \cdot 10^{-2}$ M acid. (×) Valeric acid; (◎) capric acid; (□) pentadecanoic acid; (△) palmitic acid; (●) margaric acid.

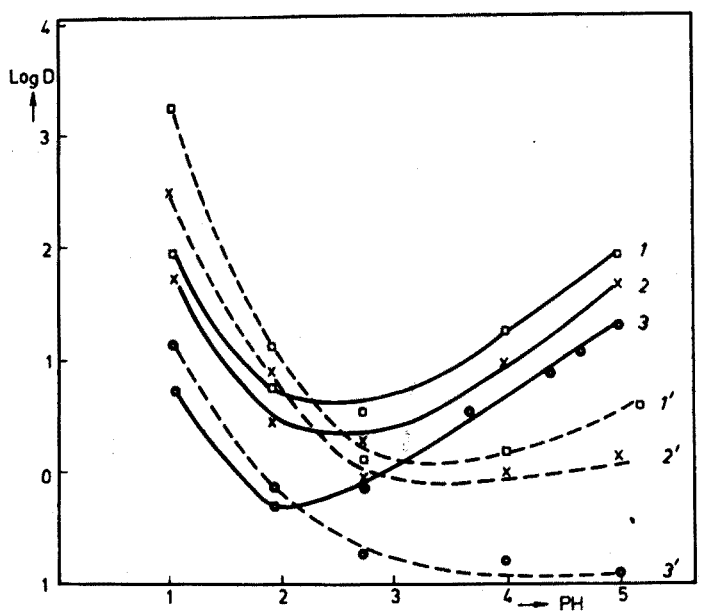

Fig. 2. Variation of log D for uranium(VI) with pH for $2 \cdot 10^{-2}$ M solutions of TOPO (1′, 2′, 3′) and for mixtures of $2 \cdot 10^{-3}$ M TOPO and $1 \cdot 10^{-2}$ M palmitic acid (1, 2, 3) in: (◎) carbon tetrachloride; (×) cyclohexane; (□) benzene.

Influence of the diluent

The influence of the diluent on the extraction properties of neutral organophosphorus compounds has been studied and discussed by many authors[14–16]. There are not enough data about the physicochemical properties of these systems[17], so that it is difficult to make quantitative estimates. In the case of synergic extraction, the system becomes more complicated; the choice of a suitable diluent is more difficult[18], being commonly based on preliminary experiments. It was of interest to study the influence of some nonpolar diluents on the extraction system.

Experiments were carried out with palmitic, salicylic[1] and benzoic[1] acids. Carbon tetrachloride, cyclohexane and benzene were chosen; according to the order of Schmidt *et al.*[19], their activity is similar, as are their dielectric constants, dipole moments and molecular polarizibility. There is no hydrogen bonding between these diluents and neutral organophosphorus compounds; benzene and carbon tetrachloride may form π-electron bonds. The extraction of uranium with solutions of TOPO and mixtures of TOPO and fatty acids in the three diluents as a function of pH values of the aqueous phase was investigated. Extraction curves for uranium with pure TOPO are shown in Fig. 2 (dashed curves). The differences in the values of the distribution coefficients are extremely great at pH 1 where D increases from 14 with carbon tetrachloride to 1300 with benzene; at pH 5, the extraction curves drop sharply but the influence of the diluents is of the same character.

The extraction curves for uranium with TOPO in the presence of palmitic, benzoic and salicylic acids are shown in Figs. 3 and 4, respectively. The curves in the absence of organic acids are given for comparison. The curves involve two

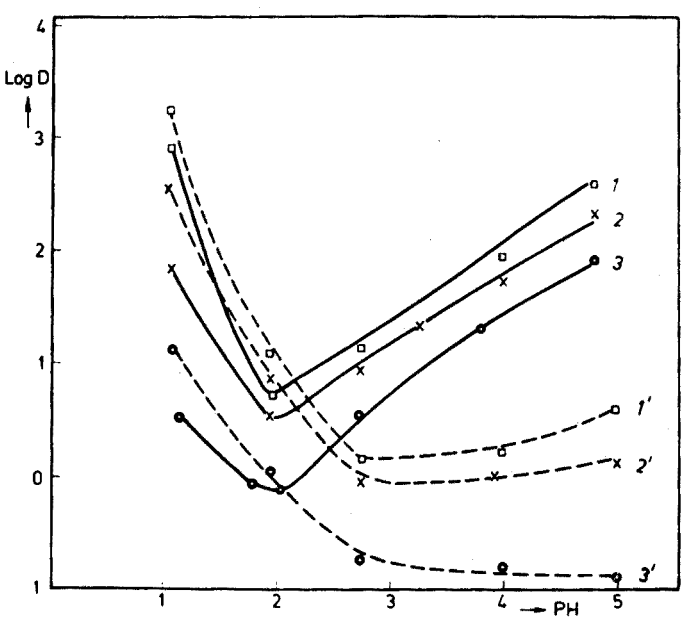

Fig. 3. Variation of log D for uranium(VI) with pH for $2 \cdot 10^{-2}$ M TOPO (1', 2', 3') and for mixtures of $2 \cdot 10^{-2}$ M TOPO and $1 \cdot 10^{-2}$ M benzoic acid (1, 2, 3) in: (◎) carbon tetrachloride; (×) cyclohexane; (□) benzene.

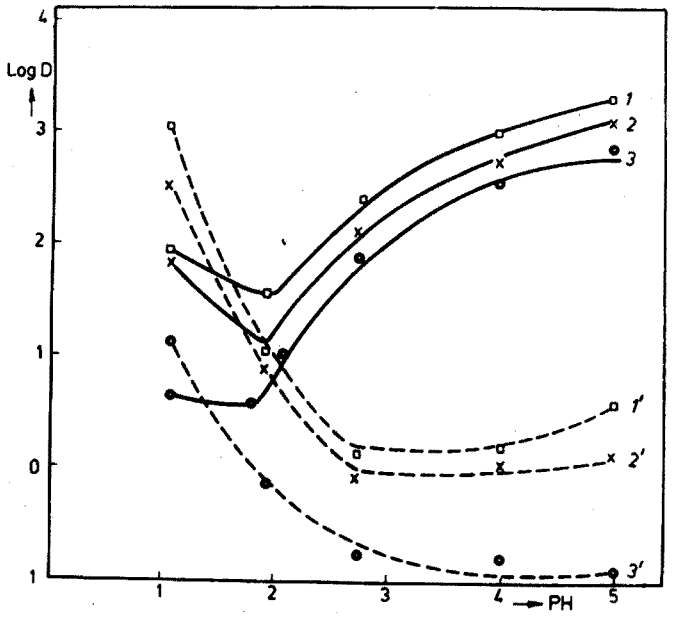

Fig. 4. Variation of log D for uranium(VI) with pH for $2 \cdot 10^{-2}$ M TOPO (1', 2', 3') and for mixtures of $2 \cdot 10^{-2}$ M TOPO and $1 \cdot 10^{-2}$ M salicylic acid (1, 2, 3) in: (◎) carbon tetrachloride; (×) cyclohexane; (□) benzene.

regions regardless of the diluent used: a region of antagonistic action (pH below 1.9) and a region of synergic action (pH above 1.9). Thus the diluents do not change the effect of the acids. D decreases in the order $D_{C_6H_6} > D_{C_6H_{12}} > D_{CCl4}$ in all cases; xylene and toluene behaved similarly to cyclohexane as diluents. The highest distribution coefficients of uranium were obtained in extraction with benzene. The results shown could not be correlated with the physical constants of the diluent. It could be assumed that benzene and cyclohexane take part in the extractable species, solvating them at low TOPO and acid concentrations.

REFERENCES

1 St. Mareva, N. Jordanov and M. Konstantinova, *Anal. Chim. Acta*, 59 (1972) 319.
2 K. S. Marcley, *Fatty Acids, Their Chemistry, Properties, Production and Uses*, Interscience, New York, 1960.
3 A. K. Sundaram and S. Banerjee, *Anal. Chim. Acta*, 8 (1953) 526; 10 (1954) 256.
4 L. M. Gindin, P. I. Bobikov, G. M. Patjukov, A. M. Rozen, E. F. Kouba and A. V. Bugaeva, *Sbornik "Ekstraktsiya"*, II, Gosatomizdat, Moscow, 1962, p. 82.
5 S. M. Karpachev, *Radiochim.*, 3 (1961) 291.
6 N. Nakasuka, *J. Inorg. Nucl. Chem.*, 32 (1970) 3667.
7 R. Pietsch and H. Sinig, *Anal. Chim. Acta*, 49 (1970) 51; 53 (1971) 287.
8 M. Tanaka, *J. Inorg. Nucl. Chem.*, 32 (1970) 2759 and 2791.
9 L. L. Galkina, *Radiokhim.*, 8 (1966) 358.
10 A. W. Ashbrook, *J. Inorg. Nucl. Chem.*, 34 (1972) 1721.
11 E. N. Merkin, *Radiokhim.*, 8 (1966) 705.
12 A. Weisberger, E. Proskauer, J. Riddin and E. Tups, *Organic Solvents*, Inostrannaya Literatura, Moscow, 1958.

13 S. B. Savvin, *Arsenazo III*, Atomizdat, Moscow, 1966.
14 A. M. Rozen and L. P. Horhorina, *Dokl. Akad. Nauk SSSR*, 153 (1963) 1387; *Zh. Neorg. Khim.*, 12 (1967) 244.
15 A. A. Nemodruk and L. P. Gluhova, *Zh. Neorg. Khim.*, 8 (1963) 2618.
16 S. Siekierski, *J. Inorg. Nucl. Chem.*, 24 (1962) 205.
17 Y. Marcus and A. S. Kertes, *Ion Exchange and Solvent Extraction of Metal Complexes*, John Wiley, Bristol, 1969, p. 712.
18 T. V. Healy, *Nucl. Sci. Eng.*, 16 (1963) 413; *J. Inorg. Nucl. Chem.*, 19 (1961) 328; 30 (1968) 1025.
19 V. S. Schmidt, E. A. Mejav and S. S. Nosikova, *Radiokhim.*, 9 (1967) 317.

Analytica Chimica Acta, 68 (1974) 243–246

SHORT COMMUNICATION

An analytically useful coulometric generation of micro amounts of metal ions

Part II. Electrogeneration of lead(II)

TH. J. M. POUW, G. DEN BOEF and U. HANNEMA

Laboratory for Analytical Chemistry, University of Amsterdam, Nieuwe Achtergracht 166, Amsterdam (The Netherlands)

(Received 21st May 1973)

In a previous paper[1] the potentialities of liquid bismuth amalgam as an electrode material for the coulometric preparation of bismuth(III) ions have been discussed. The described method is suitable for the generation of micro amounts of lead(II) ions from lead amalgam as well. As in the case of bismuth(III) ions the current efficiency can be determined by measuring, at a given generation current, the time needed to convert an accurately known amount of EDTA into the metal complex by means of spectrophotometric indication of the equivalence point. The lead–EDTA complex displays an absorbance maximum at 242 nm with a molar absorptivity of the order of 9000.

The accurate determination of concentrations of EDTA as low as 10^{-6} *M* appears to be possible, provided that the lead amalgam electrode is protected against spontaneous oxidation by a sufficiently negative potential during every interruption of the generation current.

Experimental

The equipment used throughout the experiments has already been described[1] and was used without any change.

The influence of oxygen

The influence of oxygen on lead amalgam is illustrated in Fig. 1, which shows an experimental polarization curve of a dropping lead amalgam electrode in a 0.1 *M* perchloric acid solution which had been adjusted to pH 3.5 by potassium hydroxide. The solution was 0.002% in triton X-100. The concentration of the amalgam was about 0.002 *M*. The dotted curve I represents the reduction of oxygen according to

$$O_2 + 2\,H_3O^+ + 2e \rightarrow H_2O_2 + 2\,H_2O \qquad (1)$$

Curve II describes the oxidation of lead amalgam according to

$$Pb(Hg) \rightarrow Pb^{2+} + 2e + (Hg) \qquad (2)$$

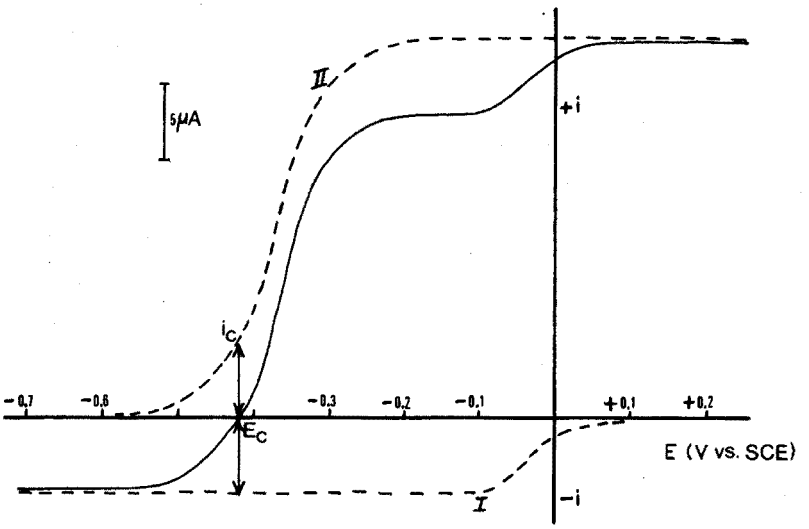

Fig. 1. Illustration of the influence of oxygen on the polarization curve of a dropping lead amalgam electrode.

If there is no external polarization, lead amalgam will be oxidized according to the reaction

$$Pb(Hg) + O_2 + 2\,H_3O^+ \rightarrow Pb^{2+} + H_2O_2 + 2\,H_2O + (Hg)$$

which can be found by combination of reactions (1) and (2).

The corrosion current i_c is larger than in the case of bismuth amalgam[1].

Coulometric preparation of lead(II) ions from liquid lead amalgam

The coulometric preparation for quantitative purposes of micro amounts of lead(II) ions would be possible if the spontaneous oxidation of lead amalgam, occurring during the interruptions of the generation current, could be prevented. Fortunately, this spontaneous oxidation can be virtually suppressed by a potential

TABLE I

TITRATIONS OF $5.19 \cdot 10^{-8}$ MOLES OF EDTA WITH ELECTROGENERATED Pb(II)

T_e (sec)	C.E. $= T_t/T_e \cdot 100\%$	Standard deviation
41.4	96.6	
39.6	101.0	
42.4	94.3	
38.0	105.2	
35.6	112.3	5.0 ($n = 10$)
38.6	103.6	
38.9	102.8	
39.7	100.8	
39.7	100.8	
41.0	97.5	

of -1.2 V *vs.* S.C.E., as was established by the following tests. The electrolysis cell, equipped with a lead amalgam electrode at a concentration of about 0.03 *M*, was filled with 0.1 *M* perchloric acid adjusted to pH 3.5 with potassium hydroxide. In advance, most of the oxygen had been removed from this solution by nitrogen. Furthermore, 0.05 ml of a 10^{-3} *M* EDTA solution was added. With a potential of -1.2 V *vs.* S.C.E. applied to the amalgam electrode, the absorbance of the solution in the electrolysis cell, measured at 242 nm, showed an increase from 0.000 to only 0.007 over a period of 30 min. Without the protecting potential, as little as 5 min sufficed to produce such an increase in absorbance as corresponded to total conversion of the EDTA present. Reduction of Pb–EDTA did not occur at the potential of -1.2 V *vs.* S.C.E.

Thus, the method previously applied for the generation of bismuth(III)[1] can also be used for the generation of micro amounts of lead(II) ions.

Results and discussion

Table I gives the results of ten successive titrations of $5.19 \cdot 10^{-8}$ moles of EDTA (10^{-6} *M*) with electrogenerated lead(II) ions. The concentration of the amalgam was about 0.03 *M*. The generation current was 0.25 mA. The titrations were carried out in a 0.1 *M* perchloric acid solution adjusted to pH 3.5 with potassium hydroxide and were followed spectrophotometrically at 242 nm. A typical titration curve is given in Fig. 2.

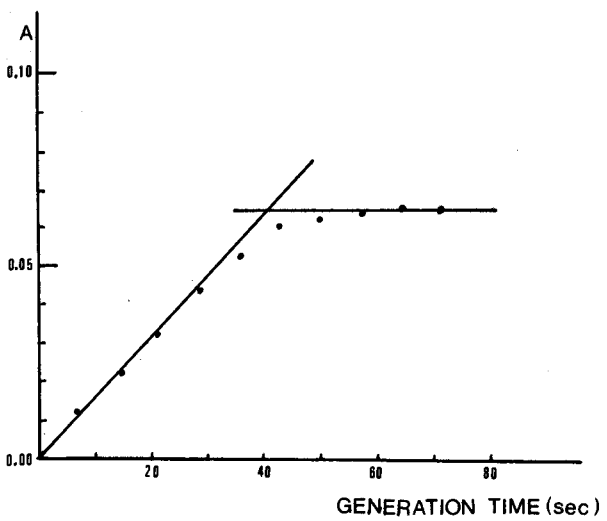

Fig. 2. Titration curve of a titration of $5.19 \cdot 10^{-8}$ moles of EDTA (10^{-6} *M*) with electrogenerated lead(II).

The amount of EDTA titrated corresponds to a concentration of the order of 10^{-6} *M* which was also the lower limit of determination of the titration with electrogenerated bismuth(III)[1].

It will not be possible to determine lower concentrations of EDTA with electrogenerated lead(II) ions by employing an amperometric method of indication, because the stability constant of the lead–EDTA complex is not large enough.

REFERENCE

1 Th. J. M. Pouw, G. den Boef and U. Hannema, *Anal. Chim. Acta*, 67 (1973) 427.

Analytica Chimica Acta, 68 (1974) 247–250

BOOK REVIEWS

H. A. Liebhafsky, H. G. Pfeiffer, E. H. Winslow and P. D. Zemany, *X-Rays, Electrons and Analytical Chemistry. Spectrochemical Analysis with X-Rays*, Wiley–Interscience, New York, 1972, xii + 566 pp., price £ 10.45.

Many analysts new to the field of X-ray analysis, have good reason to be grateful to these authors for their earlier classic work on this subject—*X-Ray Absorption and Emission in Analytical Chemistry*—first published in 1960. The literature coverage of this field is still comparatively sparse and this new publication is very welcome. The authors are at pains to point out that this is not a revised edition of their earlier work but a new book, and while the general format and much of the original material have been rightly retained, the claim is essentially true.

The work consists of an introductory chapter on the generation and properties of X-rays, followed by nine self-contained chapters dealing with measurement of X-ray intensity, X-ray detectors and detector systems, absorptiometry with X-rays, X-ray spectra, the selection of X-ray wavelengths, X-ray diffraction in chemical analysis, measurement of film thickness, simple trace determinations, reliability of X-ray emission spectrometry, statistical considerations, and finally a chapter dealing with equipment and selected applications. An appendix provides information on safety, tables of emission lines and absorption edges, mass absorption coefficients of the elements and of selected film materials, characteristic photon yields of the elements and absorption jump ratios, and finally a guide to literature references between 1964 and 1970 on the determination of elements by X-ray fluorescence.

The authors have shown their ability to present relatively complex technical material in very simple terms which makes the book ideally suited to students and also to established analysts who wish to assimilate the fundamentals of X-ray analysis. Although the word does not appear in the title, this is a practical book containing a particularly useful section dealing with difficulties experienced in X-ray analysis and recommendations for curing them.

It is well illustrated and contains almost 900 references including generous recommendations to buy competing publications. Anyone—tyro or expert—with an interest in X-ray analysis will find this book invaluable.

D. M. Peake (Birmingham)

Differential Thermal Analyis, Vol. 2. Applications, Edited by R. C. Mackenzie, Academic Press, London and New York, 1972, xvi + 607 pp., price £ 12.50.

Three years have elapsed since the publication of the first volume of this worthy book—no less than 31 authors had to pool their experiences to produce this second volume which completes the series. Sections A–C were included into Volume 1 (subtitled: Fundamental Aspects); the present volume contains section D (chapters

26–30) on the use of DTA in physical chemistry and section E (chapters 31–46) on applications in industry. Section D could well have gone into Volume 1 as it describes a large amount of fundamental material (and contains, by the way, some of the best-written chapters in the whole series). About three-quarters of the volume of the book is devoted to section E, in which the application of DTA to the widest possible industrial problems is described. Despite the large number of authors with different backgrounds and mother-tongues, the standard of contributions is quite even and always high. The detailed table of contents is very helpful; one can easily find one's topic in the book. The text is well presented; typography is clear, figures are well drawn and thermograms are presented in such detail that peak temperatures can be read with sufficient accuracy from the charts. The price of the book is quite high, though it costs only 50 p more than Volume 1 cost three years ago. There is no point in buying Volume 2 separately as one has to look up Volume 1 frequently for fundamentals. For private individuals the price of the 2-volume set may be prohibitive; the book is, however, a must for institutions or laboratories where DTA or thermal analysis in general is employed.

Gyula Svehla (Belfast)

Manzur-ul-Haque Hashmi, *Assay of Vitamins in Pharmaceutical Preparations*, John Wiley & Son, London, 1973, xxv + 512 pp., price £12.00

This book is a comprehensive review of methods of vitamin analysis published up to 1971. Dr. Hashmi must be congratulated on his diligence; over 200 methods for 18 vitamins are described. A general introduction is followed by a short chapter on the stability of vitamins in pharmaceutical preparations. Each vitamin then has a chapter devoted to it, in which the methods are listed, briefly discussed and then given in reasonable detail. Chapter 21 describes methods for the simultaneous determination of some vitamins and the last chapter describes published methods with Autoanalyzer equipment. The book is well presented and errors are rare, although we are told on p. 28 to weigh out the equivalent of 100 mg – 1 g Vitamin A in the examination of fish oils (a weight of oil is intended).

Does the book accomplish its aim? It certainly assembles the wealth of published literature on vitamin analysis and most pharmaceutical analysts will want a copy for its reference value. However, it is a tantalizing text. Its usefulness would be greatly improved if a more critical approach had been adopted, such as a critical review of the methods available for each compound, followed by a detailed description of only the more useful techniques (for example, the choice of 22 methods for Vitamin C is rather bewildering). The author obviously appreciates the importance of stability and a chapter on this aspect was most welcome; a study of the applicability of the methods to stability testing would have been even more welcome. Finally the book claims to contain sufficient detail to be a practical text; however, there seems a continual need to follow up the relevant references. For example, under Vitamin A we are told to avoid a Morton and Stubbs correction if we know that interfering substances are absent—we are not told how to detect these.

J. Tillman (Loughborough)

C. E. Weaver and L. D. Pollard, *The Chemistry of Clay Minerals*, Developments in Sedimentology, Vol. 15, Elsevier Scientific Publishing Company, Amsterdam, 1973, viii + 213 pp., price Dfl. 65.00 (*ca.* $20.25).

This authoritative work presents a vast selection of data on the composition and the structures of twenty-five varieties of clay minerals. These data, which focus much-needed attention on interstratified minerals, emphasize the variations in the compositions of the more commonly occurring clays. In many instances the chemical compositions are related to the possible modes of origins of the minerals.

Post-graduate students, and research workers in general in the field of clay science, will consider this a well referenced book of very considerable merit. It cannot, however, be recommended to those who are less involved in the field. The use of diagrams to illustrate structures, some emphasis on experimental procedures (only the short chapter which deals with clay synthesis is satisfying in this respect), particularly with regard to analysis and to techniques used in determining structures, and a treatment of the surface chemistry of clays, would greatly broaden interest in the book.

M. A. B. Hayes (Birmingham)

Howard A. Strobel, *Chemical Instrumentation*, Addison–Wesley Publishing Company, Reading, Mass., 2nd Ed., 1973, xxii + 903 pp., price $13.95.

The second edition of this book represents in many ways the dramatic changes that are taking place in analytical chemistry. There is a total of 903 pages and 31 chapters. The subject matter that is covered, is covered well, and the author is to be congratulated on devoting so much time and energy to gathering together so many facts from so many fields. Eight chapters are devoted to electronics, starting from Ohm's law and carrying through to digital computers. Not many years ago this subject matter would have been considered purely physics, but today it is becoming more important for the practicing analytical chemist to be versatile in electronics. The second most important feature of the book is the devotion of six chapters to various parts of electrochemistry. All these chapters, both on electronics and electrochemistry, are well written with the student in mind. Of particular note are the references at the end of each chapter, which present a thorough bibliography of pertinent textbooks.

Seven chapters are devoted to spectrometry; two chapters occupy the bulk of this section and are concerned with basic optics and absorption spectrometry. The choice of the remaining subject matter for the spectrometry section is perplexing. Good coverage is given to flame photometry and emission spectroscopy, and reasonably good coverage to nuclear magnetic resonance. However, there is no chapter on infrared spectrometry although the topic is mentioned in various parts of the book. Two pages only, are devoted to atomic absorption spectroscopy and there is no discussion on any aspects of X-ray analysis. The chapter on chromatography dealts with basic principles of chromatography, but does not discuss programmed-temperature, capillary-column or preparative gas chromato-

graphy, or the combination of g.c. with other techniques. Thermal methods are not discussed at all.

The general conclusion is that the material which is covered, is covered well. But many of the major techniques which are part of the analytical chemist's arsenal today are barely mentioned. No doubt this book could be used for some courses in instrumentation analysis, but it would have to be supplemented by other texts.

J. W. Robinson (Baton Rouge)

Annual Reports on NMR Spectroscopy, Vol. 5A, Edited by E. F. Mooney, Academic Press, London, 1972, xii + 696 pp., price £13.00.

This book follows the same general pattern as the previous volumes as it combines annual reviews with subject reviews of a more specialised nature. The first two chapters (by T. N. Huckerby and R. Fields respectively) review developments in proton and fluorine-19 nuclear magnetic resonance published during 1970. Both reviewers have arranged their material very well indeed, and it is only of minor note that one section on the fluorine-19 n.m.r. of natural products overlaps with chapter three on the n.m.r. of carbohydrates and related compounds. The latter review by T. D. Inch covers the literature from 1968 to 1970; earlier work has been reviewed by the same author in volume two of this series. Chapter four (by W. McFarlane) on homonuclear magnetic double resonance and chapter five (by M. Witanowski and G. A. Webb) on nitrogen n.m.r. (^{14}N and ^{15}N) also up-date reviews in earlier volumes. In chapter six, J. W. Akitt reviews the n.m.r. spectroscopy of compounds containing aluminium and gallium. This chapter should appeal to many inorganic chemists as well as n.m.r. specialists. The final chapter by D. G. Gillies and D. Shaw discusses the application of Fourier transform methods to high-resolution n.m.r. This clearly presented review is particularly timely in view of the recent explosion of interest in this area, and it should have great appeal to the non-specialist.

The contributors to this volume deserve credit for maintaining the very high standard of this series. However, one might have hoped that the price of these volumes could have been maintained below £10, perhaps by reducing the size which has doubled since Volume one.

W. B. Jennings (Birmingham)

Analytica Chimica Acta, 68 (1974) 251

ANNOUNCEMENT

21st Canadian Spectroscopy Symposium, Ottawa, 1974

The 21st Canadian Spectroscopy Symposium will be held in Ottawa, October 7–9, 1974.

For details contact: Mr. J. L. Dalton, Secretary, 21st Canadian Spectroscopy Symposium, Department of Energy, Mines and Resources, Mines Branch, 555 Booth Street, Ottawa, Ontario, K1A 0G1, Canada.

ERRATA

K.L. Crochet and J.G. Montalvo, Jr., Enzyme electrode system for assay of serum cholinesterase, *Anal. Chim. Acta*, 66 (1973) 259–269.

This paper should have included a reference to an earlier procedure for cholinesterase: L.H. von Storp and G.G. Guilbault, A new assay for cholinesterase potentiometric determinations in flow streams, *Anal. Chim. Acta*, 62 (1972) 425–430.

G. Raspi, P. Zanello, A. Cinquantini and P. Corti, Voltammetric behaviour of copper(III) and its analytical applications, *Anal. Chim. Acta*, 66 (1973) 435.
Page 437, Table I, the units of $\bar{i}_d/C$ should read (μA mmol^{-1} l).

(Continued from page 4 of cover)

CONTENTS

(continued on inside page of cover)